The Role of Viral Sensing in the Development of Autoimmunity

Claudia Loetsch

A thesis in fulfilment of the requirements for the degree of
Doctor of Philosophy

University of New South Wales
Faculty of Medicine, St. Vincent's Clinical School
Garvan Institute of Medical Research

September 2016

PLEASE TYPE

THE UNIVERSITY OF NEW SOUTH WALES
Thesis/Dissertation Sheet

Surname or Family name: Loetsch

First name: Claudia

Other name/s:

Abbreviation for degree as given in the University calendar: PhD

School: St. Vincent's Clinical School

Faculty: Medicine

Title: The Role of Viral Sensing in the Development of Autoimmunity

Abstract 350 words maximum: (PLEASE TYPE)

Type I diabetes (T1D) is an autoimmune disease caused by a combination of genetic and environmental factors. Previous studies have linked infections with enteroviruses, such as coxsackievirus B4 (CVB4), with an increased risk of T1D. This dissertation examines the impact of both exogenous virus (i.e. CVB4) and endogenous retroviruses (ERVs) residing in the mammalian genome on the development of chronic inflammation and autoimmunity.

Following CVB4 infection, T1D-susceptible mice displayed exaggerated tissue damage and signs of chronic inflammation after viral clearance. Ongoing inflammation in these mouse strains was linked to an increased infiltration of T follicular helper cells (Tfh) and germinal centre-like B cells in the pancreas. Furthermore, genome-wide expression analyses of pancreatic beta cells from CVB4-infected mice revealed the activation of virus response genes associated with type I/II interferon (IFN) signalling, accompanied by tissue-specific induction of ERVs. In addition, our data highlight an important role for ERVs in the transcriptional regulation of immune response genes. Remarkably, pancreatic beta cells from uninfected T1D-susceptible mice revealed similar gene enrichment profiles to those found in CVB4-infected mice, emphasizing the role of viral sensing in autoimmune diabetes.

To further explore the role of viral recognition in autoimmunity, we made use of a novel mutant mouse strain that carries a point mutation within the MAVS (mitochondrial antiviral-signalling) protein, a crucial mediator of cytoplasmic nucleic acid sensing. MAVSlos mice immunised with RNA substrates exhibited diminished production of type I IFN and subsequent reduction of Tfh expansion and germinal centre formation. These findings demonstrate the significant role of (viral) nucleic acid sensing for appropriate activation of effector cells, but also illustrate how dysregulation of innate anti-viral signalling may translate into inappropriate (diminished or exaggerated) adaptive immunity.

Declaration relating to disposition of project thesis/dissertation

I hereby grant to the University of New South Wales or its agents the right to archive and to make available my thesis or dissertation in whole or in part in the University libraries in all forms of media, now or here after known, subject to the provisions of the Copyright Act 1968. I retain all property rights, such as patent rights. I also retain the right to use in future works (such as articles or books) all or part of this thesis or dissertation.

I also authorise University Microfilms to use the 350 word abstract of my thesis in Dissertation Abstracts International (this is applicable to doctoral theses only).

21/09/16
Date

The University recognises that there may be exceptional circumstances requiring restrictions on copying or conditions on use. Requests for restriction for a period of up to 2 years must be made in writing. Requests for a longer period of restriction may be considered in exceptional circumstances and require the approval of the Dean of Graduate Research.

FOR OFFICE USE ONLY

Date of completion of requirements for Award:

ORIGINALITY STATEMENT

'I hereby declare that this submission is my own work and to the best of my knowledge it contains no materials previously published or written by another person, or substantial proportions of material which have been accepted for the award of any other degree or diploma at UNSW or any other educational institution, except where due acknowledgement is made in the thesis. Any contribution made to the research by others, with whom I have worked at UNSW or elsewhere, is explicitly acknowledged in the thesis. I also declare that the intellectual content of this thesis is the product of my own work, except to the extent that assistance from others in the project's design and conception or in style, presentation and linguistic expression is acknowledged.'

Signed ……..

Date ……..

SUMMARY

Type I diabetes (T1D) is an autoimmune disease caused by a combination of genetic and environmental factors. Previous studies have linked infections with enteroviruses, such as coxsackievirus B4 (CVB4), with an increased risk of T1D. This dissertation examines the impact of both exogenous virus (i.e. CVB4) and endogenous retroviruses (ERVs) residing in the mammalian genome on the development of chronic inflammation and autoimmunity.

Following CVB4 infection, T1D-susceptible mice displayed exaggerated tissue damage and signs of chronic inflammation after viral clearance. Ongoing inflammation in these mouse strains was linked to an increased infiltration of T follicular helper cells (Tfh) and germinal centre-like B cells in the pancreas. Furthermore, genome-wide expression analyses of pancreatic beta cells from CVB4-infected mice revealed the activation of virus response genes associated with type I/II interferon (IFN) signalling, accompanied by tissue-specific induction of ERVs. In addition, our data highlight an important role for ERVs in the transcriptional regulation of immune response genes. Remarkably, pancreatic beta cells from uninfected T1D-susceptible mice revealed similar gene enrichment profiles to those found in CVB4-infected mice, emphasizing the role of viral sensing in autoimmune diabetes.

To further explore the role of viral recognition in autoimmunity, we made use of a novel mutant mouse strain that carries a point mutation within the MAVS (mitochondrial antiviral-signalling) protein, a crucial mediator of cytoplasmic nucleic acid sensing. $MAVS^{los}$ mice immunised with RNA substrates exhibited diminished production of type I IFN and subsequent reduction of Tfh expansion

and germinal centre formation. These findings demonstrate the significant role of (viral) nucleic acid sensing for appropriate activation of effector cells, but also illustrate how dysregulation of innate anti-viral signalling may translate into inappropriate (diminished or exaggerated) adaptive immunity.

Table of Contents

Acknowledgements

This work would have not been possible without the invaluable contribution of many people. First and foremost, I would like to express my sincere appreciation to my supervisor Cecile King, for her guidance, encouragement and expertise throughout this PhD - her passion for science has certainly shaped this project. I would further like to express my gratitude to my co-supervisor Tatyana Chtanova for her continuing support and advice. A huge thanks goes to the members of the King lab – past and present – for all the scientific advice and training. A special thanks goes to Joanna Warren for all her help with gargantuan experiments, for being a fantastic friend, for rectifying my musical education and for reminding me that lack of talent is no reason not to sing. I would further like to thank Jon Sprent, Kylie Webster and Marcel Batten for their invaluable suggestions during lab meetings and beyond. I would also like to thank members of the Grey lab, and in particular Stacey Walters for teaching me how to master islet isolations. A huge thanks goes to the entire immunology department for creating a wonderful and warm working environment – I feel very lucky to have undertaken my PhD at such a professional, supportive and friendly workplace.

A very special thanks to my dearest partners in crime, Rushika and Eli, who really shaped the social hours of my PhD life with visionary couch parties, mood enhancers and bake off victories (“Chess fever”, “MacMan”), and showed me how much Austria and Australia truly have in common.

One person I can barely thank enough is my partner Rodrigo, for his incredible encouragement, his patience, his moral and scientific support, for sharing the

love for the German soccer team, and for coming up with seemingly unlimited resources of sugar and caffeine whenever needed.

Finally, I would like to thank my entire family, and especially my mum. If it had not been for your inspiration, your understanding, and your endless support in any possible way, I would not have been able to study half the world's circumference away from home.

Publications by the author during this candidature

McGuire HM, Vogelzang A, Warren J, **Loetsch C**, Natividad KD, Chan TD, Brink R, Batten M, King C. IL-21 and IL-4 Collaborate To Shape T-Dependent Antibody Responses. J Immunol. 2015 Dec 1;195(11):5123-35.

Loetsch, C., Warren, J., Jandl. C., King, C. Cytosolic recognition of RNA drives the germinal centre response to red blood cells. (*Manuscript in Submission)*

Vazquez-Lombardi, R., **Loetsch, C.**, Zinkl, D., Jackson. J., Schofield, P., Deenick, E.K., King, C., Phan, T.G., Webster, K.E., Sprent, J., & Christ, D. Potent antitumour activity of IL-2-Fc fusion proteins requires Fc**γ**R-dependent depletion of regulatory T cells. (*Manuscript under Revision)*

Jandl C. and **Loetsch C.** Cytokine expression by T follicular Helper Cells in Germinal Centers: Methods and Protocols. Springer Methods, 2016 (*Manuscript under Revision)*

Experiments that were not the sole work of the author

Nenad Bartonicek performed the read mapping, counting and normalization, extraction of repeat regions and the EdgeR-based modelling for RNA-sequencing analysis. With regard to ggplot2 data visualization, Nenad Bartonicek generated the violin plots, while Jeremy Parsons generated the density plots for co-enrichment of LTR elements.

Abbreviations not defined in the text

Bcl2	B-cell lymphoma 2
bp	Base pair
CARD	Caspase activation and recruitment domain
CD	Cluster of differentiation
CFSE	Carboxyfluorescein succinimidyl ester
DAB	3,3'-Diaminobenzidine
DMSO	Dimethyl sulfoxide
DNA	Deoxyribonucleic acid
EDTA	Ethylenediaminetetraacetic acid
ELISA	Enzyme-linked immunosorbent assay
CpG	5'–C–phosphate–G–3'
h	Hour
HeLa	Immortalised cell line derived from cervical cancer cells
HRP	Horseradish peroxidase
IF	Immunofluorescence
Ig	Immunoglobulin
IHC	Immunohistochemistry
kb	Kilobase pair
kDa	Kilodalton
lncRNA	long non-coding RNA
MEF	Mouse embryonic fibroblasts
min	Minutes
MyD88	Myeloid differentiation primary response gene 88
O/N	Overnight
PBS	Phosphate-buffered saline
PCR	Polymerase chain reaction
PFU	Plaque-forming unit
PWM	Position weight matrix
RNA	Ribonucleic acid
RPMI	Roswell Park Memorial Institute medium

RT	Room temperature
SDS	Sodium dodecyl sulphate
STAT	Signal transducer and activator of transcription
TBS	Tris-buffered saline
TMB	3,3’,5,5’-Tetramethylbenzidine
UTR	Untranslated region
WT	wild-type

1. GENERAL INTRODUCTION

1.1. At a glance

The mammalian immune system coordinates a complex network of cellular and molecular mechanisms that ensure host protection from invading pathogens. In order to limit immune destruction to invading pathogens, it is critical to discriminate self from non-self tissues. The loss of this ability (loss of self-tolerance) results in aberrant immune responses to host tissue and ultimately in the development of autoimmunity. While the exact aetiology of many autoimmune diseases, including type I diabetes (T1D), is still unknown, it has been established that both genetic and environmental factors play a major role in disease development. Indeed, T1D, an autoimmune disease caused by selective destruction of insulin-producing beta cells in the pancreas, has been commonly linked to virus infections as environmental triggers. This dissertation aims to improve our understanding of how endogenous viral elements and exogenous virus infections can contribute to chronic inflammation and autoimmunity within the framework of T1D.

1.2. The immune system

1.2.1. Primary lymphoid organs

Lymphatic organs are implicated in leukocyte development, maturation and proliferation and are classified into primary and secondary lymphoid organs

accordingly. Lymphocyte development takes place in primary lymphoid organs, which comprise the thymus and the bone marrow, the latter providing stem cells from which all lymphocytes arise.

1.2.1.1. T cell development in the thymus

The process of T (**t**hymus-derived) cell development in the thymus involves migration to the thymus and divergence to different T cell lineages. T cells leave the thymus as antigen inexperienced naïve single positive (CD4+ or CD8+) T cells, and undergo further differentiation in the periphery to obtain effector functions.

At first, early lymphocyte progenitor cells migrate from the bone marrow to the thymus and subsequently start their commitment to the T cell lineage. Early T cell progenitors do not express the CD4 or CD8 T cell co-receptors (i.e. double negative), but will become double positive (DP $CD4^+CD8^+$) once they successfully assemble the T cell receptor β-chain (Raulet et al., 1985). DP thymocytes undergo both positive and negative selection to become single positive (SP) $CD4^+$ or $CD8^+$ T cells. The process of positive selection generates SP thymocytes with sufficient T cell receptor affinity and/or avidity for self-peptides. In return, thymocytes with a high affinity for self-antigen are eliminated during negative selection (clonal deletion), thereby avoiding autoimmunity (Ashton-Rickardt et al., 1994; Cook et al., 1997; Kappler et al., 1987; Sebzda et al., 1994). Finally, selected T cells relocate to the medulla, where they continue to undergo deletion and maturation before exiting the thymus as immune-competent T cells (Takahama, 2006).

1.2.1.2. B cell development in the bone marrow

Similarly to T cells, B cell development occurs in several distinct stages. Early B cell development takes place in primary lymphoid organs (foetal liver and bone marrow) followed by maturation stages in secondary lymphoid organs (spleen and lymph nodes). Initial stages in the bone marrow are defined based on the surface expression of several CD (cluster of differentiation) antigens and the rearrangement of the immunoglobulin heavy and light chain loci (Coffman, 1982). During early developmental stages, hematopoietic stem cells (HSC) differentiate into early lymphocyte progenitors, pro-B cells and pre-B cells to become immature B cells that express a mature B cell receptor (BCR) capable of binding antigen (Hardy et al., 1991; LeBien, 2000). Before leaving the bone marrow, immature B cells have to undergo a negative selection process that eliminates clones with a high affinity to self-antigen (central B cell tolerance, (Grandien et al., 1994; Loder et al., 1999). After successfully passing this crucial checkpoint, immature B cells further differentiate into transitional B cells that will continue their maturation after migration to secondary lymphoid organs (Loder et al., 1999). The mature B cell population can be divided into follicular B cells, which colonize the lymphoid follicles of spleen and lymph nodes, and marginal zone (MZ) B cells. While murine MZ B cells are mainly found within the marginal zone of the spleen, human MZ B cells are less restricted and have access to the circulation. Upon antigen encounter, both B cell populations can terminally differentiate into antibody-producing plasmablasts or generate antigen-experienced B cells that will rapidly produce high-affinity antibodies upon a secondary antigen challenge (Cerutti et al., 2013).

1.2.2. Secondary lymphoid organs

Secondary or peripheral lymphoid organs are structured sites in which antigen-driven differentiation and proliferation of lymphocytes takes place. Major secondary lymphoid organs include the spleen, regional lymph nodes and isolated lymphoid follicles, tonsils, mucosa-associated lymphoid tissue (MALT) and Peyer's patches (Goodnow, 1997; Kunisawa et al., 2005). Strategic positioning of these lymphoid structures throughout the body enables efficient antigen sampling and presentation. The basic structural organization of secondary lymphoid organs involves compartmentalization into T cell zones and B cell follicles, the presence of antigen-presenting cells (APCs) such as macrophages and dendritic cells, as well as a high degree of vascularization that supports fast antigen delivery and cellular responses (Anderson and Shaw, 2005; Cyster, 1999). Circulating immune cells, such as APCs displaying antigen, can reach secondary lymphoid organs through lymphatic and/or blood vessels. Notably, lymph nodes exclusively filter leukocytes and associated antigens that circulate in lymphatic vessels. Immune cells enter the lymph node via afferent lymphatic vessels and exit it through efferent lymphatic vessels. Efferent vessels can drain into a larger lymph node and, eventually, into the bloodstream through subclavian veins. Leukocytes that circulate in blood vessels are filtered through the spleen, which exclusively filters blood. Furthermore, entry of immune cells into other lymphoid organs, such as the tonsils, occurs via both lymphatic and blood vessels.

1.2.3. Tertiary lymphoid structures

Tertiary lymphoid structures, also referred to as ectopic lymphoid structures, can only be found in the state of chronic inflammation, in which tissue-infiltrating immune cells can form organized lymphoid structures within non-lymphoid tissues. These organized ectopic structures show a great similarity to secondary lymphoid organs in terms of B and T compartmentalization, vasculature and function (Drayton et al., 2006).

1.3. Innate and adaptive immunity

Throughout the course of evolution, the mammalian immune system has adopted two different strategies to protect the host from pathogen invasion. While innate immunity is critical for the recognition of a wide range of common pathogenic patterns and the initiation of rapid defence mechanisms, adaptive immunity requires a longer time to react but provides pathogen-specific defence, as well as immunity that protects against subsequent infection.

1.3.1. Key components of the innate immune system

Innate immunity depends on a limited number of germ-line encoded receptors that are able to recognize common pathogen-associated molecular patterns (PAMPs) exclusively found on pathogenic microbes such as bacteria, fungi, viruses and parasites (Janeway, 1989). Engagement of PAMPs with their respective receptors triggers rapid and non-specific immune responses,

thereby providing a first layer of defence against invading pathogens. The innate immune system is furthermore responsible for initiating immune responses towards host-related stress signals such as local tissue injury or cell necrosis, and, last but not least, essential for the activation of the adaptive immune system (Iwasaki and Medzhitov, 2015).

1.3.2. Microbial sensing Pattern-Recognition Receptors (PRRs)

Mammalian cells express two major classes of PRRs: membrane-associated receptors, which include toll-like receptors (TLRs) and C-type lectin receptors (CLRs); and cytosolic receptors, such as RIG-I-like receptors (RLRs), NOD-like-receptors (NLRs), AIM2-like receptors (ALRs) and the more recently described class of cytosolic DNA sensors (CDSs). PRRs are expressed by several leukocyte populations (e.g. dendritic cells, macrophages and B cells) but also by various nonprofessional immune cells such as fibroblasts, epithelial cells and endothelial cells. Many PAMPs are able to activate multiple PRRs, which subsequently results in complex receptor interactions that can amplify or inhibit downstream signalling (Takeuchi and Akira, 2010).

1.3.2.1. Membrane-bound PRRs

The initial notion of the innate immune system lacking specificity and complexity was quickly overruled by the discovery of TLRs in the mid-90s (Lemaitre et al., 1996; Medzhitov et al., 1997). To date, the TLR family is undoubtedly the most widely studied PRR class with 10 members described in

humans and 12 members reported in mice. Depending on their cellular localization, TLR signalling takes place either at the cell surface (TLR1, TLR2, TLR4, TLR5, TLR6 and TLR10) or intracellularly at endosomal or endolysosomal membranes (TLR3, TLR7, TLR8, TLR9, TLR11, TLR12, TLR13). TLRs at the plasma membrane are able to recognize lipopolysaccharide (LPS), proteins, lipoproteins and lipids, whereas intracellular TLRs within endosomal membranes recognize single- and double-stranded nucleic acids. Ligand-receptor interactions activate a multitude of signalling pathways that promote the release of proinflammatory cytokines, chemokines and/or interferons, thus triggering a precise, ligand-specific immune response (Kawai and Akira, 2010).

C-type lectin receptors (CTRs) make up the second class of transmembrane receptor families and are indispensable for sensing carbohydrate structures present on fungi, viruses and mycobacteria. Activation of CTRs results either in the induction of proinflammatory cytokines or in the inhibition of TLR-mediated signalling (Geijtenbeek and Gringhuis, 2009).

1.3.2.2. Cytoplasmic PRRs

A substantial body of work has been directed at understanding intracellular recognition of viral nucleic acids. The three most relevant members of the RIG-I-like receptors family (RLRs) – RIG-I, MDA5 and LGP2 – are important for recognition of single-stranded RNA (ssRNA), double-stranded RNA (dsRNA) and 5'-triphosphate RNA (ppp-RNA) (Yoneyama et al., 2015). Almost all cells except for plasmacytoid dendritic cells (pDCs), which favour TLR

signalling in response to viral infections (Kato et al., 2005), rely on RLR-mediated anti-viral immunity.

Retinoic acid-inducible gene I (RIG-I) is specialised in detection of virus-derived dsRNA and possibly 5'-ppp-ssRNA, while melanoma differentiation-associated antigen 5 (MDA5) is critical for binding to long dsRNAs. Laboratory of genetics and physiology 2 (LGP2) is the third and least characterized RLR member and has been proposed to be involved in regulating RIG-I and MDA5 function (Yoneyama et al., 2005). Immune activation downstream of RIG-I and MDA5 is orchestrated by the adaptor mitochondrial antiviral signalling protein (MAVS), which leads to the induction of type I interferons and proinflammatory cytokines that mediate antiviral immune responses.

Nucleotide-binding domain, leucine-rich repeat-containing (NLR) proteins are the second class of cytoplasmic sensors, with NLRP3 as the most recognized family member. While NLRs seem little involved in host defences against various viruses (Sabbah and Bose, 2009), they play a major role in initiating inflammasome assembly (Schroder et al., 2010), transcriptional activation of proinflammatory cytokines and regulation of apoptotic processes in the setting of bacterial infections.

Similar to NLRs, AIM2-like receptors (ALRs) are crucial for the assembly of inflammasomes (Lamkanfi and Dixit, 2014), which are multiprotein oligomers that induce caspase-1-mediated inflammation. Members of the ALR family share a DNA-binding motif that allows for recognition of single- (ssDNA) and double-stranded DNA (dsDNA) from various microbes. Although is it assumed that additional ALRs exist, AIM2, which binds to dsDNA, and IFI16, which

binds to ssDNA and dsDNA, are the two most prominent members of this family.

Finally, few members of the DExD/H-box (DDX, DHX) superfamily are also involved in nucleic acid sensing and have recently been proposed to be included in the list of cytoplasmic nucleic acid sensors (Orzalli and Knipe, 2014).

1.3.3. Phagocytic cells

Pathogens that have crossed epithelial barriers and successfully entered the host are instantly recognized by tissue resident phagocytic cells. Professional phagocytic cells, including monocytes/macrophages, dendritic cells and neutrophils, are of myeloid lineage and operate against both extracellular and intracellular pathogens. Extracellular pathogens are recognized by membrane-bound PRRs (e.g. TLRs) on the cell surface of phagocytes, most commonly neutrophils, and are subsequently eliminated via release of antimicrobial granules, lysosomal degradation following phagocytosis and/or neutrophil extracellular traps (Brinkmann et al., 2004; Faurschou and Borregaard, 2003). By contrast, intracellular invaders (viruses and certain bacteria) are detected through soluble PRRs within the cytoplasm of phagocytes, most commonly macrophages. Internalized pathogenic material can also be recruited to endolysosomes and bind to endosomal TLRs. The engagement of foreign pathogens with cytoplasmic and/or endosomal receptors leads to the induction of antiviral signalling pathways that control viral replication and also induces apoptosis of the infected cell (Broz and Monack, 2013; Michallet et al., 2008).

The interaction of intra- and extracellular phagocyte receptors with microbial patterns results in the release of pro-inflammatory cytokines and chemokines that further attract effector leukocytes to the site of inflammation and stimulate antigen-presenting cells to initiate adaptive immunity. Notably, scavenger phagocytes, mainly macrophages, are also involved in the uptake of cellular debris from tissue remodelling and apoptosis, and participate in fine tuning of innate immune responses (Mukhopadhyay and Gordon, 2004).

1.3.4. NK cells and NKT cells

Natural killer (NK) cells are a unique component of the innate immune response as they are classified as lymphocytes but lack a clonally specific receptor, thus distinguishing them from B or T lymphocytes (Cerwenka and Lanier, 2001). It was initially believed that NK recognition is based on the absence of self major histocompatibility class I (MHC I) on the surface of target cells (e.g. viruses), a concept described as ‘missing self recognition’ (Kärre, 1981). However, the later discovery of stimulatory and inhibitory receptors on the surface of NK cells has shaped the idea of NK plasticity, and defined NK responsiveness as a result of integrated NK receptor signalling (Shifrin et al., 2014).

NK-mediated cytotoxicity is mediated through several known mechanisms, including secretion of cytolytic granules, death receptor-mediated cytolysis and cytokine-mediated recruitment of additional cytotoxic lymphocytes (Lee et al., 2007).

Similar to NK cells, natural killer T (NKT) cells are considered as innate lymphocytes. In addition to the expression of typical NK markers on the cell

surface, NKT cells also harbour an unconventional T cell receptor (TCR) restricted to the monomorphic MHC class-I-like molecule CD1d on antigen-presenting cells (Bendelac et al., 1995). Due to their characteristic features, NKT cells are thought to function at the interface of innate and adaptive immunity and have been implicated in the host defence to infections and in inflammation (Van Dommelen and Degli-Esposti, 2004). With respect to viral infections, NKT and NK cells have demonstrated considerable functional overlap (e.g. production of IFN-y). Moreover, depletion of NKT cells in mouse models of virus infection is generally associated with normal viral clearance (Tyznik et al., 2014), suggesting a limited contribution of NKT cells to host defence against viruses. A notable exception is the disseminated varicella infection repeatedly observed in NKT-deficient patients, thereby supporting a unique role of NKT cells in controlling replication of herpes virus (Banovic et al., 2011; Levy et al., 2003)

1.3.5. Innate immunity to viral infections

Antiviral immune responses are initiated upon recognition of viral components, predominantly viral nucleic acids, by the host. As all living organisms contain nucleic acids, the innate immune system has evolved pattern-recognition PRRs that allow the discrimination of self nucleic acids from non-self (viral) nucleic acids. This discrimination is mainly based on modifications intrinsic to eukaryotic mRNA. For instance, foreign transcripts of bacterial or viral origin can be recognized based on the presence of 5’-triphosphate ends, whereas most self-RNAs bypass detection by expressing 5’-monophosphates or

through masking potential 5'-triphosphate groups through a 5'-cap (Bowie and Fitzgerald, 2007). In addition, only the 5'-cap structures of eukaryotic mRNAs are methylated at the at the N7 position of the capping guanosine residue and the ribose-2'-O position of the 5'-penultimate residue (Zust et al., 2011). Similarly, eukaryotic CpG DNA contains methylated cytosine, and can be discriminated from bacterial DNA that exhibits numerous unmethylated cytosine residues. As a result of these base modifications, nucleic acid material from apoptotic and/or necrotic cells does not induce immune activation either. Also, it has been reported that few host RNAs contain 5'-triphosphate (e.g. 7SL RNA) without actually triggering immune recognition (Hornung et al., 2006). Therefore, it is likely that additional features (e.g. other base modifications) are in place to facilitate self versus non-self sensing. Further discrimination between self and viral transcripts depends on the strandedness (single or double) of the RNA molecule: double-stranded RNA - characteristic for viral replication and typically absent in mammalian systems - is recognized by a number of endosomal and cytoplasmic sensors (Saito and Gale, 2008). Importantly, to avoid recognition of single-stranded (ss) self-RNA present within the cytosol, pathogenic ssRNA is compartmentalized within endosomes, which are not accessible to the former (Barton and Kagan, 2009).

On the downside, the inappropriate engagement of PRRs by self nucleic acids harbours a potential autoimmune threat. Indeed, self nucleic acid containing immune complexes play an important role in initiating TLR-mediated autoimmune attack in systemic lupus erythematosus (SLE) and rheumatoid arthritis (RA) (Goh and Midwood, 2012; Lande et al., 2011). Also, consistent with the idea that modifications of host RNA prevents aberrant responses,

loss-of-function mutations in the RNA-editing enzyme ADAR1 (adenosine deaminase 1), which is responsible for the common deamination of adenosine to inosine, have been associated with several autoimmune conditions, including Aicardi Goutières syndrome (AGS) (Rice et al., 2012). Overall, while PRRs are crucial to recognize transcripts of pathogenic origin, the nucleic acid detection system is error-prone and can mediate immune activation against self nucleic acids.

Activation of virus-specific PRRs leads to the production of type I interferons (IFNs), type III IFNs, proinflammatory cytokines and chemokines, and increased expression of co-stimulatory molecules such as CD40, CD80 and CD86 (Odendall et al., 2014; Sevilla et al., 2004; Stetson and Medzhitov, 2006b). The production of type I IFNs, the main cytokines involved in the host's defence to viruses, is primarily induced by endosomal TLR and cytoplasmic RLR signalling. Endosomal TLRs, including TLR3, TLR7, TLR8 and TLR9, are important for the recognition of RNA viruses that enter the cell via budding or receptor-mediated endocytosis and engage down-stream signalling cascades via the adaptor molecules TIR-domain-containing adapter-inducing interferon-β (TRIF) or myeloid differentiation primary response gene 88 (MyD88) (Kawai and Akira, 2006). TLRs at the cell surface (e.g. TLR2, TLR4) have also been described to be involved in sensing viral components, but appear to play a minor role in inducing type I IFN production (Kawai and Akira, 2006).

Intracellular viral RNA is mainly recognized by either RIG-I, which recognizes 5'-ppp-ssRNA and short dsRNA (Pichlmair et al., 2006; Takahasi et al., 2008) or MDA5, which recognizes long dsRNA (Kato et al., 2006). Activation of these

receptors triggers their association with the adaptor protein MAVS (Seth et al., 2005). On the other hand, viral DNA is commonly recognized via endosomal TLR9 and multiple cytoplasmic sensors (e.g. DAI, RNA polymerase III, IFI16), most of which converge on the adaptor protein STING (stimulator of interferon genes), a transmembrane protein within the endoplasmic reticulum membrane (Ishikawa et al., 2009). Activation of either endosomal or cytoplasmic system results in the phosphorylation of IRF3 and IRF7 by various kinases (e.g. TBK1 and IKK) and subsequently in the production of type I IFN.

Table 1.1. Major pattern recognition receptors implicated in sensing nucleic acids

PRR		Localization	Sensed pathogens	Natural agonists	Synthetic agonists	Adaptor
TLRs	TLR3	Endosome	dsRNA viruses ssRNA viruses dsDNA viruses	dsRNA	Poly(I:C), polyU	TRIF
	TLR7/8	Endosome	ssRNA viruses	GU-rich ssRNA	Imidazoquino-lines (R848), guanosine analogues	MyD88
	TLR9	Endosome	dsDNA viruses	DNA	CpG ODNs	MyD88
RLRs	RIG-I	Cytoplasm	ssRNA viruses DNA viruses	Short RNA with 5'-ppp	LMW Poly(I:C)	MAVS
	MDA5	Cytoplasm	ssRNA viruses DNA viruses	Long dsRNA	HMW Poly(I:C)	MAVS
ALRs	IFI16	Cytoplasm Nucleus	DNA viruses	dsDNA	-	STING ASC
	AIM2	Cytoplasm	DNA viruses	DNA	Poly(dA:dT)	STING
DDXs DHXs	DDX3	Cytoplasm	RNA viruses	RNA	-	MAVS
	DDX1 DDX21 DHX36	Cytoplasm	RNA viruses	dsRNA	HMW Poly(I:C)	TRIF
	DDX60	Cytoplasm	DNA viruses RNA viruses	ssRNA dsRNA dsDNA	-	MAVS
	DHX9	Cytoplasm	DNA viruses RNA viruses	dsRNA dsDNA	CpG-B ODNs	MAVS MyD88
	DHX36	Cytoplasm	DNA viruses	dsDNA	CpG-A ODNs	MyD88 TRIF
	DHX41	Cytoplasm	DNA viruses	DNA	-	STING
Other	ZBP1 (DAI)	Cytoplasm	DNA viruses	dsDNA	Poly(dA:dT)	STING
	Pol III	Cytoplasm	DNA viruses	AT-rich dsDNA	-	RIG-I
	cGas	Cytoplasm	DNA viruses	dsDNA	-	STING

5'ppp, 5' triphosphate end; AIM2, absent in melanoma 2; dsRNA, double-stranded RNA; IFI16, IFNγ-inducible protein 16; MDA5, melanoma differentiation-associated protein 5; ODN, oligodeoxynucleotide; LMW/HMW poly(I:C), low-molecular weight/high-molecular weight polyinosinic–polycytidylic acid; RIG−I, retinoic acid-inducible gene I; ssRNA, single-stranded RNA; STING, stimulator of IFN genes; TLR, Toll-like receptor; ZBP1, Z-DNA-binding protein 1; dsDNA, double-stranded DNA; MyD88, myeloid differentiation primary response gene 88; Poly(dA:dT), poly(deoxyadenylic-deoxythymidylic) acid; ASC, Apoptosis-associated speck-like protein containing a CARD; cGas, Cyclic GMP-AMP synthase; Pol III, RNA polymerase III. (Table adapted from (Desmet and Ishii, 2012)

1.3.6. Key components of the adaptive immune system

The innate PRR-mediated detection of common pathogen patterns propagates the secretion of various interferons, cytokines and chemokines as well as the up-regulation of co-stimulatory molecules (e.g. CD40, CD80, CD86) and major histocompatibility class II (MHC II) on antigen-presenting cells (APCs). The migration of activated APCs, such as DCs, to secondary lymphoid organs allows the induction of a powerful and highly specific adaptive immune response. While the number of PRR epitopes is limited, random re-arrangement of B and T cell antigen receptors generates a seemingly limitless lymphocyte receptor repertoire (Jackson et al., 2013). The survival of each lymphocyte clone depends on natural selection, as only lymphocytes that are activated via antigen binding to their receptor will proliferate and differentiate (clonal selection theory, (Burnet and Holmes, 1965). At the same time, lymphocytes that are potentially self-reactive are deleted during early developmental stages (clonal deletion), an important mechanism for immunological tolerance. Arguably the most crucial feature of adaptive immunity is the generation of memory cells that persist after complete elimination of the pathogen (i.e. immunological memory). These memory cells provide fast and efficacious protection in case of a secondary infection with the same pathogen (Kalia et al., 2006). There are two main effector mechanisms carried out by the adaptive immune system: humoral immunity (antibody-mediated) and cell-mediated immunity.

1.3.7. Humoral immunity

Humoral immunity is achieved by antibody-secreting B cells that protect the host from invading pathogens within extracellular spaces such as blood or lymphatic fluid. Upon antigen encounter, circulating naïve B cells become activated and differentiate into both antibody-secreting plasma cells and long-lived memory B cells. The secreted antibodies are capable of binding antigens on the surface of a targeted microbe, thereby preventing its adhesion and/or entry to the host cell (i.e. neutralization). Antibodies are also able to coat the pathogen's surface, which marks the pathogen for recognition and elimination by phagocytes (i.e. opsonisation) (Radaev and Sun, 2002). Furthermore, antibodies bound to the surface of pathogens can activate the complement system, leading to enhanced opsonisation through recruitment of other phagocytes or direct elimination of the pathogen through complement-dependent cytotoxicity (Ricklin et al., 2010). Notably, antibodies display a half-life of several days, while long-lived memory B cells persist after elimination of the pathogen and quickly proliferate in case of a reinfection (Radbruch et al., 2006).

The initial response to pathogen infections depends to a wide extent on the presence of natural ('spontaneous') antibodies with broad antigen specificities. These antibodies are encoded by germ-line variable gene segments that do not undergo somatic hypermutation, and therefore constitute a relatively limited repertoire of low affinity antibodies (Kocks and Rajewsky, 1988). While the majority of natural antibodies belong to the IgM isotype that provides immediate protection from systemic infections (i.e. neutralization), secretory IgA is the key antibody in initial restriction of local infections at mucosal

surfaces. Importantly, natural antibodies induce adaptive IgM and IgG antibody responses through activation of the complement system, but also by enhanced targeting of antigen to lymphoid organs (Boes, 2000; Ochsenbein and Zinkernagel, 2000).

1.3.7.1. T-Independent B cell responses

Antibody responses to non-protein antigens such as polysaccharides or lipids are independent of MHC II-restricted B-T cell interaction. The production of antibodies to T-independent (T-I) antigen takes place after simultaneous engagement with TLRs (T-I type 1 antigens) or upon extensive antigen-mediated crosslinking of the B cell receptor (T-I type 2 antigens) (Mond et al., 1995; Pasare and Medzhitov, 2005). B cell responses to T-I antigens mainly involve marginal zone (MZ) B cells and B1b cells. Notably, these responses occur outside of the B cell follicle (extrafollicular) and generate short-lived plasma cells. Antibodies directed at T-I antigens are of IgG and IgM isotypes and generally display low antigen affinity. It has been suggested, that T-I B cells give rise to memory type B cells but this concept is yet to be elucidated (Tangye and Good, 2007).

1.3.7.2. T-Dependent B cell responses

Antibody responses to most protein antigens require direct interaction of both T cells and B cells. As T cell help is essential for B cell maturation, terminal differentiation and isotype switching, these responses are termed T-dependent (T-D) B cell responses. Antibodies generated during T-D B cell responses

display a high affinity to the antigen of interest, translating into a highly effective neutralization of invading pathogens (Crotty, 2015).

Initially, naïve B cells within secondary lymphoid organs bind to soluble antigen or collect antigen from the surface of other APCs (e.g. DCs, macrophages). Subsequently, antigens will be internalized, processed and presented in form of a peptide fragment on the surface of B cells. Subsequent upregulation of the chemokine receptor CCR7 allows the migration of the B cells to the interface of the B cell follicle with the T cell zone (T-B border). Naïve CD4+ T cells are primed within the T cell zone by interdigitating dendritic cells that present peptide antigen in the context of MHC II. This results in downregulation of CCR7 and facilitates the migration of T cells to the T-B border. Here, B cells present antigen fragments to cognate CD4+ T cells on MHC II. Upon activation through cognate T cells, B cells migrate to the outer B cell follicles and undergo proliferation. At this stage, some proliferating B cells differentiate into short-lived plasma cells that generally display a low affinity for antigen. Alternatively, B cells can migrate to the centre of the B cell zone to form a primary follicle, known as germinal centre (GC). The structural division of GCs into dark zones and light zones has functional implications. The dark zone features rapid proliferation of antigen-specific B cells (i.e. clonal expansion) as well as somatic hypermutation (SHM), which introduces point mutations within variable regions of the BCR to increase diversity (Tarlinton and Smith, 2000). The light zone of the GC is critical for affinity maturation of GC B cells through interactions with follicular dendritic cells (FDCs) and antigen-experienced T follicular helper cells (T_{FH} cells). Based on their sensitivity to the chemokines CXCR4 (dark zone) and CXCL13 (light zone), GC B cells can move between

both compartments. However, only suitable B cell clones receive survival signals from co-stimulatory signals on the surface of T_{FH} cells (e.g. ICOS, CD40, IL-21, IL-4) and from FDC-presented antigen (Allen et al., 2007a; Allen et al., 2007b; Garside et al., 1998). Affinity-matured GC B cells exit the GC as either memory B cells or long-lived plasma cells and initiate immunoglobulin isotype switching. Alternatively, GC B cells can re-engage in another cycle of somatic hypermutation within the GC.

Recent advances in intravital imaging have changed our view of GCs as highly conserved anatomical entities with restricted intercompartmental migration, and introduced the concept of GCs being dynamic structures with 'open access' - not only for antigen-specific GC B cells, but also for follicular (naïve) B cells that were not actively recruited to this site (Schwickert et al., 2007; Victora and Nussenzweig, 2012). By increasing the competition for antigen within the GC, these previously unappreciated dynamics seem to maximise the chances of rare high-affinity clones to participate in GC reactions.

1.3.8. Cell-mediated immunity

In contrast to antibody-mediated humoral immunity, cell-mediated immunity depends on the recognition of intracellular pathogens by T lymphocytes. While B cell receptors (BCRs) directly bind to antigen, T cell receptors can only recognize short peptide fragments bound to MHC complexes on antigen-presenting cells (APCs).

1.3.8.1. T cell activation

As previously described, mature T cells exiting the thymus co-express either CD8 or CD4 co-receptors on the cell surface. This is crucial, as CD8+ T cells can only detect peptide antigen in the context of MHC I, while CD4+ T cells only recognize peptides displayed on MHC II antigen complexes (Germain, 2002). MHC II is predominantly expressed by professional APCs such as dendritic cells (DCs), macrophages (MPs) and B cells, while MHC I is expressed on all nucleated cells (Rock et al., 2016). APCs are most likely to deliver cognate antigen to T cells in the T cell zone of secondary lymphoid organs. The fate of a T cell following cognate antigen encounter depends on the presence or absence of co-stimulatory molecules. One of the most prominent examples of T cell co-stimulation is the interaction between CD28 on the T cell surface and members of the B7 (CD80 (B7.1) or CD86 (B7.2)) family on the surface of mature APCs (Lanier et al., 1995). By contrast, other receptor-ligand interactions such as PDL-1 (APCs) and PD-1 (T cells) can strongly inhibit T cell activation (Keir et al., 2007). Furthermore, APCs can also modulate T cell responses through the production of various cytokines (e.g. IL-6, IL-1β, TNFα, TGF-β). These cytokines can be produced in response to binding of a PRR on the APC's surface to its respective PAMP that thereby functions as an adjuvant and enhances immunogenicity of protein antigens.

Importantly, T cell activation requires the simultaneous engagement of TCR and MHC-peptide as well as co-stimulation (Grakoui et al., 1999). Therefore, T cells that have encountered cognate antigen but lack co-stimulatory signals will remain hyporesponsive (i.e. T cell anergy). Upon activation, downstream signalling within T cells promotes the expression and secretion of various T

cell effector molecules, including IL-2, IL-21, TNF-α and IFN-γ (Sallusto et al., 2004).

1.3.8.2. $CD8^+$ T cells

CD8+ T cells, or cytotoxic T lymphocytes (CTLs) are crucial for limiting the spread of intracellular pathogens such as viruses and intracellular bacteria (Wong and Pamer, 2003). Like self-antigens, pathogen-derived components are processed through proteosomal degradation and presented in the context of MHC I. CTLs induce programmed cell death (apoptosis) of antigen-specific target cells by calcium-dependent release of cytotoxic effector proteins (e.g. perforin and granzyme B) or by Fas-Fas ligand interactions. While the former mechanism introduces pores in the cell membrane of target cells, the latter activates the caspase-dependent apoptosis pathway. Furthermore, CTLs can shape the host defence by releasing cytokines such as IFN-γ, TNF-α, and TNF-β, which facilitate the recruitment and activation of additional effector cells.

1.3.8.3. $CD4^+$ T helper cells

As outlined above, $CD4^+$ T cells recognize peptide antigen in the context of MHC II on the surface of professional APCs. Similar to CTLs, $CD4^+$ T cells require co-stimulatory signals provided by APCs for sufficient and effective activation. Following activation, naïve $CD4^+$ T cells differentiate into different T helper (T_H) cell lineages that display lineage-specific effector functions. Initially, $CD4^+$ T cells were simply divided into IFN-γ-producing T_H1 cells that drive cell-mediated immunity, and IL-4-producing T_H2 cells that promote antibody-

mediated immunity (Mosmann et al., 1986). Over the last few years, a growing number of functional T_H subsets (T_H1, T_H2, T_H9, T_H17, T_H22, T_{FH}) has been proposed and associated with novel roles in health and disease. However, it remains controversial whether distinct T helper cell subsets are terminally committed. Recent studies indicate that T_H cells retain plasticity throughout differentiation (Luthje et al., 2012; O'Shea and Paul, 2010).

Although the expression of master controller transcription factors are used to delineate T_H lineage commitment, their unique expression may not completely define T_H cell fate. Epigenetic modifications influence the binding of transcription factors to promoter regions of genes, contributing to the heritability of T_H lineage decisions and evidence is emerging that these decisions remain open to revision. Through the analysis of the chromatin state in resting and effector T cells (including T_H1, T_H2, T_H17 cells cultured *in vitro* and Treg subsets) a recent study has revealed the retention of both permissive and repressive transcription factor binding (bivalent) marks in T_H cell specific genes, including those of transcription factors (Wei et al., 2009). Transcription factor genes in a bivalent state have the potential for subsequent activation or silencing, suggesting that T_H cells retain the potential for functional revision (King, 2009; Wei et al., 2009).

1.3.8.4. T follicular helper cells

T follicular helper (T_{FH}) cells are specialized $CD4^+$ T cells residing within B cell areas of secondary lymphoid structures (Vinuesa et al., 2016). In order to obtain this unique B cell proximity, T_{FH} cells down-regulate the T cell zone homing chemokine receptor CCR7, whilst inducing the B cell zone homing

chemokine receptor CXCR5, which binds to CXCL13 produced by FDCs. As previously described, T_{FH} cells are essential for the production of long-lived, high-affinity antibodies. T_{FH} cell differentiation initially depends on the strength of the TCR signal (Fazilleau et al., 2009; Tubo et al., 2013) and on interleukin 6 (IL-6) as the earliest TCR-independent signal. IL-6-mediated signalling induces the expression of master regulator Bcl-6, which orchestrates T_{FH} differentiation and represses alternative phenotypes. Fully differentiated T_{FH} cells can be identified as $CXCR5^{hi}PD1^{hi}Bcl6^{hi}$ CD4 T cells that secrete C-X-C motif chemokine 13 (CXCL13), interleukin 21 (IL-21) and interleukin 4 (IL-4) (Haynes et al., 2007; Reinhardt et al., 2009).

Importantly, both IL-21 and IL-6 play a role in the generation of a GC reaction of optimal magnitude, but appear to have redundant functions for Tfh cell differentiation. Whilst the absence of either IL-6 or IL-21 alone only has a modest impact, eliminating signals from both cytokines severely diminished the percentages of Tfh cells following infection (Eto et al., 2011; Karnowski et al., 2012).

T_{FH} differentiation is a tightly regulated process (King et al., 2008), and its dysregulation can result in the formation of ectopic GCs and subsequent autoantibody production. Although the role of T_{FH} cells in autoimmunity remains incompletely understood, increasing evidence points at T_{FH} cells as central players in several autoimmune disorders such as Sjögren's syndrome (Simpson et al., 2010; Szabo et al., 2013), systemic lupus erythematosus (He et al., 2013; Terrier et al., 2012), rheumatoid arthritis (Liu et al., 2012; Ma et al., 2012) and multiple sclerosis (Romme Christensen et al., 2013; Tzartos et

al., 2011). As the present dissertation focuses on the development of autoimmunity in the context of viral infections, it is critical to discuss the role of type I IFNs as essential drivers in shaping T_{FH} development. Type IFNs have been reported to promote T_{FH} differentiation via stimulation of IL-6 production (Cucak et al., 2009), and through induction of Bcl-6, CXCR5 and PD1 on T_{FH} cells in a STAT1-dependent manner (Nakayamada et al., 2014). This feature may have important implications for linking imbalanced innate immune responses against viral infections to dysregulated TFH function and autoimmunity.

1.3.8.5. T follicular regulatory cells

The observation that GC B cells exhibit very high mutation rates during T-dependent GC reactions evokes the imminent danger of producing self-reactive B cell clones (Brink, 2014). Therefore, in order to circumvent the development of autoimmunity, the GC reaction must be well regulated. The discovery of T follicular regulatory (T_{FR}) cells that regulate both Tfh cells and B cells within the GC has shed light on this important process. Like T_{FH} cells, T_{FR} cells reside within the GC and represent up to 25% of GC T cells (Linterman et al., 2011). As the name suggests, T_{FR} cells derive from T regulatory cells and combine characteristics of natural T regulatory cells (Tregs), such as the expression of forkhead box protein 3 (Foxp3), and of T_{FH} cells (expression of CXCR5 and PD-1) (Chung et al., 2011; Wollenberg et al., 2011). T_{FR} cells directly antagonize T_{FH} cell function and thereby limit the potential risk of expanding auto-reactive B cells. For this reason, the T_{FH} to T_{FR} ratio is now

considered critical for fine-tuning the antibody production within the GC (Sage et al., 2013).

While the role of type I IFNs on T_{FR} activity is yet to be revealed, the effects of these cytokines might have the potential to increase the T_{FH}:T_{FR} ratio, thereby possibly tipping the balance towards autoimmunity.

1.4. Autoimmunity

Autoimmunity is defined as the loss of tolerance towards the body's own tissues and cells, and autoimmune disorders the result of an aberrant self-targeted immune attack. Paul Ehrlich, who famously coined the term "*Horror Autotoxicus*", was the first to introduce the concept of autoimmunity in the early 20th century (Ehrlich, 1901). As of 2015, more than 12% of the world's population is affected by an autoimmune disorder and there is commonly a far greater prevalence in females than in males (Ngo et al., 2014).

1.4.1. Mechanisms of self-tolerance

Immunological tolerance or "self-tolerance" refers to the notion that the immune system does not respond to self-antigens, whilst mounting strong responses against foreign (or non-self) antigens (Schwartz, 1989). Mechanistically, this is mediated via thymus-dependent central tolerance and by peripheral tolerance, both functioning to suppress self-reactive lymphocytes.

As discussed earlier, T cells undergo positive and negative selection in the thymus. However, it is now well accepted that not all potentially self-reactive T cell clones are fully eliminated by this process, as the thymus does not harbour the complete spectrum of peripheral self-antigens (Henderson et al., 2015). Therefore, the operation of a second layer of protection, peripheral tolerance, is necessary to ensure ongoing tolerance. As discussed above, efficient T cell activation requires the presence of co-stimulatory signals. If this co-stimulatory signal is of inhibitory nature, T cell differentiation is actively repressed, which induces a state of T cell anergy or mediates the differentiation into T regulatory cells (Tregs). Key interactions causing T cell anergy are mediated by the inhibitory receptors PD-1 and CTLA-4 (Keir et al., 2008). The importance of these receptors became evident when mice lacking PD-1 or CTLA-4 developed different forms of systemic autoimmunity (Nishimura et al., 1999; Tivol et al., 1995). Whether TCR engagement results in T cell activation or induction of tolerance often depends on the immediate cytokine environment. Anti-inflammatory cytokines such as IL-10 or TGF-β can maintain or induce a pool of tolerogenic APCs (e.g. DCs) that mediate self-tolerance through the expression of inhibitory co-molecules such as PD-L1 on their surface. Another key mechanism contributing to peripheral tolerance is apoptosis. Similar to negative selection occurring within the thymus, T cell clones in the periphery that are chronically stimulated by self-antigen are forced into cell apoptosis in a Fas- or Bim-mediated manner (Hildeman et al., 2002; Strasser and Pellegrini, 2004).

B cell tolerance is obtained through negative selection of immature self-reactive B cell clones during B cell development in the bone marrow (central

tolerance) and through further peripheral tolerance mechanisms, mainly within the spleen. The concept of central B cell tolerance comprises several mechanisms including clonal deletion, anergy and receptor editing (Gay et al., 1993; Goodnow et al., 1988; Nemazee and Burki, 1989; Russell et al., 1991). Immature B cell clones that bind to self-antigen with high avidity either undergo apoptosis (i.e. clonal deletion) or reactivate their immunoglobulin gene rearrangement process in order to obtain a B cell receptor (BCR) that does not react to self-antigen. B cells that chronically display low avidity to self-antigen will enter a state of anergy due to a lack of stimulation and consequently have a short life span (Cambier et al., 2007).

Despite the existence of central tolerance mechanisms, an average of 10% of transitional B cells remain auto-reactive when leaving the bone marrow. These peripheral B cells are further selected based on the specificity of their BCR, the strength of the BCR signal, which may lead to clonal deletion or anergy, and on the presence of B cell survival factors such as B-cell activating factor (BAFF) (Vossenkamper et al., 2012). Recent evidence also suggests a significant role of TLR/MyD88 signalling in shaping the B cell repertoire (Rawlings et al., 2012).

1.4.2. Autoimmune diseases

Autoimmune diseases are the clinical symptoms inflicted upon B and/or T cell failure to sustain immune tolerance towards self-antigen (Davidson and Diamond, 2001). Broadly, autoimmune diseases can be organ-specific such as type I diabetes (T1D) and rheumatoid arthritis (RA), and systemic, such as

systemic lupus erythematosus (SLE). Autoimmune attacks are directed against a multitude of antigen types and can target specific cell subsets (e.g. pancreatic beta cells in T1D or oligodendrocytes in multiple sclerosis) or nuclear antigens (RNA/DNA in SLE). The underlying mechanisms leading to disruption of tolerance are yet to be fully understood, however, it is clear that both genetic and environmental factors are highly influential.

1.4.3. Type I diabetes

Autoimmune or type I diabetes (T1D) is a chronic autoimmune disease characterized by the destruction of insulin-producing pancreatic beta cells by infiltrating immune cells (Atkinson and Eisenbarth, 2001). Disease onset typically occurs early during childhood or adolescence but may also develop later in life. While insulin replacement therapy has been the standard treatment for the past 90 years, immunotherapies for T1D are the current focus of basic and clinical research.

The ongoing discovery of auto-reactive T cells and islet cell autoantibodies in patients and mouse models of T1D has resulted in a long and likely incomplete list of targeted antigens (e.g. pre-proinsulin, GAD65, IAPP, IGRP, ICA) (Baekkeskov et al., 1990; Bottazzo et al., 1974; Palmer et al., 1983; Roep et al., 1990). With respect to etiopathogenesis, research over the past four decades has led to the conclusion that T1D is indeed a complex multifactorial disease caused by a combination of genetic pre-disposition, insufficient immune regulation and environmental factors (Eisenbarth, 1986). However, little understanding of the exact mechanisms leading to disease has been

gained and the extent to which each risk factor contributes to disease is currently a subject of discussion.

1.4.4. Genetic contribution to type I diabetes

Undoubtedly, host genetics play an important role in the development of T1D. Amongst the more than 50 susceptibility genes reported to be associated with autoimmune diabetes, most evidence has been presented for alleles within the MHC gene cluster. Several MHC haplotypes including *HLA-DRB1*04–HLA-DQA1*0301–HLA-DQB1*0302* and *HLA-DRB1*03–HLA-DQA1*0501–HLA-DQB1*0201* have been shown to confer a high genetic risk, while other distinctive alleles such as *DRB1*1501-DQA1*0102-DQB1*0602* are protective against disease development (Caillat-Zucman et al., 1997; Fernando et al., 2008). The application of SNP (single-nucleotide polymorphism) technology has promoted the discovery of further non-MHC risk alleles including mutations within the insulin gene region, protein tyrosine phosphatase, non-receptor type 22 (PTPN22), interleukin-2RA (IL-2RA) or cytotoxic T lymphocyte protein 4 (CTLA4) (Bell et al., 1984; Lowe et al., 2007; Smyth et al., 2004; Ueda et al., 2003). It is important to note that many T1D risk loci are shared by multiple autoimmune disorders, which might reflect the existence of common underlying pathways (Li et al., 2015; Prahalad et al., 2009; Ramos et al., 2011).

1.4.5. Environmental contribution to type I diabetes

Despite the lack of definitive evidence, a number of observations underscore the role of environmental factors in triggering autoimmune diabetes in genetically susceptible individuals. Critically, T1D incidence rates have shown an annual increase of approximately 3% worldwide, and vary significantly amongst different countries and age groups to the extent that they cannot be accounted for by genetic factors alone (Gardner et al., 1997; Moses et al., 1995; Patterson, 2000; Tuomilehto et al., 1995). Although T1D risk is 15-fold increased if having an affected sibling, concordance rates of only 30-60% amongst monozygotic and 6-10% amongst dizygotic twins, strongly point towards an environmental component (Kyvik et al., 1995; Redondo et al., 2008). Moreover, more than 85% of newly diagnosed T1D patients show no family history of the disease (Hamalainen and Knip, 2002), and only about 5% of people with one diabetic parent will develop the disease later in life (Redondo et al., 2001).

So far, not a single environmental factor has been proven responsible for T1D development. This could possibly be explained by a large temporal gap between disease initiation and clinical onset, at which time the causative agent might be completely cleared (‘hit-and-run event”) or undetectable by standard assays. In addition, there is the potential of several environmental factors acting synergistically towards disease progress. A further complicating factor is that disease susceptibility to the same agent(s) may differ depending on the genetic constitution of the host. To date, virus infections rank on top of the suspect list of environmental triggers (van Belle et al., 2011), nevertheless,

bacterial infections (Sechi et al., 2008), cows milk (Kostraba et al., 1993), wheat protein (MacFarlane et al., 2003) and vitamin D levels have also been proposed to influence the development of T1D (Bailey et al., 2007).

1.4.6. The role of enterovirus infections in type I diabetes

The potential role of viral infections in T1D was first described in 1926 when seasonal patterns in disease onset were observed (Adams, 1926). Notably, the concept of T1D seasonality has been intensively investigated and validated for several geographic regions within the northern and southern hemispheres (Kalliora et al., 2011; Moltchanova et al., 2009; Weets et al., 2004). Importantly, sero-epidemiological and experimental animal studies have identified enteroviruses, and in particular coxsackievirus B (CVB), as key candidates for environmental triggers of T1D (Rodriguez-Calvo et al., 2016). That said, the frequent detection of anti-enteroviral antibodies and enteroviral RNA in blood and pancreas samples from T1D patients does not prove a causal relationship between enterovirus infection and autoimmunity (Alidjinou et al., 2015; Banatvala et al., 1985; Clements et al., 1995; Frisk et al., 1992; Gamble et al., 1969; Tuvemo et al., 1989). Furthermore, one should be cautious when interpreting the commonly described detection of viral capsid protein VP1 in the pancreas of affected individuals, as concerns regarding the specificity of antibodies utilized for immunohistochemistry experiments have been raised (Richardson et al., 2009). More convincingly, Notkins and colleagues reported that direct infection of pancreatic beta cells with coxsackievirus B4 (CVB4) resulted in subsequent induction of insulitis and diabetes in genetically susceptible mouse strains, further reinforcing the notion

of a pivotal interplay of genetic and environmental factors (Yoon et al., 1978). Further (circumstantial) evidence is provided by the large number of recent-onset T1D patients reporting a viral infection prior to their diagnosis (Dotta et al., 2007; Krogvold et al., 2015), and by the isolation of a CVB4 strain from the pancreas of a diabetic 10-year old patient during post-mortem examination (Yoon et al., 1979). Very recently, an unprecedented study by Krogvold *et al*. reported the presence of enterovirus in pancreata from living individuals with recent T1D onset (Krogvold et al., 2015). Samples were collected by performing minimal tail resection, an improved procedure that was developed as part of the Diabetes Virus Detection (DiViD) study (Krogvold et al., 2014). Altogether, the involvement of enterovirus infections in the development of T1D under the premise of a susceptible genetic background seems very plausible. Although it is highly unlikely that a single enterovirus strain (e.g. CVB4) is able to precipitate T1D, identification of responsible serotypes could potentially facilitate the development of future vaccines.

1.4.7. The pancreatic beta cell might seal its own fate

In addition to environmental factors, the target tissue itself might provide another important piece of the puzzle. As discussed above, certain pancreatrophic viruses are able to directly infect beta cells, leading to the production of type I IFNs and elevated levels of MHC I. If this “viral signature” was induced by the beta cells themselves, it might subsequently facilitate their destruction by self-reactive CD8 T cells, while neighbouring alpha cells remain fully intact. Indeed, pancreatic islets of recently diagnosed patients have been found to express elevated levels of both MHC I and type I IFNs (Foulis et al.,

1987). Moreover, a prospective study by Ferreira et al. was able to link the development of islet autoimmunity to a transient induction of type I IFNs (Ferreira et al., 2014).

The idea that the pancreatic beta cell can act autonomously - without the assistance of specialized immune cells - serves as rationale for the beta cells' capacity to produce type I IFNs and other pro-inflammatory cytokines (Cardozo et al., 2001; Flodstrom et al., 2002; Flodstrom-Tullberg et al., 2003; Ortis et al., 2010), which has long been a matter of dispute. However, this active participation seems to come with the trade-off of a potential autoimmune assault.

1.4.8. Lessons from genome-wide association studies (GWAS)

The immune response to environmental stimuli such as viruses is largely manipulated by underlying host genetics and hence might vary across different individuals. The GWAS-mediated discovery of novel T1D risk loci that are associated to immune genes, and in particular to genes involved in anti-viral host responses (Cooper et al., 2008; Hakonarson et al., 2007; Smyth et al., 2006b; Todd et al., 2007), further supports the notion that virus infections impose an environmental threat for genetically susceptible hosts. Newly identified T1D risk genes include *IL10*, *IL19*, *IL20*, *IL27*, *CD69* and *IFIH1*, with the latter possibly being the most intriguing candidate (Barrett et al., 2009; Smyth et al., 2006a). As discussed earlier, IFIH1, also known as MDA5, is one of the two main cytoplasmic sensors for the recognition of viral RNA (Kato et al., 2006; Takeuchi and Akira, 2008), and its activation is crucial for the initiation of anti-viral immune responses. Moreover, MDA5 is the predominant

receptor for the detection of picornaviruses such as CVB4 (Feng et al., 2012; Feng et al., 2013). Strikingly, MDA5 has been found to confer opposing T1D disease risk based on the presence of protective (i.e. loss-of-function) or enhancing (i.e. gain-of-function) alleles (Downes et al., 2010; Liu et al., 2009; Nejentsev et al., 2009). Other studies have identified a signalling network driven by interferon regulatory factor 7 (IRF7) that is highly enriched for virus response genes (e.g. *IFIH1*, *CD68*, *Ifi27* and others) and shows a very strong association with risk for T1D and other autoimmune disorders (Heinig et al., 2010). IRF7 is the master regulator of type I IFN-dependent immunity (Honda et al., 2005) and single-nucleotide polymorphisms (SNPs) in genes or genetic regions within the IRF7-driven network described by Heinig et al. have been shown to increase the production of type I IFNs and type I IFN response genes (Figure 1.1).

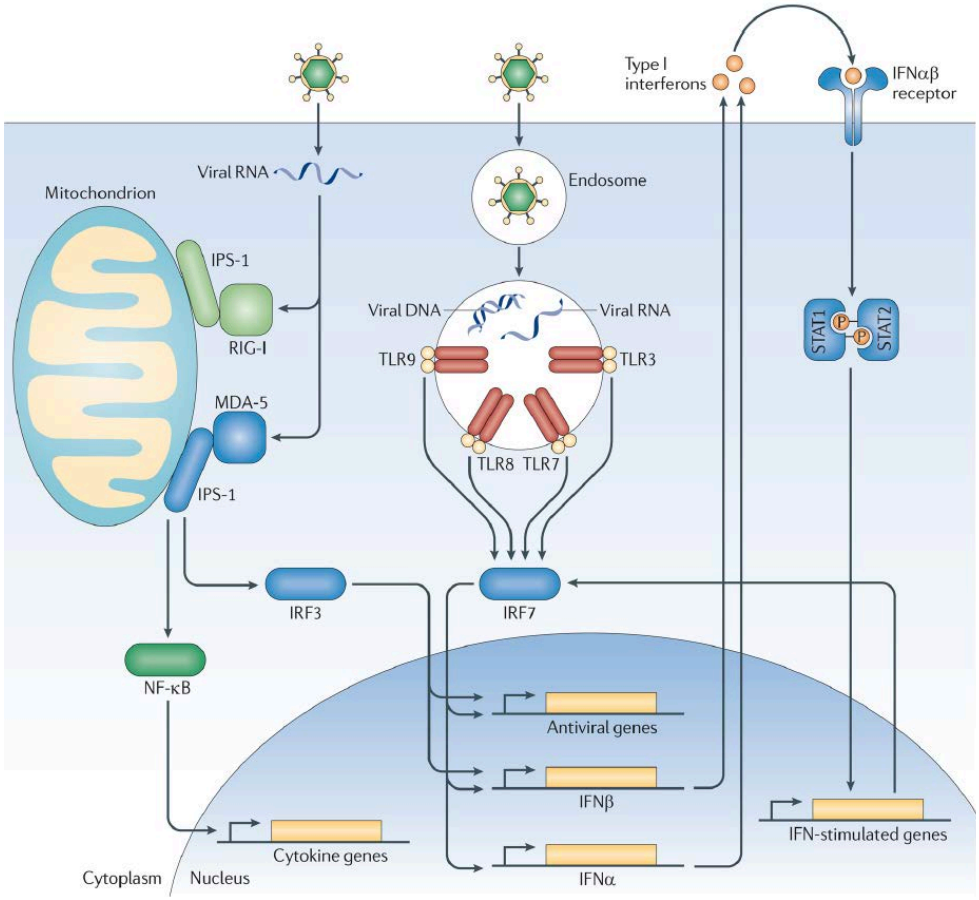

Figure 1.1 Components of the anti-viral immune response genetically linked to Type I Diabetes. Viruses are recognized in general by two separate pathways. Intrinsic recognition occurs through detection of viral nucleic acids by cytosolic RLRs and other nucleic acid sensors in the infected cells. MDA-5/IFI1H is a cytosolic RLR that can recognize Picornavirus genomes. Activated MDA-5 activates the transcription factors IRF-3 and NF-κB. In contrast, extrinsic recognition of virus occurs through Toll-like receptors (TLR) 3, 7, 8 and 9, which can recognize viral DNA and RNA within endosomes and activate transcription factors IRF-7 and NF-κb. IRF-3 and IRF-7 function in homo- or heterodimers to initiate transcription of Type I interferons and other anti-viral genes, as shown. Via NF-κB, both pathways induce the expression of pro-inflammatory cytokines. Secreted Type I interferons bind to the IFNαβR on the cell surface, which signals via STAT1 and STAT2 to induce expression of ~300 interferon-stimulated genes (ISGs) including MDA-5 and IRF-7. Type 1 diabetes is linked to genetic polymorphisms in MDA-5/IFI1H, IRF-7, and an IRF-7 driven network of 305 genes. Figure reproduced from (Foxman and Iwasaki, 2011).

Thus, one possible scenario is that (repeated) viral infections in genetically susceptible individuals might trigger prolonged and exacerbated anti-viral immune responses dominated by the production of type I IFNs, thereby promoting the encounter of self-antigen with self-reactive lymphocytes and may ultimately result in autoimmunity.

1.4.9. Endogenous retroviruses

Most of the research investigating the connection between viral response and autoimmunity clearly focuses on infections with exogenous virus. However, accumulating evidence argues for the likelihood of endogenous retroviruses (ERVs) as contributors, if not mediators, of autoimmune events. Although they comprise about 8% of the human and up to 10% of the mouse genome, it is only due to the completion of full genome sequencing that the vast existence of (functional) ERVs was fully appreciated (Cohen et al., 2009; McCarthy and McDonald, 2004). Endogenous retroviruses are retroviruses that have integrated into the hosts' genome after reverse transcription of viral RNA during the course of evolution, and as such can be seen as fossil records of ancient germ-line infections. As part of the group of transposable elements, they have the ability to change their relative position within the genome (Baillie et al., 2011; Boeke et al., 1985). Based on their phylogenic similarity to exogenous viruses, ERVs are loosely categorized into 3 classes. They possess a simple genomic structure, characterized by the functional genes *gag*, *pol* and *env* and two long-terminal repeats (LTRs) (Stoye, 2012). Most ERVs have acquired countless inactivating mutations that prevent the formation of infectious particles within the host cell (Johnson and Coffin, 1999). However, ERVs can still impact their host in a beneficial or detrimental manner. While ERV transcripts may serve as promoter or enhancer elements for proximal and distal genes, thereby shaping cellular responses; their retrotransposition into the host's genome may result in damaging mutations and chromosome instability (Boeke and Stoye, 1997; Hughes and Coffin, 2004; Mi et al., 2000). The facilitating role of ERVs in developing the

mammalian placenta is only one example of how ERVs have earned their existence during the course of evolution (Harris, 1998; Rote et al., 2004).

By contrast, accumulating evidence indicates that reverse-transcribed ERV cDNA is able to precipitate chronic innate immune responses and thereby imposes an autoimmune threat (Jacob et al., 2002; Stetson et al., 2008; Yu, 2016). The mechanisms that prevent the inappropriate detection of endogenous retroviral DNA are yet to be fully understood. As observed for foreign RNA, DNA sensors are likely to bind to characteristic features that are exclusively found in pathogens, although it has been argued that DNA sensors may be completely insensitive to its targets' structure (Civril et al., 2013). Also, self-DNA is generally sequestered within the nucleus and thereby protected from cytosolic recognition. However, reverse transcription of retroviral RNA into cDNA circumvents the subcellular limitation as it takes place within the cytoplasm. The accumulation of endogenous DNA elements within the cytoplasm is therefore further restricted by host-intrinsic exo- and endonucleases.

Detection of cytosolic DNA results in activation of the interferon stimulatory DNA (ISD) pathway, leading to IRF3-dependent production of type I IFNs (Ishii et al., 2006; Stetson and Medzhitov, 2006a), and inflammasome-dependent production of pro-inflammatory cytokines (Wu and Chen, 2014) (figure 1.2). Chronic stimulation of the ISD pathway by uncontrolled accumulation of endogenous DNA can supposedly mimic the RIG-I/MDA5-dependent type I IFN-mediated autoimmunity, as observed in studies on 3' repair exonuclease 1 (Trex1)-deficient mice. Trex1 is the most abundant exonuclease within the

cytosol of mammalian cells and as such the major negative regulators of ISD signalling (Stetson et al., 2008).

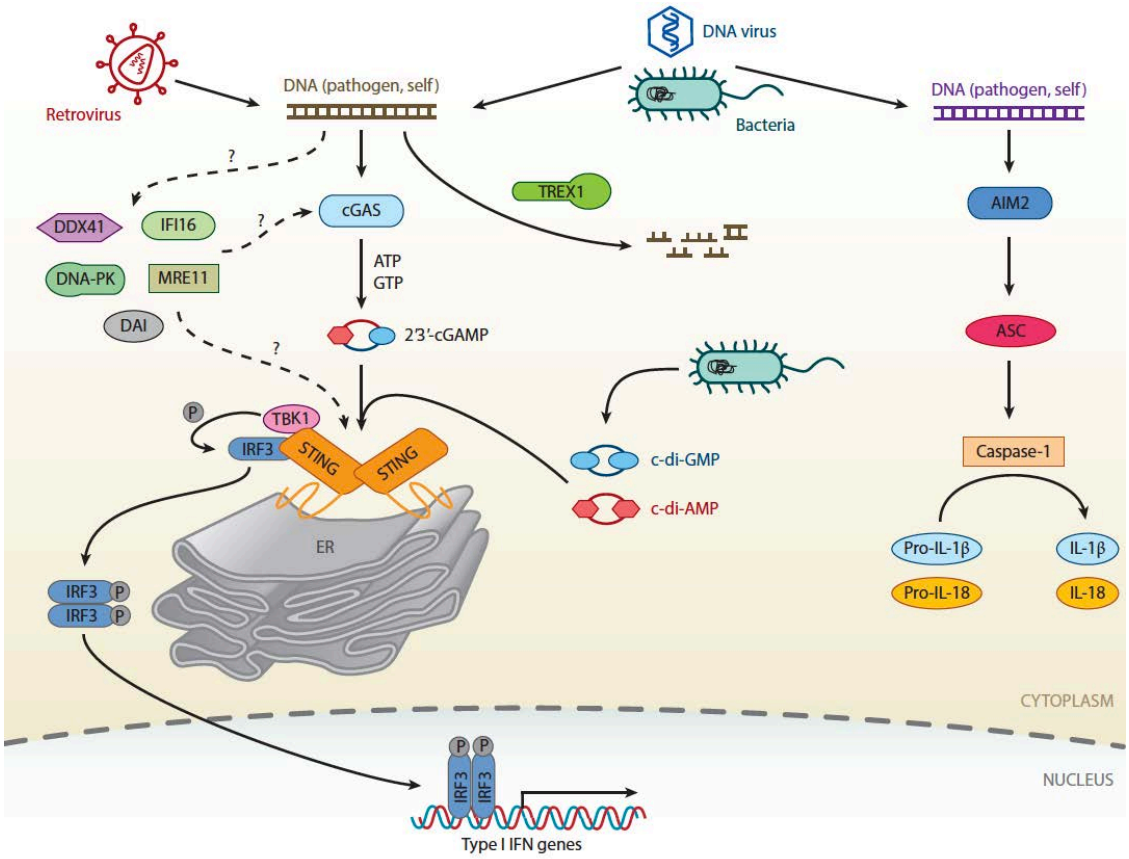

Figure 1.2 Cytosolic DNA–sensing system
Cytoplasmic DNA of self or microbial origin could activate cGAS and potentially other putative DNA sensors, which are all proposed to transduce signals to the ER-localized adaptor protein STING. STING recruits and activates the kinase TBK1, which then activates the transcription factor IRF3 to induce type I IFNs. Endogenous DNase, such as Trex1, could degrade self-DNA to prevent the aberrant activation of the DNA-sensing pathway. In addition to inducing type I IFNs, cytosolic DNA could also activate the AIM2 inflammasome, leading to caspase-1 activation and IL-1β maturation. (Abbreviations: AIM2: absent in melanoma 2; c-di-AMP, cyclic diadenylate; c-di-GMP, cyclic diguanylate; cGAMP, cyclic GMP-AMP; cGAS, cyclic GMP-AMP synthase; DAI, DNA-dependent activator of IRFs; DDX41, DEAD box polypeptide 41; DNA-PK, DNA-dependent protein kinase; ER, endoplasmic reticulum; IFI16, interferon gamma-inducible protein 16; IFN, interferon; MRE11, meiotic recombination 11; STING, stimulator of interferon genes; Trex1, three prime repair exonuclease 1.). Figure reproduced from (Wu and Chen, 2014)

Trex1-deficient mice accumulate endogenous DNA transcripts including reverse-transcribed retroviral elements within their cytosol and suffer from

premature death caused by cell-intrinsic autoimmunity (Morita et al., 2004; Yang et al., 2007). In humans, homozygous and heterozygous loss-of-function mutations within the Trex1 gene have been associated with auto-inflammation found in patients with Aicardi-Goutières syndrome (AGS) and systemic lupus erythematosus (SLE) (Crow et al., 2006; Lee-Kirsch et al., 2007a; Lee-Kirsch et al., 2007b; Namjou et al., 2011). In addition, AGS and SLE patients show elevated levels of type I IFNs in the absence of an exogenous viral trigger (Lebon et al., 1988), often granting them the term “congenital virus infection” (Rice et al., 2009).

In conclusion, the processing, compartmentalization and metabolism of nucleic acids is critical for both an effective anti-viral immune response and for immune tolerance to self nucleic acids. However, host mechanisms designated to differentiate between self and non-self nucleic acids are fallible and the defective control of endogenous retroviral DNA, as seen in the case of Trex1-deficiency, outlines another possible setting of virus-precipitated autoimmunity.

1.5. The role of MAVS in immunity and autoimmunity

Research interest in the mitochondrial adaptor protein MAVS has grown significantly during recent years. MAVS was simultaneously discovered by four different groups in 2005, each introducing a different name: mitochondrial antiviral signalling protein (MAVS (Seth et al., 2005)), IFN-β promoter stimulator protein 1 (IPS-1 (Kawai et al., 2005)), virus-induced signalling adaptor (VISA, (Xu et al., 2005)) and CARD adaptor inducing IFN-β (Cardif (Meylan et al., 2005). In line with its essential role in antiviral immunity, MAVS is ubiquitously expressed in various tissues and cell types (Seth et al., 2005), and its crucial binding domains show a high degree of conservation amongst species (Shi et al., 2015; Xu et al., 2014). Remarkably, MAVS can perform its anti-viral functions in different subcellular localizations. The largest fraction of MAVS protein is localized at the outer mitochondrial membrane, while smaller fractions are found at peroxisomes or at the mitochondrion-associated membrane (MAM) (Dixit et al., 2010; Horner et al., 2011; Seth et al., 2005).

1.5.1. MAVS: a central player in antiviral innate immunity

Immune responses to RNA viruses essentially depend on the recognition of viral features by RIG-I-like receptors within the cytosol of infected cells. Although TLRs are also able to detect viral RNAs, their localization at the endosome lumen prevents their encounter with viruses that have successfully entered the cytoplasm. Furthermore, most of the non-immune cells that efficiently fight invading viruses (e.g. fibroblasts and epithelial cells) express

insignificant levels of TLRs and induce type I IFNs independent of TLR signalling (Diebold et al., 2003; Goubau et al., 2013).

RIG-I and MDA5 both recognize distinct RNA ligands (see Table 1.1), while LGP2, the third RIG-I-like receptor appears to hold regulatory functions (Venkataraman et al., 2007; Yoneyama et al., 2005). Binding of an appropriate viral target to either MDA5 or RIG-I results in a conformational change that facilitates the association of their N-terminal caspase activation and recruitment domain (CARD) with the CARD domain present in the MAVS adaptor protein (Jiang et al., 2012). This CARD-CARD interaction induces the polymerization of MAVS CARD domains on the outer mitochondrial membrane into prion-like fibres (Figure 1.3). This aggregation process is self-perpetuating and allows the formation of large MAVS aggregates in response to a small amount of viral RNA (Hou et al., 2011; Xu et al., 2014). Due to their prion-like nature, aggregated MAVS fibres are resistant to detergent and protease and can only be removed through autophagy (Mathew et al., 2014; Tal et al., 2009). The formation of prion-like fibres that mediate a beneficial biological function is very unique and has only been observed for MAVS and ASC, the latter being an adaptor protein involved in inflammasome activation (Cai et al., 2014).

The MAVS-mediated production of type I IFNs and proinflammatory cytokines is propagated through a complex signalling cascade. Aggregated MAVS fibres are potent activators of multiple ubiquitin E3 ligases (e.g. TRAF2, TRAF3, TRAF5, TRAF6, cIAP1/2, MIB1/2) that subsequently recruit the downstream effector kinases IKK (inhibitor of kappa B kinase) and TBK1 (TANK-binding kinase 1) (Liu et al., 2013; Mao et al., 2010; Paz et al., 2011).

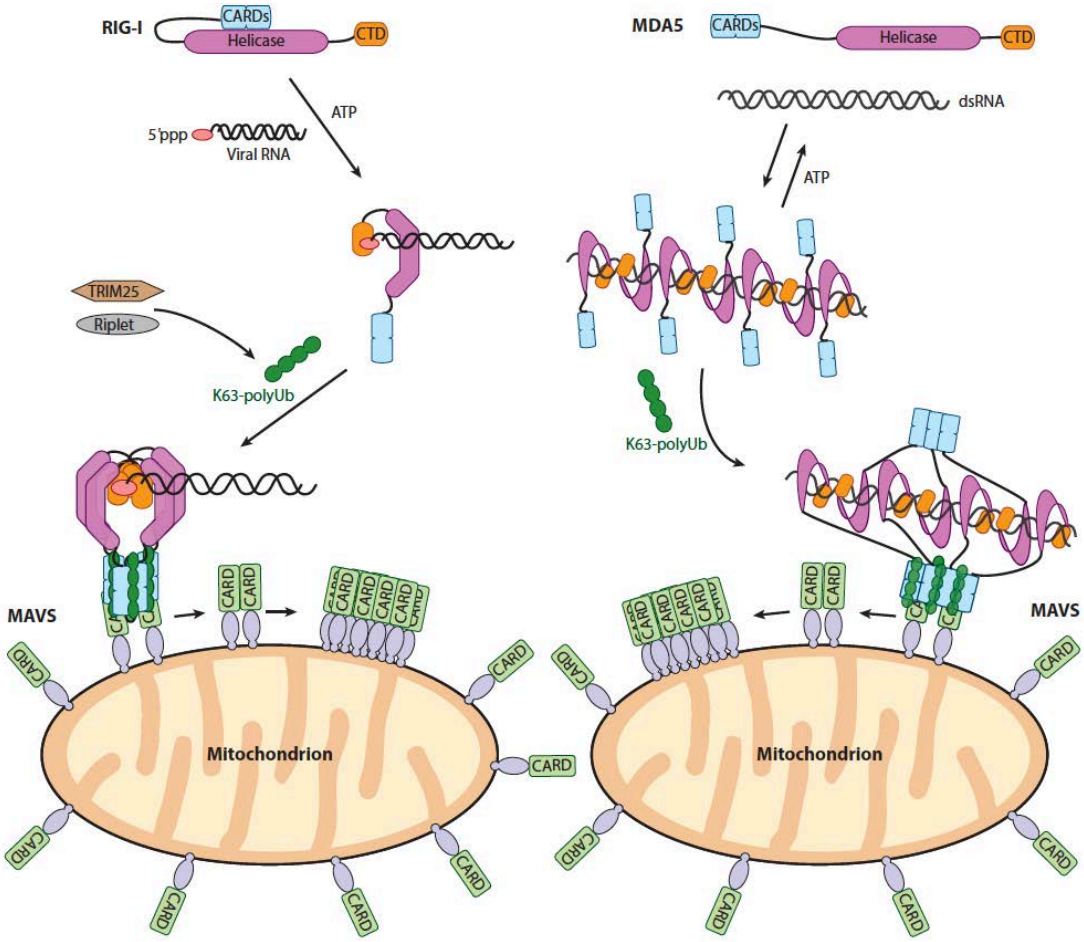

Figure 1.3 Model for cytosolic RNA-induced activation of RLR-MAVS pathway.
Binding to 5'ppp-containing viral RNA induces a structural rearrangement in RIG-I that liberates its CARDs for subsequent association with unanchored K63-linked ubiquitin chains to form oligomers. MDA5 stacks along dsRNA in a head-to-tail fashion to form helical filaments, which facilitate the formation of discrete CARD oligomers along the filaments. Oligomerized CARD domains of RIG-I and MDA5 interact with the CARD domain of MAVS. This interaction promotes the polymerization of MAVS CARD, which in turn serves as a "seed" to trigger the prion-like conversion of other MAVS on the mitochondrial outer membrane. (Abbreviations: CARD, caspase activation and recruitment domain; CTD, C-terminal domain; dsRNA, double-stranded RNA; Hel-1 and Hel-2: helicase domain 1 and 2; Hel-2i: helicase insertion domain; MAVS, mitochondrial antiviral signalling; MDA5, melanoma differentiation associated gene 5; P, pincer domain; pro-rich, proline rich; RLR, RIG-I-like receptor; TM, transmembrane domain.). Figure reproduced from (Wu and Chen, 2014)

Activation of IKK and TBK1 kinases results in the phosphorylation of the transcription factors IRF3 (IFN regulatory factor 3) and IRF7 (IFN regulatory factor 7), respectively, leading to the induction of IFN-α and IFN-β, proinflammatory cytokines and other antiviral interferon-stimulated genes.

Despite extensive advances in the field, the localization of MAVS at the mitochondrial and peroxisomal membranes still represents a great gap in knowledge. Mislocalization of MAVS to the plasma membrane results in an almost complete abrogation of its antiviral potential (Seth et al., 2005). Various viruses (e.g. HCV, EV71, CVB4) take advantage of this spatial requirement and cleave MAVS at its transmembrane region, which releases MAVS from its mitochondrial localization and abolishes the production of type I IFN (Li et al., 2005; Mukherjee et al., 2011; Wang et al., 2013). A number of findings might explain the significance of MAVS localization to the mitochondria. First, it has recently been proposed that redox-sensitive MAVS residues may trigger favourable conformational changes in the presence of reactive oxygen species (ROS), which are produced at high levels by mitochondria and peroxisomes during the course of an infection (Koshiba, 2013; Tal et al., 2009; Zhao et al., 2012). Second, Koshiba and colleagues discovered that the mitochondrial membrane potential ($\Delta\Psi m$) plays a pivotal role in MAVS-mediated antiviral signalling, as type I IFN production was completely abolished in response to chemically-induced $\Delta\Psi m$ dissipation (Koshiba et al., 2011). Third, proteins of the mitochondrial fusion machinery (e.g. mitofusin 1 and 2) can either promote or inhibit efficient MAVS signalling, thus highlighting the involvement of mitochondrial dynamics (Castanier et al., 2010; Onoguchi et al., 2010; Yasukawa et al., 2009). Finally, other studies have suggested that this spatial phenomenon may allow MAVS to be in close proximity to the NLRP3 inflammasome, thereby facilitating its optimal activation (Park et al., 2013; Subramanian et al., 2013). Although future work is required to further address

the functional implications of MAVS positioning, evidence supporting the importance of its mitochondrial localization is certainly compelling.

1.5.2. The impact of MAVS on adaptive immunity and autoimmunity

It has long been acknowledged that innate immune signals are able to shape adaptive immune responses in a qualitative and quantitative manner, and thus have potential implications in the development of autoimmunity. In the case of MAVS, most efforts have been made to disentangle the innate mechanisms of prion-like-fibre-mediated signalling, while few studies have investigated the role of MAVS in adaptive immunity. As one of the key players within antiviral signalling cascades and type I IFN production, MAVS provides a crucial link between innate and adaptive immunity. Type I IFNs participate in T cell activation, differentiation and survival; either directly or indirectly through activation of co-stimulatory molecules on antigen-presenting cells, typically DCs (Honda et al., 2003). Furthermore, type I IFNs display a non-redundant role in anti-viral immunity by mediating the induction of cytotoxic T lymphocytes (CTL) and antigen-specific antibodies (Muller et al., 1994; van den Broek et al., 1995). In line with this, a study by Bhoj et al. confirmed the vital role of MAVS in generating antigen-specific antibodies in response to respiratory syncytial virus (RSV). MAVS-deficient mice in this study showed complete abrogation of type I IFN signalling, a drastic reduction of dendritic cell activation and a significant increase in initial viral load. Surprisingly, these mice displayed normal activation and expansion of antigen-specific CTL and were able to clear the virus in a similar time frame as WT mice (Bhoj et al., 2008),

opening up the possibility that - at least for some viruses - other type I IFN-independent pathways or cell types (e.g. NK cells) can step in.

As described earlier, gain-of functions mutations in the *IFIH1* gene coding for MDA5 confer a chronic type I IFN signature that is linked to an increased susceptibility to various autoimmune conditions (Crampton et al., 2012; Rice et al., 2014). As its only adaptor molecule, MAVS is critical for mediating MDA5-induced antiviral immune responses, and mice deficient for MAVS expression have been shown to rescue the autoimmune phenotype in mice with increased MDA5 signalling (Funabiki et al., 2014). Accordingly, gain-of-function and loss-of-function mutations within MAVS have a strong potential in defining virus-related pathogenesis. To the best of our knowledge, only one MAVS variant with clinical implications has been reported so far. This uncommon loss-of-function variant (C79F, rs11905552) is dominantly found within the African-American population and has been associated with decreased levels of type I IFN and pro-inflammatory cytokines, which translate into defective antiviral immunity in *in vitro* studies (Pothlichet et al., 2011). In other studies, overexpression of MAVS *in vitro* led to significant increases in type I IFN production (Biacchesi et al., 2009; Seth et al., 2005), suggesting that variants linked to gain-of-function could potentially contribute to an autoimmune phenotype. However, further research efforts are needed in order to get a better understanding of the role of MAVS in autoimmunity *in vivo*. Finally, as a central hub for antiviral immune responses, MAVS is likely involved in directing the outcome of endogenous (e.g. ERV) and exogenous (e.g. CVB4) stimuli and thereby represents an important target for immunotherapy.

1.6. Research aims of this study

The overarching aim of this study is to obtain further insights into pathways and mechanisms underlying chronic infection and autoimmunity in response to endogenous and exogenous viral stimuli in the context of type I diabetes (T1D). This aim has been based on the following three hypotheses, which are discussed in chapters 2, 3 and 4 of this dissertation:

1. Infections with an exogenous virus trigger chronic inflammation and autoimmune processes in T1D

2. The expression of endogenous virus in the pancreatic beta cell is associated with the development of chronic inflammation and T1D

3. A single nucleotide polymorphism (SNP) within the transmembrane region of MAVS has functional implications related to chronic inflammation and autoimmunity

2. THE ROLE OF COXSACKIEVIRUS B4 IN CHRONIC INFLAMMATION AND AUTOIMMUNITY

2.1. INTRODUCTION

Mouse models of type I diabetes are a valuable tool for investigating genetic and environmental contributions to disease pathogenesis, and for testing the therapeutic potential of novel drugs. In particular, the non-obese-diabetic (NOD) mouse is the most widely utilized experimental model in experimental T1D research. This spontaneous model of autoimmune diabetes was first developed in 1974 and recapitulates many aspects of human disease (Hanafusa et al., 1994). NOD mice develop insulitis between the ages of 3-4 weeks, which can transition into cell–mediated destruction of pancreatic beta cells, resulting in overt diabetes. Similar to T1D in humans, the incidence rates in NOD mice show a strong gender bias towards females (60-90%) as compared to males (10-30%) (Hanafusa et al., 1994). Furthermore, the genetic susceptibility for autoimmunity in NOD mice is associated with specific MHC variants (designated $H2^{g7}$) and is influenced by additional non-MHC risk loci, as observed in humans (Lyons et al., 2001; Wicker et al., 2005a; Wicker et al., 2005b). These common features have been extremely useful for investigating disease mechanisms and for identifying novel T1D genes and pathways that provide potential therapeutic targets.

NOD mice are equipped with a unique genetic background that precipitates disease in the absence of any known environmental stimuli (Delovitch and

Singh, 1997). However, studies collectively indicate that environmental factors do play a role as the spontaneous incidence of T1D in NOD mice varies considerably between colonies, is influenced by virus infection, immunisation, diet and microbiota (Elliott et al., 1988; King and Sarvetnick, 2011; Muir et al., 1995; Serreze et al., 2005). In humans, T1D is characterized as a complex and multifactorial disease that may require a multitude of environmental triggers. In the NOD mouse, infections with CVB can result in either acceleration (e.g. CVB4) or prevention (e.g. CVB3) of the disease, depending on the viral strain, the inoculated dose, tropism for beta cells and most importantly, the time point of infection (Drescher et al., 2004; Serreze et al., 2000; Serreze et al., 2005; Tracy et al., 2002). Therefore, the use of additional mouse models may be required in order to establish a causal relationship between environmental factors such as virus infections and the risk for T1D. Other inbred mouse strains, such as SJL/J or NIH Swiss, fail to spontaneously develop disease, but are susceptible to virus-induced T1D (Yoon et al., 1978). Furthermore, some mouse strains are resistant to T1D, such as C57BL/6 and NOR/Lt (Prochazka et al., 1992; Yui et al., 1996).

Virus-induced T1D studies in NOD mice have greatly advanced our knowledge of how viral infections can modulate autoimmune responses within a “fertile” genetic background. However, this approach is likely to mask the full spectrum of viral contribution to disease initiation and progression. This section describes comparative studies assessing the role of CVB4 infection in the development of chronic inflammation and T1D in three inbred mouse strains with different disease susceptibility: C57BL/6, SJL and NOD. This approach

enables a thorough analysis of both viral kinetics and antiviral immune responses under different genetic environments. Furthermore, in order to investigate the contribution of the innate immune system to virus-induced tissue damage, the immunodeficient strains NOD.SCID and B6.RAG1, both of which lack a functional adaptive immune system (B and T lymphocytes), were analysed.

2.2. RESULTS

2.2.1. Tissue tropism and replication kinetics of CVB4

Virus-induced T1D is predominantly linked to enteroviruses, and in particular coxsackievirus B4 (CVB4). In order to assess the impact of CVB4 infection on the development of chronic inflammation and autoimmunity, the diabetogenic strain variant CVB4 E2 (see section 6.12) was obtained.

With the aim to study the effects of CVB4 infection on normoglycemia and T1D, an appropriate dose regimen resulting in severe pancreatitis whilst minimizing virus-induced mortality was established. Accordingly, a dosage of 10^5 PFU given intraperitoneally was found to be an appropriate for both NOD and SJL mice, resulting in 95% survival over a period of 28 days (Fig. 2.1F). Despite their reported resistance to develop T1D after viral infection (Yui et al., 1996), B6 mice were found to be considerably more sensitive to CVB4-induced *mortality* and were therefore given a non-lethal dose of 20 PFU. Finally, the immunodeficient strains NOD.SCID and B6.RAG1 (RAG) were injected with the same dose as their respective immunocompetent strain.

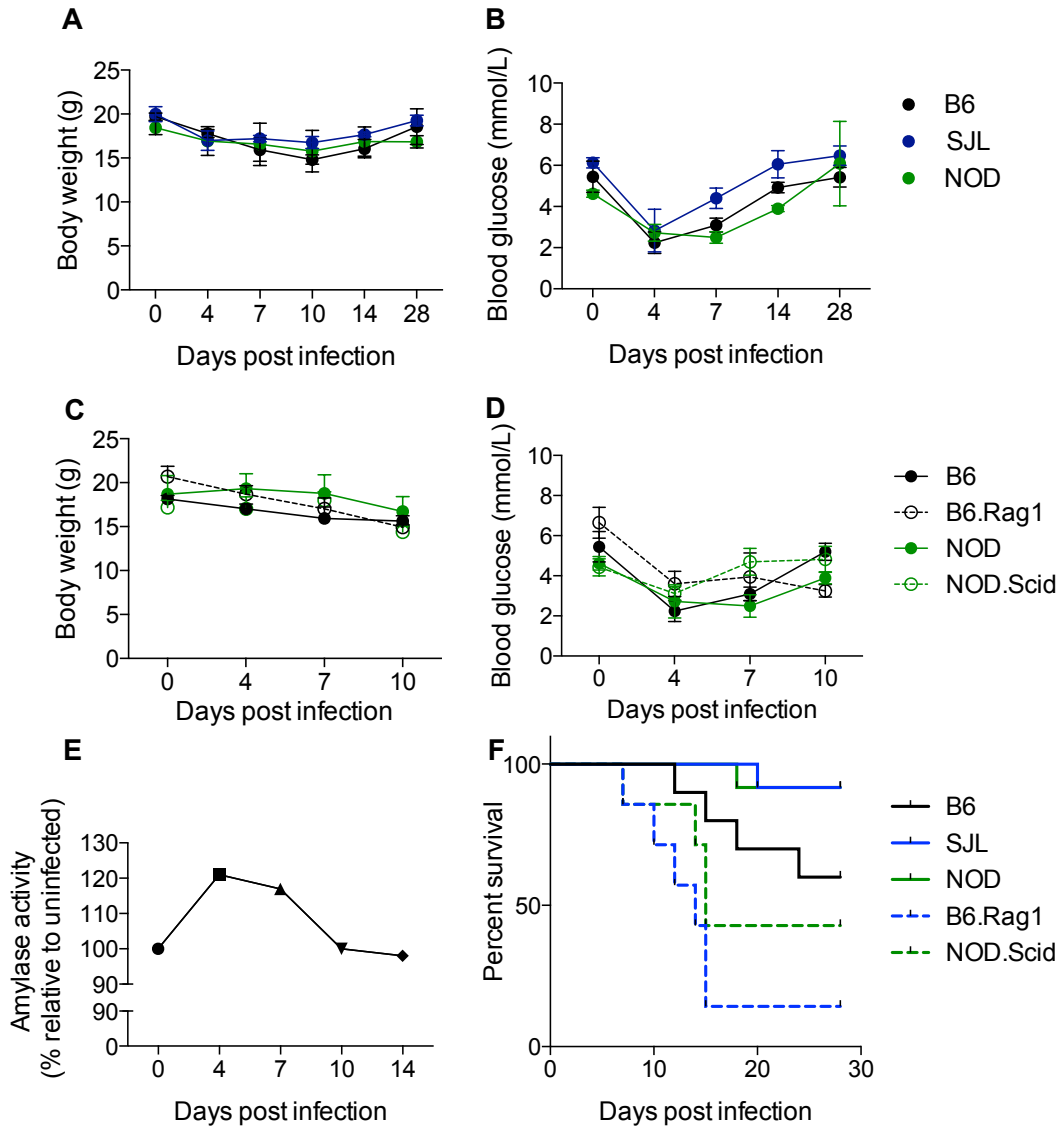

Figure 2.1. Effect of CVB4 infection on body weight and blood glucose levels in immunocompetent and immunodeficient mouse strains

9- to 10-week old female mice were i.p. injected with CVB4 (20 PFU for B6 and B6.Rag1; 10^5 PFU for NOD, NOD.SScid and SJL). (A) Body weights and (B) nonfasting blood glucose levels in immunocompetent mice were determined at indicated time points. (C) Body weights and (D) nonfasting blood glucose levels of immunodeficient and immunocompetent mice were monitored on day 0, 4, 7 and 10 post-infection. Results are expressed as mean ± SEM (n = 9). (E) Serum amylase activity in CVB4-infected B6 mice relative to uninfected B6 mice (n = 5). (F) Comparison of survival rates using the Kaplan–Meier method following CVB4 infection. Data are shown as mean percentages. A significant difference was noted between B6 and B6.Rag1 ($p < 0.05$) and between NOD and NOD.Scid ($p < 0.05$). PFU, plaque forming units, i.p., intraperitoneally. Data (n = 12 for B6, SJL and NOD; n = 8 for NOD.Scid and B6.Rag1. are representative of 2 independent experiments.

Upon CVB4 inoculation, immunocompetent mice displayed significant weight loss during the initial 10 days of infection, but almost completely recovered their initial body weight by day 28 post-infection (pi) (Fig. 2.1A).

Measurement of blood glucose levels revealed early and pronounced hypoglycemia, peaking around day 4 pi in B6 and SJL, and day 7 pi in NOD mice (Fig. 2.1B). Early hypoglycemia following viral infection was accompanied by increased blood amylase activity (Fig. 2.1E), which indicated severe destruction of the exocrine pancreas (i.e. pancreatitis), leading to compromised digestion. On the other hand, hyperglycemia (blood glucose levels above 15mmol/L), indicative of T1D, was only detected in about 10% of NOD mice, but not in any of the other analysed strains during the course of 28 days following infection. Immunodeficient mice showed a similar trend in weight loss and also developed severe hypoglycemia following CVB4 infection (Fig. 2.1C and Fig. 2.1D). Notably, assessment of immunodeficient mice past the 10-day time point was compromised by a dramatic increase in the mortality rate (Fig. 2.1F). By contrast, 95% of NOD and SJL, and 60% of B6 mice survived 28 days pi (Fig. 2.1F).

Next, it was investigated whether the susceptibility to virus-induced hyperglycemia was directly related to differences in viral tropism and replication kinetics. On day 4 pi, replicating virus was found in all major organs (pancreas, spleen, liver, heart, intestine and thymus) of CVB4 infected mice (Fig. 2.2A-E). Despite the large difference in initial viral load, viral titres were comparable across different organs and strains. Importantly, the highest level of viral replication was found in the pancreas of B6, NOD and SJL mice, confirming the strong pancreas tropism of CVB4 (Fig. 2.2A). Replicating virus

could not be detected in any tested organs by day 14 pi, indicating that the virus was cleared at that time point. Notably, the T1D-resistant B6 mice showed accelerated viral clearance in the pancreas compared to T1D-prone SJL and NOD mice, which may reflect the reduced dose of virus given to B6 mice. Due to the high mortality rate in the immunodeficient strains B6.RAG1 and NOD.SCID, viral replication data is restricted to day 10 pi. During this period, viral titres in the pancreas of NOD.SCID mice were similar to those measured in NOD mice (Fig. 2.2E), underlining the important role of innate immunity in early viral restriction. However, compared to B6 mice, B6.RAG1 mice showed elevated viral titres on day 7 pi and 10 pi. This suggests that adaptive immunity in B6 mice may play a more pronounced role in mediating viral clearance relative to the NOD strain.

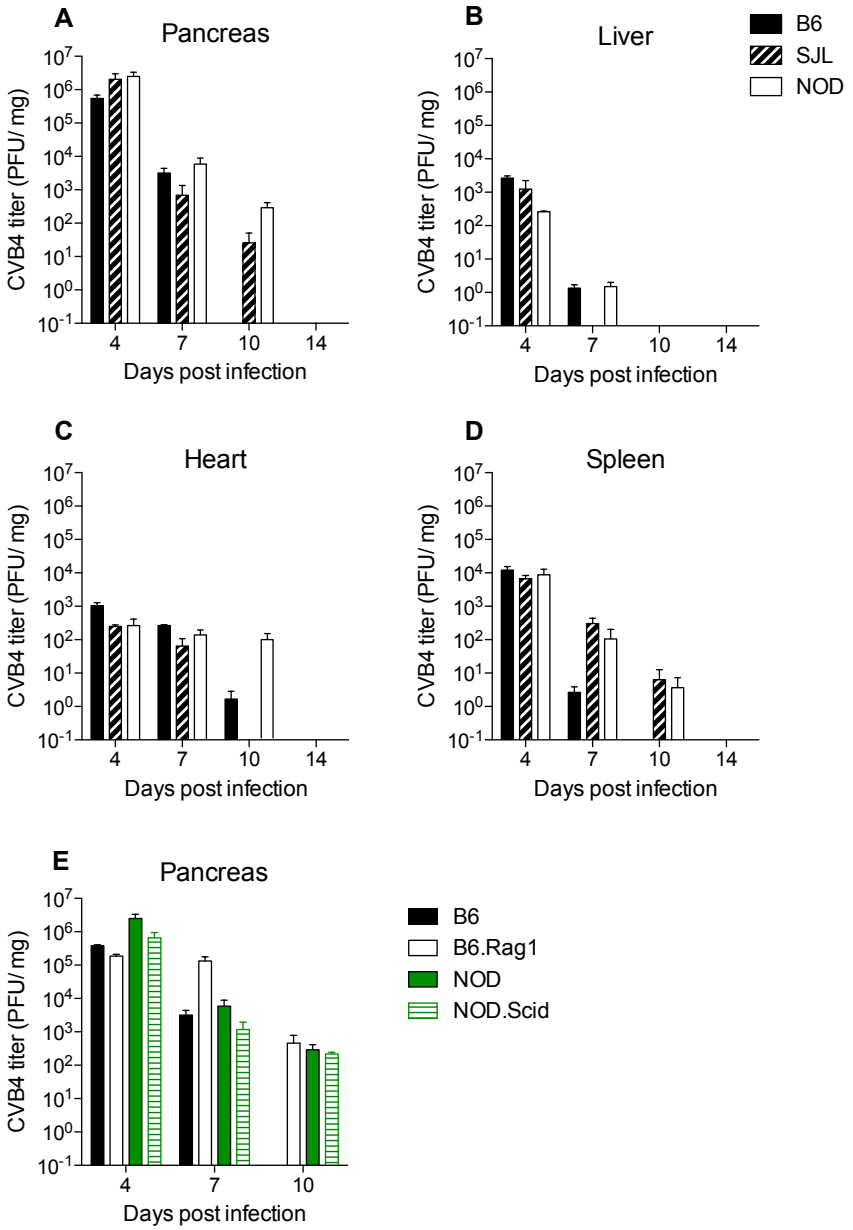

Figure 2.2. Viral titres in different tissues following CBV4 infection
9- to 10-week old female mice were i.p. injected with CVB4 (20 PFU for B6 and RAG; 10^5 PFU for NOD, SCID and SJL). Pancreas (A, E), liver (B), heart (C) and spleen (D) were harvested at day 4, 7, 10 and 14 pi (4 mice per strain and time point). Viral titres were determined by plaque assay and adjusted for tissue weight. Results are expressed as mean ± SEM (n = 4). The minimum detection limit of the assay was 0.1 PFU/ml. pi, post-infection; PFU, plaque-forming units, i.p., intraperitoneally.

To investigate the route of infection, viral kinetics at earlier time points were examined. Viral replication was detected as early as 4 hours post infection and was mainly limited to the pancreas, although virus was also present in stool samples of B6 and SJL mice (Fig. 2.3A). At 24 hours post CVB4 infection,

elevated viral titres were consistently found in pancreas and stool samples of immunocompetent mice (Fig. 2.3B). As CVB4 is classified as an enterovirus and is predominantly found in the intestine (Alidjinou et al., 2014), its early detection in stool samples supports the notion that viral replication and expansion occurs in the gut.

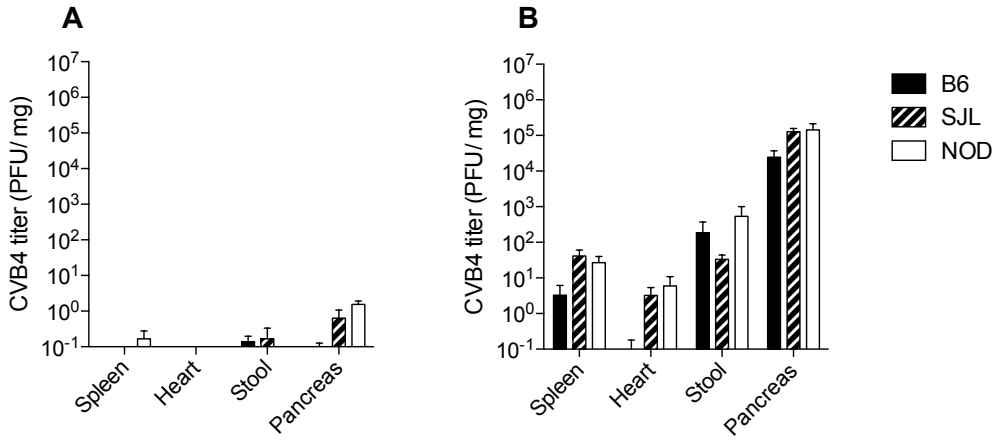

Figure 2.3. Early CVB4 replication is limited to the pancreas
9- to 10-week old female mice were i.p. injected with CVB4 (20 PFU for B6; 10^5 PFU for NOD and SJL). Spleen, heart, pancreas and stool samples were harvested 4 hours pi (A) and 24 hours pi (B) (4 mice per strain and time point). Viral titres were determined by plaque assay and adjusted for tissue weight. Results are expressed as mean ± SEM. The minimum detection limit of the assay was 0.1 PFU/ml. pi, post-infection; PFU, plaque forming units, i.p., intraperitoneally.

Finding replicating virus in stool samples early after intraperitoneal inoculation raises the question of how the virus spreads from the peritoneal cavity to the intestinal lumen. Cautiously performed i.p. injections do not perforate intraperitoneal organs, and are therefore an unlikely source of spread. It was hypothesized that monocytes/macrophages and dendritic cells (DCs), which are key mediators for the initiation of antiviral immune responses (Banchereau and Steinman, 1998; Mogensen, 1979), may facilitate early viral spread.

Although DCs can readily be infected by several enteroviral strains, they have been shown to be non-permissive to CVB both *in vitro* and *in vivo* (Kramer et al., 2007; Schulte et al., 2013). Thus, focus was set on the susceptibility of peritoneal macrophages to CVB4 infection. The majority of peritoneal macrophages obtained by lavage from B6 mice expressed the coxsackievirus and adenovirus receptor (CAR), as determined by fluorescent microscopy (Fig. 2.4A). Notably, CAR is essential for viral entry and has been correlated with viral tropism (Carson, 2001; Martino et al., 2000). We next inoculated B6 mice with CVB4 and harvested peritoneal macrophages 24 hours later. Analysis of fluorescent microscopy revealed that a considerable proportion of inflammatory ($Ly6C^{hi}$) macrophages were permissive to CVB4 infection as suggested by positive staining for the enterovirus capsid protein VP1 (Fig. 2.4B). This finding supports the notion that macrophages may constitute an additional CVB4 reservoir, and raises the question about the specific role of this immune cell population on the development of chronic inflammation in T1D.

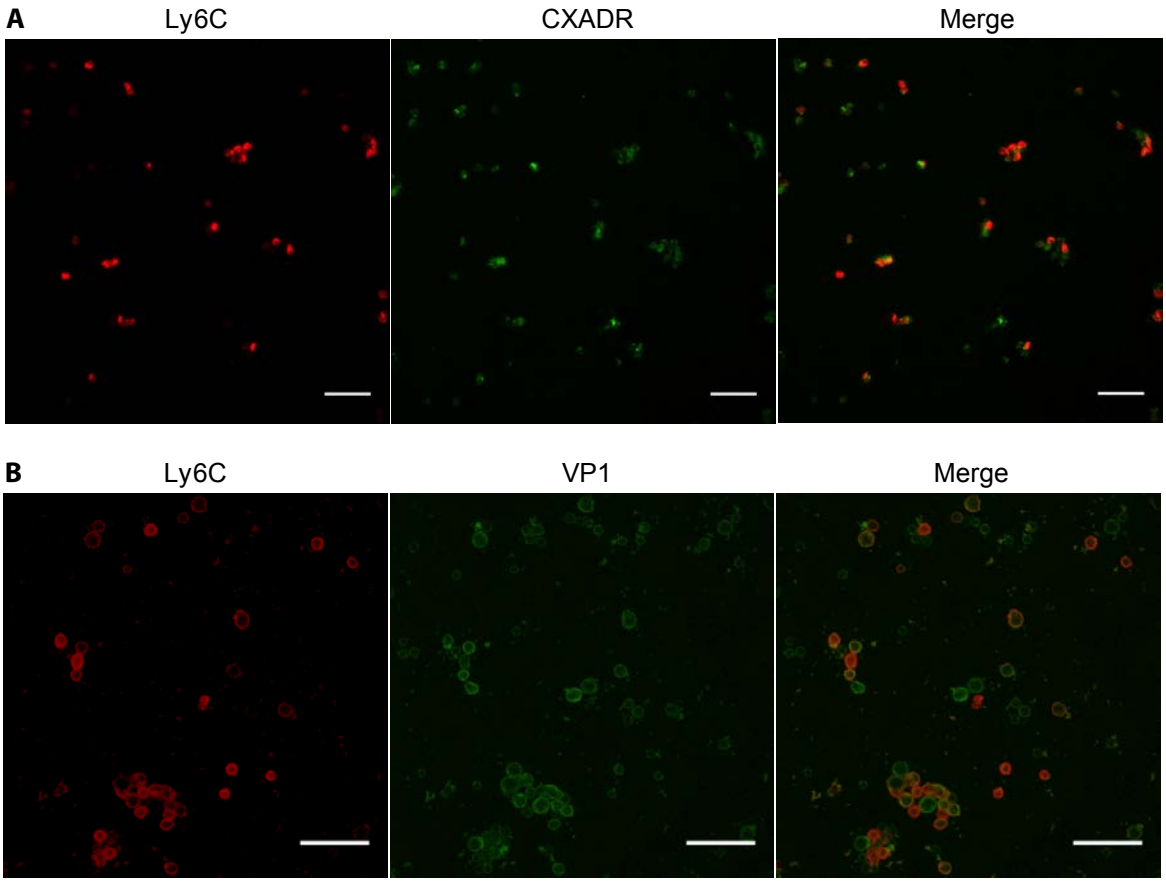

Figure 2.4. Peritoneal macrophages express CXADR and are susceptible to CVB4 infection

A. Peritoneal macrophages from 9-10-week old B6 mice were obtained by lavage and stained for CXADR (green) and Ly6C (red). (B) 9- to 10-week old female B6 mice were i.p. injected with 20 PFU of CVB4. 24 hrs pi, peritoneal macrophages were obtained by lavage, formalin fixed and stained for VP1 (green) and Ly6C (red). Scale bars indicate 50 µm (original magnification x20). pi, post-infection; PFU, plaque-forming units, i.p., intraperitoneally.

2.2.2. Histopathological changes within the pancreas of CVB4-infected mice

As demonstrated above, CVB4 shows strong tropism for pancreatic tissue in mice. To clarify whether this tropism is related to the endocrine and/or exocrine pancreas – which has important mechanistic implications for disease pathogenesis –pancreatic sections were carefully examined for the presence of VP1. In agreement with the viral replication data (Fig. 2.2A), the maximum level of VP1-positive staining was detected on day 4 pi (Fig. 2.5, top right panel), while specimens taken after day 10 pi indicated negative staining (data not shown). Importantly, VP1 expression was exclusively found within the exocrine pancreas of B6, SJL and NOD mice, and completely absent within pancreatic islets, suggesting that tropism of CVB4-E2 is related to acinar cells within the exocrine pancreas.

Subsequently, it was examined whether this tropism is associated with the (qualitative and quantitative) expression levels of CAR (coxsackievirus and adenovirus receptor) and DAF (decay-accelerating factor) by acinar cells, as previously suggested (Hafenstein et al., 2007; He et al., 2001). Surprisingly, positive CAR and DAF staining in mock-infected pancreas sections was not observed within exocrine tissue, but was restricted to pancreatic islets (Fig. 2.5, middle left and bottom left panel). Upon CVB4 infection, both islets and exocrine regions indicated high expression of CAR (Fig. 2.5, middle right panel) and DAF (Fig. 2.5, bottom right panel). As the VP1 staining profiles described above were limited to exocrine tissue, these results do not support

the notion of CAR- and/or DAF-mediated cell entry of CVB4 and require further investigation.

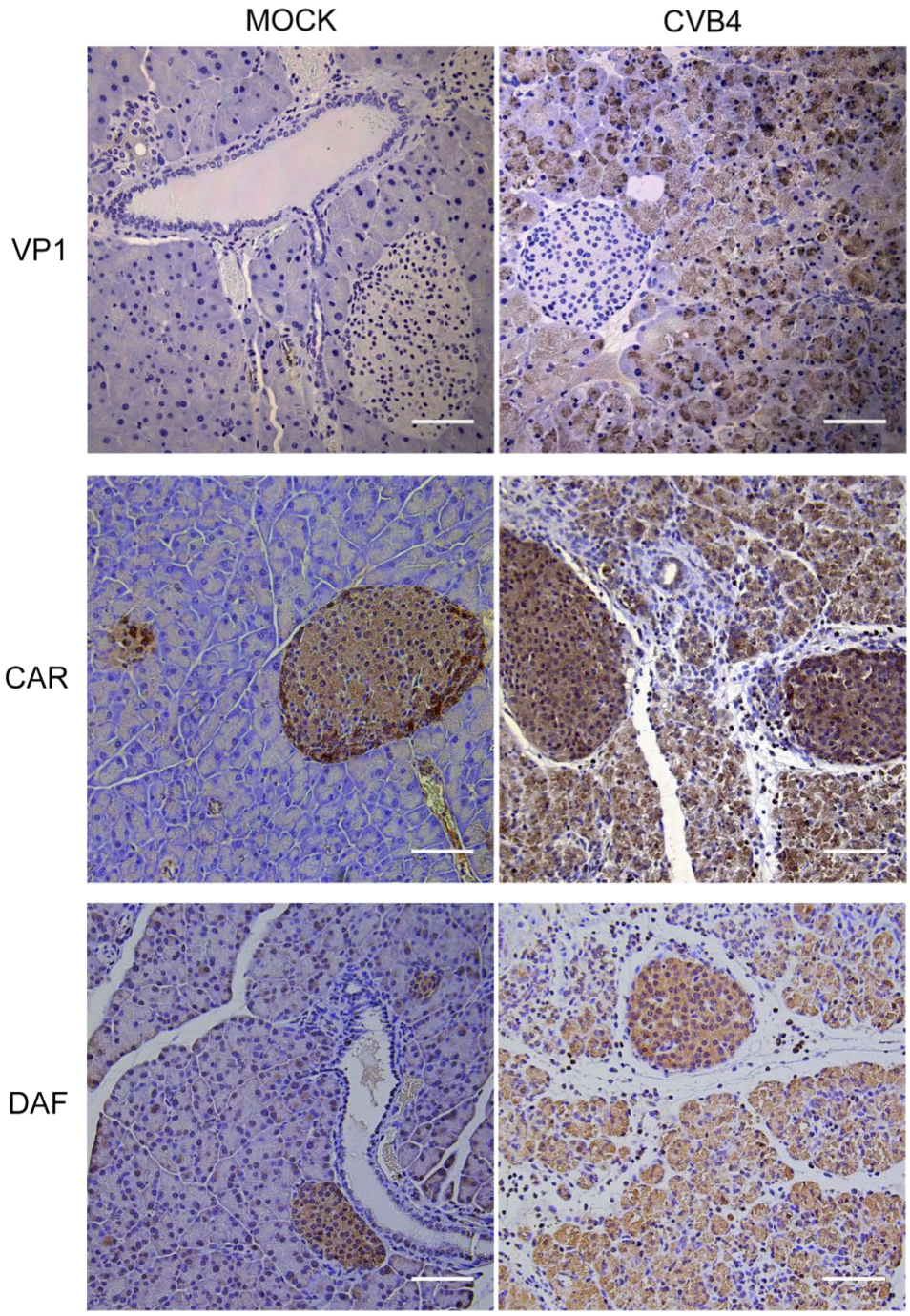

Figure 2.5. Expression of VP1, CAR and DAF in the pancreas
9-10-week-old female B6 mice were i.p. injected with 20 PFU/mouse of CVB4 and sacrificed 4 days pi. Pancreas sections were stained with antibody against VP1 (clone 5D8/1), CAR or DAF. Mock-infected sections are shown in the left column, CVB4-infected sections are shown in the right column. Scale bars indicate 75 µm (original magnification x20). DAF, Decay accelerating factor; CAR, Coxsackievirus and adenovirus receptor; VP1, viral protein 1; PFU, plaque forming units, i.p., intraperitoneally. Images are representative for 2 independent experiments (n = 3).

Taking into consideration that exaggerated tissue damage following CVB4 infection may be linked to increased T1D susceptibility, it was next assessed whether T1D-prone strains display increased levels of tissue destruction. Thus, a histopathological evaluation of pancreas sections was performed for 28 days following CVB4 infection. On day 4 pi, pancreas sections showed extensive immune cell infiltration and signs of acute acinar tissue damage (Fig. 2.6). Immune cell infiltrates peaked around day 7 pi in B6, SJL and NOD mice, and were found throughout the exocrine pancreas of all analysed strains, although NOD mice appeared to have the highest degree of inflammation.

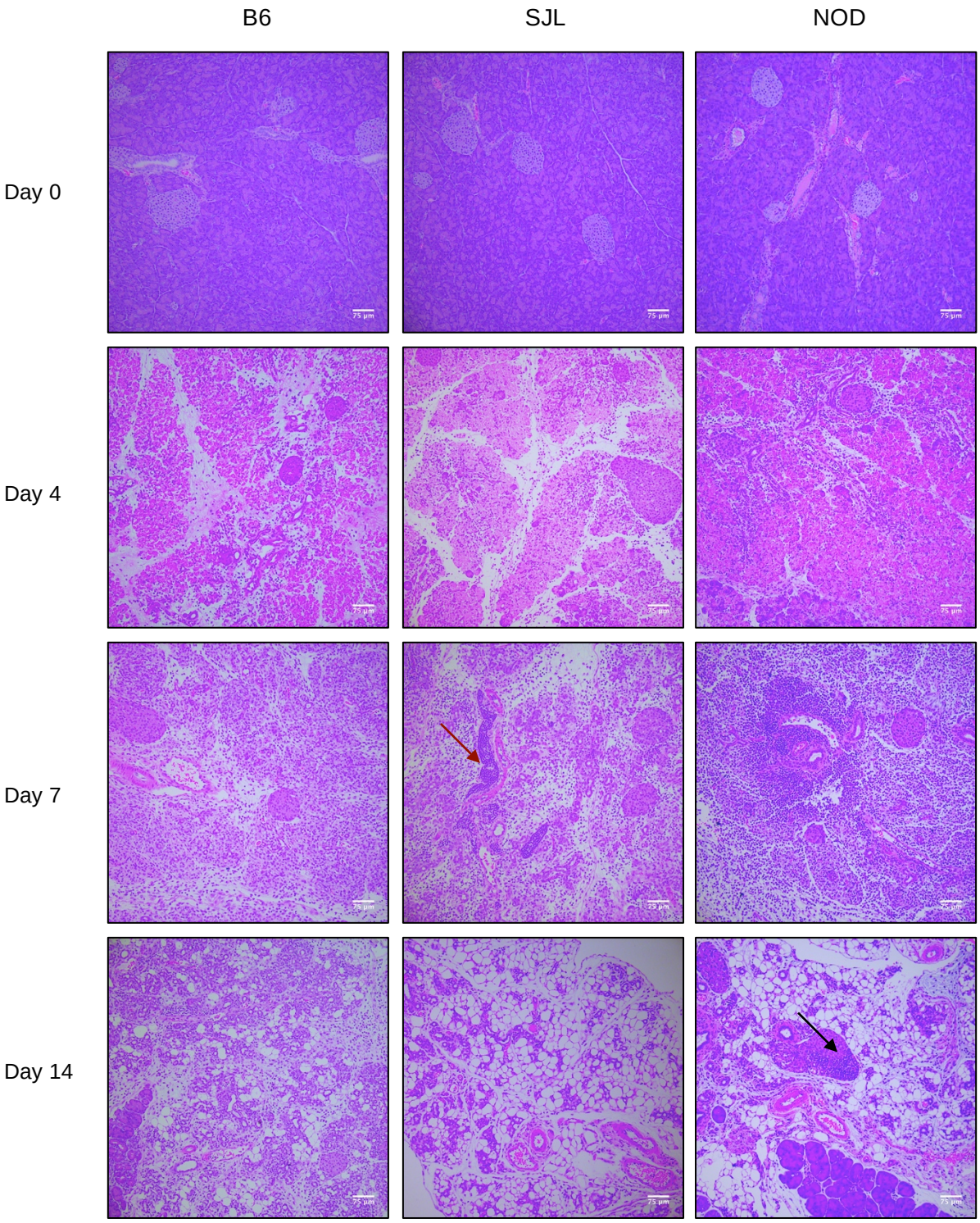

Figure 2.6. CVB4 infection is associated with severe pancreatitis.
Representative images from pancreas sections of B6, SJL and NOD mice at indicated time points after CVB4 infection. 9- to 10-week old female mice were i.p. injected with CVB4 (20 PFU for B6; 10^5 PFU for NOD and SJL) and pancreata harvested on day 0, 4, 7 and 14 pi. Pancreas sections were routinely processed and stained with H&E. Scale bars indicate 75µm (original magnification x10). Black arrow indicates peri-insulitis, red arrow indicates tertiary lymphoid structures. H&E, hematoxylin & eosin; pi, post-infection; PFU, plaque-forming units, i.p., intraperitoneally.

In regards to islet infiltration, differences were observed amongst strains. CVB4-infected B6 mice showed fully intact islets, while islets in SJL and NOD mice were occasionally infiltrated by few small mononuclear cells. However, peri-insulitis (i.e. infiltration in the islet periphery) was only exhibited by a minor proportion of NOD mice, and not detected in SJL mice. Importantly, only the T1D-prone SJL and NOD mice showed *de novo* formation of tertiary lymphoid structures, which was observed as early as day 7 pi in SJL mice (Fig. 2.6; red arrow).

By day 14 pi, B6, SJL and NOD mice experienced severe destruction of acinar cells within the exocrine pancreas and their replacement with fat tissue. The latter is commonly a result of ongoing pancreatitis causing the release of digestive enzymes and subsequent autodigestion of pancreatic tissue (Wang et al., 2009). While surviving islets in B6 and SJL mice seemed intact, a large proportion of NOD islets displayed mild to moderate insulitis (Fig. 2.6; black arrow).

In order to study the role of adaptive immunity in virus-induced tissue pathology, pancreas sections from B6.RAG1 and NOD.SCID mice were evaluated on day 4 and 7 post CVB4-infection. Compared to NOD mice (Fig. 2.6), immunodeficient NOD.SCID displayed slightly reduced immune cell infiltration and tissue damage (Fig. 2.7, right panel), suggesting that infiltrating B and T cells contribute to the tissue destruction observed in NOD mice after CVB4 infection. In contrast, the acute pancreatitis found in B6.RAG1 mice (Fig. 2.7, bottom left panel) was more pronounced compared to B6 mice (Fig. 2.6), particularly on day 7 pi. Although both immunodeficient strains tested lack

functional B and T cells, differences observed in histopathology and viral clearance might reflect their distinct genetic backgrounds.

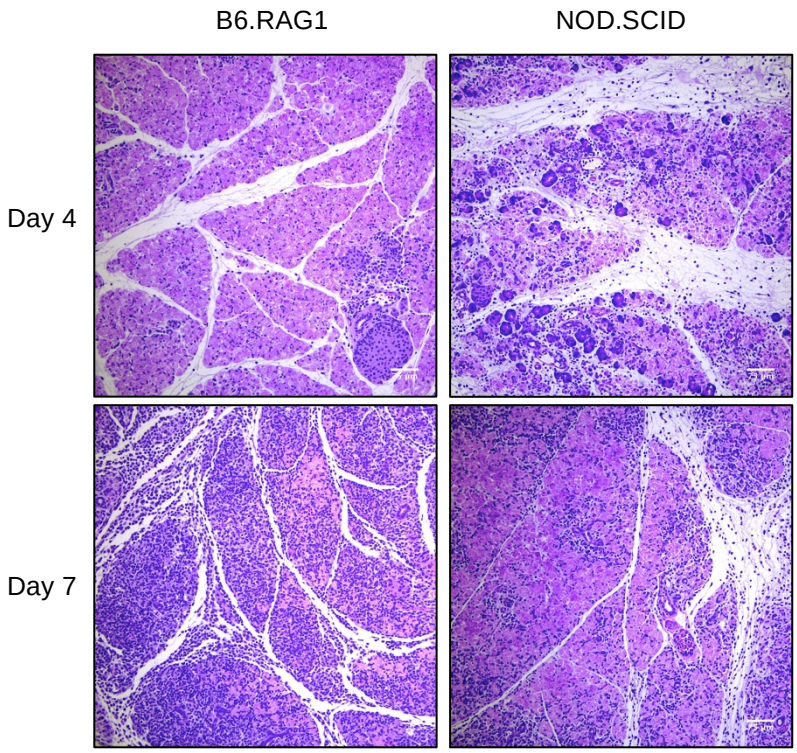

Figure 2.7. Immune cell infiltration and tissue damage in immunodeficient mice. Representative images from pancreatic sections of immunodeficient mice following CVB4 infection. 9- to 10-week old female B6.RAG1 and NOD.SCID mice were i.p. injected with CVB4 (20 PFU for B6.RAG1; 10^5 PFU for NOD.SCID). Pancreata were harvested on day 4 pi and 7 pi and stained with H&E. Scale bars indicate 75 µm (original magnification x10). H&E, hematoxylin & eosin; pi, post-infection; PFU, plaque forming units; i.p., intraperitoneally.

As mentioned above, tertiary lymphoid structures (TLS) were observed in the pancreas during acute CVB4 infection in SJL and NOD, but not in B6 mice. TLS formation is characteristic of chronic inflammation in severely damaged tissues, where organized immune responses are required onsite. However, the persistence of TLS is also associated with an increased risk of autoimmunity, as autoreactive lymphocytes are more likely to encounter their cognate antigen (Neyt et al., 2012). In line with this, TLS were found in the T1D-susceptible

strains (NOD and SJL) two weeks after viral clearance (Fig. 2.8C and D), and were completely absent in T1D-resistant B6 mice at any given time point. Hence, the formation of TLS in response to viral infections appears to be an inherent feature of T1D-susceptible strains, essentially driving chronic inflammation. To assess the severity of chronic inflammation across the three strains, both insulitis and pancreatitis were evaluated on day 28 pi (Fig. 2.9).

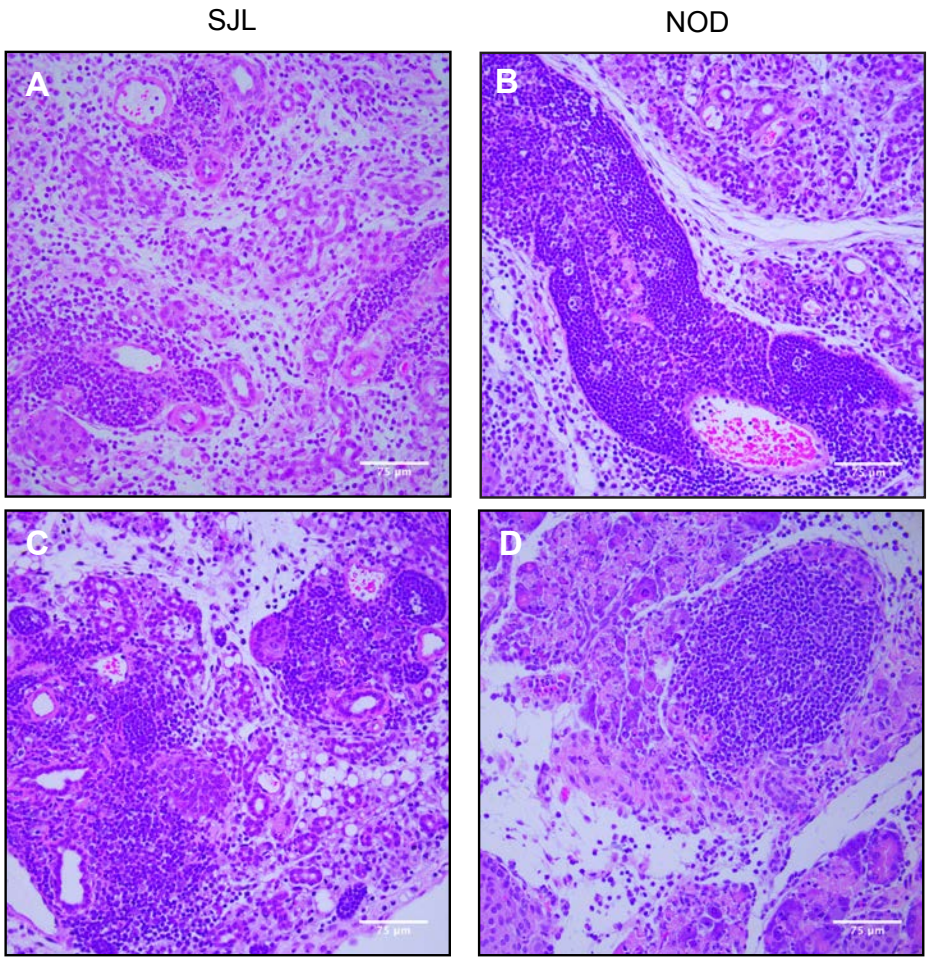

Figure 2.8. CVB4 infection drives the formation of tertiary lymphoid structures within the pancreas of T1D-prone SJL and NOD mice

Representative pancreas sections from CVB4-infected NOD and SJL mice show evidence of de novo formation of tertiary lymphoid structures (TLS). 9- to 10-week old female mice were i.p. injected with 10^5 PFU of CVB4. Pancreata were harvested on day 28 pi. Processed pancreas sections were stained with H&E and inspected for TLS by light microscopy. TLS were found in pancreas sections from SJL mice (A, day 4pi; C, day 28 pi) and from NOD mice (B, day 7 pi; D day 28 pi), but not in pancreas sections from B6 mice (data not shown). Scale bars indicate 75µm (original magnification x20). H&E, hematoxylin & eosin; pi, post-infection; PFU, plaque-forming units, i.p., intraperitoneally.

While few mice were able to regenerate pancreatic tissue, the majority of B6, SJL and NOD mice exhibited severe pancreatitis (Fig. 2.9D). Notably, the amount of insulitis observed in B6 mice was negligible and possibly restricted to necrotic lesions. By contrast, the great majority of NOD mice showed a high degree of insulitis involving more than 50% of the islets (Fig. 2.9A, Fig. 2.9B and Fig. 2.9C). Importantly, islet infiltration in CVB4-infected NOD mice was considerably greater compared to spontaneous infiltration in age-matched control mice (Fig. 2.9B and Fig. 2.9C).

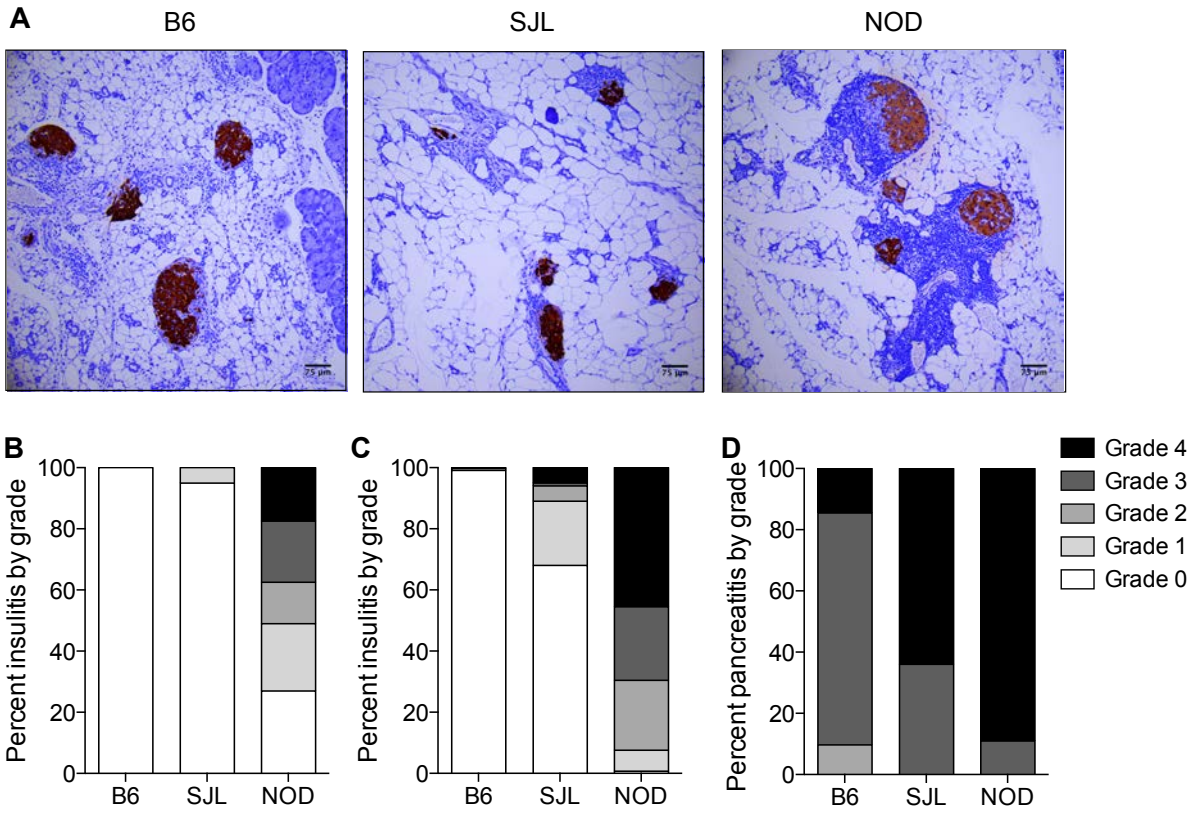

Figure 2.9. Severity scores of insulitis and pancreatitis
9-10-week-old female mice were i.p. injected with CVB4 (20 PFU for B6; 10^5 PFU for NOD and SJL) and sacrificed 28 days pi. (A) Representative histological sections of the pancreas stained for insulin. Severity scores for insulitis in mock-infected (B) and CVB4-infected mice (C) and for pancreatitis (D) in CVB4–infected mice; (B6: n=6, SJL: n=5, NOD: n=6). Scores were determined as described in experimental procedures. Scale bars indicate 75 µm (original magnification x20). pi, post-infection; PFU, plaque-forming units, i.p., intraperitoneally.

This observation was particularly apparent in severely infiltrated islets (grade 4 insulitis). Insulitis in SJL mice was less prevalent than in NOD mice (Fig. 2.9A, middle panel). Although a considerable percentage of SJL mice showed mild insulitis (i.e. peri-insulitis), the majority of islets in this strain were negative for insulitis. Notably, a small percentage of SJL mice displayed moderate to severe insulitis (Fig 2.9C) and might therefore constitute a high-risk group for autoimmunity.

2.2.3. Leukocyte profiling in pancreas and secondary lymphoid organs

Pancreatic tissues taken from T1D patients characteristically exhibit substantial mononuclear cell infiltration (Coppieters et al., 2012; Gepts, 1965; Willcox et al., 2009). However, the functional mechanisms by which the immune infiltrate induces and/or amplifies insulitis are incompletely understood.

The histopathological assessment of pancreas sections from CVB4-infected mice revealed severe pancreatitis peaking around day 7 pi. Importantly, two weeks after viral clearance, considerable immune cell infiltration remained in the exocrine pancreas of T1D-resistant B6 and T1D-prone SJL and NOD mice. To expose qualitative and quantitative differences, a comparative flow cytometric analysis of the pancreas infiltrate was performed on day 7, 14 and 21 following CVB4 infection.

In agreement with histopathological findings, relative and total numbers of infiltrating CD45+ leukocytes were highest on day 7 pi (Fig. 3.10A and B). Due to massive tissue destruction, the total pancreatic mass is drastically reduced by day 14 and day 21. As a consequence, the absolute numbers of CD45+ leukocytes were decreased at these time points (Fig. 3.10B), but their relative proportion remained high above those of non-infected controls.

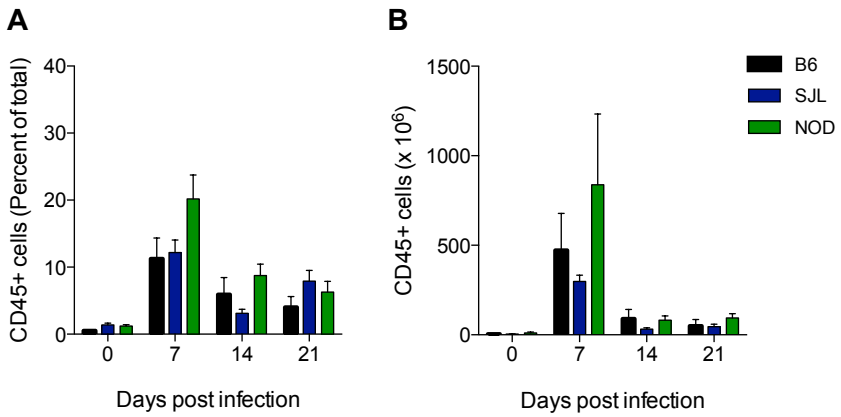

Figure 2.10. CVB4-induced leukocyte infiltration persists after viral clearance
9-10-week-old female mice were i.p. injected with CVB4 (20 PFU for B6; 10^5 PFU for NOD and SJL) and sacrificed on day 7 pi, 14 pi and 21 pi. Isolated immune cells were analysed by flow cytometry. Results are expressed as mean ± SEM (n = 5). There was no statistical difference ($p > 0.05$; ANOVA) in CD45+ cell fractions or total numbers between the groups. pi, post-infection; PFU, plaque forming units, i.p., intraperitoneally.

To identify the major cell types within the immune cell infiltrate at each time point, cells were stained for CD3 and B220, allowing the detection of B cells (CD45+ B220+), T cells (CD45+ CD3+) and myeloid cells (CD45+B220-CD3-). During acute infection on day 7, the infiltrate of B6 and NOD mice was mainly dominated by myeloid cell infiltration (Fig. 2.11A). This was also true for SJL mice, which also displayed increased frequencies of infiltrating B and T cells on day 7 compared to B6 and NOD mice (Fig. 2.11A). This finding, together with the formation of tertiary lymphoid structures observed in SJL mice at this

time point, might indicate differences in the kinetics or the magnitude of the adaptive immune response in this strain.

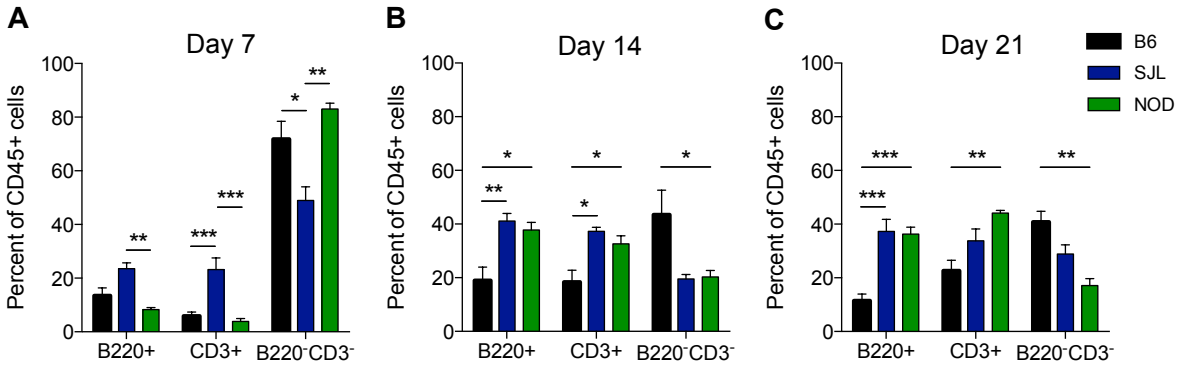

Figure 2.11. Leukocyte profile of T1D-susceptible strains contains increased proportions of adaptive immune cells
9-10-week-old female mice were i.p. injected with CVB4 (20 PFU for B6; 10^5 PFU for NOD and SJL) and sacrificed at day 7 pi (A), 14 pi (B) or 21 pi (C), followed by flow cytometric analysis of the pancreata. Results are expressed as mean ± SEM (n=5); statistical significance was determined by a one-way analysis of variance (ANOVA) using Bonferroni's post hoc test ($^{*}p \leq 0.05$, $^{**}p \leq 0.01$, $^{***}p \leq 0.001$). pi, post-infection; PFU, plaque-forming units, i.p., intraperitoneally.

Further phenotyping on day 7 pi showed that dendritic cells (CD11c+), neutrophils (Ly6G+) and NK cells (NK1.1+) only constituted a minor fraction of the myeloid infiltrate (B220-CD3-), while more than 70% of this lineage in B6, SJL and NOD mice consisted of F4/80+ macrophages (Fig. 2.12A). This suggests that macrophages may be important for controlling viral clearance and responding to tissue damage early in the response to CVB4. Although macrophages were also detected in the pancreas on both day 14 and day 21 pi, their relative contribution to the infiltrate was drastically reduced at these later time points and did not differ between T1D-resistant and T1D-susceptible strains (Fig. 2.12B and C). By contrast, frequencies of CD11c+ dendritic cells were increased during the adaptive phase of the immune response (day 14

and 21 pi), but no significant differences were noted between the three mouse strains at these time points (Fig. 2.12B and C).

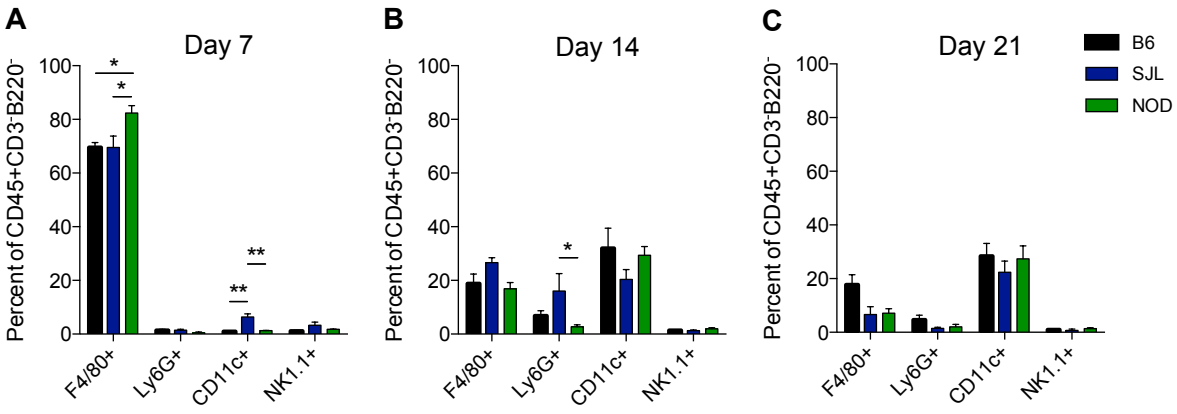

Figure 2.12. Initial immune infiltrates are dominated by macrophages
9-10-week-old female mice were i.p. injected with CVB4 (20 PFU for B6; 10^5 PFU for NOD and SJL) and sacrificed at day 7 pi (A), 14 pi (B) and 21 pi (C). Isolated immune cells were analysed by flow cytometry. Staining definitions for individual populations: macrophages, CD45+/CD11b+/F4/80+; neutrophils, CD45+/CD11b+/Ly6G+; dendritic cells, CD45+/CD11c+; natural killer cells CD45+/CD3-/NK1.1+. Results are expressed as mean ± SEM (n=5); statistical significance was determined by a one-way analysis of variance (ANOVA) using Bonferroni's post hoc test ($^{*}p \leq 0.05$, $^{**}p \leq 0.01$). pi, post-infection; PFU, plaque-forming units, i.p., intraperitoneally.

No significant differences were found between mouse strains in terms of relative amounts of infiltrating neutrophils and NK cells on day 7 and 21 pi. Notably, however, SJL mice revealed increased levels of neutrophils on day 14 pi. While other studies have reported an influx of NK cells and neutrophils into the pancreas at very early time points after CVB4 infection (De Palma et al., 2009; See and Tilles, 1995), it is likely that the majority of these cells were cleared by day 7 pi in the current study, thus imposing a negligible contribution to chronic inflammation.

The pancreatic infiltrate on day 14 pi was predominated by B and T cells in T1D-susceptible SJL and NOD mice, whereas myeloid cells still represented

the highest proportion of the B6 infiltrate (Fig. 2.11B). However, the relative proportion of activated $CD4^+$ and $CD8^+$ T cells within the total T cell pool was similar amongst the three strains (Fig. 2.13A and B).

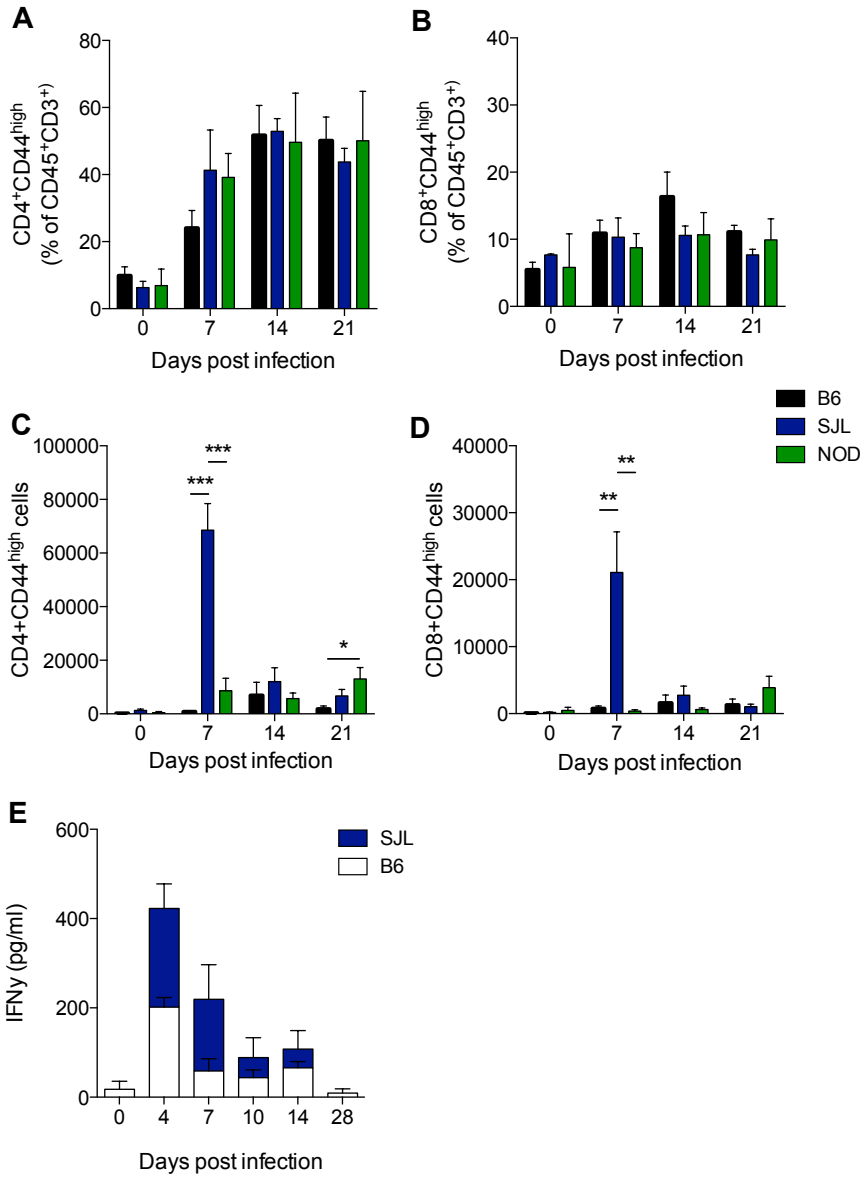

Figure 2.13. CVB4 infection results in a CD4+ T cell-dominant islet infiltration
9-10-week-old female mice were i.p. injected with CVB4 (20 PFU for B6; 10^5 PFU for NOD and SJL) and sacrificed at day 0 pi, 7 pi, 14 pi and 21 pi. Isolated immune cells were analysed by flow cytometry for percentages (A) and absolute numbers (C) of activated CD4 T cells (CD3+/CD4+/CD44high), and percentages (B) and absolute numbers (D) of activated CD8 T cells (CD3+/CD8+/CD44high). Results are expressed as mean ± SEM (n=5); statistical significance was determined by a one-way analysis of variance (ANOVA) using Bonferroni's post hoc test ($^{**}p \leq 0.01$, $^{***}p \leq 0.001$). (E) Serum levels of IFNγ were measured by ELISA on day 0 pi, 7 pi, 14 pi and 21 pi in B6 and SJL mice. pi, post-infection; PFU, plaque-forming units, i.p., intraperitoneally.

Importantly, the majority of activated ($CD44^{hi}$) T cells belonged to the $CD4^+$ T cell lineage, suggesting that T cell mediated immune responses to CVB4 depend on T helper cells (i.e. Th1 response) (Fig. 2.13A and Fig. 2.13B). In line with this, increased levels of IFN-y were detected early after CVB4 infection in the serum of B6 and SJL mice (Fig. 2.13E, NOD mice yet to be tested). Furthermore, the activation status of CD4 T cells did not decrease from day 14 pi to day 21 pi, indicating that this subset contributes to chronic inflammation in the absence of virus.

Significant differences between the strains were only apparent when assessing absolute numbers of activated/memory phenotype ($CD44^{hi}$) $CD4^+$ and $CD8^+$ T cells. In line with the more rapid adaptive immune response observed in SJL mice (Fig. 2.11), this strain mounted significantly greater expansion of $CD4^+$ and $CD8^+$ T cells early after infection (Fig. 2.13C and D). By contrast, persistent inflammation on day 21 pi was only observed in NOD mice, which showed significantly increased infiltration of activated/memory phenotype $CD4^+$ T cells and $CD8^+$ T cells at this time point (Fig. 2.13C-D).

Despite lower quantities of activated $CD8^+$ T cells relative to $CD4^+$ T cells, this subset is crucial for recognition and direct killing of virus-infected cells in the context of MHC class I expression (Borrow et al., 1994; Varela-Calvino et al., 2004; Yang et al., 1994). As such, the persistent induction of MHC I in the absence of virus could potentially attract auto-reactive CD8+ T cell clones to the vicinity of beta cells and pose an increased risk of beta cell insult. As expected, all three strains demonstrated induced MHC I expression in CVB4-infected versus mock-infected tissue on day 7 pi (Fig. 2.14). Notably,

upregulation of MHC I in all strains persisted for several days after viral clearance (day 21 pi) and could explain the presence of activated $CD8^+$ T cells in the pancreas of B6, SJL and NOD mice.

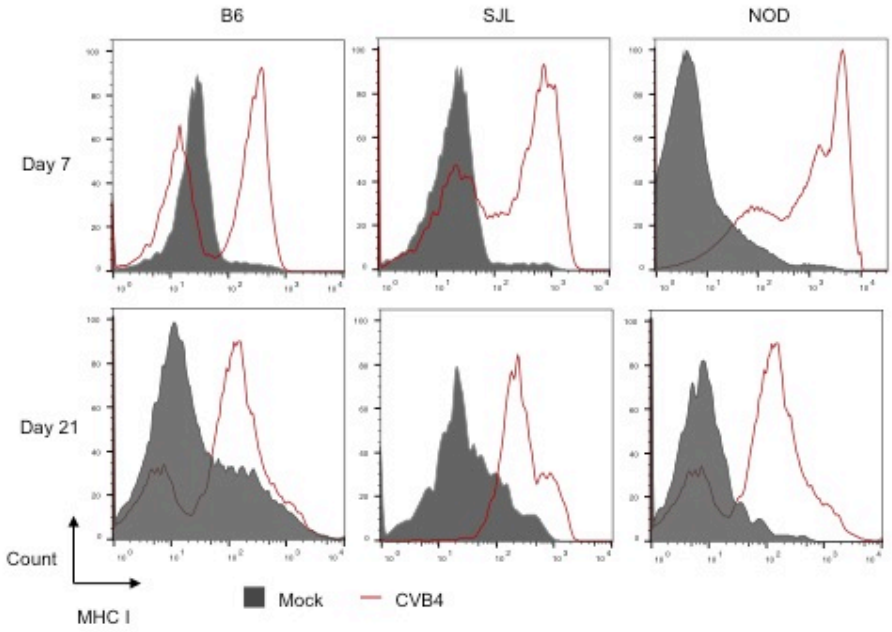

Figure 2.14. Persistent inflammation is associated with increased MHC I expression in SJL but not B6 or NOD mice
9-10-week-old female mice were i.p. injected with CVB4 (20 PFU for B6; 10^5 PFU for NOD and SJL) and sacrificed on day 7 pi and 21 pi. Antibodies used for each MHC class I haplotype: B6, H2-kb; SJL, H-2Ks; B6, H2-kd. Data are representative of 3 to 4 mice per time point. pi, post-infection; PFU, plaque forming units, i.p., intraperitoneally; MHC I, major histocompatibility class I; MFI, mean fluorescent intensity.

While CD8+ T cells might contribute to chronic inflammation following CVB4 infection, the higher infiltration of activated $CD4^+$ T cells and the increased production of IFN-y indicates that immunity to CVB4 in B6, SJL and NOD mice is predominantly linked to a T-helper-cell type 1 (Th1) response.

In addition, the discovery of tertiary lymphoid structures, which are organised in distinct T cell and B cell zones (Drayton et al., 2006; Germain et al., 2014), suggests the involvement of another helper T cell subset: T follicular helper

(T_{FH}) cells. To support this hypothesis, the presence of T follicular helper (T_{FH}) and germinal centre-like (GC) B cells within the pancreatic infiltrate of these strains were investigated.

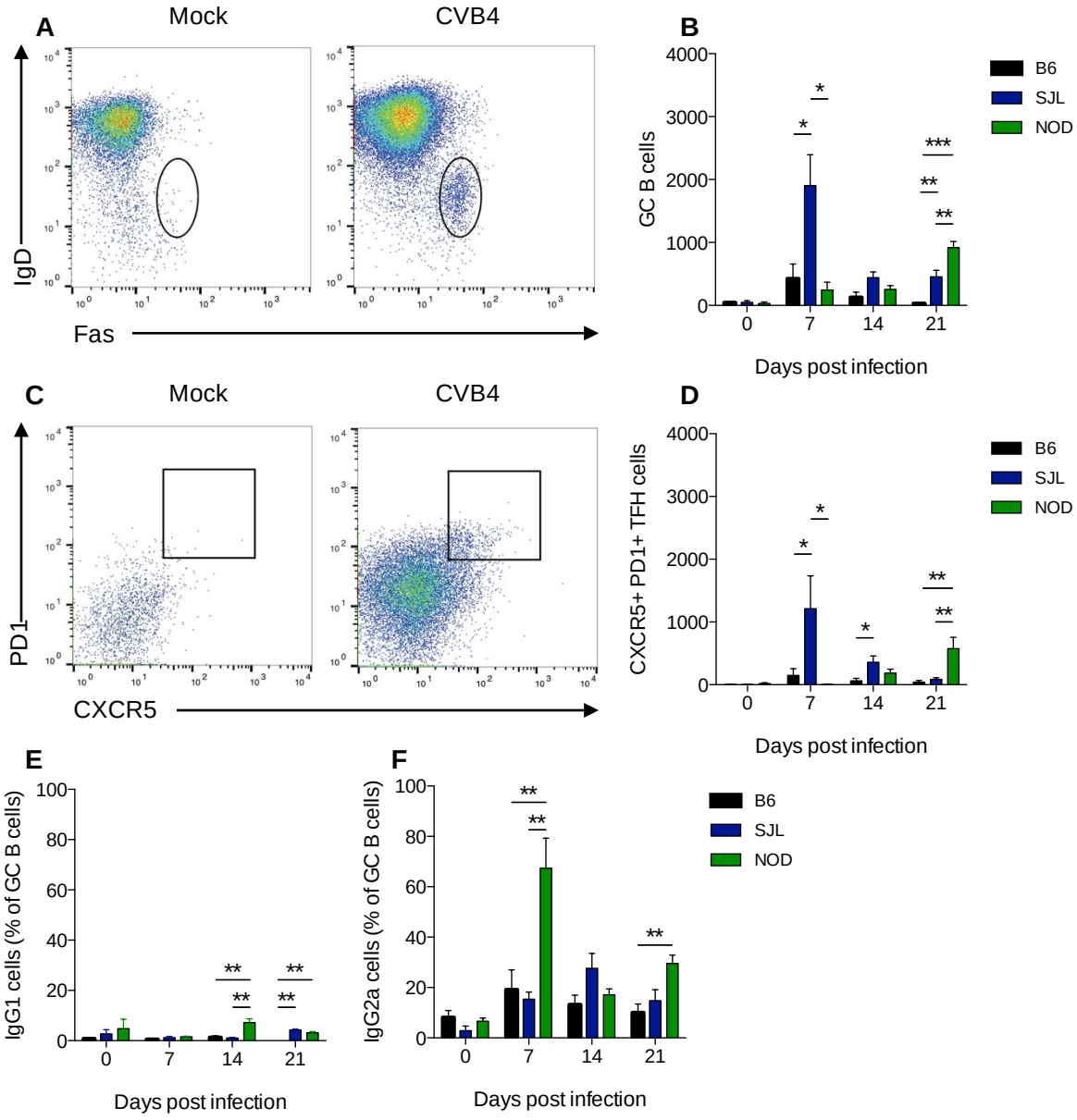

Figure 2.15. Increased numbers of GC B cells and TFH cells in T1D-prone NOD mice
9-10-week-old female mice were i.p. injected with CVB4 (20 PFU for B6; 10^5 PFU for NOD and SJL) and sacrificed at day 0 pi, 7 pi, 14 pi and 21 pi for flow cytometric analysis of pancreata. (A) Representative pseudocolour plots showing IgD and Fas expression in CD19+ B cell populations profiles in mock- and CVB4-infected SJL samples on day 7 pi. (B) Frequencies of CD45+CD19+Fas+GL7+ germinal centre B cells in the pancreas at different time points post-infection. (C) Representative flow cytometry of CXCR5 and PD-1 expression in CD4+ T cells in

mock- and CVB4-infected SJL samples on day 7 pi. (D) Frequencies of CD45+CD3+CD4+CXCR5+PD1+ T follicular helper cells in the pancreas at different time points post-infection. (E) Frequencies of IgG1+ GC B cell populations in the pancreas at different time points post-infection. (F) Frequencies of IgG2a+ in GC B cell populations in the pancreas at different time points post-infection. Results are expressed as mean ± SEM (n=4); statistical significance was determined by a one-way analysis of variance (ANOVA) using Bonferroni's post hoc test ($^{*}p \leq 0.05$, $^{**}p \leq 0.01$, $^{***}p \leq 0.001$). pi, post-infection; PFU, plaque forming units, i.p., intraperitoneally; TFH cell, T follicular helper cell; GC B cells, germinal centre B cell.

T1D-resistant B6 mice demonstrated a moderate influx of GC B cells on day 7 pi that was almost completely absent after CVB4 clearance (Fig. 2.15B). Compared to B6 mice, which showed a similar viral titre (antigen) in the pancreas as NOD and SJL mice, GC B cells numbers in the pancreas of SJL mice were significantly increased on day 7 pi and persisted after viral clearance (day 21 pi). Interestingly, GC formation in NOD mice was delayed and peaked only by day 21 pi. At this time point, absolute numbers of GC B cells in NOD mice were significantly higher compared to both B6 and SJL mice. In line with the low abundance of GC B cells in B6 mice, T_{FH} responses were found to be nearly absent in this strain (Fig. 2.15D). By contrast, the robust GC formation observed early in SJL mice was paralleled by high infiltration of T_{FH} cells (Fig. 2.15D). Finally, NOD mice displayed a delayed T_{FH} response that persisted after CVB4 was cleared (day 21 pi) and that was not observed in age-matched controls.

These findings provide additional support that ongoing inflammation in autoimmune prone strains may be linked to the presence of highly differentiated cells that promote exaggerated humoral immunity. To investigate whether this was linked to a particular immunoglobulin isotype, we evaluated the expression of IgG1 and IgG2a (B6 mice express the highly similar IgG2c

allotype termed IgG2a here for simplification) within the GC B cell population of each strain (Martin et al., 1998). Consistently, CVB4 infection was associated with class switching to the IgG2a isotype in B6, NOD and SJL mice over the course of infection (Fig. 2.15F). While the relative contribution of IgG1 to the GC population was insignificant at all time points (Fig. 2.15E), IgG2a expression above background levels was detected as early as day 7 pi. Notably, NOD mice displayed significantly increased IgG2a proportions on both day 7 and 21 pi, possibly indicating the relevance of this isotype for autoantibody production in this strain (Quintana and Cohen, 2001; Thomas et al., 2002). Lastly, we aimed to investigate whether ectopic GC formation in the pancreas of SJL and NOD mice after viral clearance is accompanied by persistent GC formation in the spleen and pancreas draining lymph nodes. Indeed, peanut agglutinin (PNA)-positive GC B cells were found in the spleen and pancreatic lymph nodes in all B6, NOD and SJL mice (Fig. 2.16). Importantly though, GC found in the pancreatic lymph nodes of SJL and NOD mice were considerably larger compared to those in B6 mice. This finding is consistent with the flow cytometric data and suggests that ectopic GC activity may promote ongoing inflammation in autoimmune mouse strains.

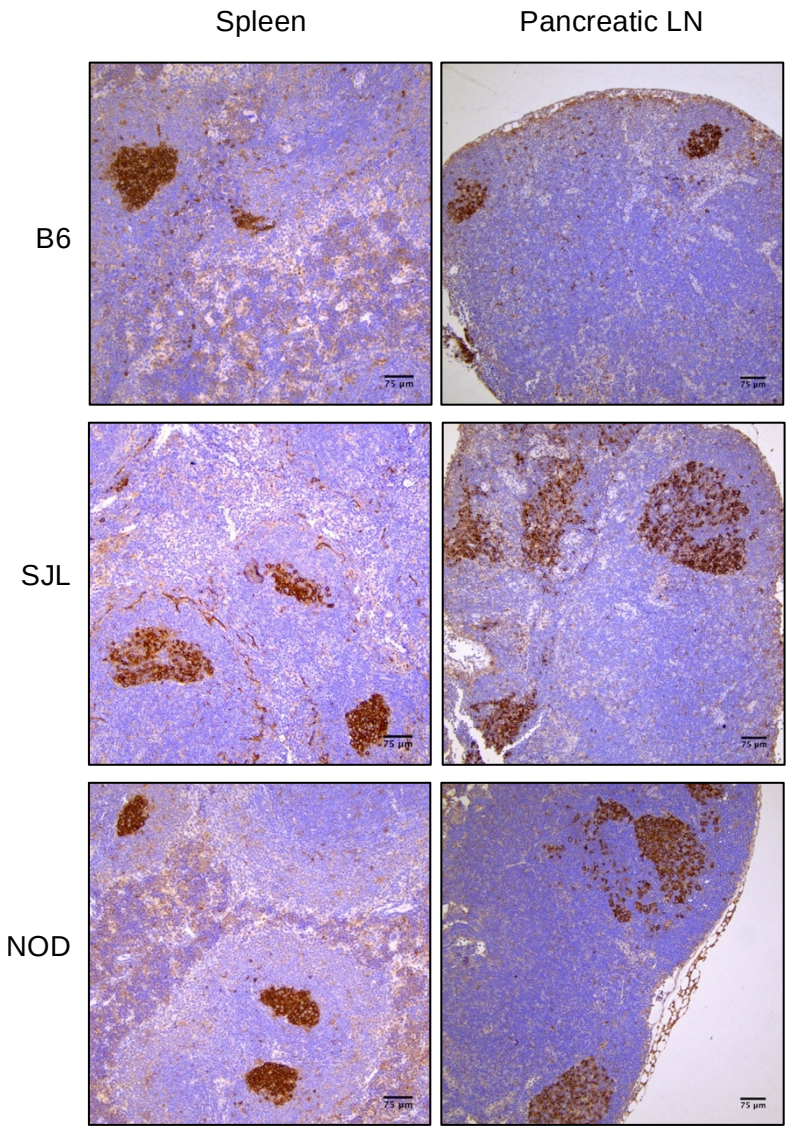

Figure 2.16. Pancreatic lymph nodes of T1D-susceptible mice reveal enlarged GC
9-10-week-old female mice were i.p. injected with CVB4 (20 PFU for B6; 10^5 PFU for NOD and SJL) and sacrificed 21 days pi. Spleen and pancreatic lymph nodes were stained by immunohistochemistry for PNA to define GC B cells. Scale bars indicate 75µm (original magnification x10). pi, post-infection; PFU, plaque forming units, i.p., intraperitoneally; GC, germinal centre; LN, lymph node.

2.3. DISCUSSION

A large body of research on type I diabetes over the past four decades has resulted in its characterization as a complex multifactorial disease that is most likely caused by a combination of genetic and environmental factors. However, the absence of symptoms prior to overt disease has made it difficult to identify definitive environmental triggers. Nevertheless, data from sero-epidemiological and genome-wide-association studies strongly support the notion that viral infections impose an increased risk of developing autoimmunity in genetically susceptible individuals. Based on this premise, animal models of virus-induced diabetes have attempted to elucidate pathogenic mechanisms that shape exaggerated immune responses to viruses. The present study focuses on differences in regards to viral tropism, viral persistence, immune cell infiltration and chronic inflammation between mouse strains with different propensities for T1D following infection with CVB4-E2.

Viral strains utilized in T1D studies, including picornaviruses (e.g. CVB), encephalomyocarditis (EMC) virus, Kilham rat virus (KRV) and lymphocytic choriomeningitis virus (LCMV), have been reported to mediate beta cell destruction either via direct infection or through initiation of autoimmune responses against beta cell antigens (Guberski et al., 1991; Jun and Yoon, 2003; von Herrath et al., 2002; Yoon et al., 1985; Yoon et al., 1978). However, due to its isolation from the pancreas of a diabetic patient and its capacity to directly infect beta cells *in vitro*, the E2 variant of the CVB4 Edwards strain (CVB4-E2) has become the most widely studied viral strain in T1D research.

Studies on the effect of CVB4 infection on beta cell integrity *in vivo* have been inconclusive, with some suggesting either tropism for the endocrine or exocrine tissue (Yap et al., 2003; Yoon et al., 1978). The data presented in this chapter support the notion that CVB4 infection in mice exclusively manifests within exocrine tissue (VP1 staining, Fig. 2.5), suggesting that destruction of pancreatic islets is likely mediated by infiltrating immune cells rather than direct virus-mediated cytolysis. As far as CVB4 tropism in humans is concerned, pancreatic islets, and in particular pancreatic beta cells seem to be predominantly affected, supporting a direct cytopathic effect of CVB4 (Dotta et al., 2007; Frisk and Diderholm, 2000). It is hypothesized, that the disagreement in cellular tropism between human and mouse possibly reflects differences in the expression of surface receptors facilitating viral entry. Notably, the immunohistochemical analysis of the previously reported viral entry receptors CAR and DAF was inconsistent with CVB4 tropism for the exocrine tissue as determined by VP1 staining patterns (Fig. 2.5). A potential source of discrepancy may be related to the utilized anti-VP1 antibody, which has been reported by some groups to bind non-viral antigen (Hansson et al., 2013). However, other groups have advised that careful protocol optimization ensures immunolabelling of enteroviral capsid protein (Richardson et al., 2014). In line with the acute tissue damage observed within the exocrine tissue, and the capacity of beta to produce insulin as suggested by IHC staining, it is believed that CVB4-E2 does not directly target pancreatic islets in mice. Unless this viral strain utilizes other unknown mechanisms of entry, positive staining of CAR and DAF within the islets of uninfected mice was probably a result of non-specific antibody interactions. Similarly, increased

'tissue stickiness' following CVB4 infection seems to provoke non-specific immunolabelling within the exocrine tissue (Fig. 3.5), although virus-mediated induction of CAR and DAF cannot be excluded. In agreement with the notion that CVB4 infection in mice targets acinar cells within the exocrine pancreas, several other groups have reported limited expression of CAR and DAF within murine islets (Hindersson et al., 2004; Mena et al., 2000). Overall, the discrepancies in cellular tropism between human and mouse CVB4 infections represent a limitation for the extrapolation into clinical settings.

In addition to cellular tropism, viral persistence within the pancreatic tissue has also been suggested as pathogenic factor threatening beta cell integrity. Ongoing viral presence is associated with exacerbated inflammation and local tissue injury, which increases the risk of sequestered beta cell antigen. However, no viral replication was found in relevant immune (thymus, spleen), peritoneal (intestine, liver) or tropism-related (pancreas, heart) organs beyond day 14 pi in any of the analysed strains (Fig. 2.2). Also, the marginally accelerated viral clearance observed in T1D-resistant B6 mice did not translate into reduced inflammation of the pancreas at that time point (Fig. 2.6). Thus, viral persistence in form of replicating virus itself does not seem to contribute to the development of chronic inflammation seen in both SJL and NOD mice. Nevertheless, the persistence of viral antigen per se has not been ruled out *per se*. Antigen depots on FDCs have been shown to be associated with CD69+ Tfh cells that survive for extended periods of time following the resolution of the germinal centre reaction (Fazilleau et al., 2007).

Of note, enteroviral RNA has been found within peripheral blood and pancreas samples of recently diagnosed T1D patients (Krogvold et al., 2015; Oikarinen et al., 2011; Yin et al., 2002). Thus, whether CVB4 mRNA persists within any of the above-mentioned organs, and if so, whether there is a qualitative and/or quantitative difference between T1D-resistant and T1D-susceptible strains, could be addressed in future studies. In that context, a study by Jaïdane and colleagues detected CVB4 E2 RNA within various organs of *Swiss Albino* mice up to 70 days after oral inoculation (Jaidane et al., 2006). However, the detection of viral RNA in humans may simply reflect acute infection, and does not provide evidence for a role of viral persistence in the development of autoimmune diabetes. So far, only few studies have detected viral RNA in tissues from long-term T1D patients, including blood (Schulte et al., 2010), and the intestine (Oikarinen et al., 2012). By contrast, a large-scale prospective study has linked the presence of enteroviral RNA with an increased risk of progression to clinical diabetes, but found no evidence of viral RNA in blood or rectal samples at the time of diagnosis (Stene et al., 2010). Accordingly, the contribution of viral persistence to disease outcome requires further evaluation.

Independent of viral persistence, exaggerated tissue damage inflicted upon the exocrine and/or endocrine pancreas during viral infections can initiate chronic inflammation and antigen sequestration. In the present study, infection with CVB4 triggered comparable levels of pancreatitis in B6, SJL and NOD mice during the first 14 days post infection. However, the level of inflammation detected by day 28 pi within exocrine tissues was more severe in T1D-prone

SJL and NOD mice compared to B6 (Fig. 3.9B), suggesting that the degree of chronic inflammation positively correlates with disease progression. In addition, autoreactive responses in form of peri-insulitis were observed early after infection in NOD mice, indicating this CVB4 strain accelerates the development of T1D in these mice under the described conditions. Despite considerable tissue injury observed by day 28 pi, B6 mice displayed no signs of islet cell damage or autoimmune insulitis (Fig. 2.9A), and completely lacked the formation of tertiary lymphoid structures observed in T1D-susceptible mice. Therefore, while the risk for antigen sequestration would have been similar across all strains, one might speculate that the disposition for establishing these organized immune cell accumulations within target organs is associated with an increased risk of attracting and/or generating autoreactive cells.

Interestingly, CVB4 infection in SJL mice caused severe destruction of the exocrine pancreas but also induced low to moderate insulitis in about 30% of the islets. However, within the 4-week observation period, none of the CVB4-infected SJL mice developed hyperglycemia or overt diabetes. Previous studies on virus-induced T1D in SJL mice have shown that 60-80% of female and male animals became hyperglycemic by day 21 following infection with EMC virus, and that this was related to direct destruction of pancreatic beta cells (Boucher et al., 1975; Jordan and Cohen, 1987; Kang and Yoon, 1993). While EMC virus has been shown to induce autoimmune diabetes in several experimental animal models, its role in clinical settings appears to be insignificant. Notably, the impact of CVB4 infections on T1D development in SJL mice has remained largely unexplored. A study by Yap and colleagues

found significantly increased glucose concentrations in CVB4-infected male SJL mice on day 22, 36 and 56 pi (Yap et al., 2003). However, glucose levels were determined in heart blood, which shows an average positive bias of +80% compared to commonly measured tail tips (Chan et al., 2012), and mice in this study were supplemented with pancreatic enzymes. The authors concluded that CVB4-induced hyperglycemia in SJL mice is related to exaggerated damage of the exocrine pancreas that prevents adequate islet neogenesis, rather than a direct autoimmune attack of the pancreatic beta cells (Chan et al., 2012). The work presented here focused on islet pathogenesis within the first 4-weeks post infection, and thus cannot draw any conclusions in regards to long-term islet neogenesis and/or survival. Similarly, differences in gender, pancreatic enzyme supplementation and glucose measurement complicate a direct comparison of our results to other studies. Notably, however, both SJL and NOD mice showed increased pancreatitis and insulitis over diabetes-resistant B6 mice (Fig. 2.9) despite equivalent viral titres detected during the peak of infection (day 4). This suggests that increased levels of inflammation early after viral infections may be associated with a higher T1D risk. Future studies will have to investigate whether SJL mice exhibiting islet inflammation develop hyperglycemia over time, and if so, whether this is related to above-threshold damage inflicted upon the exocrine pancreas.

When investigating the autoimmune destruction of pancreatic islets, it is important to separate the direct effect of the virus from de-regulated innate and/or adaptive host responses. Comparative flow cytometric analyses exposed clear differences in the immune response to CVB4 across the three

examined mouse strains, which may have important implications for T1D pathogenesis. With respect to innate immunity, the extensive macrophage infiltration of the pancreas observed across all strains by day 7 pi (Fig. 2.12A), suggests that this population is critical for controlling viral replication and monitoring tissue damage, but also opens up the possibility of macrophage-mediated viral spread and/or tissue damage. In line with the latter, NOD mice displayed significantly increased macrophage frequencies at this time point, which was paralleled by more severe pancreatitis (Fig. 2.6). Similarly, other studies have linked the severity of inflammation to the degree of macrophage influx post infection (Fairweather et al., 2006; Fairweather et al., 2003). Therefore, while early protection from CVB4 appears to be macrophage-mediated, their contribution towards chronic inflammation and autoimmunity in the context of picornavirus infections should be further addressed.

Examination of immunodeficient B6.RAG1 and NOD.SCID mice further emphasized the essential role of the adaptive immunity to CVB4 infection. Despite similar viral clearance as their immunocompetent counterparts, both B6.RAG1 and NOD.SCID showed 100% mortality by day 21 pi, clearly illustrating the requirement of functional B and T cells for the survival of CVB4-infected mice. While others have reported similar mortality rates in SCID mice on a Balb/c background (Nonoyama et al., 1993; Ramsingh et al., 1999), the findings presented in this study are in strong disagreement to those of Precechtelova et al., who found 100% survival of NOD.SCID mice at this time point despite slightly increased viral titre (Precechtelova et al., 2015). This disagreement might be related to differences in mouse gender, age of infection

and/or strain-dependent ‘leakiness’ (Nonoyama et al., 1993) - resulting in different proportions of mature lymphocytes.

Adaptive immune responses to many noncytopathic viruses are often dominated by cytotoxic T lymphocytes that recognize infected cells and prevent further viral shedding. By contrast, adaptive responses to cytopathic viruses like coxsackievirus have been reported to rather rely on neutralizing antibodies that bind to infectious virions within extracellular spaces (Kagi and Hengartner, 1996). The current study supports the notion that cytotoxic CD8+ T cells play a subordinate role in the adaptive immunity to CVB4, that is in B6, SJL and NOD mice. However, this supposition requires further verification by functional assays. Adaptive responses in all analysed strains involved both the cellular and humoral arm, but demonstrated a clear CD4+ Th1 phenotype with predominant production of IgG2a antibodies (Fig. 2.13 and 2.15). Furthermore, CVB4 infection in T1D-susceptible mice resulted in either early (SJL) or late (NOD) T_{FH} responses, accompanied by the presence of GC-like B cells (Fig. 2.15).

By three weeks post infection, T1D-resistant B6 mice showed significantly reduced frequencies of activated CD4+ T cells and of class-switched IgG2a GC-like cells, and had almost completely abrogated the T_{FH} response. SJL mice, which showed a strong Th1 phenotype early after infection, displayed moderate inflammation by day 21 pi, which may reflect that only a certain proportion of these mice develops chronic inflammation to CVB4. Strikingly, inflammation in NOD mice was characterized by significantly higher proportions of activated CD4+ T cells, T_{FH} cells and GC-like B cells of the

IgG2a isotype. Ongoing Th1 and T_{FH} responses have been shown to promote the generation of autoimmune T and B cells respectively, both of which are important pathogenic elements in human and mouse T1D (Ishigame et al., 2013; Ludewig et al., 1998; Okazaki et al., 2000; Wilson et al., 1998). For instance, blockade of the Th1 signature cytokine IFN-γ is sufficient in preventing T1D in NOD mice (Campbell et al., 1991; Debray-Sachs et al., 1991). Also, T1D patients display increased IFN-γ responses to stimulation with islet autoantigens compared to healthy subjects (Petrich de Marquesini et al., 2010; Sarikonda et al., 2014). By contrast, the potential involvement of T_{FH} cells in T1D development has only recently been appreciated. Memory phenotype T cells of T1D patients have been reported to display a strong T_{FH} signature (Kenefeck et al., 2015; Xu et al., 2013) and increased numbers of T_{FH} cells have been found in T1D patients. Accordingly, TLS detected within the exocrine pancreas of SJL and NOD mice are likely to contribute to chronic inflammation and autoimmunity by producing highly activated and differentiated B lymphocytes of the IgG2 phenotype.

In summary, this chapter represents a comparative study of CVB4 infection in different mouse strains and defines pathogenic factors that are associated with disease outcome. We found that T1D-propensity was not related to differences in CVB4 replication within the target organ. However, independent of the genetic background, T1D-prone mice displayed prolonged pancreatic inflammation after viral clearance, thereby supporting the notion that exaggerated immune responses to virus are indicative of an increased T1D risk. Furthermore, inflammation in T1D-susceptible SJL and NOD mice was

characterized by an accumulation of Tfh and GC-like B cells that were organized within tertiary lymphoid structures. In line with clinical observations, these findings suggest a crucial role of Th cell populations and autoantibodies in T1D development and may facilitate the advancement of improved therapeutics.

3. REGULATION OF IMMUNE RESPONSE GENES IN PANCREATIC BETA CELLS DURING AUTOIMMUNE AND VIRUS-INDUCED INFLAMMATION

3.1 INTRODUCTION

One of the most intriguing enigmas surrounding virus-induced T1D is the targeted autoimmune assault on pancreatic beta cells that leaves neighbouring alpha and delta cells intact (Dotta et al., 2007; Richardson et al., 2009). Due to their multitude of metabolic functions, beta cells rank among the most specialized cell types found within the human body. However, their capacity to initiate autonomous immune responses to viral infections has long been underestimated. The increased levels of type I interferons and other proinflammatory cytokines detected within virus-infected pancreatic islets have predominantly been accredited to immune cell infiltrates, while beta cells have been regarded as innocent bystanders. With the development of next generation sequencing technologies and the subsequent analysis of islet and/or beta cell transcriptomes, it became evident that beta cells not only express the required tools to sense viral RNA in the cytoplasm (i.e. RIG-I and MDA5), but they also produce an array of antiviral factors upon infection with pancreatrophic viruses (Aida et al., 2011; Ferreira et al., 2014; Marroqui et al., 2015). Generally, all cells alter their gene expression upon virus infection. This change in gene expression and protein translation is thought to focus the cells' energy on cell defence and survival. In this regard, energy consuming functions, such as insulin production, can be switched off during virus infection

(Eizirik et al., 2012; Shimizu et al., 1980) and thus, the beta cell must have cell intrinsic defences that reduce the duration of infection. However, such virus defensive programs must be regulated as they can have damaging effects on the cell itself as well as on the surrounding tissue. As a result of unbalanced antiviral responses, beta cells might directly contribute to ongoing inflammation in the pancreas and could thereby propagate their own autoimmune destruction. Since this could have important implications for disease pathology and therapeutic intervention, it is crucial to gain a better understanding of beta cell intrinsic gene signatures and functional processes following viral infection *in vivo*. However, the heterogeneous architecture of the pancreas combined with the lack of reliable antibodies to clearly distinguish between individual cell populations has considerably impeded beta cell research.

This chapter defines a robust strategy for the isolation of pure beta cell populations that enables the extraction of sufficient amounts of high-quality RNA suitable for next-generation sequencing experiments. Implementation of this methodology enabled in-depth gene expression profiling studies in pancreatic beta cells obtained from T1D-resistant and T1D-prone mice following CVB4-infection, and to compare these signatures to those obtained from autoimmune NOD mice. Furthermore, analyses of the coding and non-coding regions facilitated the generation of an atlas of the endogenous retrovirus (ERV) beta cell transcriptome during both virus infection and sterile-autoimmune inflammation. This unique inside-outside analysis of virus infection has provided insights into past interactions between our ancestors and viruses as well as an offered an intriguing explanation for selection and retainment of ERVs in the mammalian genome.

3.2 RESULTS

3.2.1 Optimization of beta cell purification and subsequent extraction of high-quality RNA

The characterization of beta cell specific gene expression patterns in physiological and pathological conditions requires the isolation of pure beta cells. Although islet cell types can be distinguished via flow cytometry by intracellular staining of their respective hormones, this technique requires chemical fixation and permeabilization of cells, thus impeding downstream extraction of high quality RNA for transcriptome analysis. While the usage of transgenic mouse models expressing a reporter gene under the insulin promoter overcomes this issue, this kind of genetic manipulation is likely to impact the expression of other gene transcripts and is therefore unsuitable for the present study.

In order to obtain pure beta cell populations, different strategies were assessed based on fluorescence-activated cell sorting (FACS). One of the most common methods of beta cell purification is based on the high content of endogenous flavins found within beta cells, mainly flavin adenine dinucleotide (FAD), which results in increased levels of autofluorescence compared to other pancreatic cell types (Van de Winkle et al., 1982; Vandewinkel and Pipeleers, 1983). However, the FAD content strongly depends on the metabolic state of the tissue and may thus vary across experimental conditions, thereby compromising the consistency of purification results (Smelt et al., 2008). Alternatively, beta cells could be separated by making use of reliable surface markers. Studies on the pancreatic beta cell surface proteome have identified

a limited number of unique surface markers that are constitutively expressed on pancreatic beta cells independent of developmental stage and metabolic condition, and that are therefore suitable to discriminate beta cell from non-beta cell populations. Two promising candidates are the transmembrane protein 27 (Tmem27), which is exclusively expressed on the surface of pancreatic beta cells and in kidney ducts (Akpinar et al., 2005; Fukui et al., 2005; Hald et al., 2012; Zhang et al., 2001), and glucose transporter Glut2 (Glut1 in humans), which is constitutively expressed by murine beta cells within their lateral microvilli (Orci et al., 1989; Pang et al., 1994). In addition to Tmem27 and Glut2, the zinc-sensitive fluorescent probe Newport Green was included in the analysis. Newport Green staining takes advantage of the high concentrations of intracellular zinc stored within the insulin crystals of pancreatic beta cells and exhibits peak excitation and emission wavelengths of 485 and 530 nm, respectively (Lukowiak et al., 2001).

Prior to FACS-based separation, pancreatic islets were isolated and subsequently dissociated into single cell suspensions using well-established methodologies (see section 6.19). Subsequently, cells were incubated with antibodies against Tmem27 or Glut2, or resuspended in PBS containing Newport Green. In order to eliminate hematopoietic cells (from possible blood contamination or from virus-induced islet infiltration), endothelial cells and dead cells from the analysis, samples were further stained for CD45.2, Pecam-1 and DAPI (4',6-diamidino-2-phenylindole), respectively. Cells were then filtered through a 70 µM strainer and subjected to FACS-based cell sorting (BD FACSAria III cell sorter). The forward and side scatter plot was used to identify

cells (gate P1 Fig. 3.1, top left panel) and to exclude debris. This gate was copied to a subsequent plot to select single cells (gate P2) based on forward scatter height and area (Fig. 3.1, second panel from top). Subsequently, it was gated on live cells (gate P3, DAPI-) and both hematopoietic cells (CD45.2+) and endothelial cells (Pecam-1+) were excluded. Finally, cells positive for Newport Green (Fig. 3.1 bottom left panel), Glut2 (Fig. 3.1, second panel from bottom) or TMEM27 (Fig. 3.1, third panel from bottom), or cells with high autofluorescence upon excitation with the 488 nm laser and the 633 nm laser (Fig. 3.1, bottom right panel), were sorted into collection tubes. In order to maximize sorting efficiency, samples were acquired at low event rates (5000 events/s) and low concentrations (10^6 cells/ml).

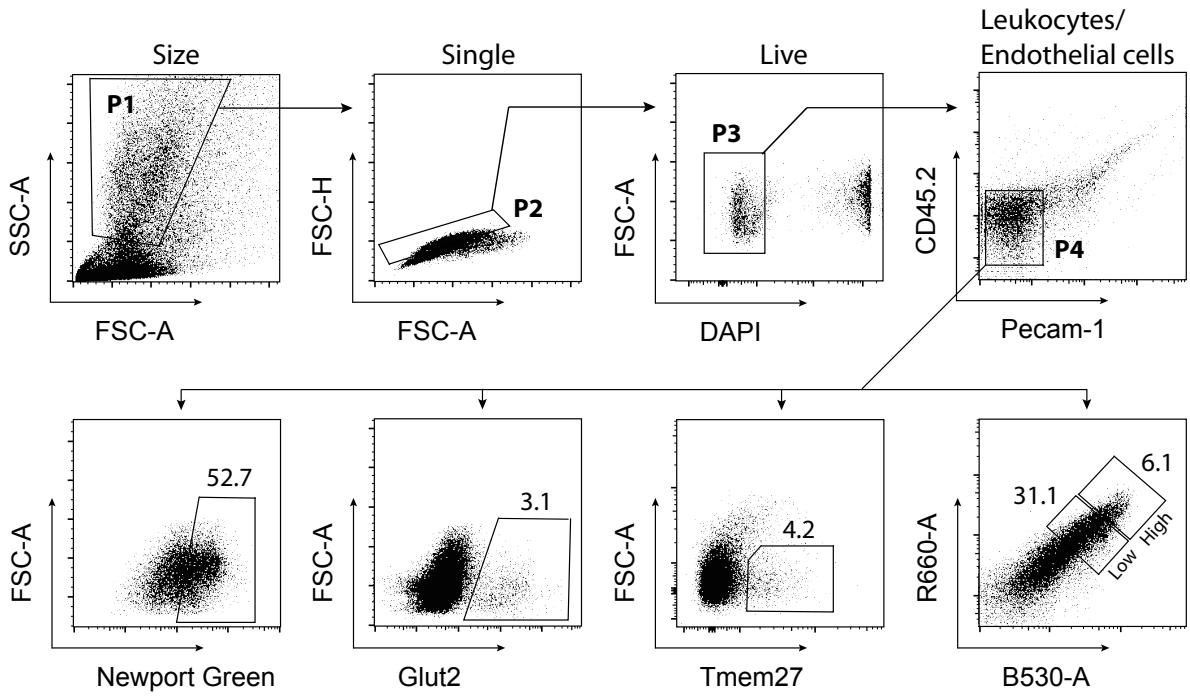

Figure 3.1. Fluorescence activated cell sorting (FACS) strategy of pancreatic beta cells
Pancreatic islets isolated from 9- to 10-week old female B6 mice were dispersed and analysed by flow cytometry. Representative plots illustrate the gating strategy. FSC, forward scatter; SSC, side scatter; Glut2, glucose transporter Glut2; Tmem27, transmembrane protein 27; DAPI, 4',6-diamidino-2-phenylindole.

To assess the beta cell purity for each sorting strategy, RNA was extracted from each sample and subjected to quantitative real-time PCR. Each sample was tested for the presence of pancreatic beta cells (insulin), exocrine tissue (amylase), endothelial tissue (Pecam), alpha cells (glucagon), delta cells (somatostatin) and major immune cell subsets (CD19 as a marker for B cells, CD3 as a marker for T cells). Furthermore, the pancreatic beta cell line (MIN6) was included in the analysis as internal control.

Importantly, gene expression levels of B cell (*CD19*) and T cell (*CD3*) markers were below the cut-off of reliable detection for all sorting strategies (Fig. 3.2), thus showing that CD45.2 based exclusion of these immune subsets was highly effective. As expected, MIN6 cells displayed high expression levels of insulin (Fig. 3.2), while non-beta cell transcripts were found to be absent. By contrast, Glut2- and Tmem27-based cell sorting not only resulted in poor yields (Fig. 3.1), but was also contaminated with glucagon-expressing pancreatic alpha cells (Fig. 3.2). This was particularly evident after Glut2-based sorting. Moreover, the absolute amount of insulin gene expression was relatively low for both antibody-based strategies (Fig. 3.2). By contrast, Newport Green- as well as autofluorescence-based strategies displayed a strong beta cell enrichment profile (insulin positive) (Fig. 3.2). However, autofluorescence-based strategies showed higher contamination with glucagon-expressing (high AF), amylase-expressing (high AF) and somatostatin-expressing (low AF) cells (Fig. 3.2). Samples sorted using Newport Green had lower levels of these contaminants, in particular of amylase-expressing exocrine cells (Fig. 3.2), which was previously reported to be the most common contaminant of beta cell isolates (Fotiadis et al., 2005; Morton et al., 2007; Nielsen et al., 1979).

Based on these results, Newport Green was selected as the optimal strategy for the isolation of highly pure pancreatic beta cells.

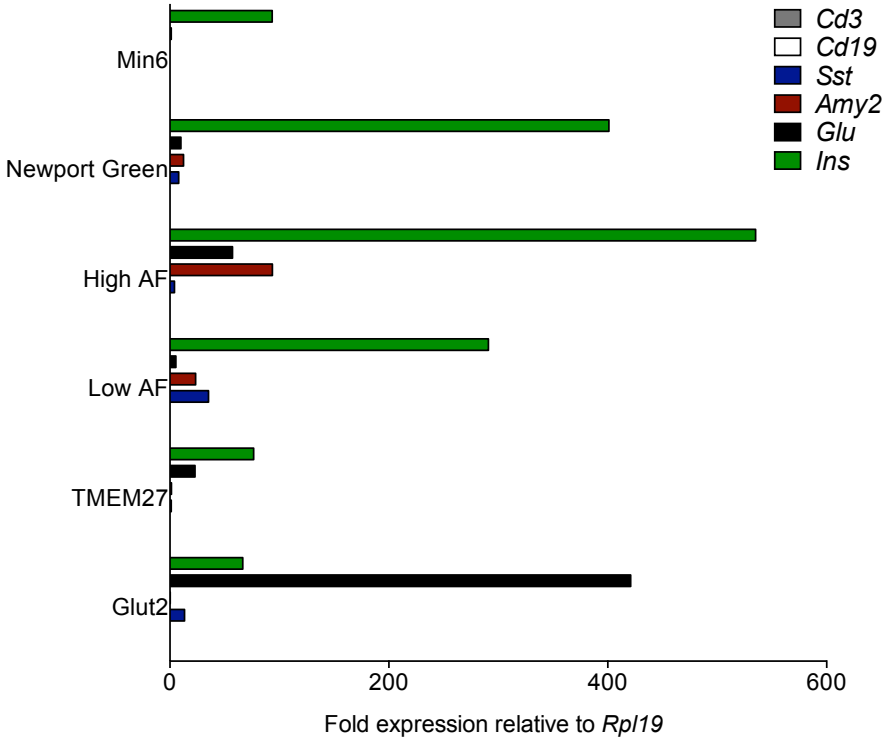

Figure 3.2. Validation of gene expression profiles of different beta cell gating strategies
FACS-sorted cells were analysed by quantitative real-time PCR. Gene expression levels of selected genes are presented relative to housekeeping gene Rpl19. AF, autofluorescence; Glut2, glucose transporter Glut2; Tmem27, transmembrane protein 27; Glu, glucagon; Sst, somatostatin; CD19, B-lymphocyte antigen; CD3, cluster of differentiation 3; Rpl19, ribosomal protein L19.

3.2.2 Beta cell specific transcriptome signatures following virus infection and autoimmunity

The causal relationship between viral infections and T1D is yet to be established. In view of that, it is critical to determine to what extent pancreatic beta cells actively direct local immune responses to virus. This will provide important clues regarding their contribution to chronic inflammation and autoimmunity in the pancreas. To address this question, the previously established Newport Green-based sorting strategy (see section 3.2.1) was utilized for the isolation of pancreatic beta cells from non-infected C57BL/6 (B6), SJL/JArc (SJL), NOD/ShiltJAusb (NOD) and NOD.SCID mice, as well as from CVB4-infected B6 and SJL mice (day 4 post infection). As shown in Chapter 2, mouse strains were chosen based upon their propensity to develop chronic inflammation following CVB4 infection (SJL), resistance to CVB4-induced chronic inflammation and propensity to develop spontaneous (sterile) autoimmune islet inflammation and T1D (NOD mice). All mice were female and 8-12 weeks-of-age at the time of tissue processing. This age represents a pre-clinical stage of diabetes in the NOD cohort. RNA sequencing (RNA-seq) was performed and the response of pancreatic beta cells to inflammation from CVB4 infection (i.e. CVB4-infected versus non-infected B6 and SJL mice) and from spontaneous autoimmunity (i.e. NOD versus NOD.SCID mice) analysed. Due to the difficulty of obtaining adequate amounts of RNA from highly purified beta cells, RNA-seq analyses was performed from 18-25 pooled mice per group. Principal component analysis (PCA) of the data demonstrated CVB4-infection as the major source of variation in gene expression levels amongst all

samples (Fig. 3.3A). Furthermore, it also highlighted the dissimilarity between immunodeficient NOD.SCID and immunocompetent NOD mice (Fig. 3.3A). Importantly, the majority of variation between datasets was accounted for by the first principal component (component 1, Fig. 3.3B), further emphasizing the clustering of T1D-prone (SJL, NOD) versus T1D-resistant (B6, NOD.SCID) mouse strains. Statistical analysis of differentially expressed (DE) genes identified 148 overlapping transcripts that were significantly induced after CVB4 infection (B6.CVB4 vs. B6, SJL.CVB4 vs. SJL) and in spontaneous autoimmunity (NOD vs. NOD.SCID) Fig. 3.4A). In addition, the total number of genes significantly activated during CVB4 infection (411 genes in SJL, 320 genes in B6) was considerably higher than those in the autoimmune model (223 in NOD). Notably, the level of gene induction was higher in T1D-prone SJL mice compared to T1D-resistant B6, as shown by the top 50 most up-regulated genes (Fig. 3.4B)

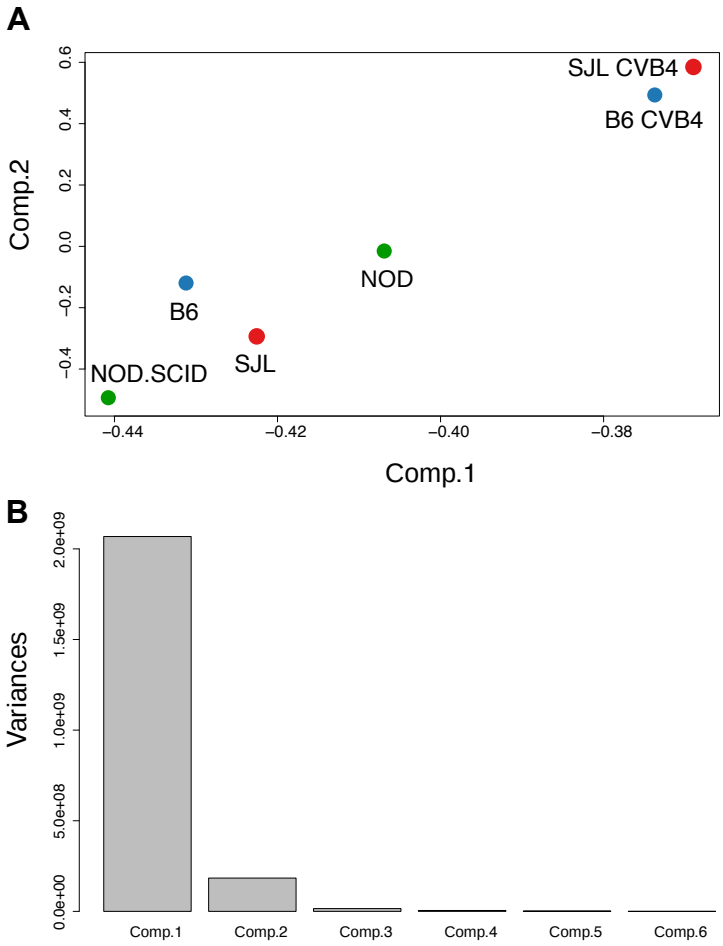

Fig. 3.3. Principal component analysis of log normalized FPKM values

(**A**) Principal-component analysis of RNA-seq transcripts from pancreatic beta cells isolated from uninfected B6 (B6), SJL (SJL), NOD (NOD) and NOD.SCID (NOD.SCID) mice, and from CVB4-infected B6 (B6 inf) and SJL (SJL inf) mice. (**B**) Variances of components 1 and 2 account for most of the variation in the data set. Individual datasets are derived from cells pooled from 18-25 mice. Comp., component.

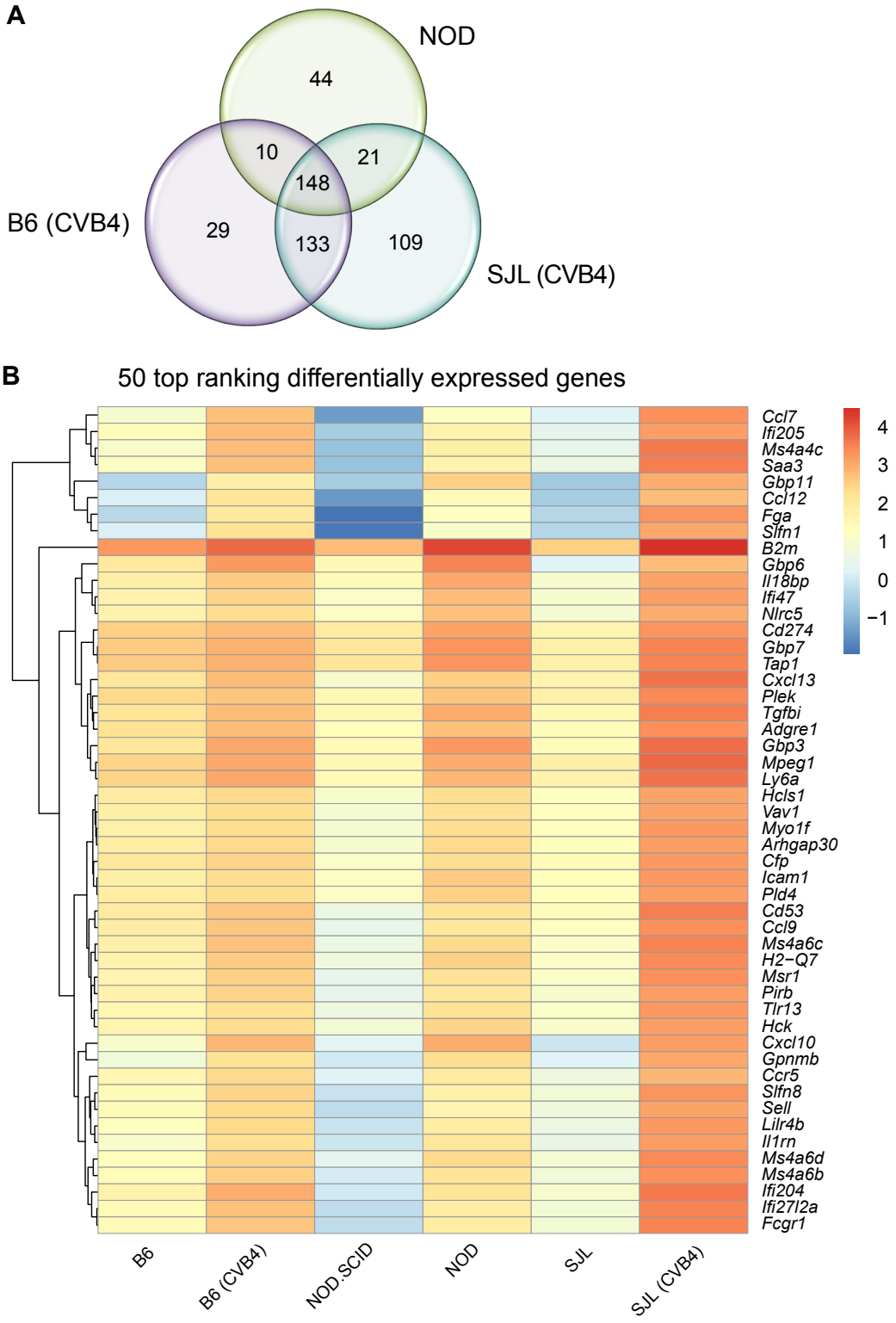

Figure 3.4. Commonly induced genes upon CVB4 infection and spontaneous autoimmunity

(**A**) Venn diagram illustrating the number of common and unique up-regulated transcripts in pancreatic beta cells in response to CVB4 infection (B6, SJL) and/or spontaneous autoimmunity (NOD vs. NOD.SCID) (≥log2-fold change in expression, FDR < 0.05). (**B**) Heatmap of the log10 counts (normalized) of the top 50 genes that are commonly up-regulated in response to both CVB4 infection and spontaneous autoimmunity (NOD vs. NOD.SCID) (FDR < 0.05). FDR, false-discovery rate.

The top-ranking genes commonly induced upon CVB4 infection and spontaneous autoimmunity comprised type I IFN-inducible genes (*Ccl7*, *Slfn1*, *Gbp11*, *Gbp6*), IFN gamma-inducible genes (*Ifi205*, *Ccl12*, *B2m*), and genes involved in acute-phase responses (*Saa3*, *Fga*) (Fig. 3.4B). GSEA (Gene set enrichment analysis) based gene ontology analysis of commonly DE genes (Subramanian et al., 2005) indicated a clear enrichment of immune response processes (Fig. 3.5).

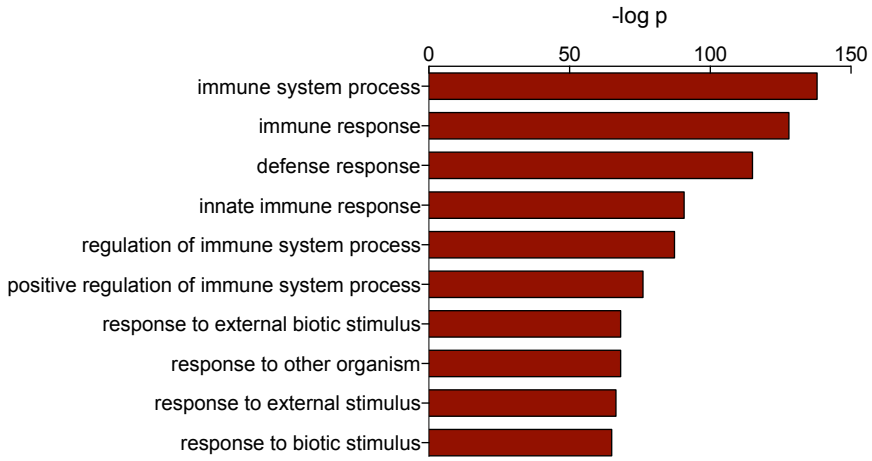

Figure 3.5. Gene ontology (GO) representation of top 10 ranking categories
Based on their p-value, listed are the top 10 most significant GO categories (subcategory biological function) that are commonly induced in response to both CVB4 infection and spontaneous autoimmunity. p, p-value. Gene ontology performed using GSEA (Gene Set Enrichment Analysis), http://www.broad.mit.edu/gsea/.

KEGG (Kyoto Encyclopedia of Genes and Genomes) pathway enrichment analysis (Kanehisa and Goto, 2000; Kanehisa et al., 2016) further illustrated the activation of pathways related to innate immune responses (Fig. 3.6A), such as *phagosome* (ID: mmu04145), *toll-like receptor signalling* (ID: mmu04620) and *natural killer cell mediated cytotoxicity* (ID: mmu04650). Interestingly, KEGG analysis also revealed enrichment of genes involved in autoimmune disorders, including *systemic lupus erythematosus* (SLE, ID: mmu05322), *type I diabetes mellitus* (ID: mmu04940) and *rheumatoid arthritis*

(ID: mmu05323). Activation of these pathways was predominantly attributed to induction of antigen processing genes (e.g. *CD40*, *CD86*, *H2-D1*, *H2-DMa*), complement cascade genes (e.g. *C1q*, *C2*, *C3*), histone genes (SLE only) and/or proinflammatory cytokines and chemokines (*Il1b*, *Il6*, *Il15*, *Ccl2*, *Ccl3*, *Ccl5*, *TNFa*). Remarkably, analysis of overlapping gene expression between pre-diabetic NOD mice and CVB4-infected mice revealed a significant enrichment of the following viral response pathways: *herpes simplex virus* (ID: mmu05168), *measles* (ID: mmu05162) and *viral myocarditis* (ID: mmu05416). Indeed, despite the absence of an exogenous virus infection, pre-diabetic NOD mice showed significant induction of anti-viral gene transcripts, including robust induction of *Ifna2* (interferon alpha 2), *Ifi44* (interferon-induced protein 44), *Mx1* (interferon-induced GTP-binding protein) and Oas1 (2'-5'-oligoadenylate synthetase 1) (Fig. 3.6). Moreover, given that CVB4 (like all picornaviruses) does not undergo a DNA stage (Holland et al., 1982), the enrichment of genes involved in cytosolic DNA sensing (ID: mmu04623, Fig. 3.6A) is somewhat surprising and suggests the presence of DNA templates unrelated to CVB4, possibly from self-DNA released during virus-induced tissue damage.

While the majority of significantly altered pathways were activated (n=108), only four were found to be significantly suppressed) (Fig. 3.6B). Down-regulated pathways were related to anabolic metabolic processes, such as *biosynthesis of amino acids* (ID: 01230), or *insulin secretion* (ID: 04911).

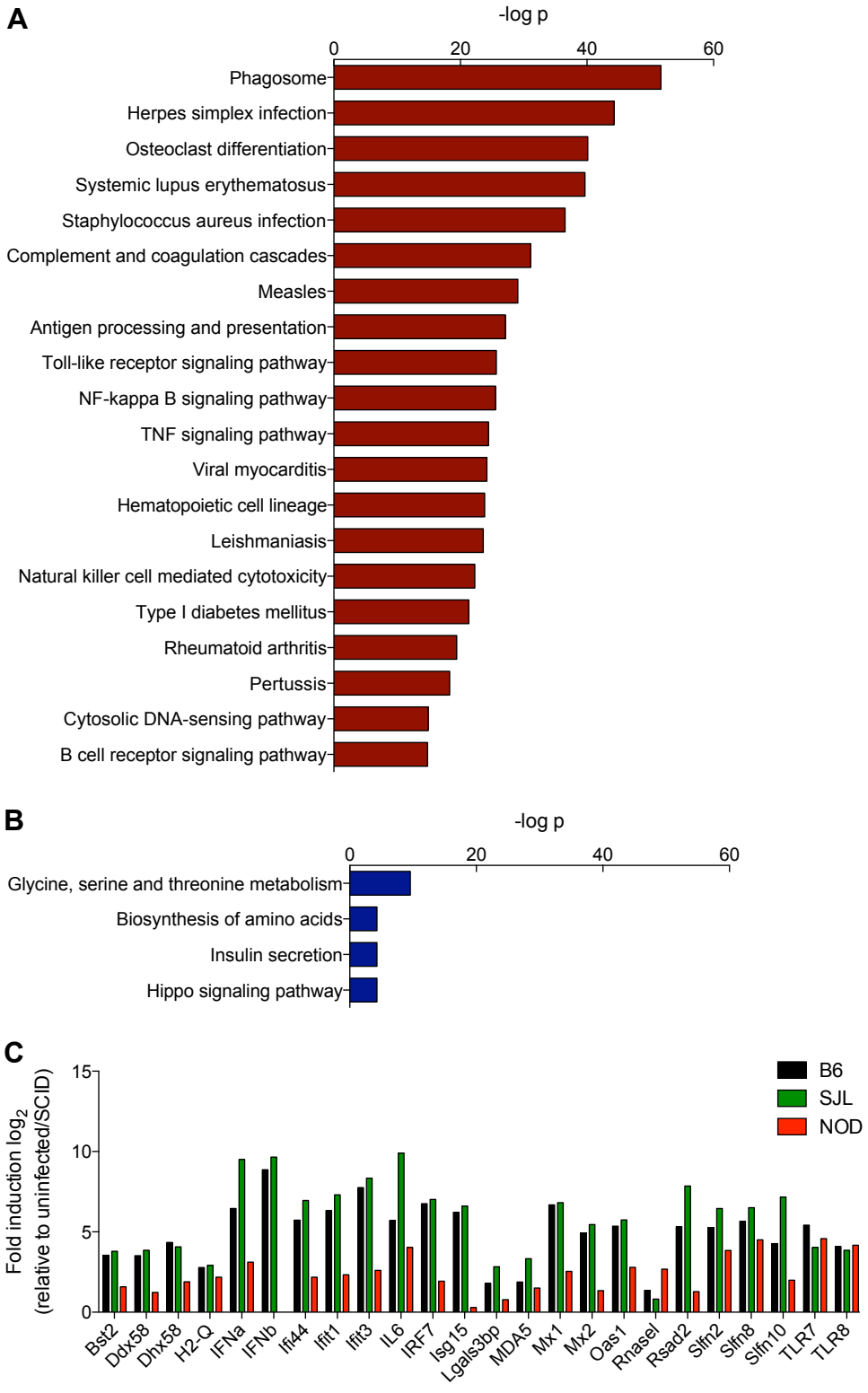

Figure 3.6. Significantly changed KEGG pathways indicate antiviral immune responses
KEGG pathways that are significantly up-regulated (A) and down-regulated (B) in response to both CVB4 infection and spontaneous autoimmunity are ranked based on their p-value. Only pathways with a minimum of 30 annotated genes were included in the analysis. (C) Log_2 fold changes of virus response genes are presented relative to mock-infected mice (B6, SJL) and to NOD.SCID, respectively. p, p-value.

Individual ranking of the top differentially expressed genes activated upon CVB4 infection mostly reflected type I IFN signalling (e.g. *Slfn1*, *Slfn4*, *Phf11b, Isg15, Ifit2*) and acute phase responses (e.g. *Fga*, *Fgg*) for both B6 and SJL mice (Table 3.1). Similarly, top up-regulated genes in pre-diabetic NOD mice also highlighted the activation of type I IFN (e.g. *Cxcl9*, *Gbp2b, Gbp11*) and type II IFN associated genes (e.g. *Gm4841* (*Ifgga3*), *F830016B08Rik* (*Ifgga4*) (Table 3.2). Taken together, the high abundance of IFN-related transcripts found both in CVB4-induced and autoimmune inflammation suggests a potential link between viral infections and exaggerated inflammation of the target tissue leading to autoimmunity.

Table 3.1. The top 10 most differentially expressed genes in response to CVB4

Gene ID	Gene name	Log_2 FC	FDR
B6 CVB4 vs. B6			
Slfn4	schlafen 4	10.1	9.6E-16
Slfn1	schlafen 1	9.7	2.2E-07
Serpina3n	serpin peptidase inhibitor A3n	9.2	1.2E-13
Fga	fibrinogen alpha	9.1	1.8E-07
Saa3	serum amyloid A 3	8.7	1.3E-11
Irg1	immunoresponsive 1 homolog	8.7	1.2E-08
Fgg	fibrinogen gamma	8.6	1.6E-11
Isg15	interferon-stimulated gene 15	8.6	7.7E-10
Ccl12	chemokine (C-C motif) ligand 12	8.5	1.3E-05
Ccl7	chemokine (C-C motif) ligand 7	8.5	1.7E-10
SJL CVB4 vs. SJL			
Slfn4	schlafen 4	10.9	1.3E-15
Lipg	lipase, endothelial	10.8	1.4E-10
Fga	fibrinogen alpha	10.5	4.0E-09
Phf11b	PHD finger protein 11B	10.3	4.5E-09
Fgg	fibrinogen gamma	10.1	9.0E-13
Slfn1	schlafen 1	9.5	1.3E-06
Ly6c2	lymphocyte antigen 6 complex, locus C2	9.5	8.0E-14
Ifit2	IFN-induced TPR 2	9.3	1.3E-15
Oasl1	2'-5' oligoadenylate synthetase-like 1	9.0	2.0E-09
Serpina3n	serpin peptidase inhibitor A3n	9.0	1.4E-13

FC, fold change; FDR, false-discovery rate.

Table 3.2. The top 10 most differentially expressed genes between NOD and NOD.SCID

Gene ID	Gene name	Log_2 FC	FDR
Gm4841	Interferon-gamma-inducible GTPase Ifgga3 protein	9.8	3.3E-08
Cxcl10	chemokine (C-X-C motif) ligand 10	9.7	6.7E-12
Cxcl9	chemokine (C-X-C motif) ligand 9	9.7	1.0E-10
F830016B08Rik	Interferon-gamma-inducible GTPase Ifgga4 protein	9.3	3.6E-08
Gbp2b	guanylate binding protein 2b	8.7	9.5E-07
Tgtp1	T cell specific GTPase 1	8.5	8.1E-15
Chil1	chitinase 3 like 1	8.4	3.2E-06
Ligp1	interferon inducible GTPase 1	8.3	3.8E-15
H2-M2	histocompatibility 2, M region locus 2	8.3	5.3E-05
Gbp11	guanylate binding protein 11	8.0	6.1E-07

FC, fold change; FDR, false-discovery rate.

Given that RNA-seq analyses had to be performed with primary beta cells that had been pooled from 15-20 mice per group, it was essential to perform quantitative real-time PCR (qRT-PCR) validation on pancreatic islet samples from individual mice. Therefore, to verify the role of type I interferons and type I IFN-inducible genes in response to CVB4 infection, qRT-PCR of selected genes (fold change > 3) was performed. As insufficient RNA remained from RNA-seq samples, additional RNA was obtained from total pancreas samples of CVB4-infected and uninfected B6 mice (n = 3 each). As depicted in Fig. 3.7, gene expression levels of *H2-K1* (histocompatibility 2, K1), *Eif2ak2* (eukaryotic translation initiation factor 2 Alpha Kinase 2), *Ifna2* (Interferon alpha 2), *Ifnb1* (interferon beta 1), *Il6* (interleukin 6) and *Irf7* (interferon regulatory factor 7) were within 4-fold of RNA-seq values, indicating a robust correlation between both techniques.

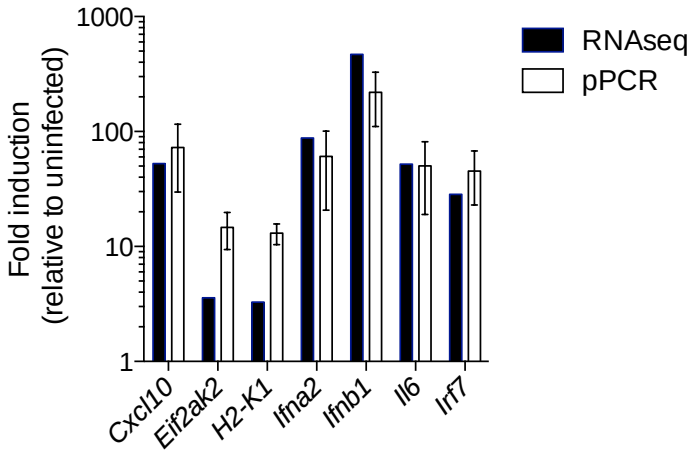

Figure 3.7. Quantitative RT-PCR validation of selected CVB4 response genes
Differential expression of selected CVB4 response genes was validated by qRT-PCR in total pancreas samples from B6 mice (n = 3). Samples were normalized to the housekeeping gene Rpl19. Fold changes are presented relative to mock-infected samples as average ± SD of three biological replicates. Results of qRT-PCR were within 4-fold of RNA-seq expression levels. Rpl19, ribosomal protein L19.

3.2.3 Expression of endogenous retroviruses in response to virus-induced and autoimmune and inflammation

Endogenous retroviral (ERV) elements comprise about 8-10% of mammalian genomes and have significantly shaped co-evolution between host and exogenous viral infections (Amariglio and Rechavi, 1993; Baltimore, 1985; McClintock, 1984; Temin, 1985). Through recognition by cytosolic PRRs, RNA and cDNA elements of endogenous retroviral origin have been reported to provoke innate immune responses that precipitate a general antiviral state (Jacob et al., 2002; Stetson et al., 2008). With the exception of germ cells, the placenta and pre-implantation embryos, the majority of endogenous retroviral genes in adult tissues are transcriptionally silenced through DNA methylation

and cellular restriction factors (Lerner et al., 1976; Seifarth et al., 2005). However, epigenetic and cellular dysregulation may result in re-activation of ERV elements in somatic cells (Maksakova et al., 2008; Rowe and Trono, 2011), and has been reported in the context of cancer (Chiappinelli et al., 2015; Roulois et al., 2015) and autoimmunity (Gray et al., 2015; Lee-Kirsch et al., 2007b; Namjou et al., 2011; Rice et al., 2012).

The previous section of this dissertation illustrated an elevated expression of viral recognition and anti-viral immune response genes in uninfected NOD mice (Fig. 3.6). Furthermore, this T1D-susceptible mouse strain displayed activation of the cytosolic DNA sensing pathway in the absence of an exogenous virus (Fig. 3.6), suggesting an accumulation of endogenous DNA. In addition, several cytosolic nucleic acid sensors, including *Mb21d1* (cyclic GMP-AMP synthase, also cGas), *Ddx58* (DEXD/H-Box Helicase 58, also RIG-I), *Aim2* (absent in melanoma 2) and *Zbp1* (DNA-dependent activator of IFN-regulatory factors) were significantly induced in uninfected NOD mice and in CVB4-infected B6 and SJL mice (Fig. 3.8A and B). As illustrated in a detailed map of the cytosolic DNA sensing pathway (Fig. 3.8A), molecular targets downstream of the receptors listed above were similarly activated (highlighted in red) and are likely to contribute to the previously identified type I interferon signature (section 3.2.2). Notably, increased expression of classic RNA sensors such as *Ddx58, Dhx58 or Ifih1* in uninfected NOD mice might reflect augmented levels of endogenous DNA, such as DNA from retroviral elements or damaged tissues, as these receptors have also been reported to respond to DNA ligands (Ablasser et al., 2009; Chiu et al., 2009; Choi et al., 2009). In addition to transcriptional silencing of endogenous retroelements, cell-intrinsic

checkpoints are in place to limit the exposure of the host immune system to self-nucleic acids including ERV elements and cellular debris. In particular, endogenous and exogenous retroviral DNA is digested by *TREX1* (3-prime repair exonuclease 1), the most abundant cytoplasmic exonuclease (Gray et al., 2015; Hoss et al., 1999; Lindahl et al., 1969; Yang et al., 2007), and by the ribonuclease function of the triphosphohydrolase *SAMHD1* (SAM domain and HD domain-containing protein 1) (Crow et al., 2006; Laguette et al., 2011; Powell et al., 2011). As SAMHD1 binds to both RNA and DNA templates, induction of this gene in response to CVB4, a ssRNA virus, was less surprising (Fig. 3.8A and B).

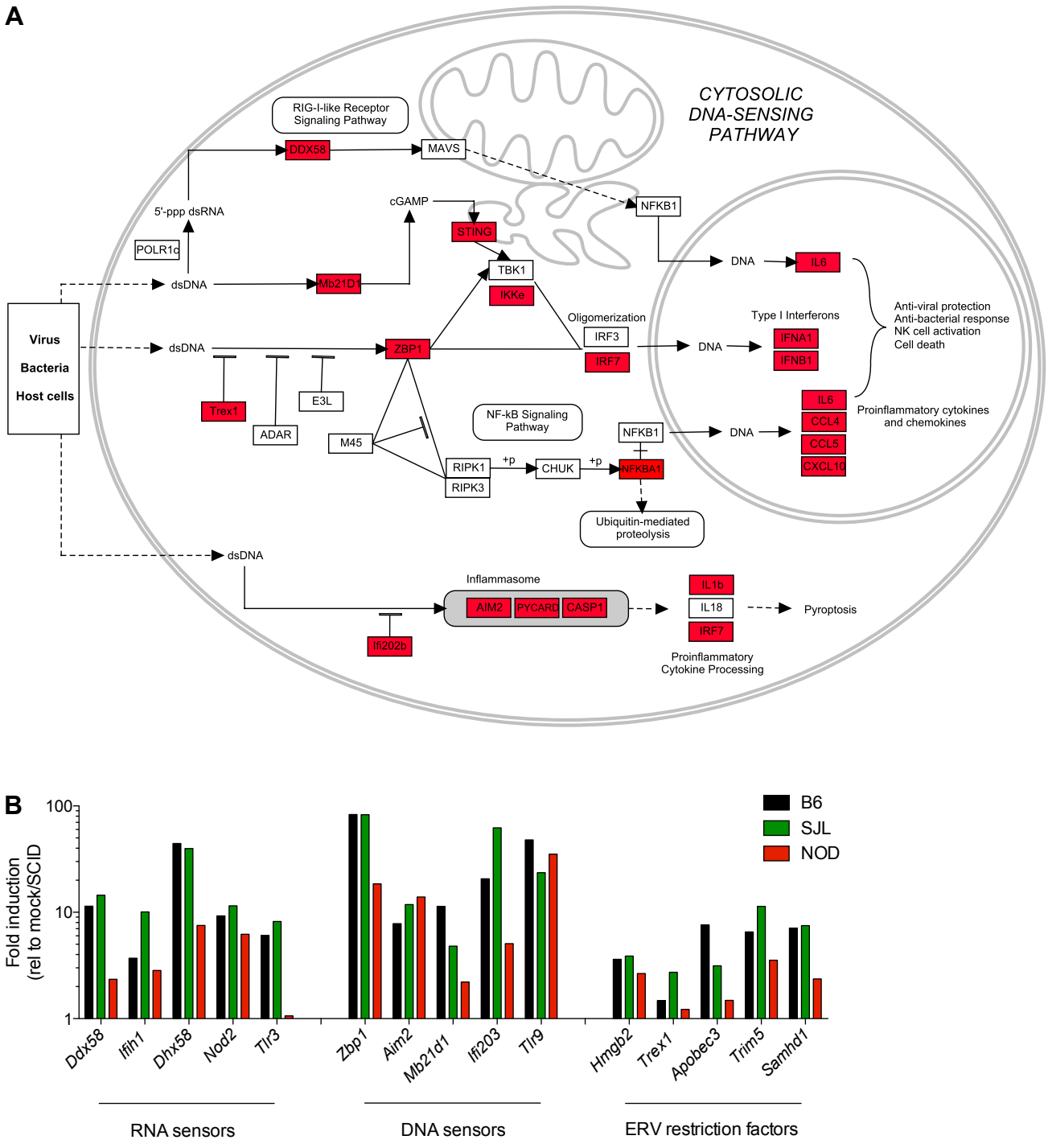

Figure 3.8. Activation of nucleic acid sensing pathways in uninfected NOD mice
(A) Illustration of the cytosolic DNA sensing pathway, adapted from the mmu04623 KEGG database. Genes that are significantly ($p < 0.05$) up-regulated in response to both CVB4 infection (B6, SJL) and spontaneous autoimmunity (NOD) are highlighted in red. Pathway map was generated using PathVisio (Kutmon et al., 2015). (B) Log10 fold inductions of indicated genes in response CVB4 infection and spontaneous autoimmunity are presented relative to mock-infected samples (B6, SJL) and to NOD.SCID, respectively. p, p-value.

The induction of Trex1, which specifically excises DNA substrates, was somewhat unexpected and is likely to reflect the accumulation of DNA templates. Other cellular restriction factors known to suppress replication and reverse transcription of endogenous and exogenous retroelements are *Apobec3* (apolipoprotein B mRNA editing enzyme, catalytic polypeptide 3), *Trim5α* (tripartite motif containing 5) and *Hmgb2* (high mobility group box 2) (Chiu and Greene, 2008; Esnault et al., 2005; Esnault et al., 2006; Hatziioannou et al., 2004; Ueda et al., 2002; Yap et al., 2004), all of which showed increased expression levels in CVB4-induced as well as in autoimmune inflammation (Fig. 3.8B). Taken together, the analyses of immune response genes identified a resonance in the upregulation of nucleic acid sensing pathways in both CVB4 infected islets and islets that were exposed to autoimmune inflammation. The reason for this commonality remains unknown, but likely reflects increased responses to self-nucleic acids during inflammation. The source of the nucleic acids may be from apoptotic or necrotic islet beta cells or acinar tissue, or may be due to the vastly increased transcription of certain genes that occurs during cellular stress. The type of nucleic acid recognised under inflammatory conditions includes mutated DNA, oxidised DNA or endogenous retroelements (Engelhorn et al., 2006; Gehrke et al., 2013; Stetson et al., 2008). Given the reports of accumulation of ERVS in Trex-1-/- mice leading to type-1 IFN production and subsequent cell intrinsic autoimmunity (Morita et al., 2004), it was hypothesised that increased production of endogenous retroviral transcripts may lead to the triggering of inflammation due to innate sensing of nucleic acid. Such a mechanism could

explain the chronic islet inflammation observed in genetically prone mice (and humans) following infection with pancreatrophic virus and would provide a bridge between virus induced inflammation and that observed in spontaneous autoimmunity. Therefore, the genome-wide transcriptional activity of ERVS in CVB4-infected and autoimmune-inflamed beta cells was analysed.

To identify ERV families and/or single ERV that are transcriptionally activated in response to CVB4 infection and/or in prediabetic NOD mice in pancreatic beta cells, differential expression analysis of retroviral reads mapping to the genomic Repbase repository was performed (Bao et al., 2015; Jurka, 1998). In line with their predominant presence within the mouse genome, the two oldest ERV subfamilies, ERVL-MaLR (mammalian apparent LTR retrotransposons) and ERVK (Endogenous Retrovirus Group K) showed the highest transcription frequency in both uninfected and CVB4-infected samples (Fig. 3.9A). Overall, the relative counts of ERV transcripts were significantly higher in NOD.SCID mice compared to pre-diabetic NOD mice (Fig. 3.9B). By contrast, CVB4 infection was associated with a significantly higher abundance of ERV transcripts (Fig. 3.9C). Similarly, the majority of differentially expressed individual ERV were re-activated (up-regulated), rather than suppressed, as illustrated by volcano plot analysis (Fig. 3.9D).

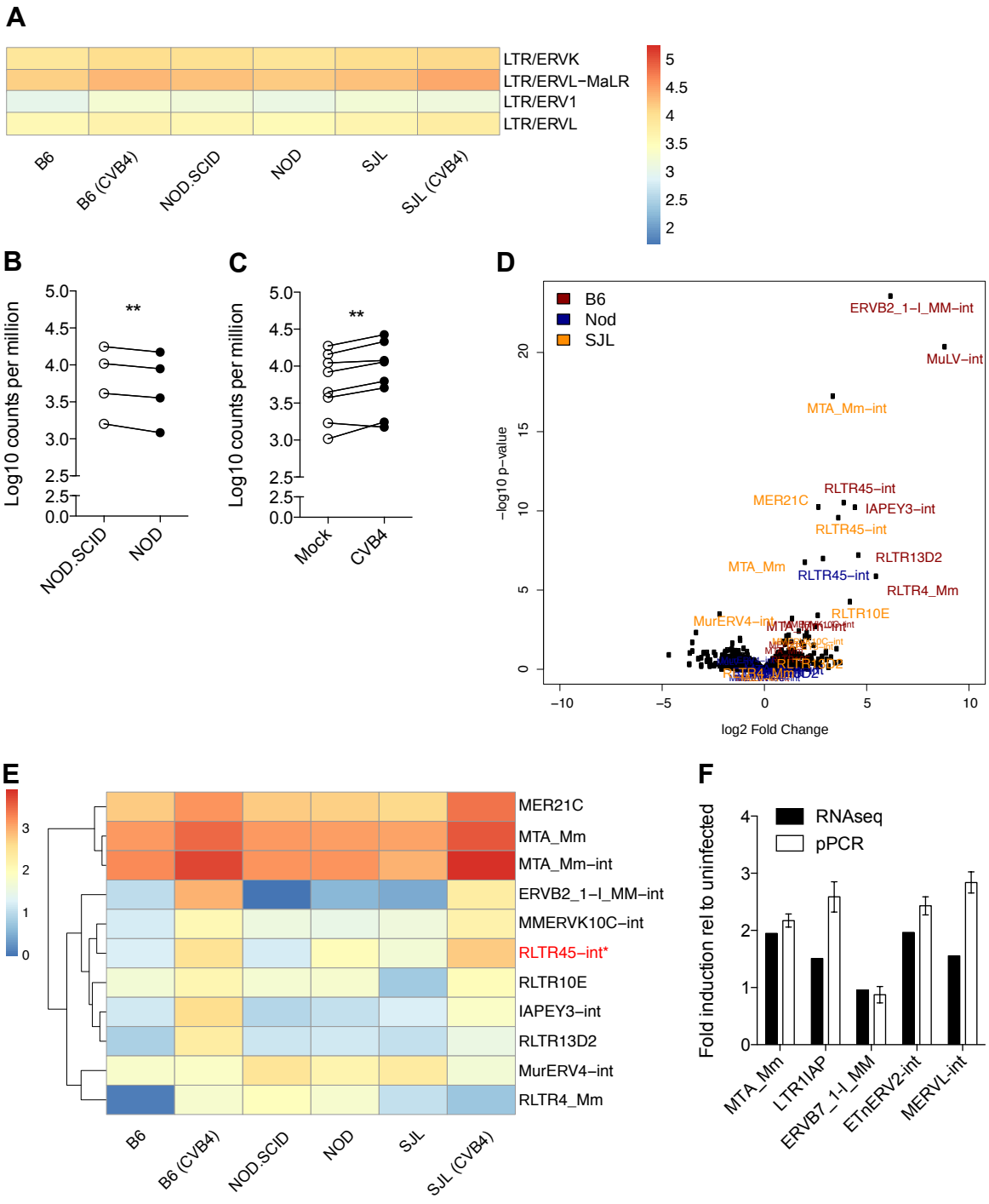

Figure 3.9. Differential expression of endogenous retroviruses

(A) Heatmap representation of ERV subfamilies presented as normalized counts. (B) Log10 counts of individual ERV subfamilies comparing NOD.SCID and NOD samples or (C) mock- and CVB4-infected B6 and SJL samples (combined); **p < 0.01. (D) Volcano plot representation of differentially expressed ERV in response to both CVB4 infection and spontaneous autoimmunity. Each square represents are statistically tested ERV member. Log_2 fold changes are presented relative to mock-infected samples (B6, SJL) and to NOD.SCID, respectively. (E) Heatmap representation and hierarchical clustering of ERV members that are significantly changed (adjusted p < 0.05) in response to CVB4 (B6, SJL) and/or autoimmunity (NOD). ERV significantly increased in response to CVB4 (relative to uninfected) and in NOD mice (relative to NOD.SCID) are highlighted in red. Data are presented as normalized counts.

(F) Differential expression of selected endogenous retroviruses was validated by qRT-PCR in total pancreas samples from mock- and CVB4-infected B6 mice (n = 3). Samples were normalized to the housekeeping gene *Rpl19*. Fold changes are presented relative to mock-infected samples as average ± SD. Results of qRT-PCR were within 2-fold of RNA-seq expression levels. p, p-value, Rpl19, ribosomal protein L19.

Again, activation of individual ERV was predominantly observed after CVB4 infection of B6 (red) or in SJL mice (yellow), whereas pre-insulitis in NOD mice (blue) appeared to have little impact on ERV expression at this stage (Fig. 3.9D). The heatmap representation of all significantly changed ERV (adjusted p-value < 0.05), either due to CVB4-induced inflammation in B6 or SJL, and/or during autoimmune inflammation (NOD), shows an over-representation of members of the ERVK subfamily, e.g. *IAPEY3-int* or *ERVB2_1-I_MM-int* (Fig. 3.9E). Notably, *RLTR45-int,* also a member of the ERVK subfamily, was the only ERV significantly induced in response to both CVB4-induced and autoimmune inflammation (Fig. 3.9E).

Transcriptional activation of retroviral elements was validated by quantitative real-time PCR (qRT-PCR) of selected differentially expressed and unchanged ERV across different subfamilies. As for validation of coding genes, RNA was obtained from pancreas samples of CVB4-infected and uninfected B6 mice. As shown in Fig. 3.9F, expression levels of ERVK members (*ERVB7_1-I_MM,* ETnERV2-*int*, *IAPEz-int*), ERVL (*MERVL-int*) and ERVL-MaLR (*MTA_Mm*) were within 2-fold of RNA-seq values, demonstrating a robust correlation between both techniques and indicating reliable detection of low-abundance retroviral transcripts by RNA-sequencing.

Transcriptional regulation of ERV elements in somatic cells is likely mediated in a tissue specific manner and hence may contribute to a tissue-intrinsic risk of immune responses to self. It was therefore examined whether CVB4-induced (re-)activation of ERV elements is specific to pancreatic beta cells and whether there is a direct relation between ERV transcription and CVB4 titres. Furthermore, to determine whether infection with an exogenous virus differentially affects ERV transcription levels in T1D-susceptible compared to T1D-resistant mice, CVB4-infected NOD mice were included in this experiment.

On day 4 post CVB4 infection, selected retroelements were highly induced in the pancreata of B6, SJL and NOD mice (Fig. 3.10A, left panel), and to a lower extent in their livers (Fig. 3.10, left panel). In addition, moderate ERV activation was found in the thymus of B6, but not of SJL or NOD mice (Fig. 3.10D, left panel). Notably, despite ongoing CVB4 replication in the spleen (see section 3.2.1), splenic ERV expression levels remained unchanged (Fig. 3.10C, left panel), suggesting that ERV transcription in this organ might be controlled by different regulatory mechanisms. On day 28 post-infection, frequencies of ERV transcripts in the pancreas remained high above control levels in T1D-susceptible SJL and NOD mice, while T1D-resistant B6 mice displayed activation patterns similar to uninfected controls (Fig. 3.10A, right panel). Importantly, differences in ERV RNA levels in other analysed tissues, including liver (Fig. 3.10B, right panel), spleen (Fig. 3.10C, right panel) and thymus (Fig. 3.10D, right panel), were not significantly different at this time point.

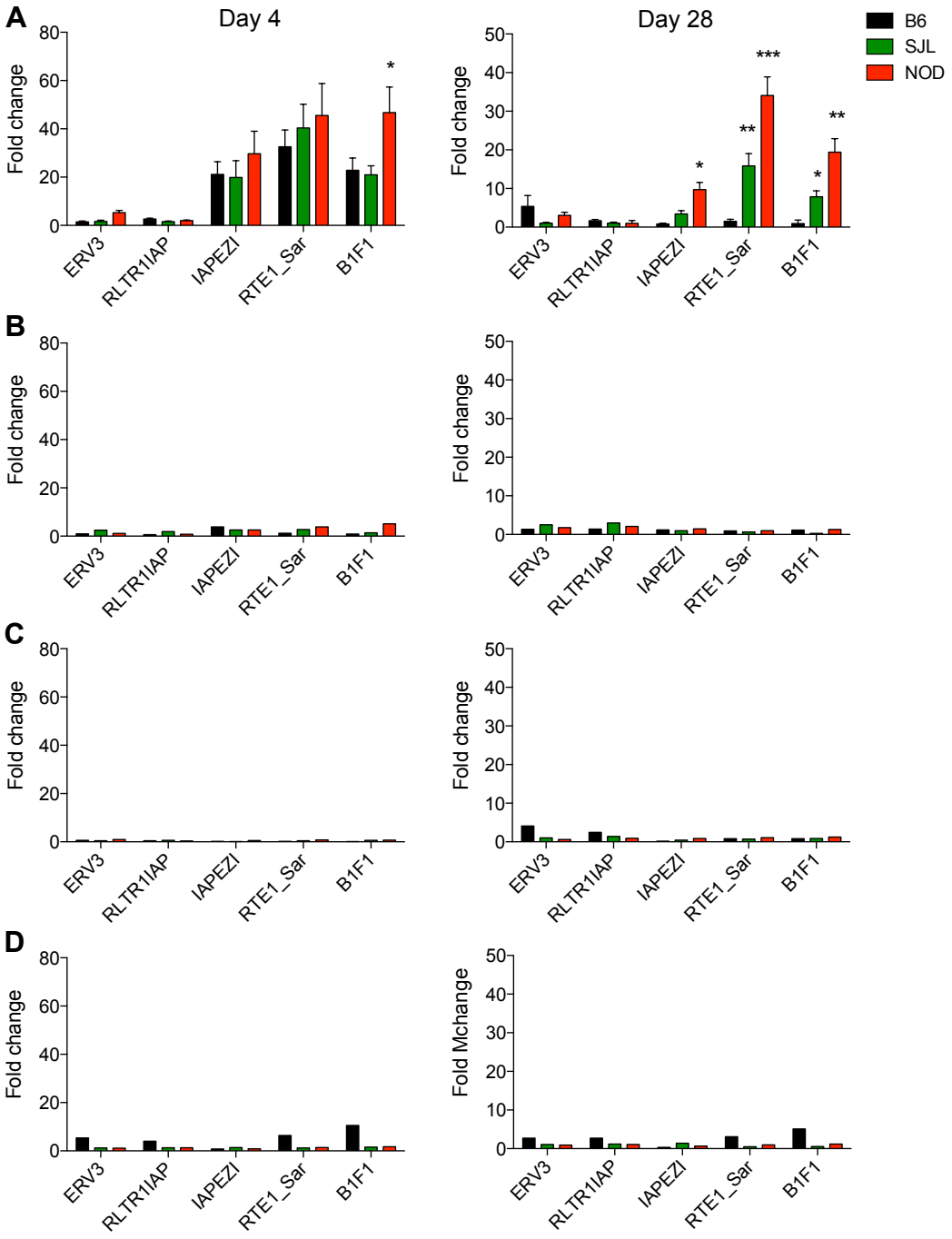

Figure 3.10. Differential tissue expression of ERV transcripts in response to CVB4 infection

Selected endogenous retroviruses were measured by qRT-PCR in pancreas (A, n = 5), liver (B, n = 1), spleen (C, n = 1) and thymus (D, n = 1) on day 4 (left panel) and on day 28 (right panel) following CVB4 infection. Values were normalized to *Rpl19* and are expressed as fold change ± SEM to uninfected controls. *P<0.05, **P<0.01, ***P<0.001. Statistical significance was assessed by 2-way ANOVA using Bonferroni's multiple comparisons test. *Rpl19*, ribosomal protein L19.

Given that chronic induction of ERV elements following viral infections can contribute to ongoing tissue inflammation and thus increase the risk of discovery by auto-reactive immune cells, it was hypothesized that inhibition of ERV accumulation may reduce the incidence of autoimmune diabetes in NOD mice. Since DNA sensors appear to show less ligand specificity compared to the more stringent RNA sensors (Civril et al., 2013), it appeared that reverse transcribed cDNA from endogenous retroviruses is likely to be a more potent inducer of innate immune activation. In this scenario, it is important to note that somatic tissues are equipped with reverse transcriptase activity through the ORF2p (open reading frame 2P) of their LINE1 (long interspersed nuclear element 1) that allows an increased production of ERV cDNA (Feng et al., 1996; Mathias et al., 1991). To inhibit or reduce the abundance of endogenous retroviral cDNA, 6-week old (mild insulitis) and 12-week old (acute insulitis) NOD mice were treated with a combination of the reverse transcriptase inhibitors Truvada (combination of 2 nucleoside reverse transcriptase inhibitors) and Viramune (non-nucleoside reverse transcriptase inhibitor). After 15 weeks of anti-retroviral therapy (ART), mice that had been treated from 12 weeks of age displayed a considerable delay, but overall no significant difference in T1D incidence relative to the control group (Fig. 3.11A). Similarly, mice being administered ART from 6 weeks of age showed no improvement in disease incidence, resulting in premature termination of the treatment at the age of 21 weeks. As expected, 3 weeks into ART, no significant change in pancreatic levels of endogenous retroviral RNA was detected (Fig. 3.11B). Critically, pancreatic cDNA expression of selected highly abundant ERV showed ambiguous results (Fig. 3.11C). While ART considerably reduced

MERVL copy numbers and appeared to have induced *ERVB7_1-I,* it had little impact on *LTR1IAP*, *MTA_Mm* and *MTC*. Thus, the influence of ERV cDNA accumulation on T1D incidence remains inconclusive and requires further experimental investigation.

Although ART displayed no major impact on spontaneous T1D incidence, it showed a small effect in the context of CVB4-induced inflammation. Serum taken from B6 mice on day 4 post CVB4 infection showed a trend towards increased levels of IFN-β (Fig. 3.11D) and IL-6 (Fig. 3.11E) compared to mice that were simultaneously treated with ART, suggesting a potential role of ERV accumulation in virus-induced diabetes.

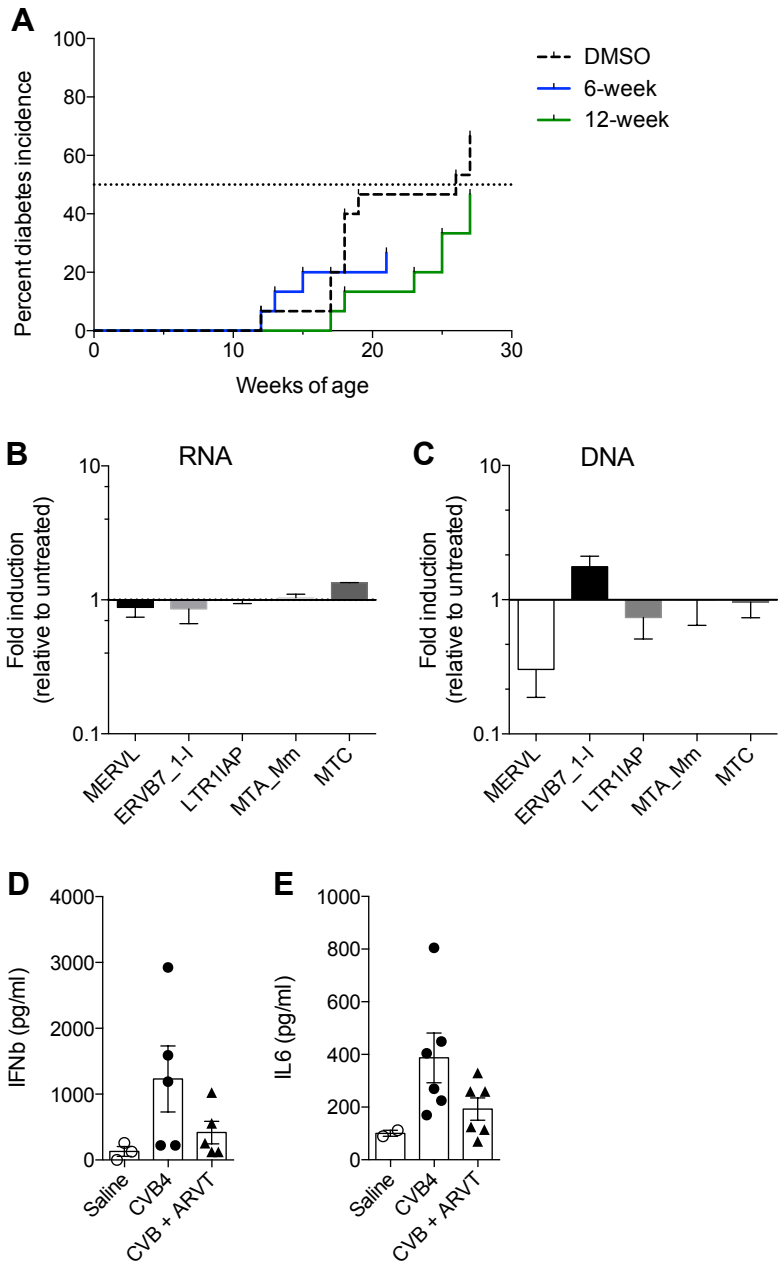

Figure 3.11. Effect of ARVT on diabetes incidence and cytokine production

A) Diabetes incidence curves in NOD mice (n=15) receiving ongoing Truvada (tenofovir/emtricitabine) and Viramune (nevirapine) treatment. Drugs were added to drinking water containing 0.02% DMSO at 3 x 10^{-4} M nevirapine, 1.6 × 10^{-4} M emtricitabine and 1.5 × 10^{-4} M tenofovir. Therapy was initiated at 6 weeks or 12 weeks of age. The control group (12-week old NOD) received water containing 0.02% DMSO only. The effect of ARVT on endogenous retroviral RNA (B) and cDNA (C) levels in the pancreas was measured by qRT-PCR after 3 weeks of treatment. Values were normalized to *Rpl19* and are expressed as fold change to untreated controls. (D) Effect of Truvada and Viramune treatment on IFNβ and IL6 (E) serum levels following CVB4 infection. B6 mice (n=5) were i.p. injected with CVB4 (20 PFU) and treated daily with Truvada + Viramune. Serum was taken on day 0 and 4 post CVB4 infection and cytokine levels measured by ELISA. ARVT, anti-retroviral therapy; CVB4, Coxsackievirus B4; Rpl19, ribosomal protein L19; PFU, plaque-forming units.

3.2.4 Regulation of immune response genes by endogenous retroviruses

The large-scale invasion of vertebrate genomes by endogenous retroviruses has long been suspected to disadvantage the host. However, accumulating evidence suggests an important function of ERV for innate immunity against viruses and other pathogens (Cohen et al., 2009; Feschotte and Gilbert, 2012; Fujino et al., 2014; Stoye, 2012). In fact, co-evolution between virus and host in the form of a mutualistic relationship appears to be the chief contributor to genetic diversity continuously driven by the pressure of natural selection (Doxiadis et al., 2008; Kulski et al., 1997). Unlike stationary protein-coding genes, members of the endogenous virome retain the ability to retrotranspose throughout the genome and thereby expand and re-shuffle regulatory networks in a species- and cell-specific manner (Kunarso et al., 2010; Rebollo et al., 2012; Schmidt et al., 2012). In doing so, ERV have greatly contributed to the pool of transcription factor binding sites and have provided entire promoter and enhancer regions to vertebrate and non-vertebrate genomes (Jacques et al., 2013; Jirtle and Skinner, 2007; McClintock, 1950; Sundaram et al., 2014).

To investigate the potential role of ERV in modulating tissue-specific antiviral innate immunity, the relative ERV distribution around genes commonly activated in response to CVB4 infection (FC > 2. FDR < 0.05; hereinafter referred to as virus response genes) were explored. Under the assumption that proximal, rather than distal regulatory elements are the predominant drivers of transcriptional activation, a genetic distance analysis was performed. Genetic

distance (in bp) was defined as the shortest distance from an ERV to a given gene (either to the transcriptional start site or to gene end). Interestingly, the median distance of ERV to virus response genes (~ 3kb) was significantly shorter compared to the distance to down-regulated genes (~ 15kb, Fig. 3.12). This effect appears to be independent of the transcriptional status of ERV, as we found similar results in differentially expressed (DE) and non-DE ERV (Fig. 3.12).

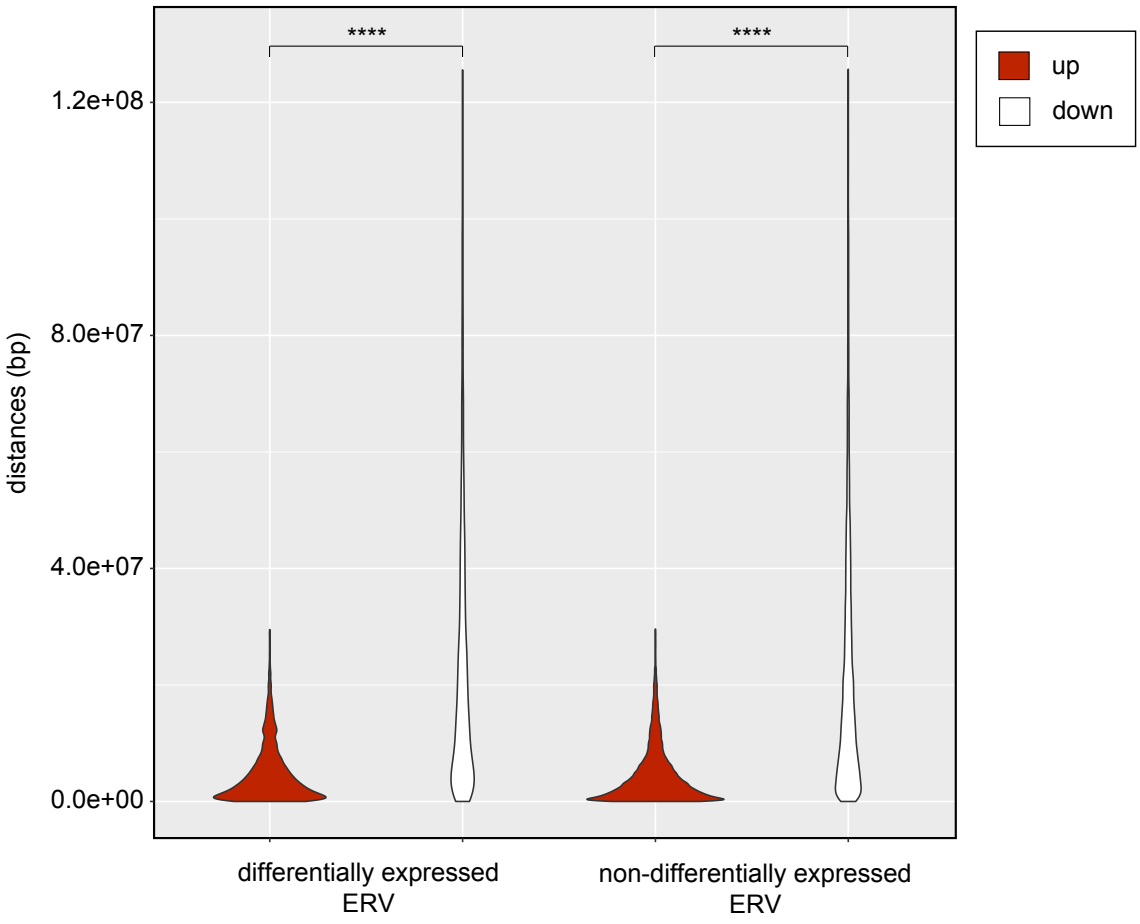

Figure 3.12. Genetic distances of ERV to immune response genes
Violin plot demonstrating the density distribution of genetic distances of differentially and non-differentially expressed endogenous retroviruses to genes that are either up-regulated (highlighted in red) or down-regulated (highlighted in white) in response to coxsackievirus B4 infection (FDR < 0.05). P-values were calculated using the Mann Whitney test, ****P < 1e-100. FDR, false-discovery rate. Violin plots were created using the ggplot2 package (Wickham, 2009).

To gain further insight into the nature of ERV that are proximal to virus response genes, the density of these ERV across different classes of transcriptional regulatory elements (Fig. 3.13) was measured. Intriguingly, the highest density of ERV coincided with distal promoter regions (commonly defined as the region 10 kb upstream of the transcription start site) of the top up-regulated virus response genes (rank 0-50, Fig. 3.13).

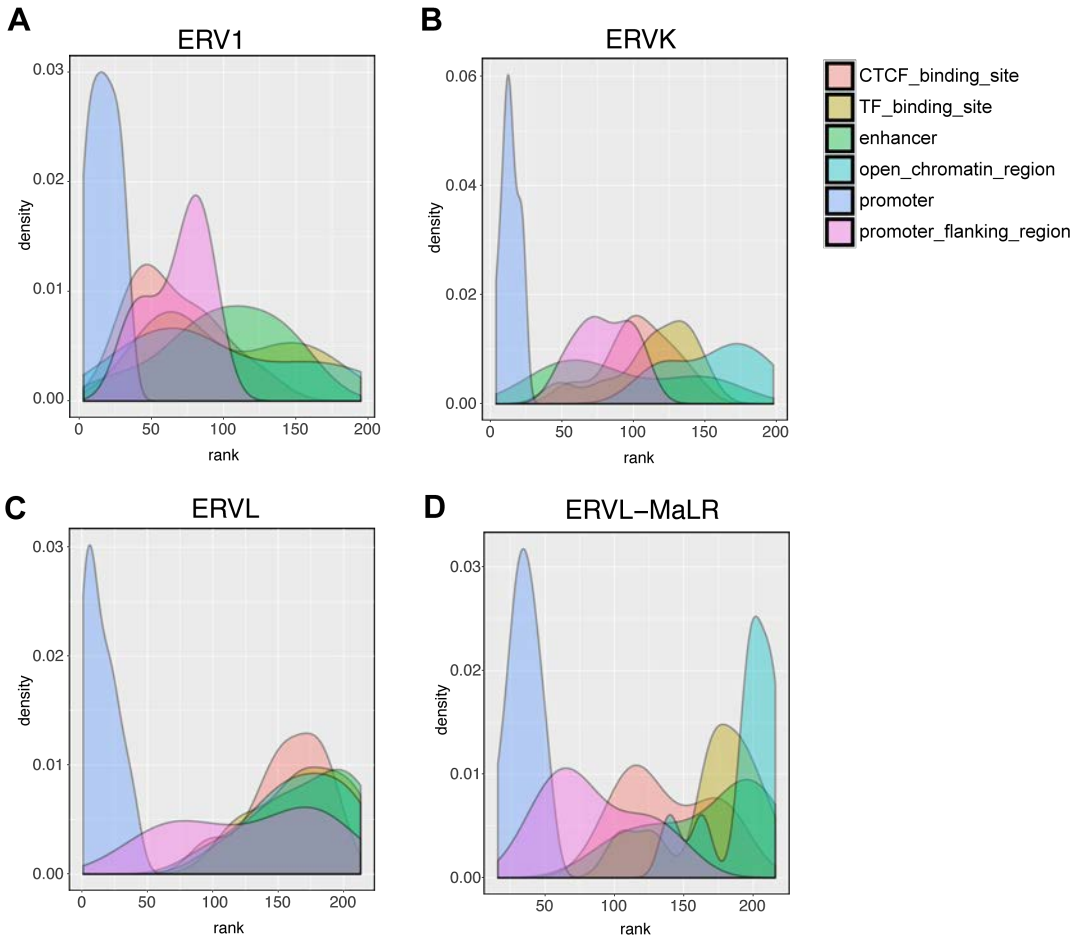

Figure 3.13. Co-enrichment of ERV elements in promoter regions of virus response genes

Density plots illustrating the frequency of ERV1 (A), ERVK (B), ERVL (C) and ERVL-MaLR (D) within regulatory regions of ranked genes (after CVB4 infection). Genes were ranked according to their fold change values in response to CVB4 infection, with down-regulated genes scoring highest values. Annotations of regulatory elements were obtained from Ensembl (Zerbino et al., 2016). Data visualization was performed using the R ggplot2 package.

This observation was most prominent for ERV-K members (Fig. 3.13B), but was also evident in ERV1 (Fig. 3.13A), ERVL (Fig. 3.13C) and ERVL-MaLR (Fig. 3.13D). In addition, ERV coinciding with enhancer and promoter flanking regions of virus response genes occurred at much lower frequencies. By contrast, ERV related to genes that remained unchanged or that were down regulated after CVB4 infection (medium to high rank) did not intersect with a distinct regulatory feature. Instead, these ERV intersected with a multitude of regulatory elements outside the defined promoter regions, including enhancer, CTCF-binding sites, TF-binding sites, promoter-flanking and open chromatin regions (Fig. 3.13).

The binding of a transcription factor (TF) to its corresponding motif, located either upstream (e.g. proximal or distal promoter, enhancer) or downstream (e.g. enhancer) of the respective gene unit initiates and/or potentiates gene transcription. In order to link the enrichment of ERV in the vicinity of virus response genes to a potential effect on gene regulation, virus response genes were analysed for common TF binding motifs. Using the genome browser PWM module of *Enrichr* (Kuleshov et al., 2016), a total of 29 significantly enriched TF binding motifs (out of 594 hits) were identified. The top-ten motifs were ranked based on the combined score and are listed in Table 3.3. Notably, motifs identified to be most over-represented in virus response genes, such as STTTCRNTTT_V$IRF_Q6_1 (interferon regulatory factor), V$IRF_Q6_2 and ICSPB_Q6 (interferon consensus sequence-binding protein) (Table 3.3), are associated with the interferon regulatory factor family and share similar consensus patterns: STTTCRNTTT (IRF_Q6_1), STTTCANTTY (IRF_Q6_2) and RAARTGAAAC (ICSBP_Q6), the latter in reverse direction.

Table 3.3 Top 10 TF binding motifs[1] in up-regulated virus response genes

ID	TF binding motif	P-value	Adj P-value	Z-score	Combined score
1	STTTCRNTTT_V$IRF_Q6_1	4.7E-10	2.8E-07	-1.76	26.65
2	V$IRF_Q6_2	1.5E-09	4.4E-07	-1.75	25.58
3	V$ICSBP_Q6	9.6E-09	1.9E-06	-1.73	22.75
4	GGGNNTTTCC_V$NFKB_Q6	6.6E-08	5.6E-06	-1.80	21.82
5	V$CREL_01	4.9E-08	4.8E-06	-1.64	20.12
6	V$NFKAPPAB65_01	4.6E-08	4.8E-06	-1.64	20.03
7	RYTTCCTG_V$ETS2_B	3.1E-08	4.6E-06	-1.63	20.02
8	V$NFKAPPAB_01	1.3E-07	9.3E-06	-1.67	19.36
9	V$NFKB_Q6	5.7E-07	3.1E-05	-1.70	17.67
10	V$IRF7_01	5.3E-07	3.1E-05	-1.65	17.14

[1]Over-represented motifs in Enrichr showing an adjusted P-value < 0.05. TF, transcription factor; C, cytosine; G, guanine; T, thymine; R, purine; Y, pyrimidine; S, strong; N, any nucleotide.

Transcription factors predicted to interact with IRF (Transfac M00772, see Fig. 3.14A) and ICSBP (Transfac M0069) include IRF-1, IRF-2, IRF-3, IRF-4, IRF-5, IRF-6, IRF-7A, IRF-7H, IRF-8, STAT1 and STAT2. Other motifs, including V$NFKB_Q6 (NF-kappaB), V$CREL_01 (CRE-like element) or $NFKAPPAB_01 are members of the Nuclear factor-κB (NF-κB)/Rel protein family and are associated with binding of NF-kappaB1, NF-kappaB2, p100, p50, p52 and RelA-p65.

Since the IRF_Q6 binding motif was identified to be the dominant driver of virus response genes (Table 3.3), ERV within 5'-UTR and 3'-UTR were analysed for intersections with this motif (Tables 4.5 and 4.6). This analysis was performed on the top 10 ranking CVB4 response genes (Table 3.4). To accommodate analysis of ERV located proximal or distal with respect to the gene unit, 5'-UTR and 3'-UTR were defined as the region 10 kb upstream and

downstream of a gene respectively, and searched for potential IRF sites using Mapper2 (Riva, 2012).

Table 3.4 Top ranking[1] virus response genes activated in both B6 and SJL

ID	Gene name	Strand	Genomic location
Slfn4	schlafen 4	+	11:83,175,186-83,190,216
Slfn1	schlafen 1	+	11:83,116,845-83,122,659
Serpina3n	serpin peptidase inhibitor A3n	+	12:104,406,708-104,414,329
Fga	fibrinogen alpha	+	3:83,026,153-83,033,617
Fgg	fibrinogen gamma	+	3:83,007,724-83,014,717
Isg15	interferon-stimulated gene 15	-	4:156,199,424-156,200,818
Ccl12	chemokine (C-C motif) ligand 12	+	11:82,101,845-82,103,399
Lipg	lipase, endothelial	-	18:74,939,322-74,961,263
Ms4a4c	membrane-spanning 4-A4C	+	19:11,407,661-11,427,246
Ifit3	IFN-induced TPR protein 3	+	19:34,583,529-34,588,982

[1]Genes showing a log2 fold change > 7.5 and FDR < 0.05 in both B6 and SJL.

Importantly, ERV sequences containing the IRF motif were found in almost all analysed 5'-UTRs (except for the 5'-UTR of *Fga*) as well as in several 3'-UTRs of virus response genes. The ERV with the highest Mapper2 identity score are presented in Table 3.5 for 5'-UTR and in Table 3.6 for 3'-UTR regions. Pair-wise alignments of the IRF motif (see Fig. 3.14A) with IRF-containing ERV located in the 5'-UTR of the top 5 virus response genes are illustrated in Figure 3.14B. While ERV with high identity scores (e.g. RodERV21-int, score = 6.6) may prove to be biologically relevant, i.e. being recognized by IRF-related TFs, others ERV with low identity scores (e.g. MTC, score = 1.8) are less likely to have a functional role. Notably, IRF-containing ERV were not associated with a particular subfamily, but were members of ERV1 (e.g. RodERV21-int), ERVK (e.g. RMER12), ERVL (e.g. LTR55) and also ERVL-MaLR (e.g. MLT1F1).

Table 3.5 Top ranking ERV intersecting IRF in the 5'-UTR of virus response genes

Gene	ERV	Genomic location (ERV)	Identity Score[1]	Direction[2]
Slfn4	RMER12	11:83,166,920-83,167,255	5.3	*trans*
Slfn1	RodERV21-int	11:83,105,844-83,107,365	6.6	*cis*
Serpina3n	RMER19C	12:104,400,013-104,400,113	5.7	*trans*
Fga	-	-	-	-
Fgg	LTR55	3:82,998,476-82,998,849	7.3	*trans*
Isg15	MLT1F1.	4:156,208,353-156,208,485	4.7	*trans*
Ccl12	RMER6A	11:82,092,138-82,092,904	4.2	*cis*
Lipg	MTC	18:74,968,906-74,969,319	1.8	*cis*
Ms4a4c	RLTR34B	19:11,403,419-11,403,945	5.3	*cis*
Ifit3	ORR1F	19:34,577,599-34,577,846	4.6	*trans*

[1]ERV selected (if multiple hits found) based on the identity score calculated by Mapper2. The identity score is a probabilistic measure of the match between the hit and the model. [2]Direction of ERV in respect to its related virus response gene

Table 3.6 Top ranking ERV intersecting IRF in the 3'-UTR of virus response genes

ID	ERV	Genomic location	Identity Score[1]	Direction[2]
Slfn4	RMER17C-int	11:83,198,428-83,199,081	6.3	*trans*
Slfn1	RLTR51B	11:83,127,528-83,127,849	5.8	*cis*
Serpina3n	RMER15-int	12:104,421,405-104,421,653	8.7	*cis*
Fga	-	-	-	-
Fgg	-	-	-	-
Isg15	-	-	-	-
Ccl12	RMER17A2	11:82,105,793-82,106,693	6.4	*trans*
Lipg	MTD	18:74,932,919-74,933,105	4.8	*trans*
Ms4a4c	-	-	-	-
Ifit3	RMER2	19:34,596,528-34,597,060	6.0	*cis*

[1]ERV selected (if multiple hits found) based on the identity score calculated by Mapper2. The identity score is a probabilistic measure of the match between the hit and the model. [2]Direction of ERV in respect to its related virus response gene

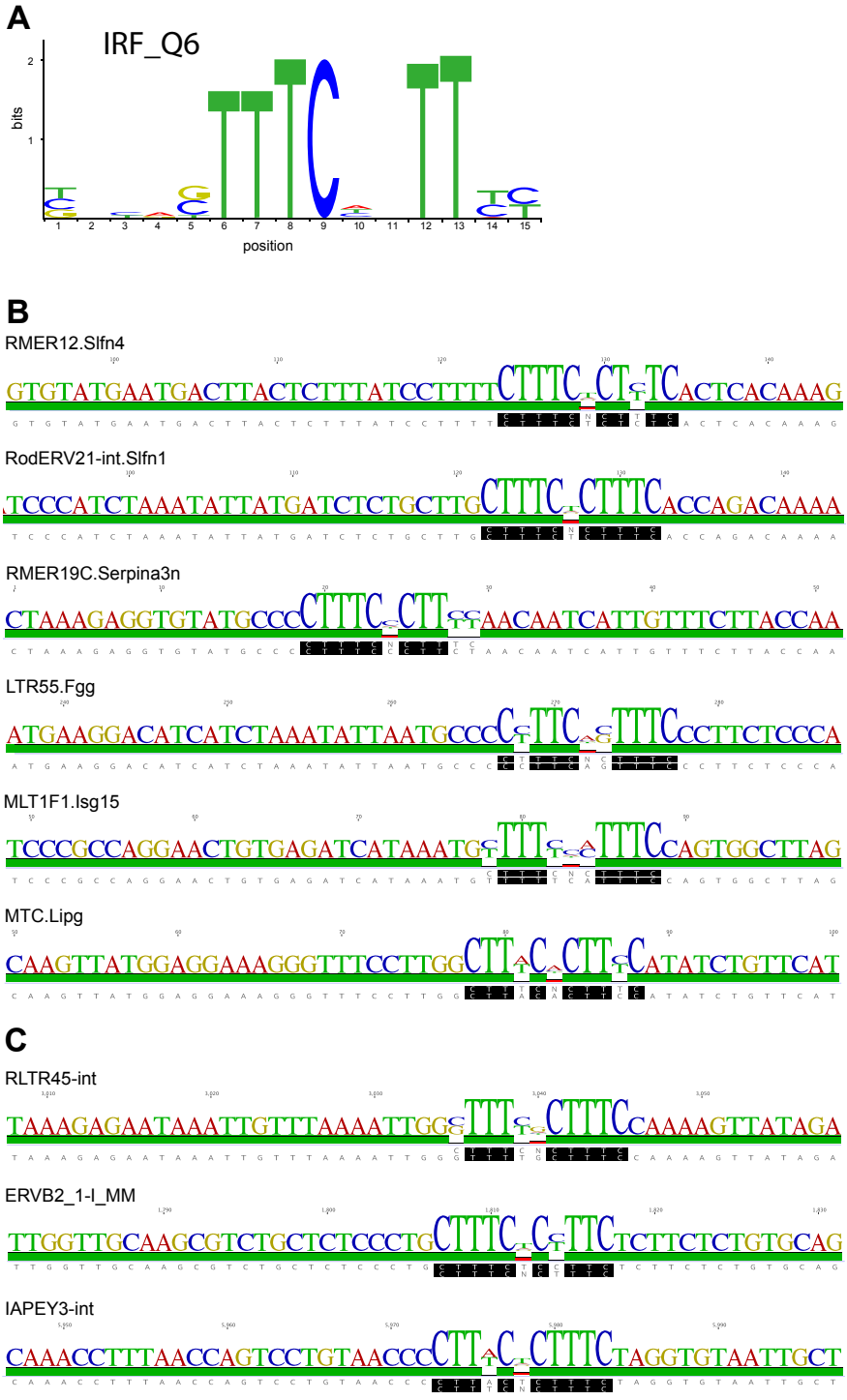

Fig. 3.14 IRF-containing ERV elements in the vicinity of virus response genes
(A) TRANSFAC motif (M00772) of IRF_Q6. (B) GSEA (gene set enrichment analysis) demonstrating enrichment of IRF_Q6 across ranked genes. Genes were ranked according to their fold change values in response to CVB4 infection, with down-regulated genes scoring highest values. (C) Alignment of ERV elements upstream of virus response genes with IRF_Q6. (D) Alignment of top differentially expressed ERV with IRF_Q6. Alignments were generated in Geneious Pro (Kearse et al., 2012). Numbers on top of the alignment indicate region within full ERV element. Black boxes indicate sequence homology.

Furthermore, the distance between ERV and its respective gene ranged between 2.3 and 9.7 kb (data not shown), indicating that these ERV may function as transcriptional enhancers, rather than operating as promoter elements. This notion is supported by the observation that a considerable amount of IRF-containing ERV harbour *trans*, rather than *cis*-acting matrices (Tables 3.5 and 3.6).

In addition to acting as *cis* and *trans* regulatory DNA elements, ERV may modulate transcription in an RNA-dependent manner. More precisely, similar to long non-coding RNAs, transcribed ERV may interact with transcription factors and/or RNA polymerase and thus impact expression of distal genes. Interestingly, the top 3 most significantly up-regulated ERV in response to CVB4 (i.e. RLTR45-int, ERVB2_1-I_MM and IAPEY3-int) also harboured the IRF_Q6 and other IRF-related motifs (Fig. 3.14C), further supporting the notion that ERV elements may modulate immune responses to exogenous virus (e.g. CVB4) by actively shaping the expression of the IFN-related gene network.

3.3 DISCUSSION

Despite more than a century of intensive T1D research, many key questions remain unanswered. While the targeted destruction of pancreatic beta cells is the hallmark of type I diabetes, the exact mechanisms leading to beta cell autoimmunity remain incompletely understood. Environmental factors are strongly suspected to contribute to disease development, yet the specific role of the beta cell in the context of immune responses to environmental triggers is poorly defined. One of the main obstacles impeding beta cell directed research is the accessibility and anatomical structure of the pancreas, as well as the lack of beta cell specific surface markers. As a result, a considerable proportion of studies use beta cell isolation methods that suffer from poor yield and/or purity (Banerjee and Otonkoski, 2009; Delmeire et al., 2003; Eizirik et al., 1994; Hadjivassiliou et al., 2000; Smelt et al., 2008; Yang et al., 2011). To improve this outcome, the present study has implemented a Newport Green-based beta cell purification strategy. Compared to autofluorescence- and antibody-based strategies, the Newport Green-based approach has demonstrated largely improved beta cell purity (Fig. 3.2). As beta cells are particularly sensitive to oxidative (e.g. trypsinisation) (Ling et al., 1994; Rasilainen et al., 2002) and mechanical stress (e.g. cell sorting), viability is severely compromised during the isolation process itself. This is particularly the case for isolation after CVB4 infection. In addition, the pancreas shows the highest RNase activity within murine tissues (Ehinger, 1965; Krosting, 2012), which complicated the extraction of sufficient amounts of high quality RNA. Thus, implementation of Newport Green-mediated beta cell isolation was

critical to overcome these technical challenges and to obtain sufficient RNA quantities to perform genome-wide sequencing.

Previous efforts studying the beta cell transcriptome have largely focussed on gene expression levels under basal conditions (Benner et al., 2014; Dorrell et al., 2011; Kutlu et al., 2009; Nica et al., 2013). A great number of these comprehensive beta cell expression profiles (human, mouse and rat) have been incorporated into the T1D database (Burren et al., 2011), which now constitutes a valuable source for beta cell research. Importantly, more than 25 T1D candidate genes (e.g. *Ifih1*) were found to be expressed in human islets (Eizirik et al., 2012), and pancreatic beta cells (Nica et al., 2013). Furthermore, a substantial amount of these predominantly immune regulating genes demonstrated elevated expression levels upon *in vitro* stimulation with proinflammatory cytokines (Eizirik et al., 2012), supporting an active role of pancreatic beta cells in coordinating immune responses to external stimuli.

This chapter presents the first transcriptome analysis of mouse pancreatic beta cells following virus infection *in vivo*. As a result of technical challenges, RNAseq was performed on one pooled sample per group. Consequently, the presented findings are of limited statistical power and require further validation in additional studies. However, in line with antiviral signatures described within the introductory section, acute infection with CVB4 provoked the activation of a wide range of interferon-stimulated genes (ISGs) and gene families, as well as pro-inflammatory chemokines and cytokines in both B6 and SJL mice. Furthermore, CVB4 infection was associated with elevated expression of

several T1D candidate genes, including *Ifih1*, *Cxcl10*, *Tnfaip3*, *TLR7/8 or* MHC class I members (e.g. *H2-Q7*, *H2-Q8*) (Fig. 3.4B and 3.6C), providing an important link between virus-induced inflammation and increased T1D susceptibility. While the observed production of interferons and pro-inflammatory cytokines may be crucial for the recruitment of mononuclear cells into the pancreas, and thereby for an efficient antiviral defence, a de-regulated over-production could result in exaggerated or chronic inflammation that increases the risk for attracting autoreactive B and T cells. In addition, it is well documented that pro-inflammatory signals can activate beta cell intrinsic pro-apoptotic signalling, thereby accelerating the loss of total beta cell mass. CVB4-infected pancreatic beta cells demonstrated a marked increase in pro-apoptotic *Bcl-2* (data not shown), whereas other pro-apoptotic markers such as *Bax* and *Bad* were not affected at the time point analysed. However, to investigate the impact of CVB4 infection on chronic inflammation and apoptosis, transcriptome analysis of pancreatic beta cells long after viral clearance (e.g. day 28) is required. In this study, technical challenges in RNA extraction during late phases of CVB4 infection (i.e. largely reduced pancreatic mass, impaired cannulation accessibility) resulted in insufficient amounts of material for RNA-seq library preparation. Notably, as a result of recent technical advances, current library protocols permit significantly lower RNA input, which will allow us to perform these studies in the future.

The current study has provided valuable insights into gene profiles of virus-infected and autoimmune-prone mice. Importantly, genes commonly induced in response to CVB4 infection and also in uninfected T1D-prone NOD mice

demonstrated a strong affiliation with type I IFN signalling, and were associated with viral response pathways (Fig. 3.6A). These observations reinforce the concept of virus infections as environmental trigger of T1D and are in line with the detection of type I IFN gene signatures in pre-clinical (Ferreira et al., 2014; Reynier et al., 2010) and clinical T1D patients (Foulis et al., 1987; Huang et al., 1995).

The fact that all nucleated cells are able to express type I interferons (Levy and Garcia-Sastre, 2001; Stark et al., 1998) demonstrates the pivotal role of these cytokines in the ongoing battle between mammalian hosts and invading viruses. Unfavourably, however, overexpression of type I IFN has been linked to exaggerated tissue damage and an increased risk of autoimmunity. For instance, chronic hepatitis C patients treated with IFN-alpha have demonstrated increased T1D incidence rates (Fabris et al., 2003). Similarly, overexpression of IFN-alpha in pancreatic beta cells of transgenic NOD mice resulted in accelerated T1D induction (Stewart et al., 1993). In addition, blockade of IFN-alpha produced by plasmacytoid dendritic cells (pDC) significantly delayed disease onset in the same model (Li et al., 2008).

The complex network of IFN-regulated genes described in the present study extends previous findings and places further emphasis on the active role of pancreatic beta cells in orchestrating immune cell crosstalk in an *in vivo* setting. Moreover, the significant enrichment of virus-response pathways together with activated cytosolic DNA sensing in beta cells of uninfected NOD mice pointed towards the presence of an endogenous viral trigger (Fig. 3.6). This notion was supported by a marked increase of Trex1, Samhd1 and other

restriction factors that are classically involved in cytoplasmic recognition of retroviral transcripts in both pre-diabetic and CVB4-infected mice. However, differential expression analysis revealed a low abundance of ERV RNA in uninfected T1D-prone NOD and immune-compromised NOD.SCID mice (Fig. 3.9A) and exposed *RLTR45-int* as the only significantly induced ERV in these mice (Fig. 3.9D). On the other hand, CVB4 infection activated the expression of numerous ERV (Fig. 3.9D and E), demonstrating that infection with an exogenous virus can result in activation of endogenous virus in a tissue-specific manner (Fig. 3.10). Moreover, pancreatic tissue of CVB4-infected T1D-prone NOD mice displayed the highest level of ERV induction at the acute phase of infection and well after viral clearance (Fig. 3.10), suggesting that CVB4 infection might alter existing tissue-specific methylation patterns leading to increased ERV expression.

DNA and/or histone methylation patterns of ERV elements in pancreatic beta cells have not yet been investigated, neither their epigenomic plasticity in the context of autoimmunity. From an evolutionary angle, the function of increased ERV expression following infection with an exogenous virus remains unclear. It is conceivable that ERV, in both DNA and RNA form, serve as immune adjuvants that improve immunity to foreign pathogens. On the other hand, this increased immune activation might result in loss of self-tolerance in tissues that are susceptible to autoimmunity. While anti-retroviral therapy (ART) showed no effect on T1D incidence in NOD mice, this might be due to the timing of treatment, or to the general low abundance of ERV transcripts found in uninfected NOD mice. In this instance, ART might prove more effective in

the context of virus-induced T1D, which is accompanied by considerable ERV induction. This notion is supported by the reduction of proinflammatory cytokines observed after short-term ART (Fig. 3.10D and E). In order to specifically investigate the contribution of ERV transcripts on beta cell inflammation and T1D incidence, future CVB4 infectious studies on T1D-susceptible NOD mice will involve a combination of different ART regimes.

Convincing evidence for the association between ERV accumulation and autoimmunity has been obtained from patients harbouring single nucleotide mutations (SNP) in cytosolic ERV restriction factors. Patients with SNP in either *Trex1* or *Samdh1* have been linked to autoimmune conditions such as AGS (Aicardi-Goutières syndrome), SLE (systemic lupus erythematosus) or CHLE (Chilblain lupus erythematosus) (Crow et al., 2006; Lee-Kirsch et al., 2007a; Lee-Kirsch et al., 2007b; Namjou et al., 2011; Powell et al., 2011). Similarly, Trex1-deficient mice display lethal autoimmune cardiomyopathy (Morita et al., 2004), a phenotype that depends on the cytosolic detection of ERV DNA by cGas (cyclic GMP-AMP synthase) (Gao et al., 2015; Gray et al., 2015) and that can be rescued by early intervention with ARV drugs (Beck-Engeser et al., 2011). However, further assessments are required to definitively link ERV accumulation following virus infections with increased autoimmune events. Ultimately, the observed stimulation of the cytosolic DNA sensing pathway during insulitis (NOD) or CVB4 infection (B6 and SJL) could also reflect innate activation through beta cell debris. Although self-DNA is usually sequestered within the cell nucleus or otherwise disposed of by a multitude of cytosolic nucleases, high cell turnover during inflammation or

infection may generate enough DNA templates to exceed cellular housekeeping capacities and thus to activate sequence-independent DNA sensors. In line with this, elevated production of type I interferons, as observed during CVB4 infection, have been reported to reduce self-tolerance to DNA derived from beta cell debris (Diana et al., 2013).

Accumulating evidence suggests that endogenous retroelements including ERV are likely to contribute to host immunity in a beneficial manner. In particular, by providing alternative promoter sites, ERV have been shown to fine tune host responses at the transcriptional level (Chuong et al., 2016; Cohen et al., 2009). The present work strongly supports the proposal that ERV modulate anti-viral host responses, however, a possible role for ERV transcripts acting as substrates for immune responses cannot be ruled out. Distribution analysis of ERV revealed that the average distance from an ERV to either the start or end of a CVB4 response gene averaged at about 3kb, as opposed to a 15kb distance to down-regulated genes (Fig. 3.12). As endogenous retroelements have presumably been inserted randomly into the genome (Bannert and Kurth, 2006; Deininger et al., 2003), the closer proximity of ERV to virus response genes may implicate a functional advantage for the host that led to the preservation of their current position. Furthermore, the highest density of ERV was detected in the promoter region of virus response genes, which was set as 10 kb upstream of the transcription start site (TSS). This value is arbitrary, and ERV could potentially represent distal promoter sites (25 kb), or even constitute promoter-acting enhancer elements more than 250 kb away from the TSS (Vavouri et al., 2006). However, the strong

enrichment of ERV within the promoter regions of CVB4-induced genes suggested a potential involvement in transcriptional activation, possibly through providing TF binding motifs.

To explore this further, TF binding motifs driving the expression of CVB4-response genes were identified, with IRF being the top-ranking motif. Intriguingly, ERV harbouring the IRF motif were found within 10 kb in nine out of the top ten up-regulated virus response genes (Tables 4.5 and 4.6). More over, many of these genes were associated with more than one ERV that contained an IRF motif (data not shown), and also showed enrichment of ERV harbouring other motifs (e.g. STAT5), indicating that transcriptional activation of these genes might be modulated by a multitude of ERV elements. In addition, increased ERV transcription could modulate the expression level of proximal genes through interaction with lncRNA, a mechanism that has been observed in human embryonic cells (Lu et al., 2014). Interestingly, this RNA-based modulation might be driven by the same TF set, as consensus sequences of all significantly increased ERV feature the IRF and other motifs. However, the different level of homology observed between individual ERV and the IRF consensus motif (Fig. 3.14C and D) may reflect that only some are of biological relevance, even though TF binding generally allows single base-pair mismatches (Chekmenev et al., 2005; Quandt et al., 1995). It should also be noted that the identified TF binding motifs are the result of computational predictions based on the conservation of the mouse genome and need to be experimentally validated.

Future work will extend the motif analysis across all CVB4-response genes; also incorporating other non-LTR repeats that might provide important clues for transcriptional regulation. Systemic queries will quantify the contribution of single ERV members and/or families to individual TF binding motifs, thereby potentially linking transcriptional regulation of gene families/networks to particular ERV. Relevant binding motifs within these ERV will be compared to activating histone modifications from existing databases. Their functional relevance in terms of TF binding will then be tested for individual TF (e.g. IRF3) by performing ChIP-seq analysis in CVB4 infected beta cells. Ultimately, the significance of ERV-derived motifs as promoter and enhancer elements in the context of CVB4 infection will be tested through CRISPR/Cas-mediated deletion of selected ERV candidates in B6 mice.

4. NUCLEIC ACID RECOGNITION VIA MAVS IS CRITICAL FOR ROBUST ADAPTIVE IMMUNITY

4.1 INTRODUCTION

Innate immune detection of RNA is an essential component of the host response to virus (Jensen and Thomsen, 2012). In vertebrates, two families of pattern recognition receptors (PRRs) recognise RNA: Toll-like receptors (TLRs) within endosomes and retinoic acid-inducible gene *1 (*RIG-I)-like receptors (RLRs) within the cytoplasm. The cytoplasmic RIG-I-like receptors, including MDA5 (melanoma differentiation-associated gene 5) and RIG-I, rely on the mitochondrial adaptor protein MAVS to induce type I interferon (West et al., 2011). MAVS is ubiquitously expressed on the outer mitochondrial membrane where upon activation it *interacts* with several molecules, including translocases of outer membrane 70 (Tom70), leading to the activation interferon regulatory factor (IRF) signalling (Liu et al., 2010). Importantly, Tom70 functions as a chaperone-docking receptor for importing cytosolic pre-proteins import into the mitochondria (Baker et al., 2007; Neupert and Herrmann, 2007a). Activation of the RLR-MAVS pathway leads to engagement of the TANK binding kinase 1 (TBK1) complex and the inducible IκB kinase (IKK-i/IKKε), which phosphorylates and dimerises interferon regulatory factor (IRF) 3 and IRF7 (Takeuchi and Akira, 2010). IRF3 and IRF7 then translocate into the nucleus and bind to corresponding response elements in order to induce the expression of type I interferon (T1-IFN).

The implications of nucleic acid sensing and T1-IFN production were firstly revealed by Charles Janeway over three decades ago: the “immunologist’s dirty little secret” was that foreign antigen alone was insufficient to elicit an immune response (Janeway, 1989). Protein antigen had to be delivered in conjunction with crude substances, termed “adjuvants”, to generate adaptive immunity. Subsequent work from Janeway’s laboratory, and others, demonstrated that conserved pathogen-associated molecular patterns (PAMPs) elicit excellent adjuvant activity through recognition by PRRs on APCs (Medzhitov et al., 1997). When a PRR is engaged to its corresponding PAMP, the APC can mature to efficiently present antigen, express high levels of co-stimulatory molecules, and secrete cytokines that direct the formation of an adaptive immune response.

This section provides evidence that the adaptive immune response to the model antigen sheep red blood cells (SRBC) is unexpectedly driven by cytosolic recognition of RNA. SRBC induce a robust germinal centre response, which was previously thought to be due to the polyvalent nature of SRBC antigen and have thus been used for decades to analyse the humoral immune response. Here, it is demonstrated that SRBC preparations contain RNA and that following engulfment of SRBC, cytosolic recognition of RNA through the RLR-MAVS pathway provides an early signal that is also important for subsequent amplification of the T1-IFN and TLR pathways.

4.2 RESULTS

4.2.1 The *machtlos* mutation in the transmembrane domain of MAVS impairs the interaction of MAVS with Tom70

The contribution of cytosolic detection of RNA by the RLR-MAVS pathway to adaptive immunity was investigated by utilising a novel mutant mouse strain, which was generated by ENU mutagenesis (Nelms and Goodnow, 2001). This strain carries a point mutation, named *machtlos*, within the transmembrane (TM) domain of MAVS ($MAVS^{los}$). The TM domain of MAVS is important for the localization of MAVS to the outer mitochondrial membrane as well as for T1-IFN induction (in conjunction with the MAVS CARD domain). The *machtlos* mutation caused a non-conservative amino acid change from leucine to proline at position 480 within the transmembrane helix (Fig. 4.1A and Fig. 4.1B). Whilst leucine is one of the most helix-stabilizing amino acids, proline is known as a "helix breaker" because it disrupts the regularity of the α helical backbone conformation (Chou and Fasman, 1978).

MAVS is known to interact with several proteins that influence its function at the mitochondrial surface. Protein import into mitochondria is mediated by the translocators of the outer and inner mitochondrial membranes (Tom proteins) (Baker et al., 2007; Neupert and Herrmann, 2007b; Young et al., 2003). Tom70 has previously been shown to interact with MAVS upon RNA virus infection when utilizing expression constructs *in vitro* (Liu et al., 2010). Since the TM domain of both MAVS and Tom70 mediates their location to the outer

mitochondrial membrane, it was investigated whether the *machtlos* mutation in the TM domain of MAVS affected the interaction of endogenous MAVS with Tom70 *in vivo*. To activate the RLR-MAVS pathway, synthetic viral RNA poly(I:C) was injected (i.v.) into MAVS^{los} and wild type (WT) C57BL/6 controls. Immunoprecipitation of MAVS was performed on splenocytes from WT and MAVS^{los} mice 8 hrs after poly(I:C) or control saline administration. Western blot analyses for Tom70 showed reduced association of MAVS with Tom70 in splenocytes from MAVS^{los} compared to WT splenocytes (Fig. 4.1C). This finding pinpoints amino acid #480 in the transmembrane domain of MAVS as critical for the interaction of MAVS with Tom70 in the outer mitochondrial membrane.

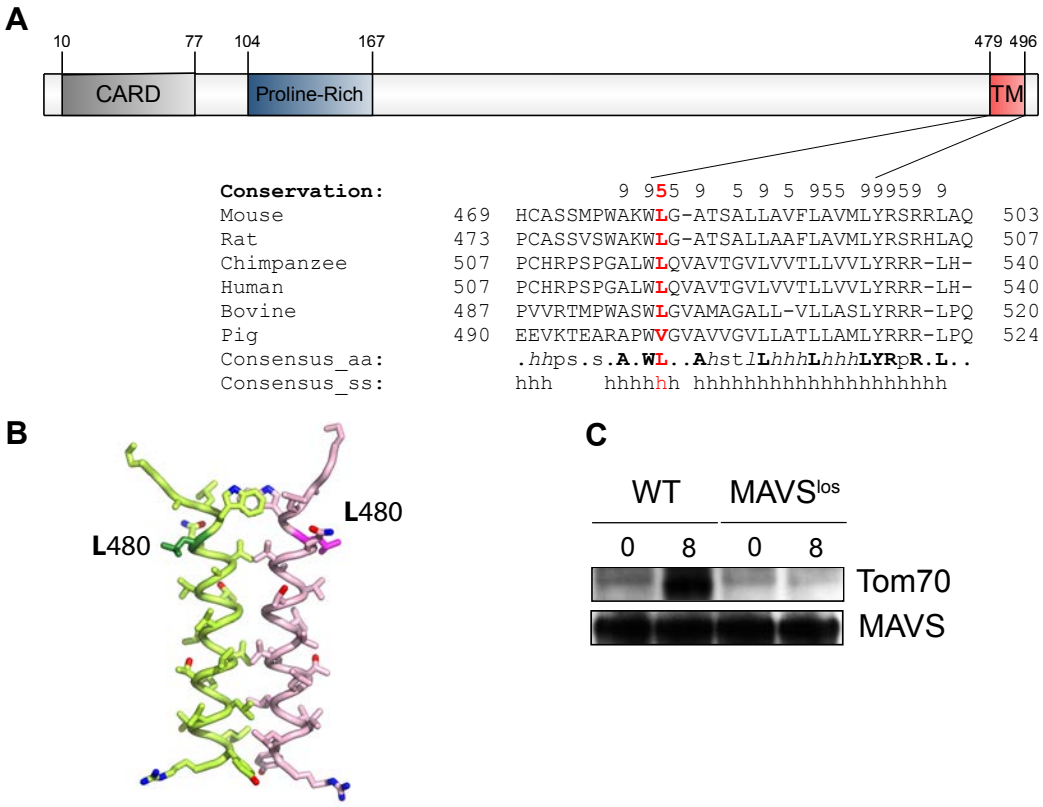

Figure 4.1. *Machtlos* mutation in MAVS TM domain impedes interaction with Tom70
(A) Schematic of MAVS domain architecture highlighting the CARD (grey), proline-rich (blue) and the transmembrane (TM) domain (red). Multiple sequence alignment of this domain shows the conservation of position 480 (leucin, highlighted in bold red), and its surrounding by hydrophobic (h) residues within the protein sequence. (B) Representative molecular model of the MAVS transmembrane domain. Residue 480L is highlighted in dark green/pink. Illustration was generated using PyMOL. (C) WT and MAVS^{los} mice were i.v. injected with 200 µg poly(I:C), and splenocytes were harvested 8 hrs after, followed by immunoprecipitation (IP) with anti-MAVS and immunoblot analysis with anti-Tom70.

4.2.2 Reduced phosphorylation of IRF3 and downstream cytokine production in MAVS^{los} mice

The transmembrane domain of MAVS has been reported to be important for both signalling and localization of MAVS to the mitochondria. To determine the influence of the *machtlos* mutation on the competence of the MAVS signalling pathway, the levels of phosphorylated IRF3 (p-IRF3) in splenocytes following poly(I:C) challenge were assessed. Eight hours after poly(I:C) injection, p-IRF3 was visible as a bright band on Western blots from WT samples (Fig. 4.2A). By contrast, MAVS^{los} splenocytes exhibited reduced IRF3 phosphorylation at the same time point (Fig. 4.2A). In support of a defect in signalling through the RLR-MAVS pathway, significant decreases in the expression levels of type III interferon (*Ifnl*) (Fig. 4.2B), type I interferon (*Ifnb*) (Fig. 4.2C) and interleukin (IL)-6 (Fig. 4.2D) mRNA 4 hrs after poly(I:C) administration, which is consistent with a defect in IRF3 activation were observed. IFN-λ (Fig. 4.2E), IFN-β (Fig. 4.2F) and IL-6 (Fig 4.2G) proteins were similarly detected in reduced amounts in the serum of MAVS^{los} mice compared with WT mice 4 hrs following injection of poly(I:C).

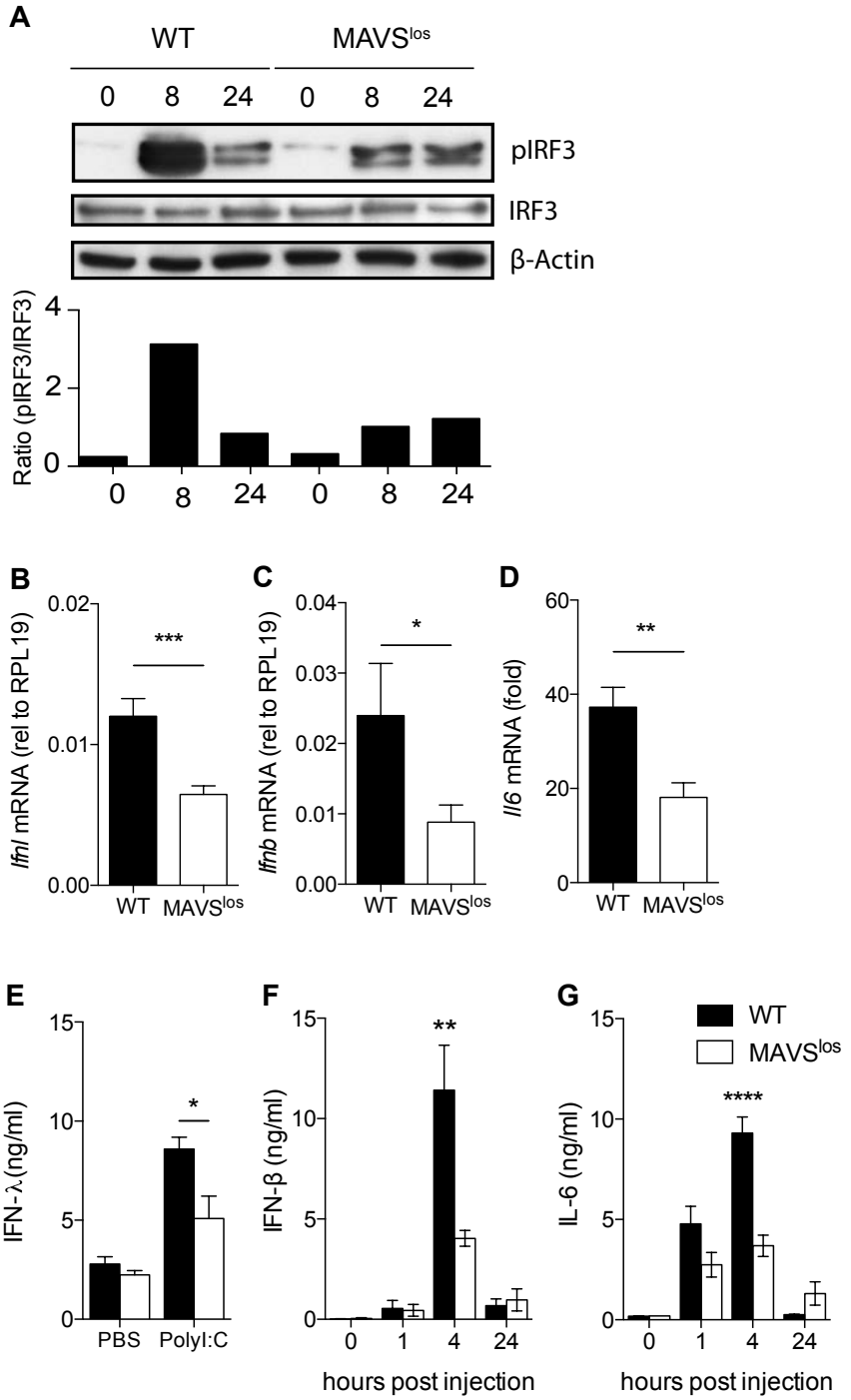

Figure 4.2. Reduced IRF3 phosphorylation in MAVS^{los} mice impairs cytokine production
(A) WT and MAVS^{los} mice were i.v. injected with 200 µg poly(I:C), and splenocytes were harvested after indicated time-points and incubated with antibodies against p-IRF3, total IRF3 and β-actin. (B) Real-time PCR analysis of *Ifnl* mRNA, (C) *Il6* mRNA and (D) *Ifnb* mRNA in splenocytes harvested 4 hours after *in vivo* poly(I:C) stimulation. Data are presented relative to RPL19 expression, n=6. (E) Mice were i.v. injected with 200 µg poly(I:C) and serum levels of IFN-λ, (F) IFN-β and (G) IL-6 measured 4 hours after by ELISA (n=6). All results are representative for at least two independent experiments. P < 0.05; **, P < 0.01; ***, P < 0.001 (1-way ANOVA).

To determine whether MAVS^{los} cells exhibited a defect in localization to the mitochondria, cultures of bone marrow derived macrophages were established and cells were transfected with poly(I:C) for 24 hours. WT bone-marrow derived macrophages (BMDM) transfected with poly(I:C) exhibited colocalization of MAVS to the mitochondria as quantified by Mander's colocalization coefficient using the Imaris colocalization function (Fig. 4.3A and B). Similarly, poly(I:C) also induced colocalization of MAVS to mitochondria in BMDM from MAVSlos mice (Fig. 4.3A and B). Finally, oligomerization of MAVS, as shown by clustering of fluorescence after activation, was also similar in MAVS^{los} and WT BMDC. Taken together, these findings demonstrate that the *machtlos* mutation did not prevent localization of MAVS to the mitochondria, but affected interaction with Tom70, reduced signalling through the RLR-MAVS pathway and downstream cytokine production.

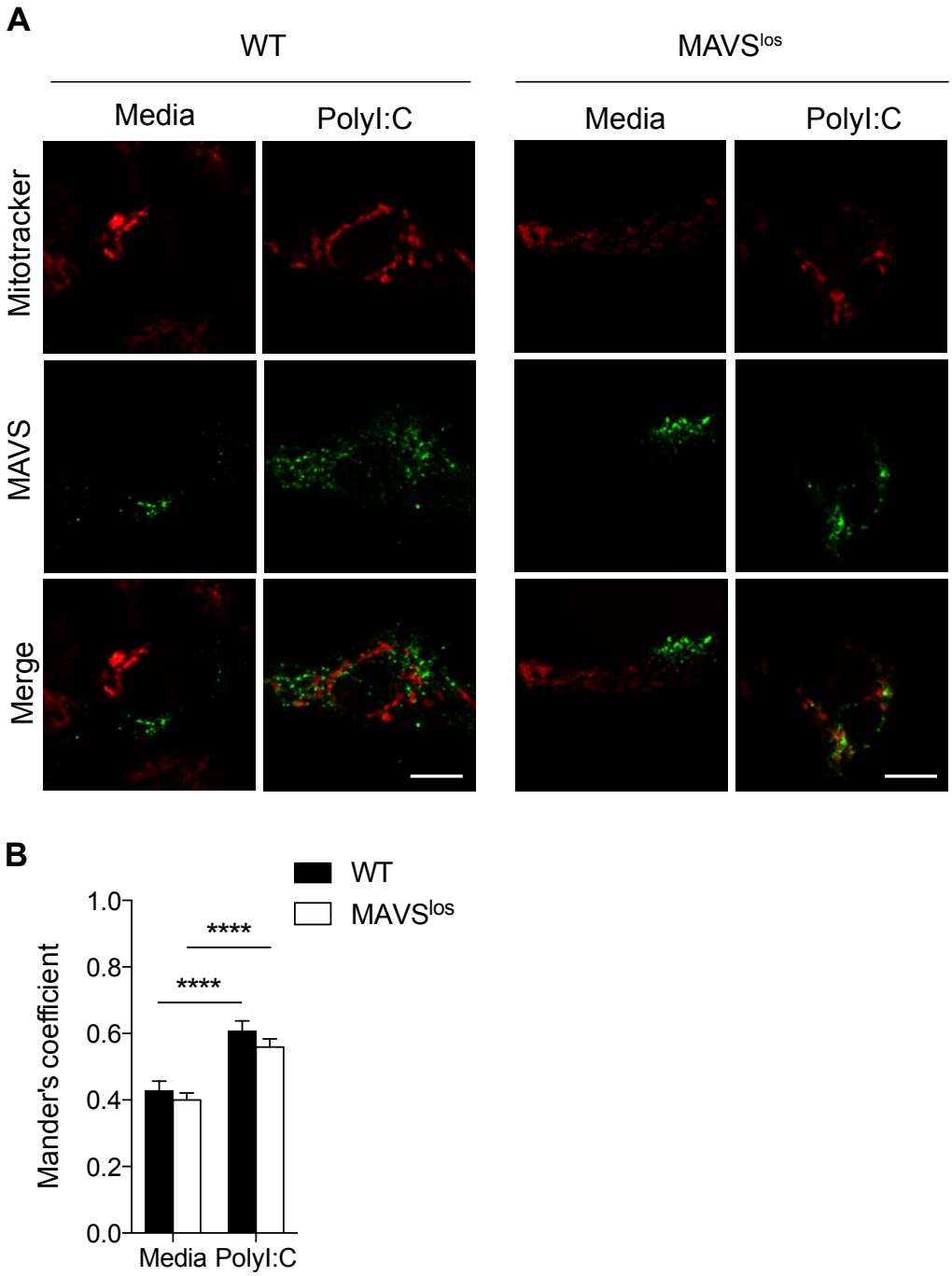

Figure 4.3. Co-localization of MAVS to mitochondria is unaffected by *machtlos* mutation
(A) Confocal images of mouse BMDM transfected for 24 hours with poly(I:C) (10 µg/ml) or cultured in media only. BMDM were stained with Mitotracker (red) and anti-MAVS (green). The merge panel shows the overlap between Mitotracker and MAVS signal. (Scale bar: 10 µm) (B) Imaris software was used to analyse co-localization of confocal images: the fraction of MAVS co-localized with Mitotracker was calculated by Mander's colocalization coefficient; n=30, averages are presented as mean ± SEM, ***P=0.0001, ****P<0.0001. Statistical significance was assessed by 2-way ANOVA using Bonferroni's multiple comparisons test. BMDM, bone marrow-derived macrophage.

4.2.3 MAVS has a role in T-dependent humoral responses

Recent studies have demonstrated that MAVS has a contributing role in T-independent immune responses toward NP-Ficoll, with a notable effect on B cell antibody production (Zeng et al., 2014). The association of the MAVS pathway with autoimmune disease is of great interest, but many autoimmune diseases involve adaptive immune responses with a T-dependent contribution. Therefore, the impact of MAVS on T-dependent germinal centre (GC) responses was tested. To this end, MAVS^{los} mice were immunised with two immunogens separately; the polyvalent antigen sheep red blood cells (SRBC) and the hapten NP conjugated to ovalbumin (OVA) in alum.

Analyses of the immune response in the spleen to the SRBC immunogens revealed a significant role for the RLR-MAVS pathway in the magnitude of the GC reaction. PNA staining of histological sections of spleen demonstrated that MAVS^{los} mice exhibited overall reduced numbers of GCs and a reduced overall area of GCs (Fig. 4.4A and Fig. 4.4B). In support of this finding, the percentages of both GC B cells (Fig. 4.4C and Fig. 4.4D) and IgG1 antibody forming GC B cells (Fig. 4.4E) 7 days after SRBC immunisation were reduced in the spleen of MAVS^{los} compared with WT mice. Analyses of antigen presenting cell (APC) populations revealed that the *machtlos* mutation resulted in decreased expression of B7.2 (CD86) on MAVS^{los} B cells (B220+TCRb-) (Fig. 4.4F), macrophages (B220-TCRb-CD11b+F4/80+) (Fig. 4.4G) and conventional dendritic cells (DCs, B220-TCRb-CD11b+CD11c+) (Fig. 4.4H), indicating reduced activation. The expression levels of CD86 in plasmacytoid

DCs (Fig. 4.4I) from MAVS^{los} and WT mice showed no significant differences at this time-point.

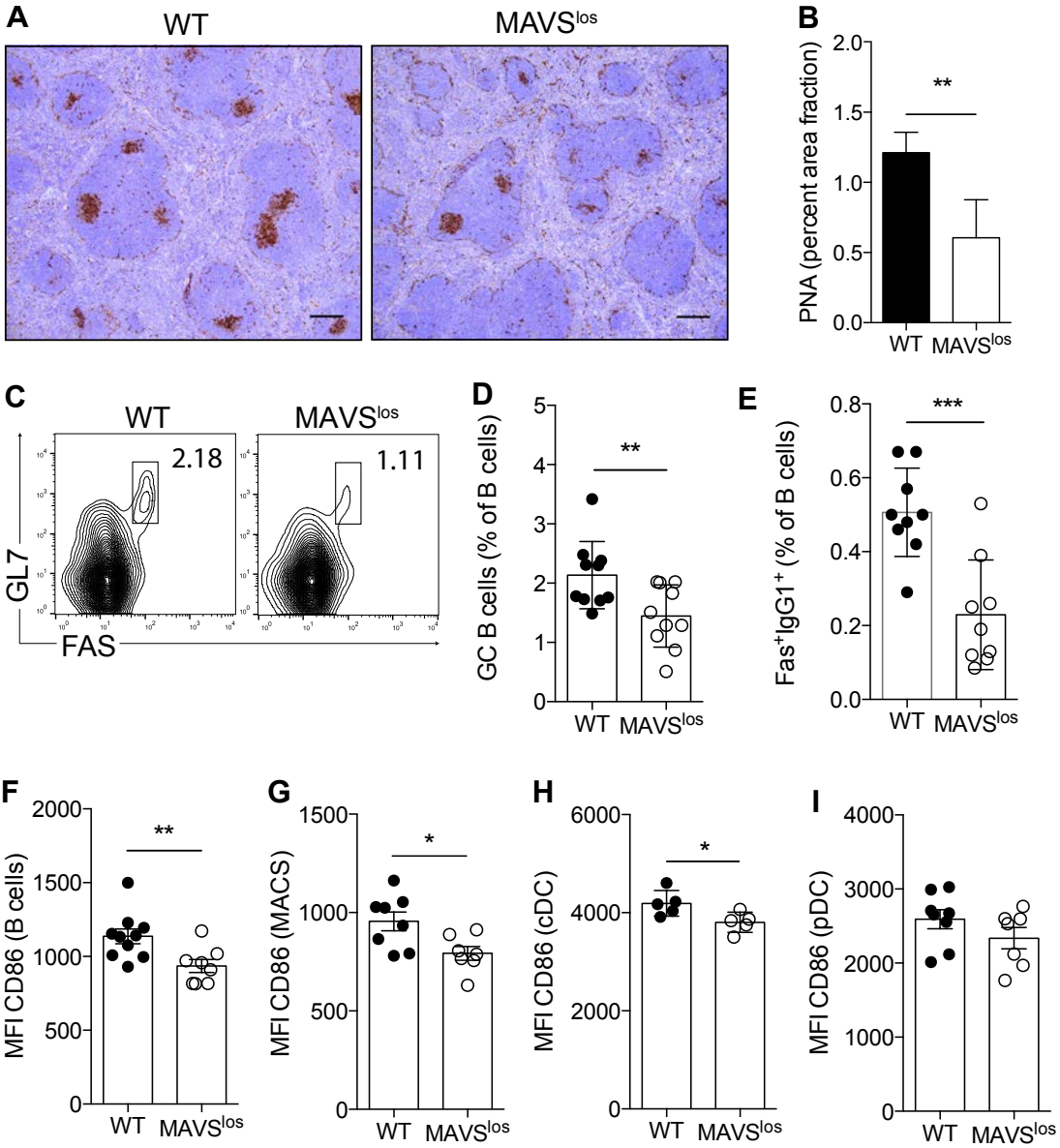

Figure 4.4. MAVS^{los} mice display impaired germinal centre formation
WT and MAVS^{los} mice were immunised with SRBC, and spleens were collected for analysis 7 days after. (A) Representative spleen sections were stained with PNA (brown) to detect GC (Scale bar: 200 µm). (B) Quantification of PNA+ area fraction is presented as mean percentage area with error bars indicating SEM. (C) Representative flow cytometric analysis of Fas+ and GL7 expression within the B cell gate (CDB220+TCRb-). (D) Mean percentage ± SEM of Fas+Gl7+ cells in each spleen. (E) Mean percentage ± SEM of Fas+IgG1+ cells in each spleen. (F-I) CD86 mean fluorescence intensity in B220+ B cells (F), F4/80+CD11b+ macrophages (G), B220-CD11c^{high} dendritic cells (DCs) and B220+CD11c+ plasmacytoid DCs (I). $P < 0.05$; **, $P < 0.01$; ***, $P < 0.001$ (unpaired Student's t test). The data are indicative of three individual experiments. GC, germinal centre; MFI, Mean fluorescence intensity; SRBC, sheep red blood cells; PNA, Peanut agglutinin.

In conjunction with an effect on GC B cells, the percentages of CXCR5^{hi} PD1^{hi} FoxP3^{-} Tfh cells were also reduced in MAVS^{los} mice (Fig. 4.5A and Fig. 4.5B). Paradoxically, despite the weaker GC reaction observed in MAVS^{los} mice, they also exhibited a reduction in the percentage of FoxP3^{+} T follicular regulatory (Tfr) cells (Fig. 4.5C). The reduced fraction of Tfr cells was not due to a diminished precursor population, since the percentages of Tregs were similar in MAVS^{los} and WT mice (Fig. 4.5D). Furthermore, the MAVS mutation led to decreased fractions of activated/memory phenotype T cells, as shown by reduced percentages of the total CD44^{hi} CD4+ T cell population (Fig. 4.5E).

The *machtlos* mutation affected the RLR-MAVS pathway, influencing several cell types during the GC reaction. To determine whether any observed defect was cell intrinsic, we examined GC reactions that form following SRBC immunisation in mixed bone marrow (BM) chimeras consisting of equal ratios (50%:50%) of wild-type (WT) BM expressing the congenic marker CD45.1 and MAVS^{los} BM expressing CD45.2. 8-12 weeks after transfer into irradiated immunodeficient (Rag) recipient mice and after checking chimerism following reconstitution, mice were immunised with SRBC and the relative contribution of both WT and MAVS^{los} lymphocytes to the immune response was determined. Flow cytometric analyses of CD4^{+} T cells 7 days after SRBC immunisation indicated a similar contribution from CD45.2 MAVS^{los} and WT BM (Fig. 4.5F). However, CD45.2 Tfh cells carrying the *machtlos* mutation were under-represented within the total Tfh cell population relative to WT Tfh cells (Fig. 4.5F).

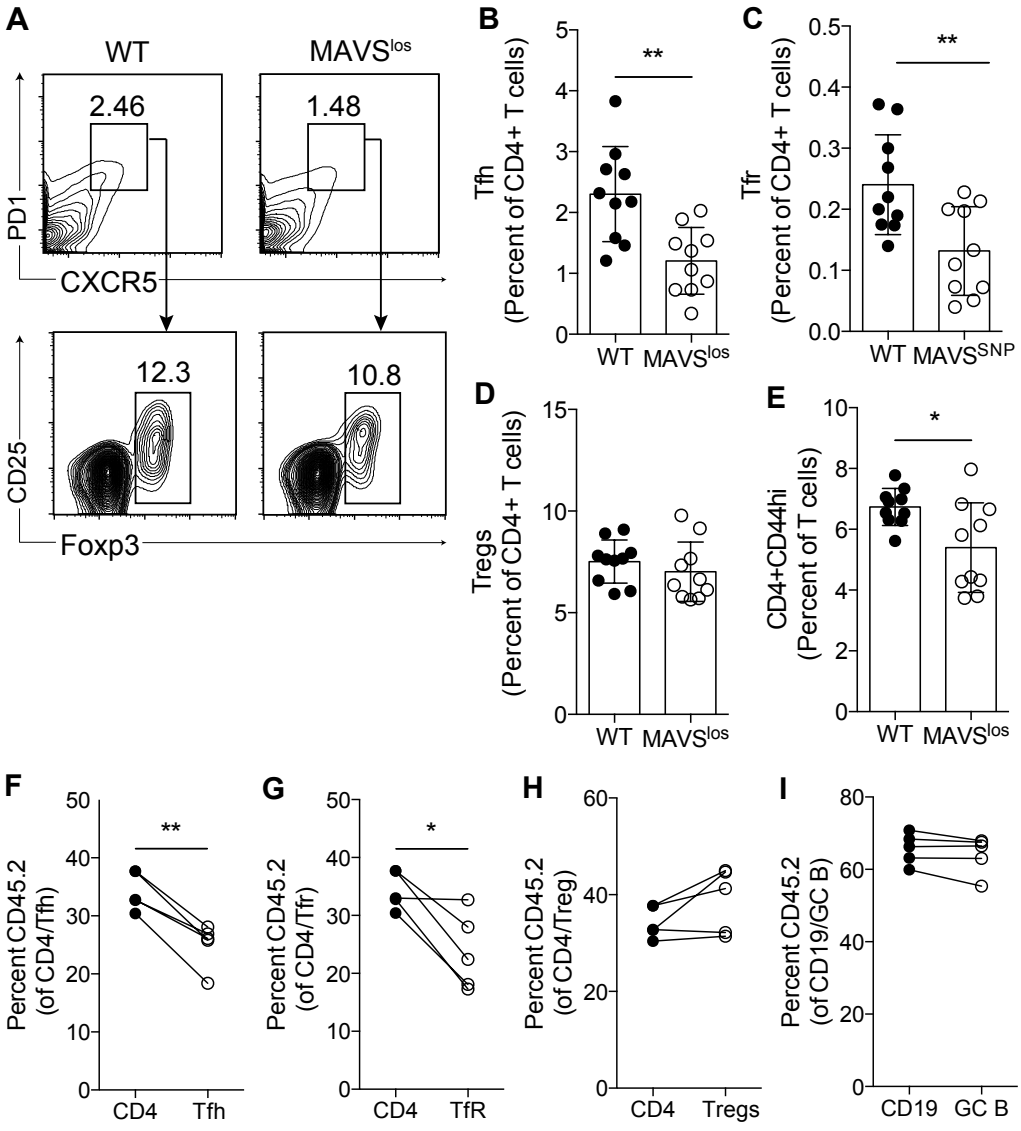

Figure 4.5. MAVS^{los} mice exhibit cell-intrinsic TFH defect

(A) Representative flow cytometric analysis of CXCR5 and PD-1 expression on CD4 helper T cells (CD19-TCRb+CD4+) from spleen 7 d after SRBC immunisation. (B-E) Mean percentage ± SEM of (B) Tfh cells (CXCR5+PD-1+Foxp3-), (C) Tfr cells (CXCR5+PD-1+Foxp3+), (D) Tregs (Foxp3+) and (E) activated CD4 T cells (CD4+CD44hi) in each spleen 7 d after SRBC immunisation. *, P < 0.05; **, P < 0.01 (unpaired Student's t test) (F-I) BM chimeras from 50:50% mixed MAVS^{los} and WT donors immunised with SRBC 8 weeks after reconstitution. Spleens were collected for analysis 7 d after immunisation. Shown are percentages of CD45.2+ MAVS^{los} of total Tfh and CD4+ T cells (F), of total Tfr cells and CD4+ T cells (G), of total Tregs and CD4+ T cells (H) and of total GC B cells (CD19+Fas+GL7+) and B cells (CD19+TCRb-) (I). *, P < 0.05; **, P < 0.01 (paired Student's t test). Tfh, T follicular helper cells; Tfr, T follicular regulatory cells; GC B, germinal centre B cells; SRBC, sheep red blood cells.

In support of this finding, the percentages of GC B cells, IgG1 containing GC B cells and T follicular helper (Tfh) cells detected by flow cytometric analyses of the spleen 10 days after immunisation with NP-OVA in alum were equivalent to that of WT controls (Fig. 4.6C, Fig. 4.6D and Fig. 4.6E). This finding indicated that the contribution of MAVS to the magnitude of the GC reaction and to the differentiation of T follicular helper cells was context dependent.

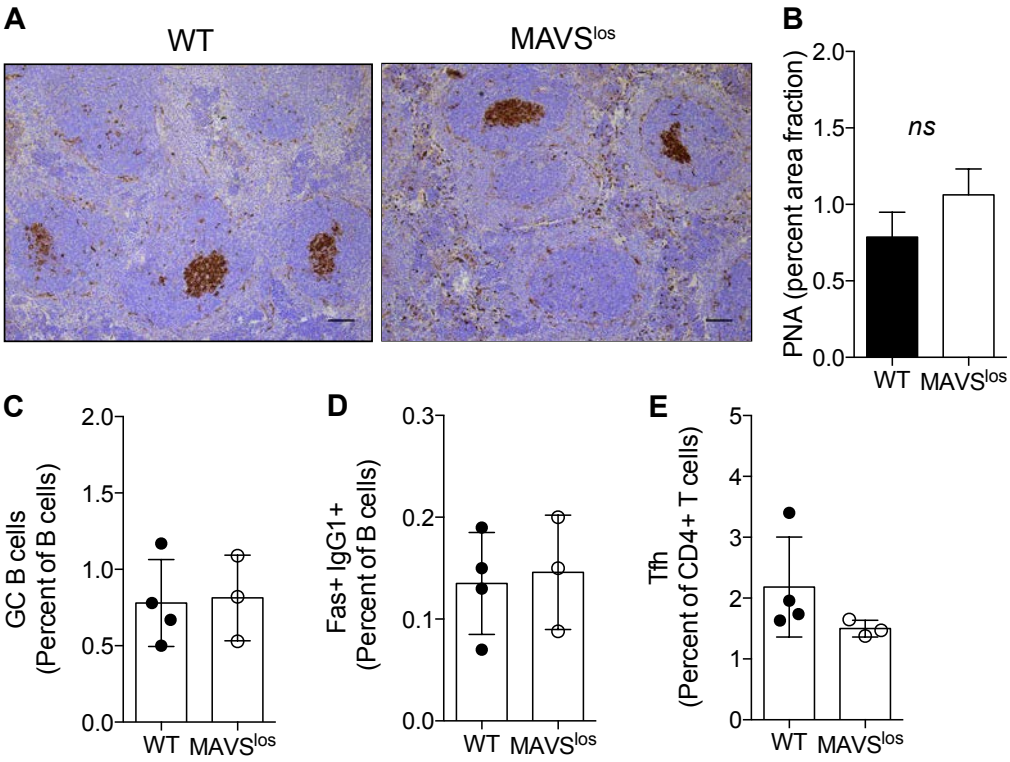

Figure 4.6. Immunisation with NP-OVA evokes potent immune response in MAVS^{los} mice
WT and MAVS^{los} mice were immunised with NP-OVA (100 µg in alum), and spleens were collected for analysis 7 days after. (A) Representative spleen sections were stained with PNA (brown) to detect GC (Scale bar: 100 µm). (B) Quantification of PNA+ area fraction is presented as mean percentage area with error bars indicating SEM. Mean percentage ± SEM of Fas+GL7+ GC B cells (C), Fas+IgG1+ GC B cells (D) and CXCR5+PD-1+Foxp3- Tfh cells (E) in each spleen. Statistical significance was assessed by unpaired Student's t test. GC, germinal centre; Tfh, T follicular helper T cells; PNA, Peanut agglutinin; NP-OVA, nitrophenyl(13)-ovalbumin.

Finally, the impact of the *machtlos* mutation on the immune response to the ssRNA virus CVB4 was tested. Similar to stimulation with poly(I:C), MAVS^{los} mice displayed reduced serum levels of IFN-β and IL-6 early after CVB4 infection compared to WT mice (Fig. 4.7A and Fig. 4.7B). In addition, MAVS^{los} mice exhibited reduced percentages of GC B cells (Fig. 4.7C), Tfh cells (Fig. 4.7D) and Tfr cells (Fig. 4.7E) compared to WT mice, indicating that the *machtlos* mutation compromised T-dependent immunity to this virus. However, no difference was found in relation to viral replication in the pancreas (Fig. 4.7F) or to overall survival following CVB4 infection (Fig. 4.7G).

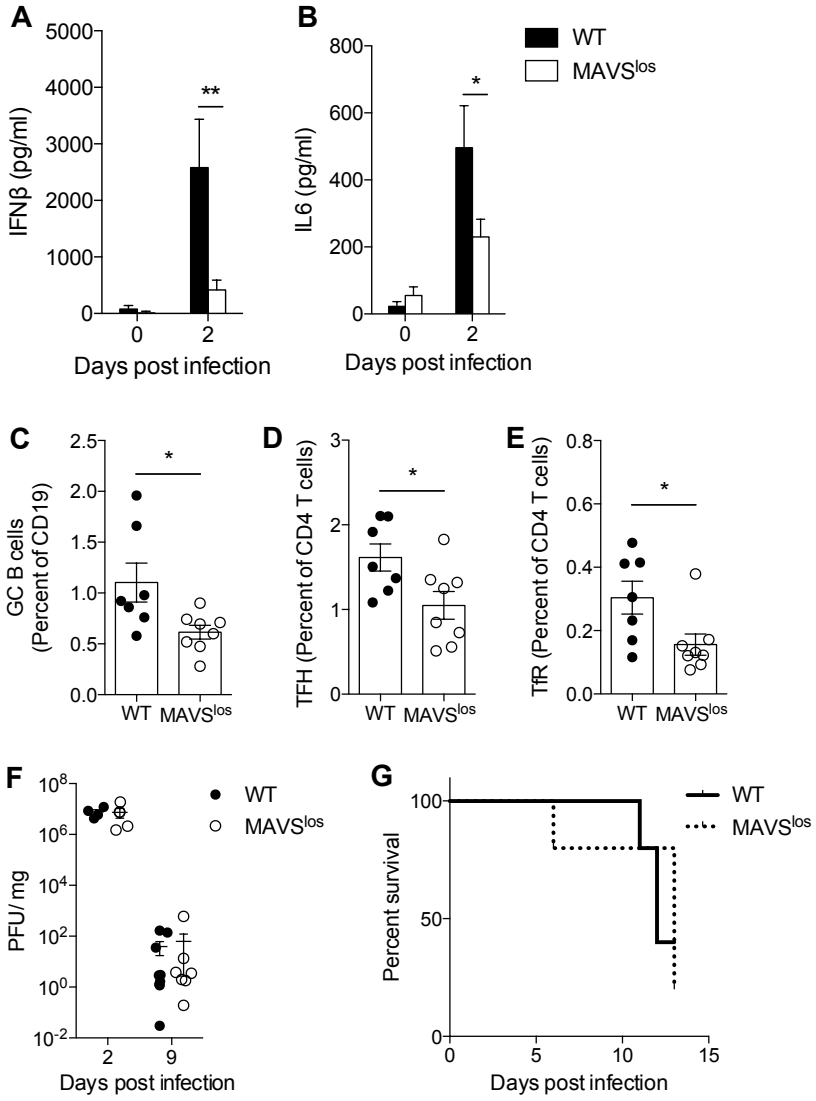

Figure 4.7. CVB4 infection in MAVS^{los} mice is associated with a reduced T-dependent B cells response

(A-F) WT and MAVS^{los} mice were i.p. infected with 20 PFU of CVB4. (A) Serum was collected on day 0 and 2 post CVB4 infection and levels of IFN-β (A) and IL6 (B) measured by ELISA (n=5). (C-E) Spleens were collected 7 days after CVB4 infection and analysed by flow cytometry. Mean percentage ± SEM of (C) GC B cells (Fas+Gl7+CD19+), (D) Tfh cells (CD4+ CXCR5+PD-1+Foxp3-) and (E) Tfr cells (CD4+ CXCR5+PD-1+Foxp3+) in each spleen. (F) Pancreata were harvested on day 2 (n=4) and 9 (n=6) post infection. Viral titres were determined by plaque assay and adjusted for tissue weight. Results are expressed as mean ± SEM. *, $P < 0.05$; **, $P < 0.01$ (unpaired Student's t test). (G) Kaplan-Meier survival curve showing survival of WT (n = 9) and MAVS^{los} mice (n = 9) following injection with 10^5 PFU of CVB4. Data shown are representative of two independent experiments. i.p., intraperitoneal; CVB4, coxsackievirus B4; PFU, plaque-forming units; GC, germinal centre; Tfh, T follicular helper T cells.

4.2.4 SRBC contain RNA and are quickly phagocytosed by APCs

SRBC are a model polyvalent protein antigen used to examine T-dependent immune responses. It was therefore unexpected that cytosolic RNA recognition through the MAVS pathway would play a role in the immune response to SRBC. However, SRBC preparations are derived from whole blood samples, which in addition to SRBCs also contain nucleated reticulocytes and a very small fraction of leukocytes. Furthermore, mature red blood cells have been shown to constitute the predominant source of plasma miRNA (Kabanova et al., 2009; Pritchard et al., 2012). Hence, TRIzol-based RNA purification from SRBC was performed and followed by DNase I treatment to remove potential DNA contamination. The extracts were run on a gel in parallel with the same extracts treated with RNase A, which provided clear evidence that the tested SRBC preparations contained RNA (Fig. 4. 8A).

To investigate how SRBC RNA could enter the cytosolic pathway of APCs, we labelled 5 x 10^8 SRBC with CFSE to a 100% labelling efficiency, transferred these cells into $MAVS^{los}$ and WT recipients and analysed the placement of the injected cells in the spleen by immunfluorescent staining. Analyses of histological sections of the spleen 30 minutes after CFSE+ SRBC transfer enabled detection of SRBC inside both CD169+ marginal zone macrophages and F4/80+ macrophages, and also indicated SRBC particles localised within CD11c+ APCs (Fig. 4.8B). Thus, APCs had consumed SRBC within 30 minutes of immunisation.

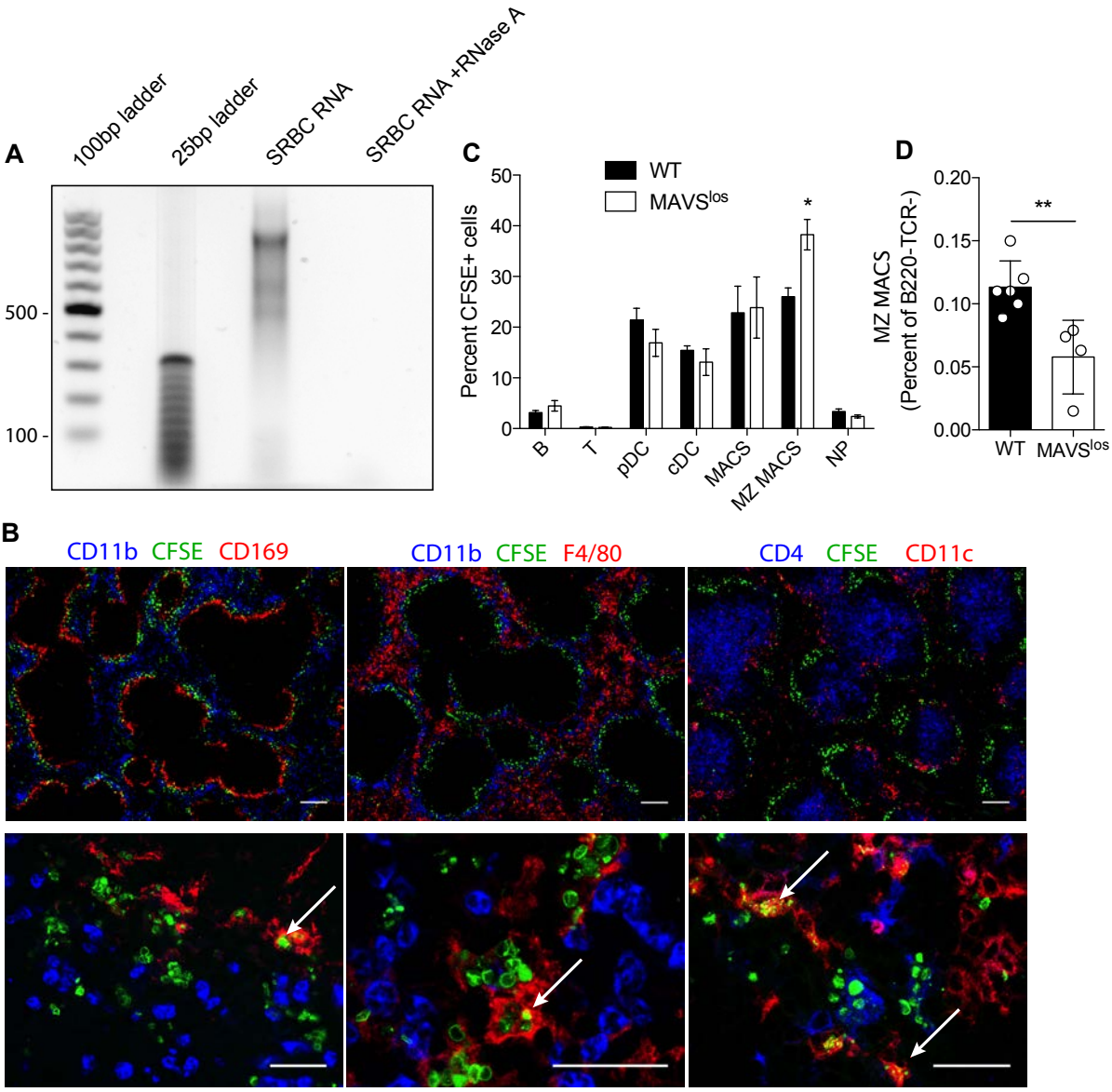

Figure 4.8. SRBC contain RNA and are taken up by antigen-presenting cells
(A) Untreated (2 µg) and RNase A-treated SRBC RNA (2 µg) was run beside on a 0.7% agarose gel containing 1x Sybr Gold. (B) Confocal images of spleen sections 30 min after immunisation with CFSE-labelled SRBC (green). Left panel: sections were immunostained with CD11b (blue) and CD169 (red). Arrow indicates SRBC uptake by MZ macrophage. Middle panel: sections were immunostained with CD11b (blue) and F4/80 (red). Arrow indicates SRBC uptake by F4/80+ macrophage. Right panel: sections were immunostained with CD4 (blue) and CD11c (red). Arrow indicates SRBC uptake by CD11c+ dendritic cell. Scale bar upper panel: 200 µm; scale bar lower panel: 25 µm. (C) Percentages of CFSE+ cells in different spleen populations 3 hrs after immunisation with CFSE-labelled SRBC. (D) Percentages of marginal zone macrophages (CD169+CD11b+TCRb-B220-) in the spleen 3 hrs after immunisation with CFSE-labelled SRBC. *, $P < 0.05$; **, $P < 0.01$ (unpaired Student's t test). SRBC, sheep red blood cell; CFSE, carboxyfluorescein succinimidyl ester; MZ, marginal zone.

Since CFSE-labelled SRBC could be detected inside APCs, flow cytometry was utilized to determine whether MAVS^{los} APCs that engulfed SRBC exhibited early phenotypic differences associated with APC function compared with WT APCs. In agreement with histological findings, CFSE+ SRBC were detected in MZ macrophages, F4/80+ macrophages and conventional DCs, but also in plasmacytoid DCs (Fig. 4.8C) three hours after immunisation. Although the percentage of MAVS^{los} MZ macrophages taking up CFSE+ SRBC was significantly increased compared to WT (Fig. 4.8C), this is likely due to an overall reduction of this population in MAVS^{los} mice in this experiment (Fig. 4.8D). We next compared the expression of CD86 and MHC class II on WT and MAVS^{los} APCs containing CFSE^{+} SRBC with CD86 and MHC class II expression on APCs from the same mice that did not contain CFSE^{+} SRBC. MAVS^{los} macrophages (Fig. 4.9A and 9B) and marginal zone macrophages (Fig. 4.9C) that had engulfed SRBC exhibited decreased expression of CD86 relative to WT APCs that had contained SRBC. Marginal zone macrophages from MAVS^{los} mice, in particular, did not upregulate CD86 (Fig. 4.9C). Similarly, the *machtlos* mutation reduced the SRBC-induced upregulation of CD86 on both conventional dendritic cells (Fig. 4.9D) and plasmacytoid dendritic cells at this 3 hr time-point (Fig. 4.9E).

Uptake of SRBC also led to increased expression of MHCII on WT macrophages (Fig. 4.9F) and conventional DCs (Fig. 4.9G), but had little effect on the expression of MHCII on macrophages and conventional DCs from MAVS^{los} mice (Fig. 4.9F and Fig. 4.9G). These findings demonstrate that the *machtlos* mutation in the TM domain of MAVS inhibits the activation of APCs

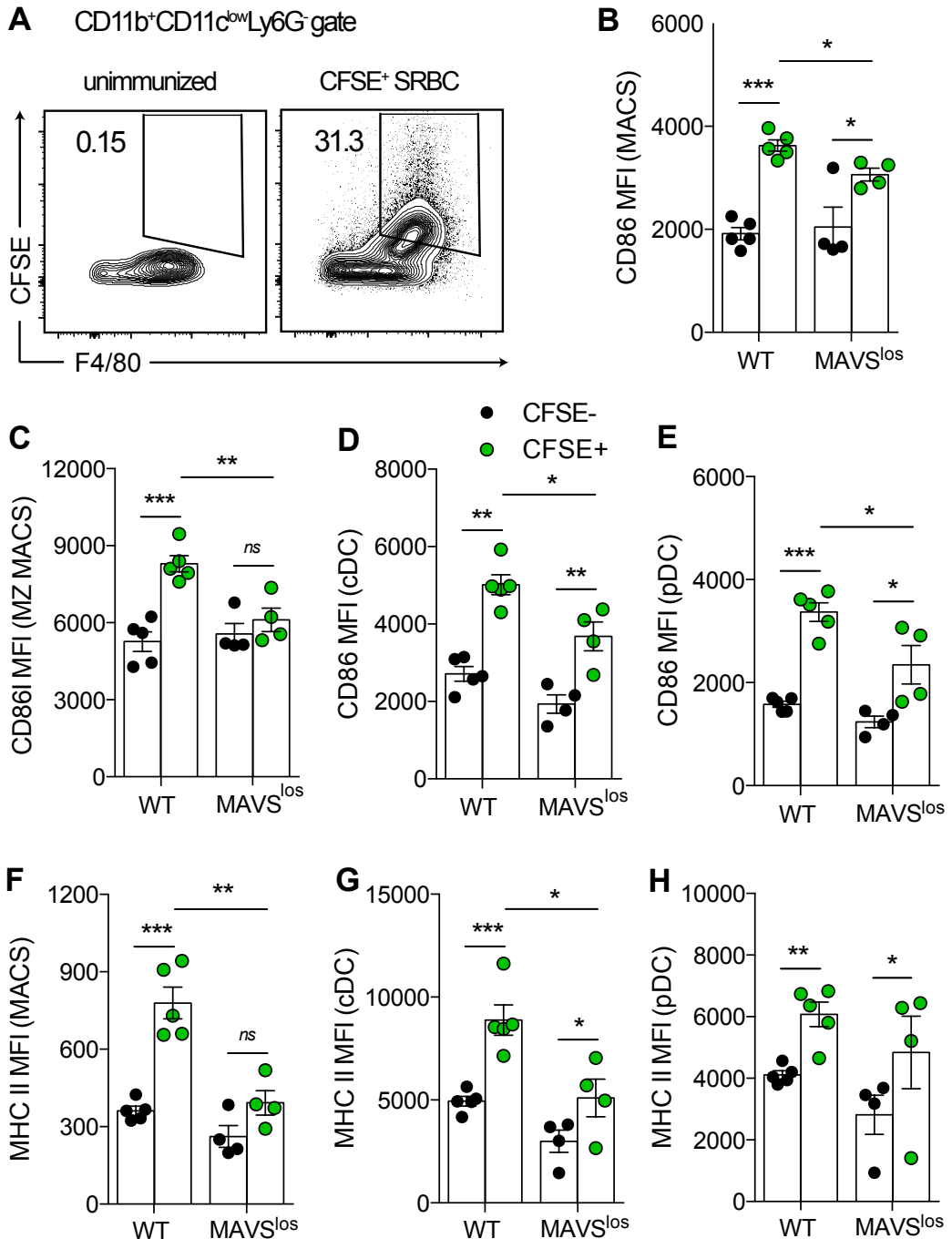

Figure 4.9. MAVS^{los} mutation attenuates SRBC-mediated activation of APCs
(A) Representative flow cytometry plot showing the percentage of CFSE+ macrophages (B220-TCRb-CD11b+CD11c^{low}F4/80+Ly6G-) in the spleen 3 hrs after immunisation with CFSE-labelled SRBC. (B-E) CD86 mean fluorescence intensity in F4/80+CD11b+ macrophages (B), CD169+CD11b+ MZ macrophages (C), B220-CD11c^{hi} conventional DCs (D) and B220+CD11c+ plasmacytoid DCs (E). (F-H) MHC II mean fluorescence intensity in F4/80+CD11b+ macrophages (F), B220-CD11c^{hi} conventional DCs (G) and B220+CD11c+ plasmacytoid DCs (H). P < 0.05; **, P < 0.01; ***, P < 0.001, ****, P < 0.0001 (2-way ANOVA). SRBC, sheep red blood cell; CFSE, carboxyfluorescein succinimidyl ester; MZ, marginal zone, DC, dendritic cells.

following engulfment of SRBC. To determine whether the effect of MAVS on APC activation was cell intrinsic, we generated mature chimeras by transferring $MAVS^{los}$ splenocytes into CD45.1 WT mice and immunised these mice 24 hrs later with CFSE-labelled SRBC. A greater (fold) induction of CD86 was observed on $CFSE^{+}$ SRBC-containing WT macrophages than on $CFSE^{+}$ SRBC-containing $MAVS^{los}$ macrophages within the same mice (Fig. 4.10B). By contrast, B cells (Fig. 4.10A), conventional DCs (Fig. 4.10C) and plasmacytoid DCs (Fig. 4.10D) did not show a clear difference in terms of the fold upregulation of CD86 in mature chimeras.

On the supposition that RNA within intact SRBC entered the cytosolic pathway of host cells to boost the immune response to SRBC, it was hypothesized that RNA-depleted SRBC would be less immunogenic. We therefore immunised mice with either whole SRBC or sonicated/RNase A-treated SRBC. Sonication followed by RNase A treatment significantly diminished the immunogenicity of SRBC, resulting in reduced percentages of Tfh cells (Fig. 4.10E) and GC B cells (Fig. 4.10F) 7 days following immunisation. Taken together, these findings demonstrate that SRBC contain RNA and suggests that foreign RNA from phagocytosed SRBC could enter the cytosolic RLR-MAVS pathway.

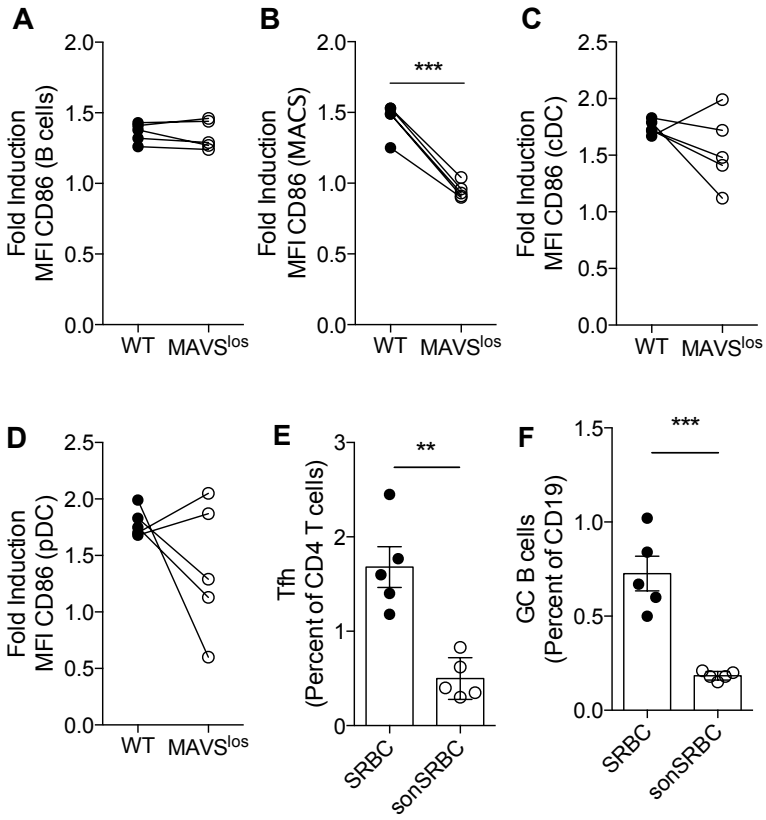

Figure 4.10. MAVS^{los} mutation attenuates SRBC-mediated activation of APCs
(A-D) Mixed chimeras were generated by injecting splenocytes from CD45.2 donor (MAVS^{los}) mice into CD45.1 (WT) recipient mice. After 24 hrs, recipient mice were immunised with CFSE-labelled SRBC and spleens collected after 3 hrs for analysis. (A) CD86 mean fluorescence intensity in B cells (CD19+TCRb-), in (B) macrophages (B220-TCRb-CD11b+CD11c^{low}F4/80+Ly6G-), in (C) conventional DCs (B220-TCRb-CD11c^{hi}) and in (D) plasmacytoid DCs (B220+TCRb-CD11c+) in the spleen. Connected symbols indicate values from the same mouse. ***, P < 0.001 (paired Student's t test). (E-F) WT mice were immunised with either intact SRBC (SRBC) or sonicated and RNase A (1 µg/ml) treated SRBC (sonSRBC) and spleens were collected for analysis 7 days after. (E) Mean percentage ± SEM of Tfh cells (CXCR5+PD-1+Foxp3-) within the CD4+ T cell population and (F) GC B cells (Fas+GL7+) within the B cell population. **, P < 0.01; ***, P < 0.001 (paired Student's t test). SRBC, sheep red blood cell; CFSE, carboxyfluorescein succinimidyl ester; DC, dendritic cells.

4.2.5 Type-1 Interferon drives IL-6 production and enhances Tfh cell differentiation

One of the contributing factors to the effect of the MAVS mutation on the activation and differentiation of T follicular subsets may be a reduced production of T1-IFN. Previous studies have suggested that T1-IFN has an activating effect on T cells, but an inhibitory effect on Tfh cell differentiation in the context of STAT3 deficiency (Ray et al., 2014). To examine the influence of T1-IFN on the GC reaction, *Ifnar1*$^{-/-}$ mice were immunised with SRBC and the GC reaction, GC B cells and T follicular subsets were examined 7 days later.

The percentage of Tfh cells was decreased in *Ifnar1*$^{-/-}$ mice relative to their WT counterparts (Fig. 4.11A). While T1IFNR deficiency had little effect on Tregs (Fig. 4.11D), the Tfr population in *Ifnar1*$^{-/-}$ displayed lower percentages compared to WT 7 days following SRBC immunisation (Fig. 4.11B). The percentages of *Ifnar1*$^{-/-}$ GC B cells were more variable than that of WT GC B cells, but were not significantly different (Fig. 4.11E). The importance of the expression of the receptor for T1-IFN in Tfh cell differentiation was tested in mixed bone marrow chimeras in which 50% of BM derived from CD45.2 *Ifnar1*$^{-/-}$ mice and 50% from CD45.1 WT mice. Despite an equal proportion of total CD4+ T cells deriving from *Ifnar1*$^{-/-}$ and WT BM, significantly fewer Tfh cells had derived from *Ifnar1*$^{-/-}$ BM. This result indicated that the effect of T1-IFN on Tfh cell differentiation was cell intrinsic (Fig. 4.11F).

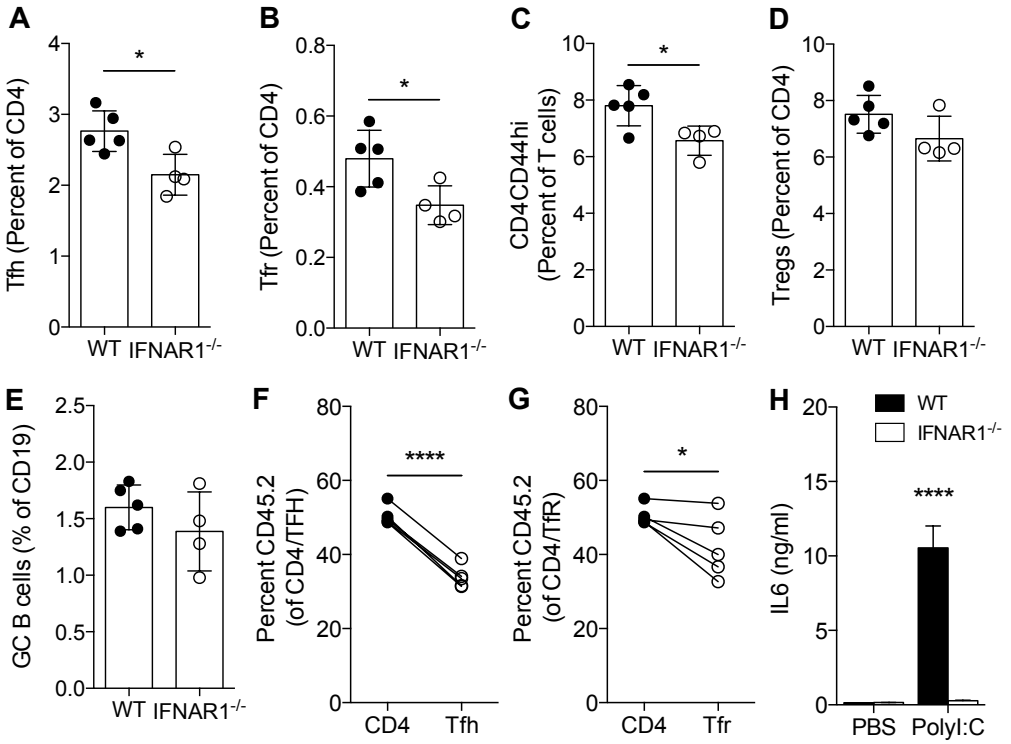

Figure 4.11. Impaired IFN-I signalling affects follicular T cell populations.
(A-E) WT and IFNAR$^{-/-}$ mice were immunised with SRBC, and spleens were collected for analysis 7 days after. (A) Mean percentage ± SEM of Tfh cells (CXCR5+PD-1+Foxp3-), (B) Tfr cells (CXCR5+PD-1+Foxp3+), (C) activated CD4+ T cells (CD4+CD44high), (D) Tregs (Foxp3+) and (E) GC B cells (Fas+GL7+) in each spleen 7 d after SRBC immunisation. *, P < 0.05 (unpaired Student's t test). (F-G) BM chimeras from 50:50% mixed IFNAR$^{-/-}$ and WT donors immunised with SRBC 8 weeks after reconstitution. Spleens were collected for analysis 7 d after immunisation. Shown are percentages of CD45.2+ MAVS^{los} of total Tfh and CD4+ T cells (G), and of total Tfr cells and CD4+ T cells (H). *, P < 0.05; ****, P < 0.0001 (paired Student's t test). (H) Mice were i.v. injected with 25 ug R848 and serum levels of IL6 were measured by ELISA. Tfh, T follicular helper cells; Tfr, T follicular regulatory cells; GC B, germinal centre B cells; SRBC, sheep red blood cells; i.v., intravenous.

Similarly, T1-IFN had a lesser, but direct effect on Tfr cells, with a reduced fraction of the total Tfr cell population deriving from *Ifnar1*$^{-/-}$ mice in the majority of chimeric mice (Fig. 4.11G). Based on these observations, a reduced T1-IFN production from the *machtlos* mutation could contribute to the decreased GC populations in MAVS^{los} mice. In addition, IL-6 production in response to poly(I:C) was markedly reduced in cells that could not respond to T1-IFN (Fig. 4.11H). It was therefore predicted that a reduced production of IL-6 may be a contributing factor to an attenuated GC reaction in both MAVS^{los} and *Ifnar1*$^{-/-}$

mice upon SRBC challenge (Fig. 4.4D and Fig. 4.11E). As a result of the observed contribution of T1-IFN signalling to the differentiation of Tfh cells, it was tested whether boosting T1-IFN could overcome the negative effect of the *machtlos* mutation on the formation of GC populations in MAVS^{los} mice. To this end, a mixture of IFN-α, IFN-β and IFN-λ 3 (s.c.), or control saline, was administered to mice 12 hrs, 24 hrs and 36 hrs post SRBC immunisation, and the effect of IFN on the GC population in MAVS^{los} and WT mice analysed on day 7. Exogenous IFN significantly increased the percentages of both WT and MAVS^{los} GC B cells (Fig. 4.12A) and IgG1 containing GC B cells (Fig. 4.12B). Tfh cells were also boosted by IFN treatment in both WT and MAVS^{los} mice (Fig. 4.12C). However, both with and without IFN treatment, the percentages of MAVS^{los} GC B cells (Fig. 4.12A), IgG1 GC B cells (Fig. 4.12B) and Tfh cells (Fig. 4.12C) remained lower that WT GC populations. In contrast to Tfh cells, IFN had little effect on the percentages of Tfr cells or Tregs in either SRBC immunised MAVS^{los} or WT mice (Fig. 4.12D and Fig. 4.12E).

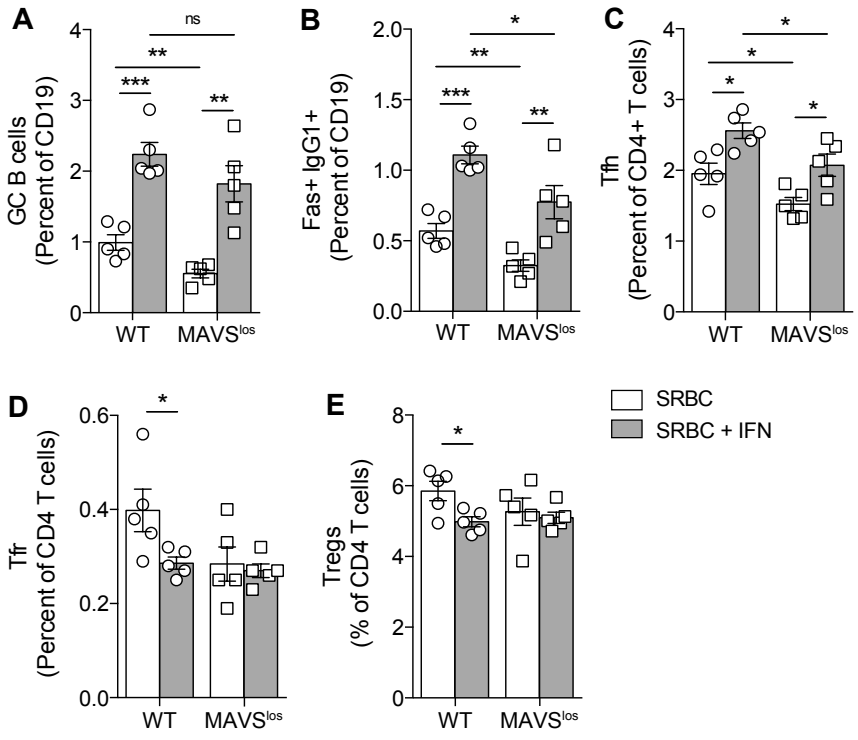

Figure 4.12. IFN-I treatment boosts T-dependent B cell response to SRBC
WT and MAVS^{los} mice were immunised with SRBC and s.c. injected with either PBS or a combination of type I interferons (0.1 µg IFN-alpha, 0.3 µg IFN-beta and 0.8 µg IFN-lambda 3) 12, 24 and 36 hrs after SRBC immunisation (SRBC + IFN); and spleens were collected for analysis on day 7. (A) Mean percentage ± SEM of GC B cells (Fas+GL7+), (B) IgG1+ GC B cells, (C) Tfh cells (CXCR5+PD-1+Foxp3-), (D) Tfr cells (CXCR5+PD-1+Foxp3+) and (E) Tregs (Foxp3+) in each spleen. ns, not significant; *, P < 0.05; **, P < 0.01; ***, P < 0.001 (2-way ANOVA). Tfh, T follicular helper cells; Tfr, T follicular regulatory cells; GC B, germinal centre B cells; SRBC, sheep red blood cells; s.c., subcutaneous, IFN, interferon.

4.2.6 The RLR-MAVS pathway influences activation of TBK1 in T follicular populations

Reduced T1-IFN may have contributed to reduced Tfh cell differentiation, but did not fully explain the cell intrinsic effect of the *machtlos* mutation. Since phosphorylation of TBK1 is an early event in the RNA-mediated activation of the RLR-MAVS pathway and TBK1 interacts with ICOS influencing the development of Tfh cells (Pedros et al., 2016), it was determined whether the RLR-MAVS pathway influences phosphorylation of TBK1 in CD4+ T cells. Eight hours after administration of poly(I:C), the levels of p-TBK1 detected by immunostaining and flow cytometry were generally lower in MAVS^{los} lymphocytes (Fig. 4.13A), but particularly in CD4+ T cells from MAVS^{los} mice compared with CD4+ T cells from WT mice (Fig. 4.13B).

Subsequently, the phosphorylation of TBK1 was analysed by flow cytometry in both Tfh cell and Tfr cell populations 7 days following immunisation with SRBC. Detection of p-TBK1 showed that the *machtlos* mutation resulted in decreased activation of TBK1. In MAVS^{los} Tfh cells, both the percentages of p-TBK1 expressing Tfh cells (Fig. 4.13C and Fig. 4.13D) and the level of expression of p-TBK1 (Fig. 4.14A) were reduced relative to WT cells. Analyses of Tfr cells, in turn, showed that a greater fraction of Tfr cells than Tfh cells expressed p-TBK1 in both strains (Fig. 4.13C and Fig. 4.13E). A similar decrease in both the mean fluorescence intensity of p-TBK1 (Fig. 4.14B) and the percentages of p-TBK1 containing Tfr cells was observed in MAVS^{los} relative to WT Tfr cells

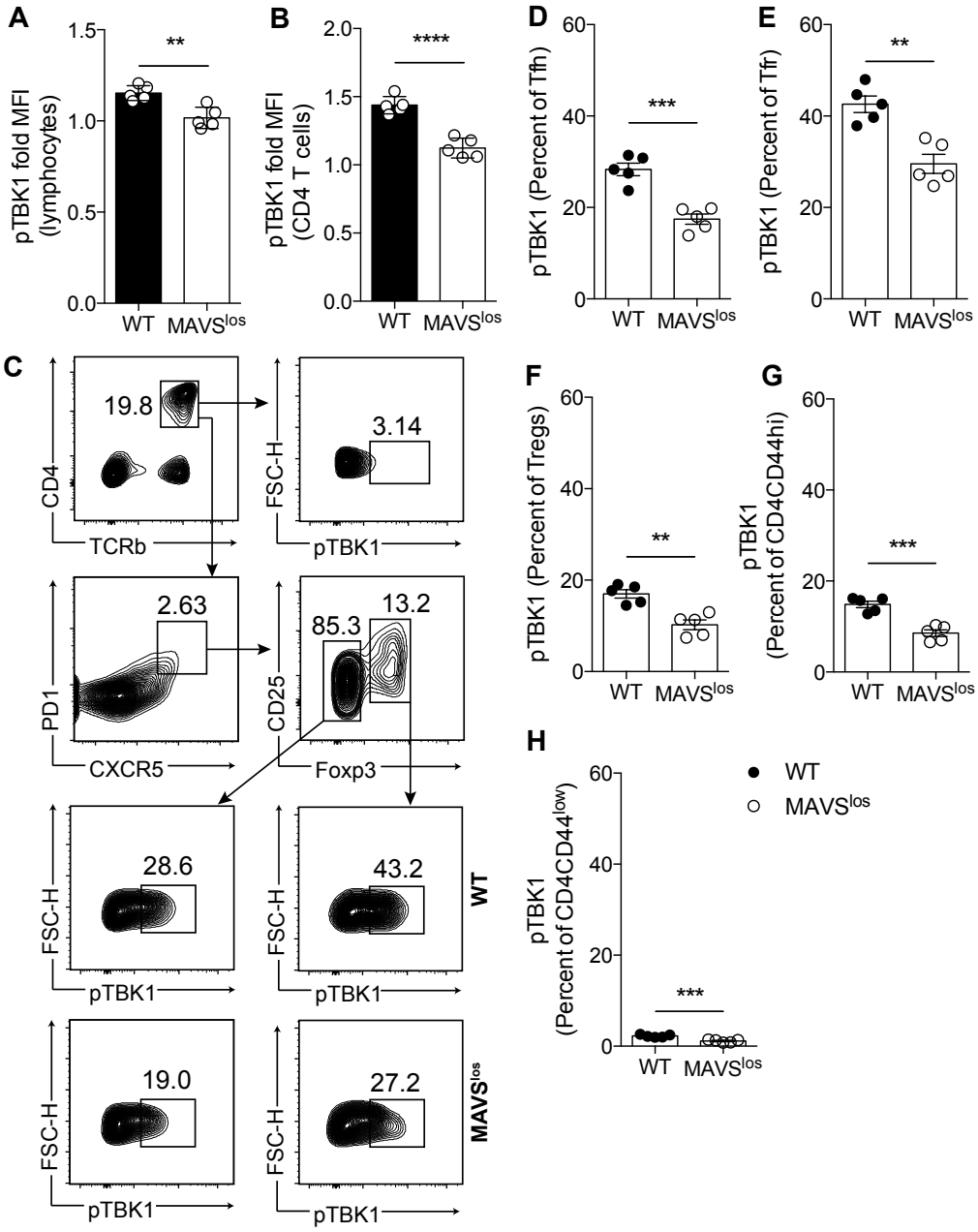

Figure 4.13. *Machtlos* mutation impairs phosphorylation of TBK1 in T cell populations. (A-B) WT and MAVS^{los} mice were i.v. injected with 200 µg poly(I:C), and spleens collected for analysis 8 hrs after. Bars indicate CD86 mean fluorescence intensity ± SEM relative to PBS-injected control mice in (A) total lymphocytes and (B) in CD4+ T cells. **, P < 0.01; ****, P < 0.0001 (unpaired Student's t test). (C-H) WT and MAVS^{los} mice were immunised with SRBC and spleens were collected for analysis on day 7. (C) Representative flow cytometry gating strategy for p-TBK1 expression in Tfh and Tfr populations in the spleen of WT and MAVS^{los} mice. (D) Mean percentage ± SEM of p-TBK1 expression in Tfh cells (CXCR5+PD-1+Foxp3-), (E) Tfr cells (CXCR5+PD-1+Foxp3+), (F) Tregs (Foxp3+), (G) activated CD4+ T cells (CD44^{high}) and (H) naïve CD4+ T cells (CD44low) in the spleen. ns, not significant; *, P < 0.05; **, P < 0.01; ***, P < 0.001 (unpaired Student's t test). i.v., intravenous; Tfh, T follicular helper cells; Tfr, T follicular regulatory cells; SRBC, sheep red blood cells.

(Fig. 4.13C and Fig. 4.13E), and was also found in Tregs (Fig. 4.13F and Fig.4.14C). Interestingly, whilst p-TBK1 was most pronounced in WT T follicular populations, its expression was not specific to these cells since p-TBK1 was greater in the total CD44hi activated/memory phenotype CD4+ T cell populations (Fig. 4.13G) compared with the naïve CD44lo CD4+ T cell populations from both MAVS^{los} and WT mice (Fig. 4.13H).

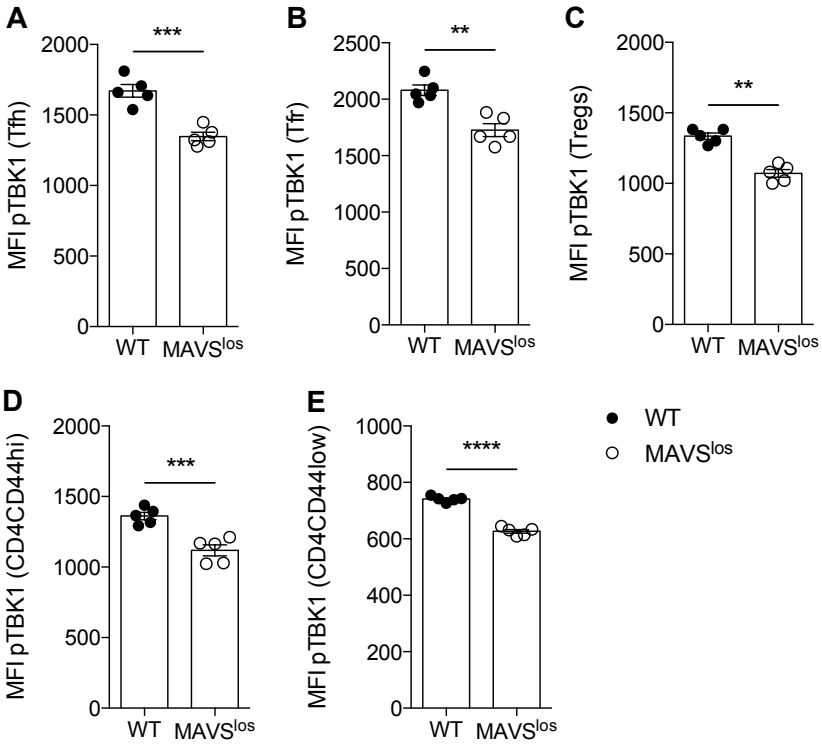

Figure 4.14. MAVS^{los} mutation is associated with decreased p-TBK1 expression in T cells

WT and MAVS^{los} mice were immunised with SRBC and spleens were collected for analysis on day 7. (A) Mean fluorescence intensity ± SEM of p-TBK1 in Tfh cells (CXCR5+PD-1+Foxp3-), (B) Tfr cells (CXCR5+PD-1+Foxp3+), (C) Tregs (Foxp3+), (E) activated CD4+ T cells (CD44^{high}) and (F) naïve CD4+ T cells (CD44low) in the spleen. ns, not significant; *, P < 0.05; **, P < 0.01; ***, P < 0.001; ****, P < 0.0001 (unpaired Student's t test). Tfh, T follicular helper cells; Tfr, T follicular regulatory cells; SRBC, sheep red blood cells.

Western blot analyses of IRF3 phosphorylation has shown that the *machtlos* mutation impairs activation of this transcription factor in response to poly(I:C)

and that this is associated with a reduced production of T1-IFN and IL-6 (see Figure 4.2). To test which cells are affected by this defect, IRF3 phosphorylation was analysed by flow cytometry. At 8 hrs after poly(I:C) challenge, T cells and MZ macrophages from MAVS^{los} mice expressed significantly reduced levels of p-IRF3 (Fig. 4.15B and Fig. 4.15C). In addition, MAVS^{los} APCs including MZ macrophages (Fig. 4.15D), F4/80+ macrophages (Fig. 4.15E) and conventional DCs (Fig. 4.15F) expressed reduced levels of CD86 compared to WT APCs, indicating reduced activation of these populations.

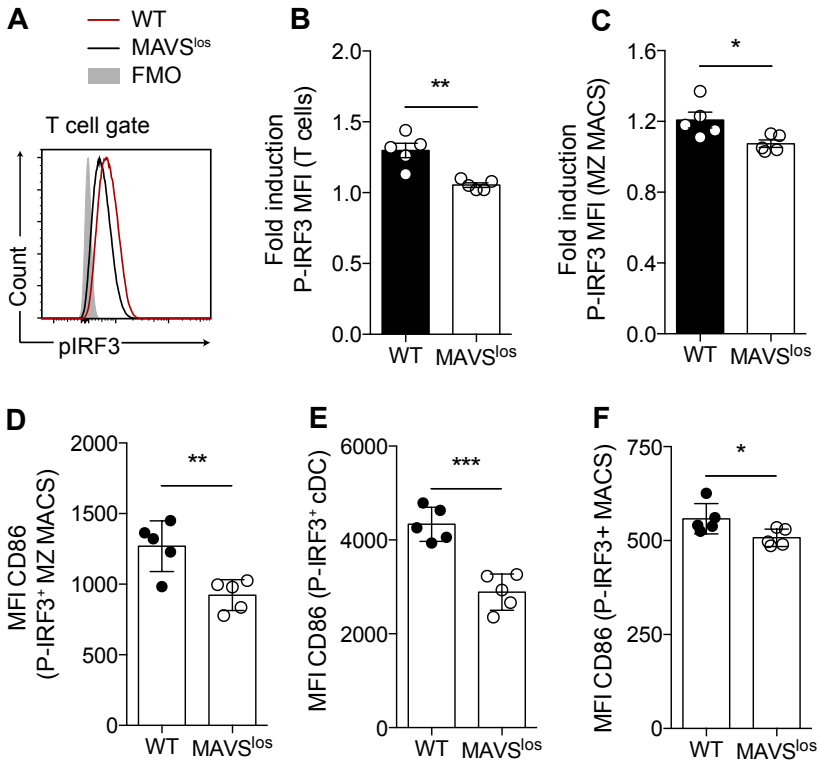

Figure 4.15. MAVS^{los} mutation is associated with decreased p-IRF3 expression in T cells
WT and MAVS^{los} mice were i.v. injected with 200 µg poly(I:C), and spleens collected for analysis 8 hrs after. (A) Representative flow cytometry plot showing expression of p-IRF3 in splenic CD4+ T cells from untreated (grey) WT mice, and from poly(I:C) treated WT (red line) and MAVS^{los} mice (black line). (B) Mean fluorescence intensity ± SEM of p-IRF3 in T cells (TCRb+B220-) and (C) MZ macrophages (CD169+CD11b+) in the spleen. (D-F) Mean fluorescence intensity ± SEM of CD86 in p-IRF3+ APCs including CD169+CD11b+MZ macrophages (D), B220-CD11c^{hi} conventional DCs (E) and F4/80+CD11b+ macrophages (F) in the spleen. *, P < 0.05; **, P < 0.01; ***, P < 0.001 (unpaired Student's t test). MZ, marginal zone; DC, dendritic cells; FMO, fluorescence minus one control.

4.2.7 The immunogenicity of SRBC is dependent upon RLR-MAVS and TLR pathways

In addition to the RLR-MAVS pathway, RNA is also recognised by TLRs contained within endosomes, but the resonance between the RLR-MAVS and TLR pathways remains incompletely understood. The RLR-MAVS pathway might influence TLR activation indirectly through T1-IFN production, amplifying recognition though PRR's. To this end, the influence of synthetic RNA on the mRNA levels of TLR3 and TLR7 as well as TLR4 (not involved in RNA recognition) was measured in MAVS^{los} splenocytes in comparison with WT and *Ifnar1-/-* cells. Poly(I:C) administration resulted in the upregulation of TLR3 mRNA in WT splenocytes, shown as fold increase over PBS controls (Fig. 4.16A). By contrast, the poly(I:C)-mediated upregulation of TLR3 mRNA was significantly reduced in both MAVS^{los} and *Ifnar1-/-* splenocytes, indicating that optimal TLR3 expression is dependent on T1-IFN responsiveness (Fig. 4.16A). TLR7 mRNA expression, in turn, was compromised by a deficiency in *Ifnar1*, but not by the *machtlos* mutation (Fig. 4.16B). Notably, supplementation of WT mice with IFN-α was associated with increased TLR3 protein expression in B cells, conventional and plasmacytoid DCs (Fig. 4.16G), but had little effect on the expression of TLR7 protein expression in these cells, confirming the strong dependency of optimal TLR3 induction on T1-IFN.

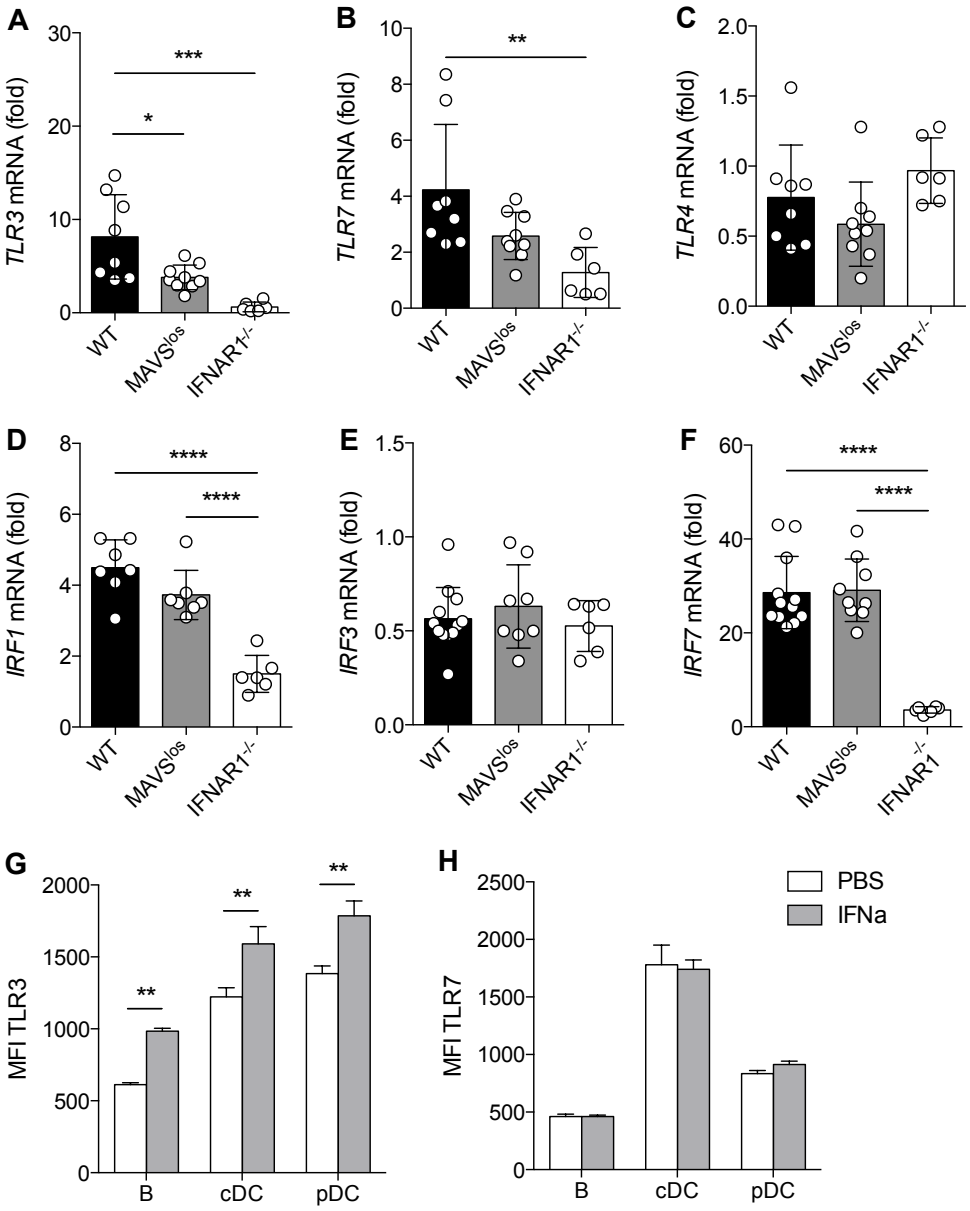

Figure 4.16. Impaired MAVS signalling is associated with reduced expression of TLR3
(A-F) WT, MAVS^{los} and IFNAR$^{-/-}$ mice were i.v. injected with 200 µg poly(I:C), and spleens collected for quantitative real-time PCR analysis 4 hrs after. Gene expression levels of selected genes are presented relative to housekeeping gene Rpl19. *, P < 0.05; **, P < 0.01; ***, P < 0.001; ****, P < 0.0001; statistical significance was assessed by 1-way ANOVA using Bonferroni's multiple comparisons test. (G-H) WT mice were s.c. injected with either PBS or 0.1 µg IFN-alpha, and spleens were collected for flow cytometric analysis on day 7 (n=5). Mean fluorescence intensity ± SEM of (G) TLR3 and (H) TLR7 in B cells (B220+), conventional DCs (B220-CD11c^{hi}) and plasmacytoid DCs (B220+CD11c+). **, P < 0.01; statistical significance was assessed by 2-way ANOVA using Bonferroni's multiple comparisons test. s.c., subcutaneous, IFN, interferon; cDC, conventional dendritic cells; pDC, plasmacytoid dendritic cells.

To further examine the effect of the *machtlos* mutation in MAVS on T1-IFN pathways, the expression of interferon stimulated genes was analysed following poly(I:C) administration relative to mice deficient in the receptors for interferon alpha and beta (*Ifnar1-/-* mice). While the mRNA expression of IRF3 was not affected in either MAVS^{los} or *Ifnar1-/-* splenocytes (Fig. 4.16E), the expression of interferon regulatory factor 1 (IRF1, Fig. 4.16D) showed a partial defect in MAVS^{los} relative to the very low expression observed in *Ifnar1-/-* splenocytes. Expression of IRF7 mRNA was distinctly reduced in *Ifnar1-/-* splenocytes, but was unaffected by the *machtlos* mutation (Fig. 4.16F). These findings indicate that the *machtlos* mutation induced a partial defect in the expression of interferon-stimulated genes.

To determine the relative contribution of RNA recognition through the TLR3 and RLR-MAVS, we administered poly(I:C) (i.v.) in the presence or absence of a TLR3-RNA complex inhibitor and measured secretion of IFN-β and IL-6 in the serum. TLR3 inhibition reduced the production of both IFN-β (Fig. 4.17A) and IL-6 (Fig. 4.17B) measured in the serum of WT mice 4 hours following poly(I:C) administration, indicating that TLR3 partially contributed to the response to poly(I:C). For MAVS^{los} mice, there was a similar trend, but no significant difference observed in IFN-β (Fig. 4.17A) or IL-6 (Fig. 4.17B) production in the presence or absence of TLR3-RNA complex inhibitor after poly(I:C) administration. This finding reflected the much lower response of MAVS^{los} mice to poly(I:C) and suggested that in the absence of a fully functioning MAVS, the role of TLR3 was less pronounced.

Similar levels of TLR7 mRNA were observed in WT and MAVS^{los} splenocytes after poly(I:C) administration (Fig. 4.16B), reflecting that (for TLRs) poly(I:C) acts mostly through TLR3 rather than TLR7. Therefore, we directly tested whether the *machtlos* mutation influenced responsiveness to a TLR7 agonist R848. Two hours after administration of the TLR7 agonist (i.v.) IL-6 was detected in serum of both WT and MAVS^{los} mice, but not in PBS treated mice (Fig. 4.17C). However, the amounts of IL-6 were significantly greater in WT than MAVS^{los} mice, suggesting that the RLR-MAVS pathway influences responsiveness to TLR7 ligand.

The RLR-MAVS pathway had an important role in the expression of TLR involved in recognition of RNA, suggesting that MAVS may generate an early signal in response to cytosolic recognition of RNA that subsequently amplifies TLR pathways. In order to test the contribution of TLR pathways to the response to SRBC, WT and MAVS^{los} mice immunised with SRBC were treated with either TLR3-RNA complex inhibitor or TLR3-RNA complex inhibitor together with Myd88 inhibitor, and the effect on GC populations by immunostaining and flow cytometry was measured. Consistent with findings shown in Figure 5, Tfh cells were significantly reduced in MAVS^{los} mice relative to WT mice on day 7 post SRBC immunisation (Fig. 4.17D). Notably, TLR3 inhibition reduced the percentages of WT Tfh cells, however, the combination of both inhibitors caused a more significant reduction in Tfh frequencies in WT mice (Fig. 4.17D). By contrast, neither TLR3 nor TLR3 plus Myd88 inhibitor significantly reduced the already low percentages of MAVS^{los} Tfh cells (Fig 17D). Similarly, TLR3 inhibition and combined TLR3 and Myd88 inhibition

significantly reduced the percentages of Tfr cells in WT mice (Fig. 4.17E), but had little effect on MAVS^{los} Tfr cells (Fig. 4.17E). A (non-significant) reduction of GC B cells was observed in WT mice with TLR3 inhibition and when TLR3 inhibition was combined with Myd88 inhibition (Fig. 4.17F). In contrast to WT GC B cells, MAVS^{los} GC B cells were not reduced following TLR3 inhibition (Fig. 4.17F). In addition, for both WT and MAVS^{los} GC populations, the administration of TLR3 combined with Myd88 inhibitor had no significant effect relative to SRBC immunisation only (Fig. 4.17F). Taken together, these findings reveal that recognition of foreign RNA is central to the immune response to SRBC and suggest that the RLR-MAVS pathway is an early signal that precedes the upregulation of TLR signalling, required for optimal humoral immunity to SRBC.

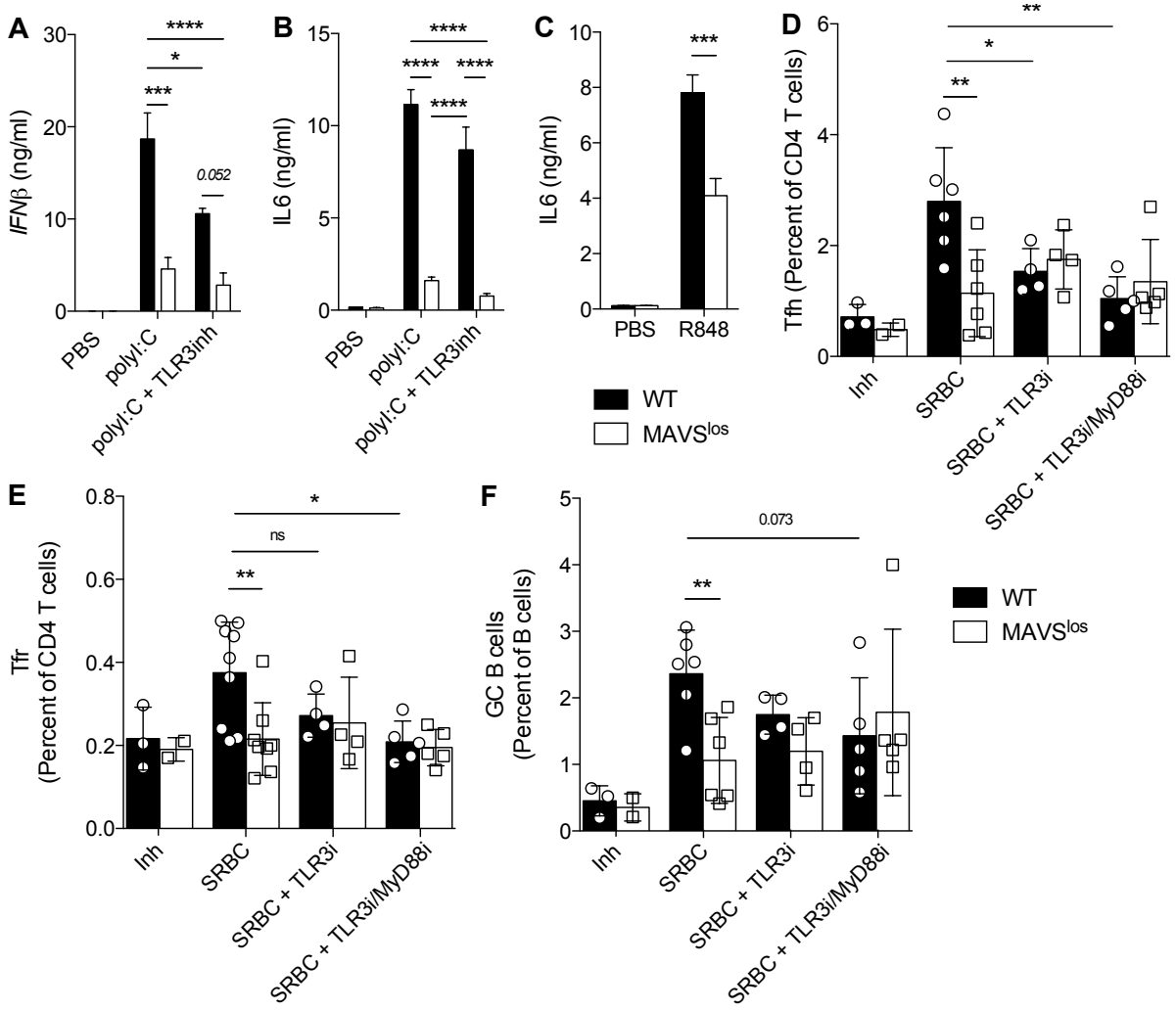

Figure 4.17. Adaptive immunity to SRBC requires MAVS-dependent TLR activation
(A-B) WT and MAVS^{los} mice were i.p. injected with PBS or 1 mg of TLR3/dsRNA complex inhibitor in PBS one hour before i.v. administration of 200 ug poly(I:C). Serum levels of IFN-β (A) and IL6 (B) were measured by ELISA. (C) WT and MAVS^{los} mice were i.p. injected with PBS or 25 ug R848 compound one hour before i.v. administration of 200 µg poly(I:C). Serum levels of IL6 were measured by ELISA. (D-F) WT and MAVS^{los} mice were immunised with SRBC and intraperitoneally administered PBS or 700 µg of TLR3/dsRNA complex inhibitor or 700 µg of TLR3/dsRNA complex inhibitor and 70 µg MyD88 inhibitor peptide 1 hour before and 1 hour after SRBC injection; control mice were given inhibitors only (Inh). Spleens were collected for analysis on day 7. Mean percentage ± SEM of (D) Tfh cells (CXCR5+PD-1+Foxp3-), (E) Tfr cells (CXCR5+PD-1+Foxp3+) and (F) GC B cells (Fas+Gl7+CD19+) in each spleen 7 d after SRBC immunisation. *, P < 0.05; **, P < 0.01; ***, P < 0.001; ****, P < 0.0001; statistical significance was assessed by 2-way ANOVA using Bonferroni's multiple comparisons test. SRBC, sheep red blood cells; GC, germinal centre; i.p., intraperitoneal; i.v., intravenous; Tfh, T follicular helper cells; Tfr, T follicular regulatory cells.

4.3 DISCUSSION

Due to their potent immunogenic properties, SRBC have been used for over half a century to study the immune response to protein antigen. In fact, experimental inoculation of SRBC into mammals predates the discovery of antibody production by B cells (Ehrich and Harris, 1942; Fagraeus, 1948). SRBC induce a robust GC reaction in mice, and as such, provide a model T-dependent antigen to analyse the humoral immune response under various genetic and metabolic host conditions. The ability of SRBC to provoke an immune response has been attributed to the foreign, polyvalent nature of SRBC antigen. Importantly, this study provides evidence that the immunogenicity of SRBC is connected to the cytosolic sensing of RNA through the RLR-MAVS pathway and that the transmembrane region (TM) of MAVS is crucially involved in this process.

The mitochondrial adaptor protein MAVS is best known for transducing antiviral signalling through its physical interaction with cytosolic RLRs that become activated following binding of RNA. The central role of the MAVS signalling complex in the immune response to viral nucleic acids is best exemplified by the number of viruses that have developed ways of evading the immune system by degrading or suppressing MAVS (e.g. hepatitis C virus, coxsackievirus, enterovirus 71) (Baril et al., 2009; Mukherjee et al., 2011; Wang et al., 2013). Notably, much of what is known about the function of the MAVS signalling pathway has been gained from studies using ectopic

overexpression of tagged MAVS and MAVS binding partners in cell lines (Hou et al., 2011; Liu et al., 2010; Seth et al., 2005; Subramanian et al., 2013; West et al., 2011). In order to probe the influence of the MAVS TM domain on the function of endogenous MAVS *in vivo*, we have utilized a mouse model that harbours a damaging SNP in the TM domain of MAVS. Our findings demonstrate that the MAVS TM domain is critical for the interaction with Tom70, which, like MAVS, is located within the outer mitochondrial membrane (Fig. 4.1C). In agreement with our finding, a previous study has shown an interaction of MAVS and Tom70 *in vitro* in Sendai virus-infected cells, and demonstrated that ectopic expression or silencing of Tom70, respectively, enhanced or impaired IRF3-mediated gene expression and IFN-β production (Liu et al., 2010). Similarly, $MAVS^{los}$ mice displayed impaired activation of both TBK1 and IRF3, which subsequently resulted in reduced production of IFN-β and IL-6, highlighting the central role of the MAVS C-terminal TM domain for T1-IFN signalling. Although here we provide evidence for the critical site in the MAVS TM domain, it remains unclear how the *machtlos* mutation affects the interaction with Tom70 and other components of the MAVS signalling complex at the molecular level. While structural data would certainly shed light on this question, a crystal structure that includes the MAVS TM domain is yet to be reported. 3D modelling of the TM region of MAVS using the HADDOCK software (v2.2) revealed a possible helical structure for the TM domain of MAVS. The effect of the *machtlos* mutation was inconclusive though, with models for proper and improper (destabilized) α-helix formations having similar likelihoods (data not shown). However, given the helix-breaking properties of the introduced proline, a disruption of the MAVS TM structure caused by the

non-conservative amino acid change (i.e. leucine to proline) is likely to be accountable for the defective binding to Tom70 and the reduced activation of both TBK1 and IRF3. In addition, an earlier report using MAVS constructs *in vitro* demonstrated that the MAVS TM domain is also responsible for its mitochondrial localization (Seth et al., 2005). Interestingly, we did not detect a defect in the ability of $MAVS^{los}$ to localize to the mitochondria (Fig. 4.3), nor did we observe an appreciable effect on MAVS oligomerization as indicated by clustered fluorescence (Fig. 4.3).

Given that MAVS is critical in the context of cytosolic RNA-sensing, the impact of the *machtlos* mutation on the immunogenicity of SRBC was unexpected. Notably, early studies using solubilized, complement-lysed or sonicated SRBC indicated that an intact SRBC structure was required for effective immune stimulation, B cell activation and optimal antibody responses (Hatten and Dunton, 1978; Nagase et al., 1982). However, the reason for this requirement remained unknown. By demonstrating the importance of cytosolic RNA for generating optimal humoral immunity, our findings provide the final piece in the SRBC puzzle. Based on the fact that mature red blood cells are anucleated, it has been a long-held view that erythrocytes have no significant RNA content. Indeed, reticulocytes show a progressive reduction in RNA content as they mature (Burka, 1969; Grasso et al., 1963; Koury et al., 2005). However, our purifications yielded SRBC RNA with a considerable size distribution (Fig. 4.8A), which is consistent with previous reports of RNA extracted from human RBC (Kabanova et al., 2009; Sangokoya et al., 2010). Moreover, the relatively small quantities of RNA detected in human erythrocytes comprise different

types of RNA, including tRNA (Kabanova et al., 2009), miRNA (Chen et al., 2008; Hamilton, 2010; Rathjen et al., 2006; Sangokoya et al., 2010; Yu et al., 2010) and several hY (human cytoplasmic) RNAs (O'Brien and Harley, 1990). Therefore, our results suggest that reduced T-dependent B cell response observed in SRBC-immunised mice harbouring the *machtlos* mutation originates from impaired signalling of SRBC RNA.

Labelling SRBC with CFSE provided further insights into the mechanism by which SRBC RNA elicits this adjuvant effect. Three hours following i.v. injection, CFSE-labelled SRBC had travelled to the spleen and amassed in the red pulp near the marginal zone, where SRBC were observed inside macrophages and dendritic cells (Fig. 4.8B). Notably, the engulfment of cells is controlled by the surface expression of CD47, which provides an antiphagocytic “don’t eat me” signal. Binding of CD47 to the immune inhibitory receptor SIRP-α (signal regulatory protein α) prevents the uptake of target cells expressing CD47 (Ishikawa-Sekigami et al., 2006; Oldenborg et al., 2000; Yi et al., 2015). A recent study has shown that *Cd47*$^{-/-}$ mouse RBC initiated an immune response following phagocytosis by mouse DCs, illustrating the immune system’s deficiency in distinguishing self and foreign material (Yi et al., 2015). In the case of SRBC, it was reported that sheep CD47 on these cells failed to bind mouse SIRP-α, providing an explanation for the uptake of SRBC by murine APCs (Yi et al., 2015).

Once SRBC had been engulfed, APCs exhibited signs of activation and maturation, with increased levels of CD86 and MHCII observed on both

macrophages and dendritic cells that contained SRBC relative to the same populations that did not contain SRBC (Fig. 4.9). Importantly, the *machtlos* mutation compromised the activation and maturation of aforementioned APCs. This finding indicated that the RLR-MAVS pathway positively regulates the maturation and antigen presenting capacity of APC populations following SRBC immunisation. The overall reduced APC function in MAVS^{los} mice may have contributed to the reduced populations of both Tfh cells and Tfr cells. In addition to the cell intrinsic MAVS effects, reduced APC function may also partly explain why MAVS^{los} Tfh cell and IgG1+ GC B cell frequencies remained low despite a reduced Tfr cell population. As SRBC provide both a source of protein antigen and, as shown in our experiments, RNA adjuvant, the ability of SRBC to generate GC reactions was compromised in MAVS^{los} mice. Similarly, CVB4 infection provoked reduced frequencies of GC B cells and follicular helper T cell subsets in mice harbouring the *machtlos* mutation. Although viral replication rates and overall survival was comparable between WT and MAVS^{los} mice, this is likely to be attributable to the host-manipulating evasion strategies of this virus (Chau et al., 2007; Mukherjee et al., 2011). Importantly, WT mice and MAVS^{los} mice responded equivalently to immunisation with NP-OVA in alum, indicating that *machtlos* did not impair the antibody response to protein antigen *per se*. These findings demonstrate the importance of MAVS signalling for the RNA adjuvant-enhanced antibody responses to protein antigens.

In contrast to both T follicular cell subsets (Tfh cells and Tfr cells), the decrease in GC B cell frequency in MAVS^{los} mice was found to be due to cell

extrinsic factors. One possible extrinsic factor is the presence of cytokines such as T1-IFN and IL-6, both of which were reduced in MAVS^{los} mice in response to poly(I:C) (Fig. 4.2). IL-6 production was also poor in mice that lacked the receptor for T1-IFN (Fig. 4.11H), indicating a positive feedback loop between both cytokines. Furthermore, the impaired activation and maturation of APCs could also have affected GC B cell frequencies in a cell extrinsic manner. On the other hand, responsiveness to T1-IFN promoted the expansion/differentiation of both Tfh cells and Tfr cells in a cell intrinsic manner (Fig. 4.11). This is in strong agreement with previous studies reporting that nucleic acid triggered T1-IFN responses are critical for APC maturation and subsequent T cell activation and differentiation (Baranek et al., 2012; Longhi et al., 2009). Administration of T1-IFN during SRBC immunisation was able to boost the percentages of GC B cells and Tfh cells to an equivalent extent in both WT and MAVS^{los} mice (Fig. 4.12). However, exogenous T1-IFN could not fully recover the GC defect in MAVS^{los} mice, suggesting that endogenous T1-IFN is present at low concentrations during SRBC immunisation.

In an effort to identify other aspects of the MAVS signalling complex that may have affected cell intrinsic differentiation of follicular T cell subsets, we focused on the activation of both TBK1 and IRF3. Notably, the phosphorylation of TBK1 was relatively restricted to T cell populations, where we observed p-TBK1 in activated/memory phenotype CD4+CD44hi T cells but not in naïve CD4+ T cells, suggesting that TBK1 phosphorylation was a result of cellular activation (Fig. 4.13). In addition, the percentages of MAVS^{los} Tfh cells containing p-TBK1 were considerably reduced compared to those in WT Tfh cells,

indicating that the MAVS TM region is critical for the robust activation of TBK1 in these cells following SRBC immunisation. Furthermore, our findings demonstrated that both total Tregs and Tfr cells activate TBK1 in response to SRBC immunisation. Indeed, the Tfr population contained the highest frequency of p-TBK1+ cells within this setting, however, the *machtlos* mutation also led to a consistent reduction in the percentages of T regulatory cells that had activated TBK1.

Consistent with a defect in the MAVS signalling complex, the activation of IRF3 was also reduced in T cells from MAVS^{los} mice (Fig. 4.15). However, in contrast to p-TBK1, poly(I:C) challenge provoked the phosphorylation of IRF3 more broadly and within both T cell and APC populations. Given that SRBC immunisations may result in low production of T1-IFN, the impaired phosphorylation of IRF3 could potentially contribute to the T cell intrinsic defect observed in MAVS^{los} mice. Consistent with our findings, a recent study has identified that the interaction of TBK1 with ICOS is an important factor in Tfh cell differentiation and demonstrated that shRNA knockdown of TBK1 reduced Tfh cell frequencies by approximately 50% following LCMV infection (Pedros et al., 2016). However, the mechanisms leading to the activation of TBK1 following SRBC immunisation and DNA virus infection are likely to differ and remain to be fully elucidated. Taken together, our findings demonstrate that the TM domain of MAVS is important for the activation of TBK1 in both Tfh cells and Tfr cells during the GC response to SRBC.

Finally, the administration of TLR3- and/or MyD88-inhibitor in the context of SRBC immunisations provided valuable insights into the contribution of TLR signalling for the immunogenicity of SRBC. Combined inhibition of MyD88 and TLR3 reduced the GC output in WT mice, as indicated by reduced percentages of Tfh cells, Tfr cells and IgG1+ GC B cells (Fig. 4.17). By contrast, combined TLR inhibition had little effect on the GC reaction in MAVS^{los} mice, suggesting that MAVS provides an early signal following SRBC immunisation that precedes the involvement of TLRs (Fig. 4.17). In support of this notion, MAVS^{los} splenocytes exhibited reduced activation of TLR3 following i.v. injection of poly(I:C) (Fig. 4.17). In a recent study, the immune response to *Cd47*$^{-/-}$ mouse RBC was shown to be associated with the activation and maturation of DCs (Yi et al., 2015). Consistent with our hypothesis that signalling through the RLR-MAVS and not the TLR pathway mediates the response to SRBC, this early effect on APC activation was not inhibited in *Myd88*$^{-/-}$*Trif*$^{-/-}$ mice that lack TLR signalling (Yi et al., 2015).

Overall, our data highlight the importance of nucleic acid sensing for optimal adaptive immunity. Based on this premise, different nucleic acid templates may be used to provide a desired adjuvant effect in the design of 'tailored' next generation vaccines. By contrast, our findings may also extend our current understanding of risk factors in autoimmunity. As exemplified with the *machtlos* mutation, individuals carrying a loss-of-function or reduced-function allele that negatively affects RLR-MAVS signalling may be protected from virus-induced autoimmunity, whilst still clearing the virus. By extension, gain-of-function mutations are likely to confer adverse host effects. Indeed, genome wide

association (GWA) studies have revealed a link between autoimmune diseases and an entire network of genes within the RLR-MAVS pathway. In particular, mutations that led to increased expression of MDA5 were shown to augment the risk for SLE and T1D (Downes et al., 2010; Nejentsev et al., 2009; Rice et al., 2014; Robinson et al., 2011), supporting the notion that chronic activation of nucleic acid sensing pathways can contribute to a number of severe autoimmune diseases (reviewed in (Banchereau and Pascual, 2006; Todd, 2014)).

5. GENERAL DISCUSSION AND PERSPECTIVE

5.1. Antiviral immunity at the expense of autoimmunity?

Although the concept of self-destruction was originally rejected over a hundred years ago (*"Horror Autotoxicus"*, Ehrlich, 1901), more than 80 autoimmune diseases have been identified. For many of these diseases, including T1D, symptom-based treatment strategies form the basis of therapeutic intervention. Understanding the events that initiate and advance autoimmunity is critical to design optimal strategies that will predict, delay, avoid or even cure autoimmune diseases. With respect to T1D, the strongest evidence for an environmental trigger points towards enterovirus infections as potential causative agents in disease pathogenesis. Based on this premise, the present study has utilized the diabetogenic coxsackievirus B4 strain to further elucidate the impact of enterovirus infections on self-destructive mechanisms leading to T1D onset.

Using the CVB4 model, we found similar kinetics of viral clearance in both T1D-resistant B6 and T1D-susceptible SJL and NOD mice, suggesting that viral persistence in the form of replicating virus did not contribute to ongoing inflammation in T1D-susceptible mice. Similarly, it has been reported that islets from T1D patients' isolated weeks after disease onset contain only very small quantities of viral RNA, indicating nearly absent viral replication during a persistent infection (Krogvold et al., 2015). Furthermore, studies on the T1D-protective CVB3 serotype found that frequently occurring spontaneous

deletions of the viral genome can lead to increased persistence of viral RNA in the pancreas and heart of CVB3-inoculated mice. Interestingly, these deletions also compromise viral replication, often resulting in the failure to detect viral protein in the aforementioned organs (Chapman and Kim, 2008; Tracy et al., 2015). This finding is in agreement with the absent CVB4 replication we observed in T1D-susceptible SJL and NOD mice (Fig. 2.2A). Further studies are required to determine which cell populations are affected by persistence of viral RNA and to evaluate the potential of this mechanism in propagating chronic inflammation. However, given that our studies and others have demonstrated a strong discrepancy in cellular tropism of CVB4 between human and mouse tissue (Dotta et al., 2007; Frisk and Diderholm, 2000; Yap et al., 2003), this evaluation would be most informative in a clinical setting.

Despite dissimilarities to human disease, T1D studies in mice have been a valuable tool for investigating the virus-mediated impact on tissue damage. The level of inflammation detected after CVB4 clearance was considerably elevated in T1D-susceptible strains compared to inflammation in T1D-resistant B6 mice. This is true for both insulitis and pancreatitis (Fig. 2.9) and reinforces the idea that de-regulated and prolonged immune responses to virus – rather than the virus itself – are associated with an elevated T1D risk. In addition, beta cell integrity in NOD mice was compromised early after CVB4 infection (i.e. peri-insulitis), suggesting that infections with pancreatropic viruses in individuals with established islet inflammation may accelerate autoimmune events (Fig. 2.6). Notably, the pancreatic innate immune cell infiltrate during acute infection was dominated by activated ($Ly6^{hi}$) macrophages, particularly in

T1D-susceptible NOD mice (Fig. 2.12A). Although macrophages are unquestionably indispensable for limiting viral replication, other studies have demonstrated that an unbalanced production of proinflammatory signals (e.g. IL-1b, IL-6, TNF-α) by either pancreatic islets or infiltrating macrophages significantly promotes the development of T1D, partially through activation of autoreactive CD4+ T cells (Calderon et al., 2006; Jun et al., 1999; Martin et al., 2008). Although this may only be one piece of the rather complex T1D puzzle, targeting macrophages by inducing an immunosuppressive phenotype could be an efficient strategy to delay disease progression in T1D patients.

Similar attention in regards to immunotherapy should be directed at the adaptive arm of the antiviral immune response. Our studies on immune-deficient B6.RAG and NOD.SCID mice have further confirmed the importance of functional lymphocytes for successful viral clearance and overall survival. However, the increased infiltration of T and B effector subsets in the pancreas of T1D-susceptible mice indicates that anti-viral immunity might come with a trade-off in the context of autoimmune susceptibility. Following viral clearance, pancreas infiltrates of T1D-prone SJL and NOD mice demonstrated higher proportions of activated/memory phenotype CD4+ T cells, GC-like B cells and Tfh cells compared to CVB4-infected B6 or age-matched uninfected NOD mice, and displayed *de novo* formation of tertiary lymphoid structures within the pancreas (Fig. 2.8, Fig. 2.13 and Fig. 2.15). Therefore, virus-mediated autoimmune destruction of beta cells in T1D-prone strains may be linked to increased production of highly differentiated, possibly autoreactive lymphocyte clones early after infection. In line with this, Th1 and Tfh phenotypes have

been described in other studies of autoimmune diabetes in mice and humans (Ferreira et al., 2015; Han et al., 2011; Katz et al., 1995; Kenefeck et al., 2015; Rabinovitch et al., 1995), with recent data suggesting a transitional period that features pathological implications for both Th1 and Tfh-like cells (Lee et al., 2012; Nakayamada et al., 2011).

Notably, SNPs linked to T1D and other autoimmune diseases have commonly been found in CD4+ T cell restricting MHC II genes (Noble and Erlich, 2012; Wang et al., 2015), and in and CD4+ T cell super enhancers (Farh et al., 2015; Vahedi et al., 2015), supporting the idea that CD4+ T effector compartments might be driving the autoimmune destruction of beta cells following virus infections. Moreover, the presence of autoantibodies commonly found in T1D patients' pinpoints a pivotal role of Th cells in T1D development (Kukko et al., 2005; Maziarz et al., 2015). Viral persistence and the subsequent ongoing production of type I IFN promotes Tfh differentiation as shown in our study (Fig. 4.12) and could therefore contribute to an increased T1D risk. While accumulating evidence emphasizes the importance of Tfh cells for anti-viral immunity (Bentebibel et al., 2013; Locci et al., 2013), their adverse implications in T1D and other autoimmune diseases (Scherm et al., 2016; Ueno, 2016) appear to be, yet again, an evolutionary trade-off. Importantly, this pathogenic mechanism is not confined to T1D – virus infections associated with other autoimmune disorders such as Sjögren's syndrome or multiple sclerosis might be partially driven by a virus-perpetuated Tfh phenotype (Belbasis et al., 2015; Igoe and Scofield, 2013). Similarly, all environmental factors able to trigger excessive differentiation of Tfh and other effector cells may be capable of

promoting autoimmune disease in genetically predisposed individuals. Finally, our studies have demonstrated that pancreatic beta cells have the capacity to upregulate an entire network of genes related to proinflammatory cytokines and T1-IFN, indicating an active involvement in antiviral defence and in the attraction of effector populations, at least during acute infection (Fig. 3.4). Thus, beta cell specific genetic variations associated with increased antiviral signalling could confer an elevated T1D risk. In line with that, our future efforts will aim to dissect the specific contribution of beta cells to chronic inflammation after viral clearance in T1D-susceptible mouse models.

Consistent with our hypothesis, recent immune intervention studies in T1D patients have aimed to block autoreactive effector lymphocytes to prevent their localization to the pancreas. However, due to disease heterogeneity, depletion resistance and a limited therapeutic time window, treatment of T1D patients with anti-CD3 (otelixizumab or teplizumab) (Herold et al., 2009; Keymeulen et al., 2010), CTLA4-Ig fusion protein (abatacept, blockade of co-stimulation) (Bluestone et al., 2006; Orban et al., 2011), anti-thymocyte globulin (ATG) (Gitelman et al., 2013), anti-CD20 (rituximab) (Xu et al., 2013) or anti-CD2 (alefacept) (Rigby et al., 2015) has only demonstrated mild or temporary improvement of beta cell function, and could not match the remission rate achieved with stem cell therapy (Couri et al., 2009; Simmons et al., 2016; Snarski et al., 2011). Current immunomodulatory strategies are shifting towards a combination of already available drugs, targeting proinflammatory cytokines (e.g. anti-TNF-a, anti-IL-1) and autoreactive effector populations (e.g. anti-CD3, anti-IL21), whilst aiming to induce tolerance to beta cells

through islet antigens (e.g. proinsulin) (Atkinson et al., 2015; Simmons et al., 2016). Given the complexity of autoimmune diabetes, this approach might allow the identification of improved therapeutic regimen tailored to individual patients.

In regards to disease prevention, large-scale prospective cohort studies are currently underway to evaluate the causality of T1D in relation to specific virus infections (e.g. CVB1, CVB4, CVB5, echovirus) and to identify more reliable and sensitive tests to detect ongoing viral infections (Group, 2008; Lonnrot et al., 2015). Notably, a recent report assessing the efficacy of CVB1-targeted vaccines has demonstrated a neutralizing immune response that prevented the onset of T1D in NOD mice (Larsson et al., 2015). In parallel, efforts are being made to commence clinical trials evaluating the efficacy of attenuated coxsackievirus vaccines in the near future (Drescher et al., 2015; Hyoty and Knip, 2014).

5.2. The virus within – friend or foe?

Endogenous retroviruses (ERVs) have retained viral characteristics and thus constitute a link between genetic and viral factors that may shape the susceptibility to autoimmune disease. Increased endogenous retrovirus activity has been implicated in autoimmune disease, mainly in the context of retroviral protein (Banki et al., 1992; Beck-Engeser et al., 2015; Freimanis et al., 2010; Laska et al., 2012; Mellors and Mellors, 1978; Moles et al., 2005). By contrast, the concept of aberrant expression of endogenous retroviral RNA and/or cDNA as autoimmune triggers has received less attention. This is somewhat

surprising, given that the majority of mammalian ERVs have lost their ability to generate viral proteins, yet retaining reverse-transcriptase activity. Other studies have shown increased ERV RNA expression in response to stimulation with cytokines or microbiota (Katsumata et al., 1999; Young et al., 2014). Our findings contribute to this field by demonstrating an elevated expression of ERV RNA following infection with a diabetogenic virus. Importantly, we found that mice prone to chronic inflammation had increased ERV RNA expression within the autoimmune target tissue even after viral clearance, supporting a potential role of ERVs as substrates for (auto-) immune recognition.

The pathogenic implications of aberrant ERV expression dependent and independent of exogenous stimuli certainly motivate further experimental investigation. For instance, simultaneous treatment of virus-infected T1D-prone mice with anti-retroviral drugs could shed further light on the contribution of ERV expression to islet infiltration and T1D risk. Similarly, tissue-specific ERV expression signatures may propagate local inflammation following infections with different viruses (e.g. herpes simplex virus, hepatitis C virus, Epstein-Barr virus) that may also be involved in the development of other autoimmune conditions.

In addition to their potential role as autoimmune substrates, ERV sequences could potentially advance immune dysregulation by modulating gene transcription. This may be mediated through binding to regulatory regions (*cis*/*trans* effect) of immune-related genes or through neutralization of gene-associated lncRNAs. Although this mechanism remains incompletely

understood, ERV regulation of immune genes has been observed for both exogenous (e.g. HIV) and endogenous retroviruses (Lu et al., 2014; Nagy et al., 2006). Our studies have identified a set of CVB4-inducible ERVs within inflamed pancreatic beta cells. Blockade of these ERVs via RNA interference will decipher the impact of each endogenous retroviral RNA on the expression of individual immune genes and on overall inflammation. Again, identifying ERV candidates that are induced by virus infections or by other stress-inducing environmental factors can provide important clues for disease pathogenesis.

Several studies have aimed to investigate the link between autoimmunity and retroviral DNA by means of antiretroviral therapy (ART). Pre-clinical studies using different combinations of ART have been able to prevent inflammation-mediated autoimmune disease in mice (Beck-Engeser et al., 2011; Sharon et al., 2015). However, early-stage clinical trials using a single reverse-transcriptase (RT) inhibitor found no effect in patients with Sjögren's syndrome (SS) (Gescuk et al., 2005; Mavragani et al., 2016). By contrast, a recent study, also on SS patients, has reinforced the notion that increased expression of retroelements is linked to an elevated autoimmune risk (Mavragani et al., 2016). Collectively, the pre-clinical and clinical studies mentioned above described a potential correlation, yet, they ultimately failed to establish the causal relationship between retroviral activity and autoimmunity. For instance, none of these studies have ruled out the possibility that dysregulated immune responses to self nucleic acids might have triggered disease. Further studies testing the efficacy of a combination of RT-inhibitors in AGS (Aicardi-Goutières syndrome) patients are currently ongoing and will hopefully clarify if and how

the accumulation of endogenous retroelements promotes autoimmune disease (*NCT02363452*; *1U01HD082806-01*).

Despite the accusations of autoimmune misconduct, there are good grounds to consider the genomic preservation of ERVs as evolutionarily advantageous. Our work has demonstrated that regulatory regions of virus response genes, in particular distal promoter sites, are enriched for ERVs (Fig. 3.13). Moreover, these ERVs were shown to harbour a multitude of TF binding motifs, including IRFs (Table 3.5 and 3.6), ISGF-3, Stat1 or Stat5 (data not shown). This suggests that ERVs are physiologically involved in the transcriptional activation of associated immune response genes, and would justify their genomic retention. By extension, the fact that the vast majority of risk-associated SNPs identified by GWA studies is located within regulatory regions outside of the exome, illustrates the strong impact of gene expression levels, rather than altered protein structure, on disease (Ernst et al., 2011; Hindorff et al., 2009; Tak and Farnham, 2015). ERVs, which constitute a large proportion of mammalian genomes, have provided alternative promoters and enhancer elements (Chuong et al., 2016; Cohen et al., 2009; Gowda et al., 1988), and have therefore significantly shaped immunity to foreign pathogens. Over the course of evolution, ERV mutations and insertions will continue to advance phenotypic traits, thus improving the overall survival outcome for the host. Ideally, the interplay between virus and host is directed towards reaching an equilibrium, in which immune defences against foreign pathogens are perfectly fine-tuned, dismissing autoimmune reactions altogether.

5.3. Making nucleic acid sensing great again

As discussed above, an aberrant expression or persistence of exogenous and/or endogenous viral nucleic acids together with a genetic predisposition could significantly augment the risk of immune reactions to self. On a molecular level, this is initiated through conserved pattern recognition receptors (PRRs), and propagated through the adaptor proteins MAVS (RNA ligands) or STING (DNA ligands). Similarly, modifications of the RNA-MAVS axis, as shown by our work, or the DNA-STING axis can impact the quality of adaptive immunity, even in a non-viral setting (Li et al., 2013; White et al., 2014). This central position of nucleic acid sensing pathways in physiological and pathological conditions makes them attractive targets for drug development.

Not surprisingly, a multitude of agonists and antagonists of these pathways are currently being evaluated in ongoing clinical trials. Antagonists, which operate by targeting nucleic acid sensors (i.e. oligonucleotide antagonists), their downstream effector molecules (e.g. TBK1 antagonists), or by neutralizing T1-IFN signalling (e.g. IFNAR1 antibody, IFN-α antibody), are now being considered for the treatment of various autoimmune and autoinflammatory disorders (Lamphier et al., 2014; Lauwerys et al., 2013; Reilly et al., 2013) (NCT01777256, NCT01622348, NCT01899729. By contrast, the therapeutic potential of agonists of nucleic acid sensing is based on their immune-enhancing properties that allow for improved adaptive responses. As a result, clinical trials are currently investigating the prophylactic and therapeutic

potential of nucleic acid sensing agonists as adjuvants for infectious disease and cancer indications, and as immunomodulatory agents for the treatment of allergies (e.g. NCT01984892, NCT01591473, NCT01607372, NCT02166047, NCT00960752). Ultimately, deciphering the contribution of discrete nucleic acid sensing pathways in the context of complex inflammatory and autoimmune diseases will allow the development of immunotherapies tailored to specific medical needs.

6. MATERIALS AND METHODS

6.1. Standard buffer solutions

Buffers/Solution	Components	Supplier
ELISA coating buffer (pH 9.4)	2.9 g/L $NaHCO_3$ 1.6 g/L Na_2CO_3,	Merck Merck
ELISA buffer	1x PBS 0.1% Tween 20	Gibco ICN Biomedicals
Red blood cell lysis buffer	8.26g NH_4Cl 1g $KHCO_3$ 0.037g EDTA 1L dH_20	Merck Merck Gibco
FACS buffer	0.02% NaN_3 0.5% BSA 2mM EDTA 1x PBS	Amersham Gibco Gibco Gibco
MACS buffer	0.5% BSA 2mM EDTA 1x PBS	Gibco Gibco Gibco
Cell culture medium I (lymphocytes)	10% Foetal calf serum (FCS) 50 U/ml penicillin G sodium 50µg/ml streptomycin sulphate 2mM L-glutamine 1x RPMI 1640	Gibco Gibco Gibco Gibco Gibco
Cell culture medium II	10% Foetal calf serum (FCS) 2mM L-Glutamine 50U/ml Penicillin 50µg/ml Streptomycin 50µM 2-mercapto-ethanol (2ME) 1x DMEM	Gibco Gibco Gibco Gibco Sigma-Aldrich Gibco
Avertin	25g 2-2-2 Tribromoethanol 25ml 2-methyl-2-butanol	Sigma-Aldrich Sigma-Aldrich
Lymphocyte isolation buffer	1x RPMI 1640 10% BCS	Gibco Gibco
Carnoys reagent	75% Methanol 25% Glacial acetic acid	BDH Prolabo Thermo Fisher
Antibody dilution buffer	0.5% Triton X-100 1% BSA 1x PBS	Sigma-Aldrich Gibco Gibco
Blocking buffer	1% BSA 3% Goat serum 1x PBS	Gibco Sigma-Aldrich Gibco
Carboxyfluorescein succinimidyl ester (CFSE) buffer	0.1% Foetal calf serum (FCS) 5µM CFSE 1x PBS	Gibco eBioscience Gibco
Isotonic Percoll solution	16.9ml Percoll 1.9ml 10x PBS 31.2ml 1x PBS	Amersham Gibco Gibco
DNA isolation buffer	670mM Tris pH8.8 166mM $(NH_4)_2SO_4$ 65mM $MgCl_2$ 10% 2-mercapto-ethanol (2ME) 5% Triton X-100 100µg/ml Proteinase K	Gibco Amersham Amersham Gibco Sigma-Aldrich Promega
Islet isolation media	Medium 199 (M199) 10% heat-inactivated bovine calf serum (BCS) 4.61mM $NaHCO_3$	Sigma-Aldrich HyClone Sigma-Aldrich
NP-40 cell lysis buffer	50mM Tris-HCL pH 8.0 150mM NaCl 1% NP-40	Sigma-Aldrich Thermo Fisher Thermo Fisher

6.2. Mice

The MAVS^{SNP} mouse strain used in this study was generated by ENU mutagenesis at the Australian Phenomics Facility on a C57BL/6 background. Thy1.1^{+} and IFNAR$^{-/-}$ were bred in house on the C57BL/6 background. µMT mice were kindly provided by Prof. Robert Brink (Garvan Institute, Sydney). C57BL/6 (B6), NOD/ShiltJAusb (NOD) and Ly5.1 congenic mice were purchased from Australian BioResources in Moss Vale, Australia. NOD.Scid, SJL/JArc (SJL) and B6.Rag1 mice (N10 background) were purchased from the Animal Resource Centre in Perth, Australia. All mice undergoing study were age- and gender-matched and between 7- and 14-weeks old.

6.3. Flow cytometry

Various tissues (spleen, thymus or lymph nodes) were collected and immediately put into lymphocyte isolation buffer. Tissues were homogenised using 70µm cell strainers. For isolation of lymphocytes from the pancreas, mice were perfused with 1x PBS (30 ml/mouse) and the pancreas extracted. The pancreas was cut into smaller pieces and digested for 13 minutes in 0.25mg/ml Liberase-Enzyme Blend-RI (Roche) in plain RPMI, before homogenized through a 70 µm cell strainer. Red blood cells (RBC) were removed by incubating the cells in 1 ml 1x RBC lysis buffer for 2 minutes on ice, before washing cells twice in lymphocyte isolation buffer. Single cell suspensions were adjusted to a concentration of 2 x 10^{7} cells/ml in ice cold FACS buffer and stained in 50-100 µl of 96-well U-bottom microtitre plates at concentrations shown in Table 2.2.

Table 2.2 Antibodies/reagents used for flow cytometry and immunohistochemistry

Antibody	Clone	Label	Company	Dilution
B220	RA3-6B2	PerCP-Cy5.5	BD Biosciences	1:300
CD11b	M1/70	FITC	eBioscience	1:200
		PE		1:300
CD11c	N418	FITC	eBioscience	1:200
		APC		1:300
CD122	5HX	Biotin	eBioscience	1:200
CD169	3D6.112	APC	BD Biosciences	1:200
CD19	ID3	PB	eBioscience	1:200
CD25	PC61	APC	eBioscience	1:200
CD3	500A2	PB	Biolegend	1:200
CD4	RM4-5	PE	BD Biosciences	1:400
		PB		1:300
		BV605		1:200
CD43	S7	Biotin	eBioscience	1:100
CD44	IM7	APC	BD Biosciences	1:300
		eFluor780		1:300
CD45.1	A20	PerCP-Cy5.5	eBioscience	1:200
		Pe-Cy7		1:200
CD45.2	104	APC-eFluor780	Biolegend	1:200
CD68	FA-11	Biotin	Biolegend	1:100
CD8	53-6.7	FITC	eBioscience	1:200
		Pe-Cy7		1:400
CD86	GL-1	BV650	Biolegend	1:200
CXCR4	2B11	Biotin	BD Biosciences	1:100
CXCR5	2G8	Biotin	BD Biosciences	1:100
F4/80	BM8	AF647	Biolegend	1:200
Fas	Jo2	FITC	BD Biosciences	1:200
Foxp3	FJK-16a	eFluor450	eBioscience	1:100
GL7	GL7	PE	BD Biosciences	1:300
Glut2	205115	Purified (rat)	R&D Systems	1:200
Goat Anti-Rabbit IgG H&L	Polyclonal	AF647	Thermo Fisher Scientific	1:300
Goat Anti-Rat IgG H&L	Polyclonal	AF488	Thermo Fisher Scientific	1:300
IgG1	A85.1	Biotin	BD Biosciences	1:100
IgG2	R19-15	Biotin	BD Biosciences	
Insulin	Polyclonal	Purified	Cell Signaling	1:100
Ly6C	AL-21	PE	eBioscience	1:100
Ly6G	1A8	PB	eBioscience	1:200
MHCII	M5/114.15.2	PE	eBioscience	1:400
NK1.1	PK136	FITC	eBioscience	1:200
		PE		1:300
		APC		1:300
PD-1	J43	FITC	eBioscience	1:100
		PE		1:200
Pecam-1	390	PE	eBioscience	1:200
pIRF3	D6O1M	PE	Cell Signaling	1:50
pTBK1	D52C2	PE	Cell Signaling	1:50
Streptavidin	-	PerCP-C5.5	eBioscience	1:400
		Pe-Cy7		1:400
		APC		1:400
		PB		1:300
TCRb	57-597	FITC	eBioscience	1:300
		APC		1:300
TLR3	11F8	PE	Biolegend	1:50
TLR7	A94B10	APC	Biolegend	1:50
Tmem27	Polyclonal	Purified (rabbit)	ProteinTech	1:100

In order to block non-specific binding of immunoglobulin to Fc receptors, cells were pre-treated with anti-mouse CD16/32 (clone 2.4G2, BD Pharmingen) for 10 min. Cells were acquired with a Canto cytometer (BD Biosciences, CA) and analysed using the FlowJo software (TreeStar, CA).

6.4. Intracellular staining

Surface molecules were detected as stated above. Intracellular molecules were detected using the Cytofix/Cytoperm™ kit from BD Biosciences according to the manufacturer's instructions. The nuclear transcription factor Foxp3 was detected using the Intracellular Fixation and Permeabilization Buffer Set from eBioscience. Cytokines were detected directly *ex-vivo* or after 4 hours *in-vitro* stimulation with phorbol myristate acetate (PMA 5 ng/ml, BIOMOL USA), ionomycin (1 µg/ml, Invitrogen) and Golgi-Stop (1:1000, BD Biosciences) at 37°C.

6.5. Isolation and sorting of pancreatic beta cells

Mice were euthanized with carbon dioxide (CO_2), before a midline incision was introduced to expose internal organs. Each mouse was given 3 ml of 0.25 mg/ml Liberase-Enzyme Blend RI (Roche) in serum-free islet isolation media via the bile duct perfusion using a 30-gauge needle. Pancreata were digested for 13 min in a 37°C water bath. The tubes were immediately put on ice and topped up with 30 ml of ice-cold islet isolation media to stop the reaction.

Tubes were shaken for 30 s to dislodge the acinar tissue from the islets of Langerhans, centrifuged at 311 x *g* for 3 minutes at 4°C and the supernatant discarded. This washing step was repeated 2 times and pellets were resuspended in 50ml islet isolation media and passed through a 380-micron sieve (Newark Wire Cloth Company). Tubes were centrifuged at 311 x *g* for 3 minutes at 4°C after which the supernatant was discarded and the tubes inverted allowing for the media to drain. Pellets were resuspended in 10 ml of Ficoll-Plaque Plus (Amersham) and vortexed at low speed for 10 s. An additional 10ml of Ficoll was added to each tube and carefully overlaid with 10 ml of serum-free islet isolation media. Tubes were centrifuges at 1730 x *g* for 23 minutes at 4°C without rotor acceleration and deceleration. Islets were collected from the interphase between media and Ficoll and transferred into a new tube containing islet isolation media. Tubes were centrifuges at 311 x *g* for 3 minutes at 4°C, the supernatant discarded and islets pooled in a 10cm petri dish. Islets were handpicked using a 1 ml pipette and transferred to a new 15 ml tube containing 10 ml islet isolation media. The tubes were rested on ice for 3 minutes and the top 6 ml aspirated. This self-sedimentation process was repeated 4 times. Tubes were centrifuges at 311 x *g* for 3 minutes at 4°C, the supernatant discarded and the pellets resuspended in 2ml of preheated 0.05% Trypsin-EDTA (Gibco) and incubated for 8 minutes at 37°C. After the reaction was stopped using ice-cold islet isolation media, pellets were centrifuged 311 x *g* for 5 minutes at 4°C at and resuspended in 1x PBS.

6.6. CFSE labelling of SRBC

SRBC were washed twice in ice-cold 1x PBS and resuspended at 10^7 cells/ml in CFSE buffer containing 5 µM CFSE. Cells were incubated at 37°C for 10 minutes and then washed 2x in ice-cold lymphocyte isolation buffer before used for *in vivo* injection.

6.7. Immunisations

8- to 10-week-old mice were i.v. injected with 2 x 10^8 sheep red blood cells (SRBC, IMVS Australia), or i.p. injected with 100 µg of nitrophenyl (13)-ovalbumin (NP_{13}-OVA) in alum, or i.p. injected with 100 µg of NP-AECM-Ficoll and spleen analysed on various time points. For monitoring SRBC uptake by splenocytes, 5 x 10^8 SRBC were labelled with CFSE (eBioscience) according to the manufacturer's instructions and injected intravenously immediately.

For TLR blocking experiments, the TLR3/dsRNA complex inhibitor (Calbiochem) and/or MyD88 inhibitor peptide (Novus Biologicals) were dissolved in DMSO and diluted in 1x PBS. Mice were intraperitoneally administered 700 µg of TLR3/dsRNA complex inhibitor and 70 µg MyD88 inhibitor peptide 1 hour before and 1 hour after SRBC injection.

Treatment of mice with type I IFN comprised s.c. administration of IFN-alpha A (0.1 µg/mouse, PBL Assay Science), IFN-beta (0.3 µg/mouse, R&D Systems) and IFN-lambda 3 (0.8 µg/mouse, R&D Systems) in 1x PBS 12 hrs, 24 hrs and 36 hours after SRBC immunisation.

6.8. Poly(I:C) and Resiquimod injections

Poly(I:C) (200 µg of high-molecular weight polyinosinic-polycytidylic acid (HMW poly(I:C), Invivogen) was injected intravenously in 200 µl 1x PBS. Resiquimod (R848, 25 µg, Invivogen) was injected intraperitoneally, also in 200 µl 1x PBS Control mice were injected with 200µl 1x PBS only. After various time points, mice were euthanized with CO_2 and serum levels of Interleukin 6 (IL-6) Interferon-β (IFN-β) measured by ELISA. For some experiments, mice were intraperitoneally injected with 1 mg TLR3/dsRNA complex inhibitor (Calbiochem, in DMSO) 1 hour before i.v. administration of 200 µg poly(I:C).

6.9. Treatment with reverse transcriptase inhibitors

6- and 12-week old NOD mice were given drinking water (changed daily), containing either 0.02% DMSO (control group) or 3 x 10^{-4} M nevirapine, 1.6 x 10^{-4} M entricitabine and 1.5 x 10^{-4} M tenofovir. Mice were monitored for changes in weight and blood glucose on a weekly basis.

6.10. Irradiation

Cohorts of mice were sublethally irradiated by a ^{137}Cs source for which Thy1.1^{+} mice received 2 doses of 450 Rads 4 hours apart, while B6.Rag1 mice received one dose of 600 Rads. Mice were reconstituted with 10^{7} bone marrow cells isolated under sterile conditions from the femurs and tibias of the respective donor mice. For mixed bone marrow chimeras, cell ratios of donor populations were checked by flow cytometry beforehand. After irradiation, mice

were given antibiotic water containing Bactrim (sulfamethoxazole and trimethoprim, Provet, Australia) for 10 days. Mice underwent immunisation studies 8-10 weeks post-reconstitution.

6.11. Polymerase chain reactions (PCR) for genotyping

2mm of mouse tail was send from the Australian BioResources (ABR) housing facility and incubated overnight at 65°C in DNA isolation buffer containing 1.13 µl Proteinase K (100 µg/ml, Promega). All primers used for genotyping are listed in Table 2.3. PCR was performed using 0.5 µl DNA digest, 0.24 µM forward and reverse primers, 50 µM of each dNTP (Promega, USA), 0.625 U Taq polymerase (Promega) and 1X Green Go Taq Reaction Buffer (Promega) in a 25 µl reaction volume. PCR products were visualized by electrophoresis on a 1.5% agarose (Sigma) gel containing 1X SYBR® Safe DNA Gel Stain (Thermo Fisher Scientific). The majority of PCRs for genotyping were carried out by Joanna Warren (Garvan Institute, Sydney, Australia).

Table 2.3 Primer sequences for genotyping

Primer	Sequence 5’ to 3’	An Temp
Thy1.1 F	GTGCTCTCAGGCACCCTC	58
Thy1.1 R	CCGCCACACTTGACCAGT	58
IFNRWT F	CTTGGGTGGAGAGGCTATTC	54
IFNRWT R	AGGTGAGAT GACAGGAGATC	52
IFNRKO F	AAGATGTGCTGTTCCCTTCCTCTGCTCTGA	65
IFNRKO R	ATTATTAAAAGAAAAGACGAGGCGAAGTGG	57
MAVS_WT_F	GCCCTGGGCTAAGTGGCT	54
MAVS_SNP_F	GCCCTGGGCTAAGTGGCC	52
MAVS_COM_R	GCCAAGAGTGCACTGGTGGCCC	65
MAVS_HRM_F	CAATGCCCTGGGCTAAGTGG	57

6.12. RNA isolation and real-time polymerase chain reaction

Total RNA was isolated using TRIzol (Invitrogen) or the RNeasy mini/miRNeasy midi kit (Qiagen) according to the manufacturer's instructions. Total RNA from FACS-sorted beta cells was isolated using the miRNeasy midi kit (Qiagen). For visualisation of SRBC RNA, 2 µg of total RNA was visualized by electrophoresis on a 0.7% agarose (Sigma) gel containing 1X SYBR® Gold RNA Gel Stain (Thermo Fisher Scientific).

For quantitative real-time PCR (qRT-PCR), 200ng RNA was treated with DNase I (Qiagen) for 30 min at 37°C, before cDNA was synthesized using the Superscript III first-strand synthesis system with oligo(dT) primers for coding and random primers for non-coding transcripts. Non-coding (endogenous retrovirus transcripts) were confirmed using the RepeatMasker software (Institute for Systems Biology). All primers were designed using the Roche UPL Primer Design Program and are shown in table 2.4 for non-coding and table 2.5 for coding transcripts. Quantitative RT-PCR of cDNA was performed at least in duplicates on the LightCycler 480 (Roche) with a pre-amplification incubation of 95°C for 10 minutes, followed by 45 cycles of 95°C for 10 sec and 55°C for 30 sec (single acquisition). Relative gene expression values were determined based on the level of the housekeeping gene RPL19 and calculated using the relative gene quantification tool from the LightCycler® 480 software (v1.5, Roche).

Table 2.4 Quantitative RT-PCR primer sequences – non-coding transcripts

Primer	Sequence	UPL probe/ amplicon length (nt)
RTE1_Sar - fwd	gatccagccttactggactacc	103/93
RTE1_Sar - rev	tgaatcgtaagtaaccaagtcatc	
B1F1 - fwd	aggatccagccttactggact	103/89
B1F1 - rev	ccatcttttgcgctctaacc	
EtnERV2 - fwd	gccaaatggtattgtgctagg	7/73
EtnERV2 - rev	tatagcctcaggtgccagga	
MERVL-LTR - fwd	aagagccaagacctgctgag	41/112
MERVL-LTR - rev	cgtttctgcaattggttacg	
RLTR1IAP - fwd	gcatgtgccaaggtatcttatg	13/92
RLTR1IAP - rev	acgtgtcactccttgattgct	
ERVB7_1 - fwd	gcctgaaacctgcttgct	4/74
ERVB7_1 - rev	tcctcaggttccagcagtg	
IAPEZI - fwd	tgtgccaagggtatcttatgact	13/95
IAPEZI - rev	tcggacgtatcactccttga	
MTA_Mm - fwd	cctgggtgacccttacacat	5/74
MTA_Mm - rev	gctgtgttccagatatagccaaa	
MTC - fwd	gccagtaagcagcactcctc	16/69
MTC - rev	actcaagcagggcaggaac	

Table 2.5 Quantitative RT-PCR primer sequences – coding transcripts (part I)

Primer	Sequence	UPL probe/ amplicon length (nt)
Mouse glucagon - fwd	tacacctgttcgcagctcag	5/89
Mouse glucagon - rev	ttgcaccagcattataagcaa	
Mouse somatostatin - fwd	cccagactccgtcagtttct	53/118
Mouse somatostatin - rev	gggcatcattctctgtctgg	
Mouse H-2K-s - fwd	gcggagaatccgagatatga	15/85
Mouse H-2K-s - rev	tggcgttctgtgtgttcc	
Mouse H-2Kb - fwd	atacctgaagaacgggaacg	107/131
Mouse H-2Kb - rev	tgatgtcagcagggtagaagc	
Mouse H-2Kd - fwd	agcccctcaccctgagat	63/60
Mouse H-2Kd - rev	ctgtgttagtcttggtggatgaa	

Table 2.5 Quantitative RT-PCR primer sequences – coding transcripts (part I)

Primer	Sequence	UPL probe/ amplicon length (nt)
Mouse IL1-beta - fwd	agttgacggaccccaaaag	38/75
Mouse IL1-beta - rev	agctggatgctctcatcagg	
Mouse IFN-lambda - fwd	tgggccagcctcttcata	33/72
Mouse IFN-lambda - rev	ctgtggcctgaagctgtgta	
Mouse IRF1 - fwd	gcaccactgatctgtataacctaca	10/75
Mouse IRF1 - rev	cctcatcctcgtctgttgc	
Mouse TLR3 - fwd	gatacagggattgcacccata	26/77
Mouse TLR3 - rev	tcccccaaaggagtacattaga	
Mouse TLR4 - fwd	ggactctgatcatggcactg	2/101
Mouse TLR4 - rev	ctgatccatgcattggtaggt	
Mouse TLR7 - fwd	tgatcctggcctatctctgac	25/95
Mouse TLR7 - rev	cgtgtccacatcgaaaacac	
Mouse TLR9 - fwd	gagaatcctccatctcccaac	79/94
Mouse TLR9 - rev	ccagagtctcagccagcac	
Mouse RPL19 - fwd	ccacaagctctttcctttcg	46/114
Mouse RPL19 - rev	ggatccaaccagaccttcttt	
Mouse IRF3 - fwd	atggctgactttggcatctt	29/76
Mouse IRF3 - rev	cgtccggcttatccttcc	
Mouse IL6 - fwd	gctaccaaactggatataatcagga	28642
Mouse IL6 - rev	ccaggtagctatggtactccagaa	
Mouse IRF7 - fwd	agcgtgagggtgtgtcct	56/76
Mouse IRF7 - rev	tcttcgtagagactgttggtgct	
Mouse MAVS - fwd	cctcacagctagtgaccaggat	96/77
Mouse MAVS - rev	agagtccccagagtgtgtcc	
CVB4 - fwd	cccggaccgagtatcaataa	41/60
CVB4 - rev	ccgggtaacgaacggttt	
Mouse IFN-beta - fwd	cacagccctctccatcaacta	78/63
Mouse IFN-beta - rev	catttccgaatgttcgtcct	
Mouse ISG15 - fwd	agtcgacccagtctctgactct	71/143
Mouse ISG15 - rev	ccccagcatcttcaccttta	
Mouse CXCL10 - fwd	gctgccgtcattttctgc	3/111
Mouse CXCL10 - rev	tctcactggcccgtcatc	
Mouse insulin - fwd	ttcagaccttggcgttgg	29/61
Mouse insulin - rev	gtgcagcactgatccacaat	
Mouse amylase - fwd	aagtaaatgttggcagtgatggt	73/88
Mouse amylase - rev	tttgagtcagcatggattgc	
Mouse CD3 - fwd	gatgcggtggaacactttct	98/61
Mouse CD3 - rev	gcaagtgccaacagctagg	
Mouse CD19 - fwd	tcctctccctgtctccttcc	16/97
Mouse CD19 - rev	cacaacattgcctccctctt	

6.13. Coxsackievirus infection

The Coxsackievirus B4 E2 (CVB4 E2) strain was kindly provided by Prof. Malin Flodström Tullberg (Karolinska Institutet, Solna, Sweden). All mouse strains were initially tested for the maximum tolerated dose (MTD) of CVB4. As a result, both NOD and SJL were injected with 105 PFU CVB4, while B6 mice received 20 PFU of CVB4. Respective doses were administered in 200 µl saline via *i.p.* injection. Mice were monitored daily and organs extracted between day 1 and day 28 post-infection. Recovery gel food was given for 14 days post infection and blood glucose levels were measured using Freestyle Lite Blood Glucose Test Strips (Abbott, Australia). To determine the severity of pancreatitis throughout the course of infection, serum amylase activity was determined using the Amylase Activity Assay Kit (Sigma-Aldrich, St. Louis, USA) according to the manufacturer's instructions.

6.14. Virus quantification

Plaque assay was performed in order to determine the viral titre of different tissues after CVB4 infection. On the day before the assay, 0.6 x 10^6 HeLa cells per well were seeded in 2 ml complete medium (RPMI with 10% FCS, 2mM L-Glut, 100 U/ml Penicillin, 100 µg/ml Streptomycin and 100 µg/ml Normocin) in 6-well plates and incubated at 37°C.

Infectious samples were collected in plain RPMI, homogenized in a dounce tissue grinder and passed through a 22 µm filter, before preparing tenfold serial dilutions. HeLa cells were ensured to have at least 90% confluency. After HeLa cells were washed with 1x PBS, 400 µl of infectious homogenate was added to each well and incubated for 60min at 37°C under gentle rotation. Infectious media was removed and 3 ml of agar mix (2x 1.8% agar, 2x MEM

containing 10% FCS) was added to each well before incubating 37°C. Three days later, cells were fixed with Carnoys reagent for 60min and subsequently stained with 0.5% Crystal Violet for 60 s. Finally, wells were extensively rinsed with H_2O and plaques counted.

6.15. Immunohistochemistry & Immunofluorescence

For immunofluorescence (IF), tissue samples were put into OCT (Tissue Tek, Australia) and stored at -80°C for a minimum of 24 hrs. 6 µm sections from various tissues (spleen, gut, lymph nodes) were cut using a cryostat (Leica, Germany) and fixed for 8 minutes in ice-cold acetone. Sections were then left to dry at room temperature (RT) for at least 30 min before rehydration in 1x PBS for 10 minutes. Afterwards, sections were incubated in blocking buffer for 1 hr to reduce non-specific background. Unless stated otherwise, primary antibodies were incubated overnight (ON), while secondary (fluorochrome-labelled) antibodies were incubated at RT for 2 hrs. All antibodies were incubated in antibody dilution buffer and are listed in table 2.2. Sections were washed 3 x 5 min in 1x PBS containing 0.1% Tween 20 and mounted with mounting agent (Fluoromount-G, SouthernBiotech).

For immunohistochemistry (IHC), tissue sections were fixed in 10% formalin for at least 24 hrs and taken to St Vincent's pathology department (Sydney, Australia) for paraffin embedding. 5 µm sections were cut by the Garvan Institute Histology facility. Sections were deparaffinised, rehydrated through washing in ethanol gradient and antigen retrieval performed (3 x 5 min in antigen retrieval buffer, DAKO, S1699) where applicable. Sections were incubated for 10 min with 0.3% H_2O_2 to block endogenous peroxidase activity,

followed by blocking buffer for 1 hour. Rabbit primary antibodies were incubated for 2 hours at RT and detected using the EnVision Detection System DAB/Rabbit (DAKO, Denmark).

Sections were analysed using a Leica DM 4000 light microscope, a Leica DM 5500 fluorescent microscope or Leica DMI 6000 confocal microscope (Leica Microsystems, Germany). Images were processed using the Leica acquisition and analysis software ImageJ (National Institute of Health, USA), Adobe Photoshop CS5 (v12, San Jose, CA) and ImarisColoc (Bitplane, Zurich, Switzerland).

For co-localization analysis, images of BMDM were analysed using the Coloc module of Imaris 8.3 (Bitplane). The Mander's coefficient was used as an indicator of the fraction of the co-localized signal over the total signal (Manders et al., 1993).

For GC quantification, spleen sections were stained with biotin-conjugated PNA followed by visualization with HRP-linked streptavidin and diamino benzidine (DAB). The sections were lightly counterstained with hematoxylin. Sections were analysed using a Leica DM 4000 light microscope, and ImageJ analysis software was used to quantitate the percentage of each image fraction that was positive for PNA staining.

6.16. Pancreatitis and insulitis scoring

All histopathological evaluation was performed by light microscopy. The severity of pancreatitis was determined by blinded scoring of the degree of cellular infiltration as described by Kanno et al. (Kanno et al., 1992): 0, none; 1, mild; 2, moderate; 3, moderate and diffuse or severe but focal; 4, severe

and diffuse. The severity insulitis was determined by blinded scoring of the degree of cellular infiltration as described by Marino et al. (Marino et al., 2014): grade 0, no insulitis; grade 1, periinsulitis; grade 2, insulitis involving <25% islet; grade 3, insulitis involving > 25% islet; grade 4, insulitis involving >75% and/or complete islet infiltration. At least 12 non-consecutive sections per animal were scored for both insulitis and pancreatitis.

6.17. Enzyme linked immunosorbent assay (ELISA)

ELISA was performed to measure (secreted) cytokines and/or immunoglobulins in either cell culture supernatant or in serum samples. In order to prepare serum, blood is allowed to clot at RT for 15-30 min, and clots are removed after centrifugation at 1000 x *g*.

For the detection of serum immunoglobulin (Ig), plates were coated overnight with anti-mouse Ig(H+L, 2 µg/ml, Southern Biotech), NP_4-BSA or NP_{23}-BSA (Biosearch Technologies) in ELISA coating buffer. Plates were blocked with 1% BSA (Gibco) diluted in 1x PBS for 2 hours at 37°C. Plates were washed 3x with PBS-T and serum samples were incubated for 2 hours at 37°C at 1:100 in ELISA buffer along with 5-10 2-fold serial dilutions. After washing the plates, analytes were incubated with Alkaline phosphatase (AP) conjugated to anti-mouse IgG_1, IgG_3 or IgM (all 1:2000, BD Biosciences) for 2 hours at 37°C. Appropriate isotype standards were purchased from Southern Biotech and used at a top concentration of 1 µg/ml. Bound alkaline phosphatase was detected with 4-Nitrophenyl phosphate (pNPP) disodium salt hexahydrate (Sigma) at 1 mg/ml and the reaction stopped with 2M sodium hydroxide solution. The titres of NP-specific IgG_1 and IgM were calculated as binary

logarithm of the last dilution factor for which the optical density (OD) was 3 times higher than the background.

IFN-γ was detected using the Murine IFN-Y Standard ELISA Development Kit (Peprotech) according to the manufacturer's instructions except that the capture antibody concentration was increased to 2 µg/ml. For the detection of cytokines, plates were coated overnight with 1 µg/ml IL6 (clone: MP5-20F3, BD Biosciences) or 4 µg/ml IFN-beta (clone: Poly5192, R&D Systems) in ELISA coating buffer. Plates were blocked with 1% BSA (Gibco) diluted in 1x PBS for 2 hours at RT. Serum or cell culture supernatant was incubated overnight in ELISA buffer. IL6 standard (BD Biosciences) and IFN-beta standard (R&D Systems) were used at a top concentration of 25.6 ng/ml. Analytes were detected using biotin-conjugated anti-mouse IFN-beta (clone: MIB-5E9.1, R&D Systems) and IL6 (clone: MP5-32C11, BD Biosciences) in ELISA buffer at 1:500 for 4 hours at RT. Biotin-labelled antibodies were detected with a streptavidin-horseradish peroxidase (SA-HRP) conjugate (BD Biosciences) at 1:1000 for 30 minutes at RT in ELISA buffer. Finally, 3,3',5,5'-Tetramethylbenzidine (TMB) substrate (BD Biosciences) was used to detect HRP activity and the reaction stopped with 1M hydrochloric acid.

6.18. Isolation and culture of bone marrow-derived macrophages

Bone marrow cells were isolated under sterile conditions from the femurs and tibias of B6 and $MAVS^{los}$ mice. After 3 washes, cells were seeded at 10^6cells/ml in complete cell culture medium II and supplemented with recombinant M-CSF (20 ng/ml, Peprotech) for macrophage (MP) differentiation. Cells were incubated at 37°C with 10% CO_2. Media was

replaced after 3 days of culture and adherent cells collected on day 6 for replating. Macrophages were harvested on day 7 by trypsinisation and cell purity was confirmed to be 90-95% as assessed by flow cytometric analysis ($CD11b^{+}CD11c^{low}F4/80^{+}B220^{-}TCRb^{-}$).

6.19. Transient transfection

Unless otherwise indicated, transient transfection was performed at 70-80% confluency using Lipofectamine 2000 (Thermo Fisher Scientific). One the day before the transfection, cells were cultured in 24-well plates in complete growth medium without antibiotics. For the transfection, 0.5 µg of (plasmid) DNA and 2µl of Lipofectamine 2000 were separately diluted in 50µl of Opti-MEM, well-mixed and incubated for 15 minutes at RT. DNA-Lipofectamine complexes were then added to each well. Cells and/or supernatants were harvested at indicated time points.

6.20. SDS-PAGE and Western Blotting

SDS-PAGE was performed on cell lysates from pancreas, spleen or bone marrow-derived macrophages directly *ex vivo* or after *in vitro* stimulation. Cells were washed twice in ice-cold 1x PBS and lysed in RIPA buffer (Sigma-Aldrich) containing protease and phosphatase inhibitors (Sigma-Aldrich) under gentle rotation for 45 minutes at 4°C. Lysates were centrifuged at 8,000 x *g* for 10 minutes at 4°C, supernatant collected and protein concentration determined using the Protein Assay Dye Reagent Concentrate (Bio-Rad) according to the manufacturer's instruction. Lysate proteins (20-100 µg) were diluted with 1X NuPAGE® LDS Sample Buffer (Thermo Fisher Scientific) and 1X NuPAGE®

Sample Reducing Agent (Thermo Fisher Scientific) and denaturated at 70°C for 10 minutes. Protein samples were separated by SDS polyacrylamide-gel electrophoresis in 1x NuPAGE MOPS SDS Running Buffer (Thermo Fisher Scientific) using a NuPAGE Novex 4-12% Bis-Tris Protein gel (Thermo Fisher Scientific). Proteins were then transferred in 1x NuPAGE® Transfer Buffer (Thermo Fisher Scientific) to a 0.2 µm pore size nitrocellulose blotting membrane (Thermo Fisher Scientific). Following transfer, membranes were blocked with 5% BSA in 1x TBS and probed overnight with either mouse (anti-beta-actin) or rabbit primary antibodies in 5% BSA in 1x TBS. Antibody binding was detected using goat anti-rabbit IgG HRP (0.1 µg/ml, Thermo Fisher Scientific) or anti-mouse IgG HRP (0.04 µg/ml, Thermo Fisher Scientific) in 5% BSA in 1x TBS. Membranes were developed in Pierce™ ECL Western Blotting Substrate (Thermo Fisher Scientific) for 1 minute and immediately exposed to X-Ray sensitive film (Fuji).

6.21. Immunoprecipitation (IP) assay

Cell lysates were washed twice in ice-cold 1x PBS and lysed under gentle rotation in NP-40 buffer containing protease and phosphatase inhibitors (Sigma-Aldrich) for 45 minutes at 4°C. After quantification, lysates were incubated with Protein A beads for 45 minutes at 4°C for pre-clearing. Lysates were incubated with MAVS antibody (2 µg/100 µg protein lysate; Abcam, ab31334) for 2-4 hours at 4°C and Protein A beads O/N. Finally, immunoprecipitates were loaded onto a SDS gel and analysed by Western blot using a Tom70 antibody (0.4 µg/ml, Santa Cruz, sc26495).

6.22. Ribosomal RNA depletion and library preparation for sequencing

RNA integrity was tested before and after depletion of ribosomal RNA (rRNA) using the Bioanalyzer2100 (Agilent, Santa Clara, CA). Samples with RNA integrity numbers (RIN) below 6 were excluded from analysis. Following rRNA depletion, samples were incubated with DNase I (Qiagen) at 37°C for 30 minutes according to the manufacturer's instructions. Indexed sequencing libraries were constructed using an Agilent Stranded RNA-seq kit (Agilent, Santa Clara, CA) and sequenced at 16 cycles (paired-end read), on an Illumina HiSeq 2000 platform.

6.23. RNA-sequencing data processing and analyses

FastQ files from sequencing libraries were first assessed for sequencing library quality using FASTQC v0.11 (Patel and Jain, 2012). Raw reads were subsequently mapped to the mouse transcriptome (Gencode release M9, GRCm38.p4), to the mouse genome (mm10 assembly), with STAR aligner v.2.4.1d, allowing for multimapping reads (Dobin et al., 2013). The reads were counted over gene models with RSEM, v.1.2.18. Counts were normalized to the transcript length and to the effective number of reads in a library (RPKM) using R package DESeq with options: method='blind', sharingMode="fit-only" (Anders and Huber, 2010). Repeat counts were calculated by finding overlaps of STAR-mapped reads and repeat regions extracted with ENSEMBL API from ENSEMBL version 84. Only repeat categories with at least 50 reads in at least two samples were considered for further analysis. Differentially expressed RefSeq transcripts and repeat elements were defined with DESeq with FDR<0.01. In order to find commonly differentially expressed genes in

“inflamed” vs. “non-inflamed” samples, EdgeR was used with a model matrix ~type + treatment, modelling out the cell type variance and including only the “treatment”. Pathway analysis on those genes was performed with R package KEGGREST (Tenenbaum, 2016). Heatmap results were visualised with R package pheatmap, while the charts were made with package ggplot2 (Wickham, 2009).

6.24. Sequence alignment of MAVS

Transmembrane domain sequences of MAVS homologues were retrieved from the UniProt knowledgebase (UniProt, 2015). Multiple sequence alignment was done using PROMALS3D Server Structure analysis of the attained model (Pei et al., 2008). Figure editing was performed in IBS (Illustrator of Biological Sequences (IBS) (Liu et al., 2015).

6.25. Statistical analyses

Where applicable, data are displayed as mean ± SEM (* $P < 0.05$, ** $P < 0.01$, *** $P < 0.001$, **** $P < 0.0001$). Statistical analyses included one-way and two-way ANOVA with Bonferroni post hoc test for multiple comparisons, and paired and unpaired Student’s t-tests in datasets containing only two groups. Diabetes incidence was displayed using Kaplan-Meier plots and compared by the Mantel-Cox log-rank test. Data were analysed using the Prism software (GraphPad).

REFERENCES

Ablasser, A., Bauernfeind, F., Hartmann, G., Latz, E., Fitzgerald, K.A., and Hornung, V. (2009). RIG-I-dependent sensing of poly(dA:dT) through the induction of an RNA polymerase III-transcribed RNA intermediate. Nat Immunol *10*, 1065-1072.

Adams, S. (1926). The seasonal variation in the incidence of acute diabetes. Arch Int Med *37*, 861.

Aida, K., Nishida, Y., Tanaka, S., Maruyama, T., Shimada, A., Awata, T., Suzuki, M., Shimura, H., Takizawa, S., Ichijo, M.*, et al.* (2011). RIG-I- and MDA5-initiated innate immunity linked with adaptive immunity accelerates beta-cell death in fulminant type 1 diabetes. Diabetes *60*, 884-889.

Akpinar, P., Kuwajima, S., Krutzfeldt, J., and Stoffel, M. (2005). Tmem27: a cleaved and shed plasma membrane protein that stimulates pancreatic beta cell proliferation. Cell Metab *2*, 385-397.

Alidjinou, E.K., Chehadeh, W., Weill, J., Vantyghem, M.C., Stuckens, C., Decoster, A., Hober, C., and Hober, D. (2015). Monocytes of Patients with Type 1 Diabetes Harbour Enterovirus RNA. Eur J Clin Invest *45*, 918-924.

Alidjinou, E.K., Sane, F., Engelmann, I., Geenen, V., and Hober, D. (2014). Enterovirus persistence as a mechanism in the pathogenesis of type 1 diabetes. Discov Med *18*, 273-282.

Allen, C.D., Okada, T., and Cyster, J.G. (2007a). Germinal-center organization and cellular dynamics. Immunity *27*, 190-202.

Allen, C.D., Okada, T., Tang, H.L., and Cyster, J.G. (2007b). Imaging of germinal center selection events during affinity maturation. Science *315*, 528-531.

Amariglio, N., and Rechavi, G. (1993). Insertional mutagenesis by transposable elements in the mammalian genome. Environ Mol Mutagen *21*, 212-218.

Anders, S., and Huber, W. (2010). Differential expression analysis for sequence count data. Genome Biol *11*, R106.

Anderson, A.O., and Shaw, S. (2005). Conduit for privileged communications in the lymph node. Immunity *22*, 3-5.

Ashton-Rickardt, P.G., Bandeira, A., Delaney, J.R., Van Kaer, L., Pircher, H.P., Zinkernagel, R.M., and Tonegawa, S. (1994). Evidence for a differential avidity model of T cell selection in the thymus. Cell *76*, 651-663.

Atkinson, M.A., and Eisenbarth, G.S. (2001). Type 1 diabetes: new perspectives on disease pathogenesis and treatment. Lancet *358*, 221-229.

Atkinson, M.A., von Herrath, M., Powers, A.C., and Clare-Salzler, M. (2015). Current concepts on the pathogenesis of type 1 diabetes--considerations for attempts to prevent and reverse the disease. Diabetes care *38*, 979-988.

Baekkeskov, S., Aanstoot, H.J., Christgau, S., Reetz, A., Solimena, M., Cascalho, M., Folli, F., Richter-Olesen, H., and De Camilli, P. (1990). Identification of the 64K autoantigen in insulin-dependent diabetes as the GABA-synthesizing enzyme glutamic acid decarboxylase. Nature *347*, 151-156.

Bailey, R., Cooper, J.D., Zeitels, L., Smyth, D.J., Yang, J.H., Walker, N.M., Hypponen, E., Dunger, D.B., Ramos-Lopez, E., Badenhoop, K.*, et al.* (2007). Association of the vitamin D metabolism gene CYP27B1 with type 1 diabetes. Diabetes *56*, 2616-2621.

Baillie, J.K., Barnett, M.W., Upton, K.R., Gerhardt, D.J., Richmond, T.A., De Sapio, F., Brennan, P.M., Rizzu, P., Smith, S., Fell, M.*, et al.* (2011). Somatic retrotransposition alters the genetic landscape of the human brain. Nature *479*, 534-537.

Baker, M.J., Frazier, A.E., Gulbis, J.M., and Ryan, M.T. (2007). Mitochondrial protein-import machinery: correlating structure with function. Trends Cell Biol *17*, 456-464.

Baltimore, D. (1985). Retroviruses and retrotransposons: the role of reverse transcription in shaping the eukaryotic genome. Cell *40*, 481-482.

Banatvala, J.E., Bryant, J., Schernthaner, G., Borkenstein, M., Schober, E., Brown, D., De Silva, L.M., Menser, M.A., and Silink, M. (1985). Coxsackie B, mumps, rubella, and cytomegalovirus specific IgM responses in patients with juvenile-onset insulin-dependent diabetes mellitus in Britain, Austria, and Australia. Lancet *1*, 1409-1412.

Banchereau, J., and Pascual, V. (2006). Type I interferon in systemic lupus erythematosus and other autoimmune diseases. Immunity *25*, 383-392.

Banchereau, J., and Steinman, R.M. (1998). Dendritic cells and the control of immunity. Nature *392*, 245-252.

Banerjee, M., and Otonkoski, T. (2009). A simple two-step protocol for the purification of human pancreatic beta cells. Diabetologia *52*, 621-625.

Banki, K., Maceda, J., Hurley, E., Ablonczy, E., Mattson, D.H., Szegedy, L., Hung, C., and Perl, A. (1992). Human T-cell lymphotropic virus (HTLV)-related endogenous sequence, HRES-1, encodes a 28-kDa protein: a possible autoantigen for HTLV-I gag-reactive autoantibodies. Proc Natl Acad Sci U S A *89*, 1939-1943.

Bannert, N., and Kurth, R. (2006). The evolutionary dynamics of human endogenous retroviral families. Annu Rev Genomics Hum Genet *7*, 149-173.

Banovic, T., Yanilla, M., Simmons, R., Robertson, I., Schroder, W.A., Raffelt, N.C., Wilson, Y.A., Hill, G.R., Hogan, P., and Nourse, C.B. (2011). Disseminated varicella infection caused by varicella vaccine strain in a child with low invariant natural killer T cells and diminished CD1d expression. J Infect Dis *204*, 1893-1901.

Bao, W., Kojima, K.K., and Kohany, O. (2015). Repbase Update, a database of repetitive elements in eukaryotic genomes. Mob DNA *6*, 11.

Baranek, T., Manh, T.P., Alexandre, Y., Maqbool, M.A., Cabeza, J.Z., Tomasello, E., Crozat, K., Bessou, G., Zucchini, N., Robbins, S.H.*, et al.* (2012). Differential responses of immune cells to type I interferon contribute to host resistance to viral infection. Cell Host Microbe *12*, 571-584.

Baril, M., Racine, M.E., Penin, F., and Lamarre, D. (2009). MAVS dimer is a crucial signaling component of innate immunity and the target of hepatitis C virus NS3/4A protease. J Virol *83*, 1299-1311.

Barrett, J.C., Clayton, D.G., Concannon, P., Akolkar, B., Cooper, J.D., Erlich, H.A., Julier, C., Morahan, G., Nerup, J., Nierras, C.*, et al.* (2009). Genome-wide association study and meta-analysis find that over 40 loci affect risk of type 1 diabetes. Nat Genet *41*, 703-707.

Barton, G.M., and Kagan, J.C. (2009). A cell biological view of Toll-like receptor function: regulation through compartmentalization. Nature Reviews Immunology *9*, 535-542.

Beck-Engeser, G.B., Ahrends, T., Knittel, G., Wabl, R., Metzner, M., Eilat, D., and Wabl, M. (2015). Infectivity and insertional mutagenesis of endogenous retrovirus in autoimmune NZB and B/W mice. J Gen Virol *96*, 3396-3410.

Beck-Engeser, G.B., Eilat, D., and Wabl, M. (2011). An autoimmune disease prevented by anti-retroviral drugs. Retrovirology *8*, 91.

Belbasis, L., Bellou, V., Evangelou, E., Ioannidis, J.P., and Tzoulaki, I. (2015). Environmental risk factors and multiple sclerosis: an umbrella review of systematic reviews and meta-analyses. Lancet Neurol *14*, 263-273.

Bell, G.I., Horita, S., and Karam, J.H. (1984). A polymorphic locus near the human insulin gene is associated with insulin-dependent diabetes mellitus. Diabetes *33*, 176-183.

Bendelac, A., Lantz, O., Quimby, M.E., Yewdell, J.W., Bennink, J.R., and Brutkiewicz, R.R. (1995). CD1 recognition by mouse NK1+ T lymphocytes. Science *268*, 863-865.

Benner, C., van der Meulen, T., Caceres, E., Tigyi, K., Donaldson, C.J., and Huising, M.O. (2014). The transcriptional landscape of mouse beta cells compared to human beta cells reveals notable species differences in long non-coding RNA and protein-coding gene expression. BMC Genomics *15*, 620.

Bentebibel, S.E., Lopez, S., Obermoser, G., Schmitt, N., Mueller, C., Harrod, C., Flano, E., Mejias, A., Albrecht, R.A., Blankenship, D.*, et al.* (2013). Induction of ICOS+CXCR3+CXCR5+ TH cells correlates with antibody responses to influenza vaccination. Sci Transl Med *5*, 176ra132.

Bhoj, V.G., Sun, Q., Bhoj, E.J., Somers, C., Chen, X., Torres, J.P., Mejias, A., Gomez, A.M., Jafri, H., Ramilo, O., and Chen, Z.J. (2008). MAVS and MyD88 are essential for innate immunity but not cytotoxic T lymphocyte response against respiratory syncytial virus. Proc Natl Acad Sci U S A *105*, 14046-14051.

Biacchesi, S., LeBerre, M., Lamoureux, A., Louise, Y., Lauret, E., Boudinot, P., and Bremont, M. (2009). Mitochondrial antiviral signaling protein plays a major role in induction of the fish innate immune response against RNA and DNA viruses. J Virol *83*, 7815-7827.

Bluestone, J.A., St Clair, E.W., and Turka, L.A. (2006). CTLA4Ig: bridging the basic immunology with clinical application. Immunity *24*, 233-238.

Boeke, J.D., Garfinkel, D.J., Styles, C.A., and Fink, G.R. (1985). Ty elements transpose through an RNA intermediate. Cell *40*, 491-500.

Boeke, J.D., and Stoye, J.P. (1997). Retrotransposons, Endogenous Retroviruses, and the Evolution of Retroelements. In Retroviruses, J.M. Coffin, S.H. Hughes, and H.E. Varmus, eds. (Cold Spring Harbor (NY)).

Boes, M. (2000). Role of natural and immune IgM antibodies in immune responses. Mol Immunol *37*, 1141-1149.

Borrow, P., Lewicki, H., Hahn, B.H., Shaw, G.M., and Oldstone, M.B. (1994). Virus-specific CD8+ cytotoxic T-lymphocyte activity associated with control of viremia in primary human immunodeficiency virus type 1 infection. J Virol *68*, 6103-6110.

Bottazzo, G.F., Florin-Christensen, A., and Doniach, D. (1974). Islet-cell antibodies in diabetes mellitus with autoimmune polyendocrine deficiencies. Lancet *2*, 1279-1283.

Boucher, D.W., Hayashi, K., Rosenthal, J., and Notkins, A.L. (1975). Virus-induced diabetes mellitus. III. Influence of the sex and strain of the host. J Infect Dis *131*, 462-466.

Bowie, A.G., and Fitzgerald, K.A. (2007). RIG-I: tri-ing to discriminate between self and non-self RNA. Trends Immunol *28*, 147-150.

Brink, R. (2014). The imperfect control of self-reactive germinal center B cells. Current Opinion in Immunology *28*, 97-101.

Brinkmann, V., Reichard, U., Goosmann, C., Fauler, B., Uhlemann, Y., Weiss, D.S., Weinrauch, Y., and Zychlinsky, A. (2004). Neutrophil extracellular traps kill bacteria. Science *303*, 1532-1535.

Broz, P., and Monack, D.M. (2013). Newly described pattern recognition receptors team up against intracellular pathogens. Nat Rev Immunol *13*, 551-565.

Burka, E.R. (1969). Characteristics of RNA degradation in the erythroid cell. J Clin Invest *48*, 1266-1272.

Burnet, M., and Holmes, M.C. (1965). Genetic investigations of autoimmune disease in mice. Nature *207*, 368-371.

Burren, O.S., Adlem, E.C., Achuthan, P., Christensen, M., Coulson, R.M., and Todd, J.A. (2011). T1DBase: update 2011, organization and presentation of large-scale data sets for type 1 diabetes research. Nucleic Acids Res *39*, D997-1001.

Cai, X., Chen, J., Xu, H., Liu, S., Jiang, Q.X., Halfmann, R., and Chen, Z.J. (2014). Prion-like polymerization underlies signal transduction in antiviral immune defense and inflammasome activation. Cell *156*, 1207-1222.

Caillat-Zucman, S., Djilali-Saiah, I., and Timsit, J. (1997). Insulin dependent diabetes mellitus (IDDM). 12th International Histocompatibility Workshop study.

Calderon, B., Suri, A., and Unanue, E.R. (2006). InCD4(+) T-cell-induced diabetes, macrophages are the final effector cells that mediate islet beta-cell killing - Studies from an acute model. American Journal of Pathology *169*, 2137-2147.

Cambier, J.C., Gauld, S.B., Merrell, K.T., and Vilen, B.J. (2007). B-cell anergy: from transgenic models to naturally occurring anergic B cells? Nat Rev Immunol *7*, 633-643.

Campbell, I.L., Kay, T.W., Oxbrow, L., and Harrison, L.C. (1991). Essential role for interferon-gamma and interleukin-6 in autoimmune insulin-dependent diabetes in NOD/Wehi mice. J Clin Invest *87*, 739-742.

Cardozo, A.K., Kruhoffer, M., Leeman, R., Orntoft, T., and Eizirik, D.L. (2001). Identification of novel cytokine-induced genes in pancreatic beta-cells by high-density oligonucleotide arrays. Diabetes *50*, 909-920.

Carson, S.D. (2001). Receptor for the group B coxsackieviruses and adenoviruses: CAR. Rev Med Virol *11*, 219-226.

Castanier, C., Garcin, D., Vazquez, A., and Arnoult, D. (2010). Mitochondrial dynamics regulate the RIG-I-like receptor antiviral pathway. EMBO Rep *11*, 133-138.

Cerutti, A., Cols, M., and Puga, I. (2013). Marginal zone B cells: virtues of innate-like antibody-producing lymphocytes. Nat Rev Immunol *13*, 118-132.

Cerwenka, A., and Lanier, L.L. (2001). Natural killer cells, viruses and cancer. Nature Reviews Immunology *1*, 41-49.

Chan, Y.K., Davis, P.F., Poppitt, S.D., Sun, X., Greenhill, N.S., Krishnamurthi, R., Przepiorski, A., McGill, A.T., and Krissansen, G.W. (2012). Influence of tail versus cardiac sampling on blood glucose and lipid profiles in mice. Lab Anim *46*, 142-147.

Chapman, N.M., and Kim, K.S. (2008). Persistent coxsackievirus infection: Enterovirus persistence in chronic myocarditis and dilated cardiomyopathy. Curr Top Microbiol *323*, 275-292.

Chau, D.H.W., Yuan, J., Zhang, H.F., Cheung, P., Lim, T., Liu, Z., Sall, A., and Yang, D.C. (2007). Coxsackievirus B3 proteases 2A and 3C induce apoptotic cell death through mitochondrial injury and cleavage of eIF4GI but not DAP5/p97/NAT1. Apoptosis *12*, 513-524.

Chekmenev, D.S., Haid, C., and Kel, A.E. (2005). P-Match: transcription factor binding site search by combining patterns and weight matrices. Nucleic Acids Res *33*, W432-437.

Chen, S.Y., Wang, Y., Telen, M.J., and Chi, J.T. (2008). The genomic analysis of erythrocyte microRNA expression in sickle cell diseases. PLoS One *3*, e2360.

Chiappinelli, K.B., Strissel, P.L., Desrichard, A., Li, H., Henke, C., Akman, B., Hein, A., Rote, N.S., Cope, L.M., Snyder, A.*, et al.* (2015). Inhibiting DNA Methylation Causes an Interferon Response in Cancer via dsRNA Including Endogenous Retroviruses. Cell *162*, 974-986.

Chiu, Y.H., Macmillan, J.B., and Chen, Z.J. (2009). RNA polymerase III detects cytosolic DNA and induces type I interferons through the RIG-I pathway. Cell *138*, 576-591.

Chiu, Y.L., and Greene, W.C. (2008). The APOBEC3 cytidine deaminases: an innate defensive network opposing exogenous retroviruses and endogenous retroelements. Annu Rev Immunol *26*, 317-353.

Choi, M.K., Wang, Z., Ban, T., Yanai, H., Lu, Y., Koshiba, R., Nakaima, Y., Hangai, S., Savitsky, D., Nakasato, M.*, et al.* (2009). A selective contribution of the RIG-I-like receptor pathway to type I interferon responses activated by cytosolic DNA. Proc Natl Acad Sci U S A *106*, 17870-17875.

Chou, P.Y., and Fasman, G.D. (1978). Prediction of the secondary structure of proteins from their amino acid sequence. Advances in enzymology and related areas of molecular biology *47*, 45-148.

Chung, Y., Tanaka, S., Chu, F., Nurieva, R.I., Martinez, G.J., Rawal, S., Wang, Y.H., Lim, H., Reynolds, J.M., Zhou, X.H.*, et al.* (2011). Follicular regulatory T cells expressing Foxp3 and Bcl-6 suppress germinal center reactions. Nat Med *17*, 983-988.

Chuong, E.B., Elde, N.C., and Feschotte, C. (2016). Regulatory evolution of innate immunity through co-option of endogenous retroviruses. Science *351*, 1083-1087.

Civril, F., Deimling, T., de Oliveira Mann, C.C., Ablasser, A., Moldt, M., Witte, G., Hornung, V., and Hopfner, K.P. (2013). Structural mechanism of cytosolic DNA sensing by cGAS. Nature *498*, 332-337.

Clements, G.B., Galbraith, D.N., and Taylor, K.W. (1995). Coxsackie B virus infection and onset of childhood diabetes. Lancet *346*, 221-223.

Coffman, R.L. (1982). Surface antigen expression and immunoglobulin gene rearrangement during mouse pre-B cell development. Immunol Rev *69*, 5-23.

Cohen, C.J., Lock, W.M., and Mager, D.L. (2009). Endogenous retroviral LTRs as promoters for human genes: a critical assessment. Gene *448*, 105-114.

Cook, J.R., Wormstall, E.M., Hornell, T., Russell, J., Connolly, J.M., and Hansen, T.H. (1997). Quantitation of the cell surface level of Ld resulting in positive versus negative selection of the 2C transgenic T cell receptor in vivo. Immunity *7*, 233-241.

Cooper, J.D., Smyth, D.J., Smiles, A.M., Plagnol, V., Walker, N.M., Allen, J.E., Downes, K., Barrett, J.C., Healy, B.C., Mychaleckyj, J.C.*, et al.* (2008). Meta-analysis of genome-wide association study data identifies additional type 1 diabetes risk loci. Nat Genet *40*, 1399-1401.

Coppieters, K.T., Dotta, F., Amirian, N., Campbell, P.D., Kay, T.W., Atkinson, M.A., Roep, B.O., and von Herrath, M.G. (2012). Demonstration of islet-autoreactive CD8 T cells in insulitic lesions from recent onset and long-term type 1 diabetes patients. J Exp Med *209*, 51-60.

Couri, C.E., Oliveira, M.C., Stracieri, A.B., Moraes, D.A., Pieroni, F., Barros, G.M., Madeira, M.I., Malmegrim, K.C., Foss-Freitas, M.C., Simoes, B.P.*, et al.* (2009). C-peptide levels and insulin independence following autologous nonmyeloablative hematopoietic stem cell transplantation in newly diagnosed type 1 diabetes mellitus. Jama *301*, 1573-1579.

Crampton, S.P., Deane, J.A., Feigenbaum, L., and Bolland, S. (2012). Ifih1 gene dose effect reveals MDA5-mediated chronic type I IFN gene signature, viral resistance, and accelerated autoimmunity. J Immunol *188*, 1451-1459.

Crotty, S. (2015). A brief history of T cell help to B cells. Nature Reviews Immunology *15*, 185-189.

Crow, Y.J., Hayward, B.E., Parmar, R., Robins, P., Leitch, A., Ali, M., Black, D.N., van Bokhoven, H., Brunner, H.G., Hamel, B.C.*, et al.* (2006). Mutations in the gene encoding the 3'-5' DNA exonuclease TREX1 cause Aicardi-Goutieres syndrome at the AGS1 locus. Nat Genet *38*, 917-920.

Cucak, H., Yrlid, U., Reizis, B., Kalinke, U., and Johansson-Lindbom, B. (2009). Type I interferon signaling in dendritic cells stimulates the development of lymph-node-resident T follicular helper cells. Immunity *31*, 491-501.

Cyster, J.G. (1999). Chemokines and cell migration in secondary lymphoid organs. Science *286*, 2098-2102.

Davidson, A., and Diamond, B. (2001). Autoimmune diseases. N Engl J Med *345*, 340-350.

De Palma, A.M., Thibaut, H.J., Li, S., Van Aelst, I., Dillen, C., Swinnen, M., Verbeken, E., Neyts, J., and Opdenakker, G. (2009). Inflammatory rather than infectious insults play a role in exocrine tissue damage in a mouse model for coxsackievirus B4-induced pancreatitis. J Pathol *217*, 633-641.

Debray-Sachs, M., Carnaud, C., Boitard, C., Cohen, H., Gresser, I., Bedossa, P., and Bach, J.F. (1991). Prevention of diabetes in NOD mice treated with antibody to murine IFN gamma. Journal of autoimmunity *4*, 237-248.

Deininger, P.L., Moran, J.V., Batzer, M.A., and Kazazian, H.H., Jr. (2003). Mobile elements and mammalian genome evolution. Curr Opin Genet Dev *13*, 651-658.

Delmeire, D., Flamez, D., Hinke, S.A., Cali, J.J., Pipeleers, D., and Schuit, F. (2003). Type VIII adenylyl cyclase in rat beta cells: coincidence signal detector/generator for glucose and GLP-1. Diabetologia *46*, 1383-1393.

Delovitch, T.L., and Singh, B. (1997). The nonobese diabetic mouse as a model of autoimmune diabetes: immune dysregulation gets the NOD. Immunity *7*, 727-738.

Desmet, C.J., and Ishii, K.J. (2012). Nucleic acid sensing at the interface between innate and adaptive immunity in vaccination. Nature Reviews Immunology *12*, 479-491.

Diana, J., Simoni, Y., Furio, L., Beaudoin, L., Agerberth, B., Barrat, F., and Lehuen, A. (2013). Crosstalk between neutrophils, B-1a cells and plasmacytoid dendritic cells initiates autoimmune diabetes. Nature Medicine *19*, 65-73.

Diebold, S.S., Montoya, M., Unger, H., Alexopoulou, L., Roy, P., Haswell, L.E., Al-Shamkhani, A., Flavell, R., Borrow, P., and Reis e Sousa, C. (2003). Viral infection switches non-plasmacytoid dendritic cells into high interferon producers. Nature *424*, 324-328.

Dixit, E., Boulant, S., Zhang, Y., Lee, A.S., Odendall, C., Shum, B., Hacohen, N., Chen, Z.J., Whelan, S.P., Fransen, M.*, et al.* (2010). Peroxisomes are signaling platforms for antiviral innate immunity. Cell *141*, 668-681.

Dobin, A., Davis, C.A., Schlesinger, F., Drenkow, J., Zaleski, C., Jha, S., Batut, P., Chaisson, M., and Gingeras, T.R. (2013). STAR: ultrafast universal RNA-seq aligner. Bioinformatics *29*, 15-21.

Dorrell, C., Schug, J., Lin, C.F., Canaday, P.S., Fox, A.J., Smirnova, O., Bonnah, R., Streeter, P.R., Stoeckert, C.J., Jr., Kaestner, K.H., and Grompe, M. (2011). Transcriptomes of the major human pancreatic cell types. Diabetologia *54*, 2832-2844.

Dotta, F., Censini, S., van Halteren, A.G., Marselli, L., Masini, M., Dionisi, S., Mosca, F., Boggi, U., Muda, A.O., Del Prato, S.*, et al.* (2007). Coxsackie B4 virus infection of beta cells and natural killer cell insulitis in recent-onset type 1 diabetic patients. Proc Natl Acad Sci U S A *104*, 5115-5120.

Downes, K., Pekalski, M., Angus, K.L., Hardy, M., Nutland, S., Smyth, D.J., Walker, N.M., Wallace, C., and Todd, J.A. (2010). Reduced expression of IFIH1 is protective for type 1 diabetes. PLoS One *5*.

Doxiadis, G.G., de Groot, N., and Bontrop, R.E. (2008). Impact of endogenous intronic retroviruses on major histocompatibility complex class II diversity and stability. J Virol *82*, 6667-6677.

Drayton, D.L., Liao, S., Mounzer, R.H., and Ruddle, N.H. (2006). Lymphoid organ development: from ontogeny to neogenesis. Nat Immunol *7*, 344-353.

Drescher, K.M., Kono, K., Bopegamage, S., Carson, S.D., and Tracy, S. (2004). Coxsackievirus B3 infection and type 1 diabetes development in NOD mice: insulitis determines susceptibility of pancreatic islets to virus infection. Virology *329*, 381-394.

Drescher, K.M., von Herrath, M., and Tracy, S. (2015). Enteroviruses, hygiene and type 1 diabetes: toward a preventive vaccine. Rev Med Virol *25*, 19-32.

Ehinger, B. (1965). On Mechanism of Ribonuclease Secretion in Murine Exocrine Pancreas. Histochemistry *5*, 326-&.

Ehrich, W.E., and Harris, T.N. (1942). The Formation of Antibodies in the Popliteal Lymph Node in Rabbits. J Exp Med *76*, 335-348.

Ehrlich, P. (1901). Die Schutzstoffe des Blutes. Verh 73 Ges Dtsch Naturforsch Arzt *27*, 865–867, 888–891, 913–916.

Eisenbarth, G.S. (1986). Type I diabetes mellitus. A chronic autoimmune disease. N Engl J Med *314*, 1360-1368.

Eizirik, D.L., Pipeleers, D.G., Ling, Z.D., Welsh, N., Hellerstrom, C., and Andersson, A. (1994). Major Species-Differences between Humans and Rodents in the Susceptibility to Pancreatic Beta-Cell Injury. P Natl Acad Sci USA *91*, 9253-9256.

Eizirik, D.L., Sammeth, M., Bouckenooghe, T., Bottu, G., Sisino, G., Igoillo-Esteve, M., Ortis, F., Santin, I., Colli, M.L., Barthson, J.*, et al.* (2012). The human pancreatic islet transcriptome: expression of candidate genes for type 1 diabetes and the impact of pro-inflammatory cytokines. PLoS Genet *8*, e1002552.

Elliott, R.B., Reddy, S.N., Bibby, N.J., and Kida, K. (1988). Dietary prevention of diabetes in the non-obese diabetic mouse. Diabetologia *31*, 62-64.

Engelhorn, M.E., Guevara-Patino, J.A., Noffz, G., Hooper, A.T., Lou, O., Gold, J.S., Kappel, B.J., and Houghton, A.N. (2006). Autoimmunity and tumor immunity induced by immune responses to mutations in self. Nat Med *12*, 198-206.

Ernst, J., Kheradpour, P., Mikkelsen, T.S., Shoresh, N., Ward, L.D., Epstein, C.B., Zhang, X., Wang, L., Issner, R., Coyne, M.*, et al.* (2011). Mapping and analysis of chromatin state dynamics in nine human cell types. Nature *473*, 43-49.

Esnault, C., Heidmann, O., Delebecque, F., Dewannieux, M., Ribet, D., Hance, A.J., Heidmann, T., and Schwartz, O. (2005). APOBEC3G cytidine deaminase inhibits retrotransposition of endogenous retroviruses. Nature *433*, 430-433.

Esnault, C., Millet, J., Schwartz, O., and Heidmann, T. (2006). Dual inhibitory effects of APOBEC family proteins on retrotransposition of mammalian endogenous retroviruses. Nucleic Acids Res *34*, 1522-1531.

Eto, D., Lao, C., DiToro, D., Barnett, B., Escobar, T.C., Kageyama, R., Yusuf, I., and Crotty, S. (2011). IL-21 and IL-6 are critical for different aspects of B cell immunity and redundantly induce optimal follicular helper CD4 T cell (Tfh) differentiation. PLoS One *6*, e17739.

Fabris, P., Floreani, A., Tositti, G., Vergani, D., De Lalla, F., and Betterle, C. (2003). Review article: type 1 diabetes mellitus in patients with chronic hepatitis C before and after interferon therapy. Aliment Pharm Ther *18*, 549-558.

Fagraeus, A. (1948). The Plasma Cellular Reaction and Its Relation to the Formation of Antibodies Invitro. J Immunol *58*, 1-13.

Fairweather, D., Frisancho-Kiss, S., Njoku, D.B., Nyland, J.F., Kaya, Z., Yusung, S.A., Davis, S.E., Frisancho, J.A., Barrett, M.A., and Rose, N.R. (2006). Complement receptor 1 and 2 deficiency increases coxsackievirus B3-induced myocarditis, dilated cardiomyopathy, and heart failure by increasing macrophages, IL-1beta, and immune complex deposition in the heart. J Immunol *176*, 3516-3524.

Fairweather, D., Yusung, S., Frisancho, S., Barrett, M., Gatewood, S., Steele, R., and Rose, N.R. (2003). IL-12 receptor beta 1 and Toll-like receptor 4 increase IL-1 beta- and IL-18-associated myocarditis and coxsackievirus replication. J Immunol *170*, 4731-4737.

Farh, K.K., Marson, A., Zhu, J., Kleinewietfeld, M., Housley, W.J., Beik, S., Shoresh, N., Whitton, H., Ryan, R.J., Shishkin, A.A.*, et al.* (2015). Genetic and epigenetic fine mapping of causal autoimmune disease variants. Nature *518*, 337-343.

Faurschou, M., and Borregaard, N. (2003). Neutrophil granules and secretory vesicles in inflammation. Microbes and infection / Institut Pasteur *5*, 1317-1327.

Fazilleau, N., Eisenbraun, M.D., Malherbe, L., Ebright, J.N., Pogue-Caley, R.R., McHeyzer-Williams, L.J., and McHeyzer-Williams, M.G. (2007). Lymphoid reservoirs of antigen-specific memory T helper cells. Nat Immunol *8*, 753-761.

Fazilleau, N., McHeyzer-Williams, L.J., Rosen, H., and McHeyzer-Williams, M.G. (2009). The function of follicular helper T cells is regulated by the strength of T cell antigen receptor binding. Nat Immunol *10*, 375-384.

Feng, Q., Hato, S.V., Langereis, M.A., Zoll, J., Virgen-Slane, R., Peisley, A., Hur, S., Semler, B.L., van Rij, R.P., and van Kuppeveld, F.J. (2012). MDA5 detects the double-stranded RNA replicative form in picornavirus-infected cells. Cell Rep *2*, 1187-1196.

Feng, Q., Moran, J.V., Kazazian, H.H., Jr., and Boeke, J.D. (1996). Human L1 retrotransposon encodes a conserved endonuclease required for retrotransposition. Cell *87*, 905-916.

Feng, Z., Hensley, L., McKnight, K.L., Hu, F., Madden, V., Ping, L., Jeong, S.H., Walker, C., Lanford, R.E., and Lemon, S.M. (2013). A pathogenic picornavirus acquires an envelope by hijacking cellular membranes. Nature *496*, 367-371.

Fernando, M.M., Stevens, C.R., Walsh, E.C., De Jager, P.L., Goyette, P., Plenge, R.M., Vyse, T.J., and Rioux, J.D. (2008). Defining the role of the MHC in autoimmunity: a review and pooled analysis. PLoS Genet *4*, e1000024.

Ferreira, R.C., Guo, H., Coulson, R.M., Smyth, D.J., Pekalski, M.L., Burren, O.S., Cutler, A.J., Doecke, J.D., Flint, S., McKinney, E.F.*, et al.* (2014). A type I interferon transcriptional signature precedes autoimmunity in children genetically at risk for type 1 diabetes. Diabetes *63*, 2538-2550.

Ferreira, R.C., Simons, H.Z., Thompson, W.S., Cutler, A.J., Dopico, X.C., Smyth, D.J., Mashar, M., Schuilenburg, H., Walker, N.M., Dunger, D.B.*, et al.* (2015). IL-21 production by CD4+ effector T cells and frequency of circulating follicular helper T cells are increased in type 1 diabetes patients. Diabetologia *58*, 781-790.

Feschotte, C., and Gilbert, C. (2012). Endogenous viruses: insights into viral evolution and impact on host biology. Nat Rev Genet *13*, 283-296.

Flodstrom, M., Maday, A., Balakrishna, D., Cleary, M.M., Yoshimura, A., and Sarvetnick, N. (2002). Target cell defense prevents the development of diabetes after viral infection. Nat Immunol *3*, 373-382.

Flodstrom-Tullberg, M., Yadav, D., Hagerkvist, R., Tsai, D., Secrest, P., Stotland, A., and Sarvetnick, N. (2003). Target cell expression of suppressor of cytokine signaling-1 prevents diabetes in the NOD mouse. Diabetes *52*, 2696-2700.

Fotiadis, C., Xekouki, P., Papalois, A.E., Antonakis, P.T., Sfiniadakis, I., Flogeras, D., Karampela, E., and Zografos, G. (2005). Effects of mycophenolate mofetil vs cyclosporine administration on graft survival and function after islet allotransplantation in diabetic rats. World J Gastroenterol *11*, 2733-2738.

Foulis, A.K., Farquharson, M.A., and Meager, A. (1987). Immunoreactive alpha-interferon in insulin-secreting beta cells in type 1 diabetes mellitus. Lancet *2*, 1423-1427.

Foxman, E.F., and Iwasaki, A. (2011). Genome-virome interactions: examining the role of common viral infections in complex disease. Nat Rev Microbiol *9*, 254-264.

Freimanis, G., Hooley, P., Ejtehadi, H.D., Ali, H.A., Veitch, A., Rylance, P.B., Alawi, A., Axford, J., Nevill, A., Murray, P.G., and Nelson, P.N. (2010). A role for human endogenous retrovirus-K (HML-2) in rheumatoid arthritis: investigating mechanisms of pathogenesis. Clin Exp Immunol *160*, 340-347.

Frisk, G., and Diderholm, H. (2000). Tissue culture of isolated human pancreatic islets infected with different strains of coxsackievirus B4: assessment of virus replication and effects on islet morphology and insulin release. Int J Exp Diabetes Res *1*, 165-175.

Frisk, G., Friman, G., Tuvemo, T., Fohlman, J., and Diderholm, H. (1992). Coxsackie B virus IgM in children at onset of type 1 (insulin-dependent) diabetes mellitus: evidence for IgM induction by a recent or current infection. Diabetologia *35*, 249-253.

Fujino, K., Horie, M., Honda, T., Merriman, D.K., and Tomonaga, K. (2014). Inhibition of Borna disease virus replication by an endogenous bornavirus-like element in the ground squirrel genome. Proc Natl Acad Sci U S A *111*, 13175-13180.

Fukui, K., Yang, Q., Cao, Y., Takahashi, N., Hatakeyama, H., Wang, H., Wada, J., Zhang, Y., Marselli, L., Nammo, T.*, et al.* (2005). The HNF-1 target collectrin controls insulin exocytosis by SNARE complex formation. Cell Metab *2*, 373-384.

Funabiki, M., Kato, H., Miyachi, Y., Toki, H., Motegi, H., Inoue, M., Minowa, O., Yoshida, A., Deguchi, K., Sato, H.*, et al.* (2014). Autoimmune disorders associated with gain of function of the intracellular sensor MDA5. Immunity *40*, 199-212.

Gamble, D.R., Kinsley, M.L., FitzGerald, M.G., Bolton, R., and Taylor, K.W. (1969). Viral antibodies in diabetes mellitus. Br Med J *3*, 627-630.

Gao, D., Li, T., Li, X.D., Chen, X., Li, Q.Z., Wight-Carter, M., and Chen, Z.J. (2015). Activation of cyclic GMP-AMP synthase by self-DNA causes autoimmune diseases. Proc Natl Acad Sci U S A *112*, E5699-5705.

Gardner, S.G., Bingley, P.J., Sawtell, P.A., Weeks, S., and Gale, E.A. (1997). Rising incidence of insulin dependent diabetes in children aged under 5 years in the Oxford region: time trend analysis. The Bart's-Oxford Study Group. BMJ *315*, 713-717.

Garside, P., Ingulli, E., Merica, R.R., Johnson, J.G., Noelle, R.J., and Jenkins, M.K. (1998). Visualization of specific B and T lymphocyte interactions in the lymph node. Science *281*, 96-99.

Gay, D., Saunders, T., Camper, S., and Weigert, M. (1993). Receptor editing: an approach by autoreactive B cells to escape tolerance. J Exp Med *177*, 999-1008.

Gehrke, N., Mertens, C., Zillinger, T., Wenzel, J., Bald, T., Zahn, S., Tuting, T., Hartmann, G., and Barchet, W. (2013). Oxidative damage of DNA confers resistance to cytosolic nuclease TREX1 degradation and potentiates STING-dependent immune sensing. Immunity *39*, 482-495.

Geijtenbeek, T.B.H., and Gringhuis, S.I. (2009). Signalling through C-type lectin receptors: shaping immune responses. Nature Reviews Immunology *9*, 465-479.

Gepts, W. (1965). Pathologic anatomy of the pancreas in juvenile diabetes mellitus. Diabetes *14*, 619-633.

Germain, C., Gnjatic, S., Tamzalit, F., Knockaert, S., Remark, R., Goc, J., Lepelley, A., Becht, E., Katsahian, S., Bizouard, G.*, et al.* (2014). Presence of B cells in tertiary lymphoid structures is associated with a protective immunity in patients with lung cancer. Am J Respir Crit Care Med *189*, 832-844.

Germain, R.N. (2002). T-cell development and the CD4-CD8 lineage decision. Nat Rev Immunol *2*, 309-322.

Gescuk, B., Wu, A.J., Whitcher, J.P., Daniels, T.E., Lund, S., Fye, K., and Davis, J.C. (2005). Lamivudine is not effective in primary Sjogren's syndrome. Annals of the Rheumatic Diseases *64*, 1326-1330.

Gitelman, S.E., Gottlieb, P.A., Rigby, M.R., Felner, E.I., Willi, S.M., Fisher, L.K., Moran, A., Gottschalk, M., Moore, W.V., Pinckney, A.*, et al.* (2013). Antithymocyte globulin treatment for patients with recent-onset type 1 diabetes: 12-month results of a randomised, placebo-controlled, phase 2 trial. Lancet Diabetes Endocrinol *1*, 306-316.

Goh, F.G., and Midwood, K.S. (2012). Intrinsic danger: activation of Toll-like receptors in rheumatoid arthritis. Rheumatology (Oxford) *51*, 7-23.

Goodnow, C.C. (1997). Chance encounters and organized rendezvous. Immunol Rev *156*, 5-10.

Goodnow, C.C., Crosbie, J., Adelstein, S., Lavoie, T.B., Smith-Gill, S.J., Brink, R.A., Pritchard-Briscoe, H., Wotherspoon, J.S., Loblay, R.H., Raphael, K., and et al. (1988). Altered immunoglobulin expression and functional silencing of self-reactive B lymphocytes in transgenic mice. Nature *334*, 676-682.

Goubau, D., Deddouche, S., and Reis e Sousa, C. (2013). Cytosolic sensing of viruses. Immunity *38*, 855-869.

Gowda, S., Rao, A.S., Kim, Y.W., and Guntaka, R.V. (1988). Identification of sequences in the long terminal repeat of avian sarcoma virus required for efficient transcription. Virology *162*, 243-247.

Grakoui, A., Bromley, S.K., Sumen, C., Davis, M.M., Shaw, A.S., Allen, P.M., and Dustin, M.L. (1999). The immunological synapse: a molecular machine controlling T cell activation. Science *285*, 221-227.

Grandien, A., Fucs, R., Nobrega, A., Andersson, J., and Coutinho, A. (1994). Negative selection of multireactive B cell clones in normal adult mice. Eur J Immunol *24*, 1345-1352.

Grasso, J.A., Woodard, J.W., and Swift, H. (1963). Cytochemical studies of nucleic acids and proteins in erythrocytic development. Proc Natl Acad Sci U S A *50*, 134-140.

Gray, E.E., Treuting, P.M., Woodward, J.J., and Stetson, D.B. (2015). Cutting Edge: cGAS Is Required for Lethal Autoimmune Disease in the Trex1-Deficient Mouse Model of Aicardi-Goutieres Syndrome. J Immunol *195*, 1939-1943.

Group, T.S. (2008). The Environmental Determinants of Diabetes in the Young (TEDDY) Study. Ann N Y Acad Sci *1150*, 1-13.

Guberski, D.L., Thomas, V.A., Shek, W.R., Like, A.A., Handler, E.S., Rossini, A.A., Wallace, J.E., and Welsh, R.M. (1991). Induction of type I diabetes by Kilham's rat virus in diabetes-resistant BB/Wor rats. Science *254*, 1010-1013.

Hadjivassiliou, V., Green, M.H., and Green, I.C. (2000). Immunomagnetic purification of beta cells from rat islets of Langerhans. Diabetologia *43*, 1170-1177.

Hafenstein, S., Bowman, V.D., Chipman, P.R., Bator Kelly, C.M., Lin, F., Medof, M.E., and Rossmann, M.G. (2007). Interaction of decay-accelerating factor with coxsackievirus B3. J Virol *81*, 12927-12935.

Hakonarson, H., Grant, S.F., Bradfield, J.P., Marchand, L., Kim, C.E., Glessner, J.T., Grabs, R., Casalunovo, T., Taback, S.P., Frackelton, E.C.*, et al.* (2007). A genome-wide association study identifies KIAA0350 as a type 1 diabetes gene. Nature *448*, 591-594.

Hald, J., Galbo, T., Rescan, C., Radzikowski, L., Sprinkel, A.E., Heimberg, H., Ahnfelt-Ronne, J., Jensen, J., Scharfmann, R., Gradwohl, G.*, et al.* (2012). Pancreatic islet and progenitor cell surface markers with cell sorting potential. Diabetologia *55*, 154-165.

Hamalainen, A.M., and Knip, M. (2002). Autoimmunity and familial risk of type 1 diabetes. Curr Diab Rep *2*, 347-353.

Hamilton, A.J. (2010). MicroRNA in erythrocytes. Biochem Soc Trans *38*, 229-231.

Han, D., Leyva, C.A., Matheson, D., Mineo, D., Messinger, S., Blomberg, B.B., Hernandez, A., Meneghini, L.F., Allende, G., Skyler, J.S.*, et al.* (2011). Immune profiling by multiple gene expression analysis in patients at-risk and with type 1 diabetes. Clin Immunol *139*, 290-301.

Hanafusa, T., Miyagawa, J., Nakajima, H., Tomita, K., Kuwajima, M., Matsuzawa, Y., and Tarui, S. (1994). The NOD mouse. Diabetes research and clinical practice *24 Suppl*, S307-311.

Hansson, S.F., Korsgren, S., Ponten, F., and Korsgren, O. (2013). Enteroviruses and the pathogenesis of type 1 diabetes revisited: cross-reactivity of enterovirus capsid protein (VP1) antibodies with human mitochondrial proteins. J Pathol *229*, 719-728.

Hardy, R.R., Carmack, C.E., Shinton, S.A., Kemp, J.D., and Hayakawa, K. (1991). Resolution and characterization of pro-B and pre-pro-B cell stages in normal mouse bone marrow. J Exp Med *173*, 1213-1225.

Harris, J.R. (1998). Placental endogenous retrovirus (ERV): structural, functional, and evolutionary significance. Bioessays *20*, 307-316.

Hatten, B.A., and Dunton, H. (1978). Age-related humoral antibody responses of AKR/J mice to T-cell dependent and independent antigens. Immunology *35*, 707-713.

Hatziioannou, T., Perez-Caballero, D., Yang, A., Cowan, S., and Bieniasz, P.D. (2004). Retrovirus resistance factors Ref1 and Lv1 are species-specific variants of TRIM5alpha. Proc Natl Acad Sci U S A *101*, 10774-10779.

Haynes, N.M., Allen, C.D., Lesley, R., Ansel, K.M., Killeen, N., and Cyster, J.G. (2007). Role of CXCR5 and CCR7 in follicular Th cell positioning and appearance of a programmed cell death gene-1high germinal center-associated subpopulation. J Immunol *179*, 5099-5108.

He, J., Tsai, L.M., Leong, Y.A., Hu, X., Ma, C.S., Chevalier, N., Sun, X., Vandenberg, K., Rockman, S., Ding, Y.*, et al.* (2013). Circulating precursor CCR7(lo)PD-1(hi) CXCR5(+) CD4(+) T cells indicate Tfh cell activity and promote antibody responses upon antigen reexposure. Immunity *39*, 770-781.

He, Y., Chipman, P.R., Howitt, J., Bator, C.M., Whitt, M.A., Baker, T.S., Kuhn, R.J., Anderson, C.W., Freimuth, P., and Rossmann, M.G. (2001). Interaction of coxsackievirus B3 with the full length coxsackievirus-adenovirus receptor. Nat Struct Biol *8*, 874-878.

Heinig, M., Petretto, E., Wallace, C., Bottolo, L., Rotival, M., Lu, H., Li, Y., Sarwar, R., Langley, S.R., Bauerfeind, A.*, et al.* (2010). A trans-acting locus regulates an anti-viral expression network and type 1 diabetes risk. Nature *467*, 460-464.

Henderson, J.G., Opejin, A., Jones, A., Gross, C., and Hawiger, D. (2015). CD5 Instructs Extrathymic Regulatory T Cell Development in Response to Self and Tolerizing Antigens. Immunity *42*, 471-483.

Herold, K.C., Gitelman, S., Greenbaum, C., Puck, J., Hagopian, W., Gottlieb, P., Sayre, P., Bianchine, P., Wong, E., Seyfert-Margolis, V.*, et al.* (2009). Treatment of patients with new onset Type 1 diabetes with a single course of anti-CD3 mAb Teplizumab preserves insulin production for up to 5 years. Clin Immunol *132*, 166-173.

Hildeman, D.A., Zhu, Y., Mitchell, T.C., Bouillet, P., Strasser, A., Kappler, J., and Marrack, P. (2002). Activated T cell death in vivo mediated by proapoptotic bcl-2 family member bim. Immunity *16*, 759-767.

Hindersson, M., Orn, A., Harris, R.A., and Frisk, G. (2004). Strains of coxsackie virus B4 differed in their ability to induce acute pancreatitis and the responses were negatively correlated to glucose tolerance. Arch Virol *149*, 1985-2000.

Hindorff, L.A., Sethupathy, P., Junkins, H.A., Ramos, E.M., Mehta, J.P., Collins, F.S., and Manolio, T.A. (2009). Potential etiologic and functional implications of genome-wide association loci for human diseases and traits. Proc Natl Acad Sci U S A *106*, 9362-9367.

Holland, J., Spindler, K., Horodyski, F., Grabau, E., Nichol, S., and VandePol, S. (1982). Rapid evolution of RNA genomes. Science *215*, 1577-1585.

Honda, K., Sakaguchi, S., Nakajima, C., Watanabe, A., Yanai, H., Matsumoto, M., Ohteki, T., Kaisho, T., Takaoka, A., Akira, S.*, et al.* (2003). Selective contribution of IFN-alpha/beta signaling to the maturation of dendritic cells induced by double-stranded RNA or viral infection. Proc Natl Acad Sci U S A *100*, 10872-10877.

Honda, K., Yanai, H., Negishi, H., Asagiri, M., Sato, M., Mizutani, T., Shimada, N., Ohba, Y., Takaoka, A., Yoshida, N., and Taniguchi, T. (2005). IRF-7 is the master regulator of type-I interferon-dependent immune responses. Nature *434*, 772-777.

Horner, S.M., Liu, H.M., Park, H.S., Briley, J., and Gale, M., Jr. (2011). Mitochondrial-associated endoplasmic reticulum membranes (MAM) form innate immune synapses and are targeted by hepatitis C virus. Proc Natl Acad Sci U S A *108*, 14590-14595.

Hornung, V., Ellegast, J., Kim, S., Brzozka, K., Jung, A., Kato, H., Poeck, H., Akira, S., Conzelmann, K.K., Schlee, M.*, et al.* (2006). 5 '-triphosphate RNA is the ligand for RIG-I. Science *314*, 994-997.

Hoss, M., Robins, P., Naven, T.J., Pappin, D.J., Sgouros, J., and Lindahl, T. (1999). A human DNA editing enzyme homologous to the Escherichia coli DnaQ/MutD protein. EMBO J *18*, 3868-3875.

Hou, F., Sun, L., Zheng, H., Skaug, B., Jiang, Q.X., and Chen, Z.J. (2011). MAVS forms functional prion-like aggregates to activate and propagate antiviral innate immune response. Cell *146*, 448-461.

Huang, X., Yuang, J., Goddard, A., Foulis, A., James, R.F., Lernmark, A., Pujol-Borrell, R., Rabinovitch, A., Somoza, N., and Stewart, T.A. (1995). Interferon expression in the pancreases of patients with type I diabetes. Diabetes *44*, 658-664.

Hughes, J.F., and Coffin, J.M. (2004). Human endogenous retrovirus K solo-LTR formation and insertional polymorphisms: implications for human and viral evolution. Proc Natl Acad Sci U S A *101*, 1668-1672.

Hyoty, H., and Knip, M. (2014). Developing a vaccine for Type 1 diabetes through targeting enteroviral infections. Expert Rev Vaccines *13*, 989-999.

Igoe, A., and Scofield, R.H. (2013). Autoimmunity and infection in Sjogren's syndrome. Curr Opin Rheumatol *25*, 480-487.

Ishigame, H., Zenewicz, L.A., Sanjabi, S., Licona-Limon, P., Nakayama, M., Leonard, W.J., and Flavell, R.A. (2013). Excessive Th1 responses due to the absence of TGF-beta signaling cause autoimmune diabetes and dysregulated Treg cell homeostasis. Proc Natl Acad Sci U S A *110*, 6961-6966.

Ishii, K.J., Coban, C., Kato, H., Takahashi, K., Torii, Y., Takeshita, F., Ludwig, H., Sutter, G., Suzuki, K., Hemmi, H.*, et al.* (2006). A Toll-like receptor-independent antiviral response induced by double-stranded B-form DNA. Nat Immunol *7*, 40-48.

Ishikawa, H., Ma, Z., and Barber, G.N. (2009). STING regulates intracellular DNA-mediated, type I interferon-dependent innate immunity. Nature *461*, 788-792.

Ishikawa-Sekigami, T., Kaneko, Y., Okazawa, H., Tomizawa, T., Okajo, J., Saito, Y., Okuzawa, C., Sugawara-Yokoo, M., Nishiyama, U., Ohnishi, H.*, et al.* (2006). SHPS-1 promotes the survival of circulating erythrocytes through inhibition of phagocytosis by splenic macrophages. Blood *107*, 341-348.

Iwasaki, A., and Medzhitov, R. (2015). Control of adaptive immunity by the innate immune system. Nat Immunol *16*, 343-353.

Jackson, K.J., Kidd, M.J., Wang, Y., and Collins, A.M. (2013). The shape of the lymphocyte receptor repertoire: lessons from the B cell receptor. Front Immunol *4*, 263.

Jacob, M., Napirei, M., Ricken, A., Dixkens, C., and Mannherz, H.G. (2002). Histopathology of lupus-like nephritis in Dnase1-deficient mice in comparison to NZB/W F1 mice. Lupus *11*, 514-527.

Jacques, P.E., Jeyakani, J., and Bourque, G. (2013). The majority of primate-specific regulatory sequences are derived from transposable elements. PLoS Genet *9*, e1003504.

Jaidane, H., Gharbi, J., Lobert, P.E., Lucas, B., Hiar, R., M'Hadheb M, B., Brilot, F., Geenen, V., Aouni, M., and Hober, D. (2006). Prolonged viral RNA detection in blood and lymphoid tissues from coxsackievirus B4 E2 orally-inoculated Swiss mice. Microbiol Immunol *50*, 971-974.

Janeway, C.A., Jr. (1989). Approaching the asymptote? Evolution and revolution in immunology. Cold Spring Harb Symp Quant Biol *54 Pt 1*, 1-13.

Jensen, S., and Thomsen, A.R. (2012). Sensing of RNA viruses: a review of innate immune receptors involved in recognizing RNA virus invasion. J Virol *86*, 2900-2910.

Jiang, X., Kinch, L.N., Brautigam, C.A., Chen, X., Du, F., Grishin, N.V., and Chen, Z.J. (2012). Ubiquitin-induced oligomerization of the RNA sensors RIG-I and MDA5 activates antiviral innate immune response. Immunity *36*, 959-973.

Jirtle, R.L., and Skinner, M.K. (2007). Environmental epigenomics and disease susceptibility. Nat Rev Genet *8*, 253-262.

Johnson, W.E., and Coffin, J.M. (1999). Constructing primate phylogenies from ancient retrovirus sequences. Proc Natl Acad Sci U S A *96*, 10254-10260.

Jordan, G.W., and Cohen, S.H. (1987). Encephalomyocarditis virus-induced diabetes mellitus in mice: model of viral pathogenesis. Rev Infect Dis *9*, 917-924.

Jun, H.S., Yoon, C.S., Zbytnuik, L., van Rooijen, N., and Yoon, J.W. (1999). The role of macrophages in T cell-mediated autoimmune diabetes in nonobese diabetic mice. J Exp Med *189*, 347-358.

Jun, H.S., and Yoon, J.W. (2003). A new look at viruses in type 1 diabetes. Diabetes Metab Res Rev *19*, 8-31.

Jurka, J. (1998). Repeats in genomic DNA: mining and meaning. Curr Opin Struct Biol *8*, 333-337.

Kabanova, S., Kleinbongard, P., Volkmer, J., Andree, B., Kelm, M., and Jax, T.W. (2009). Gene expression analysis of human red blood cells. Int J Med Sci *6*, 156-159.

Kagi, D., and Hengartner, H. (1996). Different roles for cytotoxic T cells in the control of infections with cytopathic versus noncytopathic viruses. Curr Opin Immunol *8*, 472-477.

Kalia, V., Sarkar, S., Gourley, T.S., Rouse, B.T., and Ahmed, R. (2006). Differentiation of memory B and T cells. Curr Opin Immunol *18*, 255-264.

Kalliora, M.I., Vazeou, A., Delis, D., Bozas, E., Thymelli, I., and Bartsocas, C.S. (2011). Seasonal variation of type 1 diabetes mellitus diagnosis in Greek children. Hormones (Athens) *10*, 67-71.

Kanehisa, M., and Goto, S. (2000). KEGG: kyoto encyclopedia of genes and genomes. Nucleic Acids Res *28*, 27-30.

Kanehisa, M., Sato, Y., Kawashima, M., Furumichi, M., and Tanabe, M. (2016). KEGG as a reference resource for gene and protein annotation. Nucleic Acids Res *44*, D457-462.

Kang, Y., and Yoon, J.W. (1993). A genetically determined host factor controlling susceptibility to encephalomyocarditis virus-induced diabetes in mice. J Gen Virol *74 (Pt 6)*, 1207-1213.

Kanno, H., Nose, M., Itoh, J., Taniguchi, Y., and Kyogoku, M. (1992). Spontaneous development of pancreatitis in the MRL/Mp strain of mice in autoimmune mechanism. Clin Exp Immunol *89*, 68-73.

Kappler, J.W., Roehm, N., and Marrack, P. (1987). T cell tolerance by clonal elimination in the thymus. Cell *49*, 273-280.

Karnowski, A., Chevrier, S., Belz, G.T., Mount, A., Emslie, D., D'Costa, K., Tarlinton, D.M., Kallies, A., and Corcoran, L.M. (2012). B and T cells collaborate in antiviral responses via IL-6, IL-21, and transcriptional activator and coactivator, Oct2 and OBF-1. J Exp Med *209*, 2049-2064.

Kärre, K. (1981). On the immunobiology of natural killer cells.

Kato, H., Sato, S., Yoneyama, M., Yamamoto, M., Uematsu, S., Matsui, K., Tsujimura, T., Takeda, K., Fujita, T., Takeuchi, O., and Akira, S. (2005). Cell type-specific involvement of RIG-I in antiviral response. Immunity *23*, 19-28.

Kato, H., Takeuchi, O., Sato, S., Yoneyama, M., Yamamoto, M., Matsui, K., Uematsu, S., Jung, A., Kawai, T., Ishii, K.J.*, et al.* (2006). Differential roles of

MDA5 and RIG-I helicases in the recognition of RNA viruses. Nature *441*, 101-105.

Katsumata, K., Ikeda, H., Sato, M., Ishizu, A., Kawarada, Y., Kato, H., Wakisaka, A., Koike, T., and Yoshiki, T. (1999). Cytokine regulation of env gene expression of human endogenous retrovirus-R in human vascular endothelial cells. Clin Immunol *93*, 75-80.

Katz, J.D., Benoist, C., and Mathis, D. (1995). T helper cell subsets in insulin-dependent diabetes. Science *268*, 1185-1188.

Kawai, T., and Akira, S. (2006). TLR signaling. Cell Death Differ *13*, 816-825.

Kawai, T., and Akira, S. (2010). The role of pattern-recognition receptors in innate immunity: update on Toll-like receptors. Nat Immunol *11*, 373-384.

Kawai, T., Takahashi, K., Sato, S., Coban, C., Kumar, H., Kato, H., Ishii, K.J., Takeuchi, O., and Akira, S. (2005). IPS-1, an adaptor triggering RIG-I- and Mda5-mediated type I interferon induction. Nat Immunol *6*, 981-988.

Kearse, M., Moir, R., Wilson, A., Stones-Havas, S., Cheung, M., Sturrock, S., Buxton, S., Cooper, A., Markowitz, S., Duran, C.*, et al.* (2012). Geneious Basic: an integrated and extendable desktop software platform for the organization and analysis of sequence data. Bioinformatics *28*, 1647-1649.

Keir, M.E., Butte, M.J., Freeman, G.J., and Sharpe, A.H. (2008). PD-1 and its ligands in tolerance and immunity. Annu Rev Immunol *26*, 677-704.

Keir, M.E., Francisco, L.M., and Sharpe, A.H. (2007). PD-1 and its ligands in T-cell immunity. Curr Opin Immunol *19*, 309-314.

Kenefeck, R., Wang, C.J., Kapadi, T., Wardzinski, L., Attridge, K., Clough, L.E., Heuts, F., Kogimtzis, A., Patel, S., Rosenthal, M.*, et al.* (2015). Follicular helper T cell signature in type 1 diabetes. J Clin Invest *125*, 292-303.

Keymeulen, B., Walter, M., Mathieu, C., Kaufman, L., Gorus, F., Hilbrands, R., Vandemeulebroucke, E., Van de Velde, U., Crenier, L., De Block, C.*, et al.* (2010). Four-year metabolic outcome of a randomised controlled CD3-antibody trial in recent-onset type 1 diabetic patients depends on their age and baseline residual beta cell mass. Diabetologia *53*, 614-623.

King, C. (2009). New insights into the differentiation and function of T follicular helper cells. Nat Rev Immunol *9*, 757-766.

King, C., and Sarvetnick, N. (2011). The incidence of type-1 diabetes in NOD mice is modulated by restricted flora not germ-free conditions. PLoS One *6*, e17049.

King, C., Tangye, S.G., and Mackay, C.R. (2008). T follicular helper (TFH) cells in normal and dysregulated immune responses. Annu Rev Immunol *26*, 741-766.

Kocks, C., and Rajewsky, K. (1988). Stepwise Intraclonal Maturation of Antibody-Affinity through Somatic Hypermutation. P Natl Acad Sci USA *85*, 8206-8210.

Koshiba, T. (2013). Mitochondrial-mediated antiviral immunity. Biochim Biophys Acta *1833*, 225-232.

Koshiba, T., Yasukawa, K., Yanagi, Y., and Kawabata, S. (2011). Mitochondrial membrane potential is required for MAVS-mediated antiviral signaling. Sci Signal *4*, ra7.

Kostraba, J.N., Cruickshanks, K.J., Lawler-Heavner, J., Jobim, L.F., Rewers, M.J., Gay, E.C., Chase, H.P., Klingensmith, G., and Hamman, R.F. (1993). Early exposure to cow's milk and solid foods in infancy, genetic predisposition, and risk of IDDM. Diabetes *42*, 288-295.

Koury, M.J., Koury, S.T., Kopsombut, P., and Bondurant, M.C. (2005). In vitro maturation of nascent reticulocytes to erythrocytes. Blood *105*, 2168-2174.

Kramer, M., Schulte, B.M., Toonen, L.W., de Bruijni, M.A., Galama, J.M., Adema, G.J., and van Kuppeveld, F.J. (2007). Echovirus infection causes rapid loss-of-function and cell death in human dendritic cells. Cell Microbiol *9*, 1507-1518.

Krogvold, L., Edwin, B., Buanes, T., Frisk, G., Skog, O., Anagandula, M., Korsgren, O., Undlien, D., Eike, M.C., Richardson, S.J.*, et al.* (2015). Detection of a low-grade enteroviral infection in the islets of langerhans of living patients newly diagnosed with type 1 diabetes. Diabetes *64*, 1682-1687.

Krogvold, L., Edwin, B., Buanes, T., Ludvigsson, J., Korsgren, O., Hyoty, H., Frisk, G., Hanssen, K.F., and Dahl-Jorgensen, K. (2014). Pancreatic biopsy by minimal tail resection in live adult patients at the onset of type 1 diabetes: experiences from the DiViD study. Diabetologia *57*, 841-843.

Krosting, J.L., G. (2012). RNase Activity in Mouse Tissue: Classification, Hierarchy, and Methods for Control. Thermo Fisher Scientific.

Kukko, M., Kimpimaki, T., Korhonen, S., Kupila, A., Simell, S., Veijola, R., Simell, T., Ilonen, J., Simell, O., and Knip, M. (2005). Dynamics of diabetes-associated autoantibodies in young children with human leukocyte antigen-conferred risk of type 1 diabetes recruited from the general population. J Clin Endocr Metab *90*, 2712-2717.

Kuleshov, M.V., Jones, M.R., Rouillard, A.D., Fernandez, N.F., Duan, Q., Wang, Z., Koplev, S., Jenkins, S.L., Jagodnik, K.M., Lachmann, A.*, et al.* (2016). Enrichr: a comprehensive gene set enrichment analysis web server 2016 update. Nucleic Acids Res *44*, W90-97.

Kulski, J.K., Gaudieri, S., Bellgard, M., Balmer, L., Giles, K., Inoko, H., and Dawkins, R.L. (1997). The evolution of MHC diversity by segmental duplication and transposition of retroelements. J Mol Evol *45*, 599-609.

Kunarso, G., Chia, N.Y., Jeyakani, J., Hwang, C., Lu, X.Y., Chan, Y.S., Ng, H.H., and Bourque, G. (2010). Transposable elements have rewired the core regulatory network of human embryonic stem cells. Nature Genetics *42*, 631-U111.

Kunisawa, J., Fukuyama, S., and Kiyono, H. (2005). Mucosa-associated lymphoid tissues in the aerodigestive tract: their shared and divergent traits and their importance to the orchestration of the mucosal immune system. Curr Mol Med *5*, 557-572.

Kutlu, B., Burdick, D., Baxter, D., Rasschaert, J., Flamez, D., Eizirik, D.L., Welsh, N., Goodman, N., and Hood, L. (2009). Detailed transcriptome atlas of the pancreatic beta cell. BMC Med Genomics *2*, 3.

Kutmon, M., van Iersel, M.P., Bohler, A., Kelder, T., Nunes, N., Pico, A.R., and Evelo, C.T. (2015). PathVisio 3: an extendable pathway analysis toolbox. PLoS Comput Biol *11*, e1004085.

Kyvik, K.O., Green, A., and Beck-Nielsen, H. (1995). Concordance rates of insulin dependent diabetes mellitus: a population based study of young Danish twins. BMJ *311*, 913-917.

Laguette, N., Sobhian, B., Casartelli, N., Ringeard, M., Chable-Bessia, C., Segeral, E., Yatim, A., Emiliani, S., Schwartz, O., and Benkirane, M. (2011). SAMHD1 is the dendritic- and myeloid-cell-specific HIV-1 restriction factor counteracted by Vpx. Nature *474*, 654-657.

Lamkanfi, M., and Dixit, V.M. (2014). Mechanisms and functions of inflammasomes. Cell *157*, 1013-1022.

Lamphier, M., Zheng, W., Latz, E., Spyvee, M., Hansen, H., Rose, J., Genest, M., Yang, H., Shaffer, C., Zhao, Y.*, et al.* (2014). Novel small molecule

inhibitors of TLR7 and TLR9: mechanism of action and efficacy in vivo. Mol Pharmacol *85*, 429-440.

Lande, R., Ganguly, D., Facchinetti, V., Frasca, L., Conrad, C., Gregorio, J., Meller, S., Chamilos, G., Sebasigari, R., Riccieri, V.*, et al.* (2011). Neutrophils activate plasmacytoid dendritic cells by releasing self-DNA-peptide complexes in systemic lupus erythematosus. Sci Transl Med *3*, 73ra19.

Lanier, L.L., Ofallon, S., Somoza, C., Phillips, J.H., Linsley, P.S., Okumura, K., Ito, D., and Azuma, M. (1995). Cd80 (B7) and Cd86 (B70) Provide Similar Costimulatory Signals for T-Cell Proliferation, Cytokine Production, and Generation of Ctl. Journal of Immunology *154*, 97-105.

Larsson, P.G., Lakshmikanth, T., Laitinen, O.H., Utorova, R., Jacobson, S., Oikarinen, M., Domsgen, E., Koivunen, M.R.L., Chaux, P., Devard, N.*, et al.* (2015). A preclinical study on the efficacy and safety of a new vaccine against Coxsackievirus B1 reveals no risk for accelerated diabetes development in mouse models. Diabetologia *58*, 346-354.

Laska, M.J., Brudek, T., Nissen, K.K., Christensen, T., Moller-Larsen, A., Petersen, T., and Nexo, B.A. (2012). Expression of HERV-Fc1, a Human Endogenous Retrovirus, Is Increased in Patients with Active Multiple Sclerosis. Journal of Virology *86*, 3713-3722.

Lauwerys, B.R., Hachulla, E., Spertini, F., Lazaro, E., Jorgensen, C., Mariette, X., Haelterman, E., Grouard-Vogel, G., Fanget, B., Dhellin, O.*, et al.* (2013). Down-regulation of interferon signature in systemic lupus erythematosus patients by active immunization with interferon alpha-kinoid. Arthritis Rheum *65*, 447-456.

LeBien, T.W. (2000). Fates of human B-cell precursors. Blood *96*, 9-23.

Lebon, P., Badoual, J., Ponsot, G., Goutieres, F., Hemeury-Cukier, F., and Aicardi, J. (1988). Intrathecal synthesis of interferon-alpha in infants with progressive familial encephalopathy. J Neurol Sci *84*, 201-208.

Lee, S.H., Miyagi, T., and Biron, C.A. (2007). Keeping NK cells in highly regulated antiviral warfare. Trends Immunol *28*, 252-259.

Lee, S.K., Silva, D.G., Martin, J.L., Pratama, A., Hu, X., Chang, P.P., Walters, G., and Vinuesa, C.G. (2012). Interferon-gamma excess leads to pathogenic accumulation of follicular helper T cells and germinal centers. Immunity *37*, 880-892.

Lee-Kirsch, M.A., Chowdhury, D., Harvey, S., Gong, M., Senenko, L., Engel, K., Pfeiffer, C., Hollis, T., Gahr, M., Perrino, F.W.*, et al.* (2007a). A mutation in

TREX1 that impairs susceptibility to granzyme A-mediated cell death underlies familial chilblain lupus. J Mol Med (Berl) *85*, 531-537.

Lee-Kirsch, M.A., Gong, M., Chowdhury, D., Senenko, L., Engel, K., Lee, Y.A., de Silva, U., Bailey, S.L., Witte, T., Vyse, T.J.*, et al.* (2007b). Mutations in the gene encoding the 3'-5' DNA exonuclease TREX1 are associated with systemic lupus erythematosus. Nat Genet *39*, 1065-1067.

Lemaitre, B., Nicolas, E., Michaut, L., Reichhart, J.M., and Hoffmann, J.A. (1996). The dorsoventral regulatory gene cassette spatzle/Toll/cactus controls the potent antifungal response in Drosophila adults. Cell *86*, 973-983.

Lerner, R.A., Wilson, C.B., Villano, B.C., McConahey, P.J., and Dixon, F.J. (1976). Endogenous oncornaviral gene expression in adult and fetal mice: quantitative, histologic, and physiologic studies of the major viral glycorprotein, gp70. J Exp Med *143*, 151-166.

Levy, D.E., and Garcia-Sastre, A. (2001). The virus battles: IFN induction of the antiviral state and mechanisms of viral evasion. Cytokine Growth Factor Rev *12*, 143-156.

Levy, O., Orange, J.S., Hibberd, P., Steinberg, S., LaRussa, P., Weinberg, A., Wilson, S.B., Shaulov, A., Fleisher, G., Geha, R.S.*, et al.* (2003). Disseminated varicella infection due to the vaccine strain of varicella-zoster virus, in a patient with a novel deficiency in natural killer T cells. J Infect Dis *188*, 948-953.

Li, Q., Xu, B., Michie, S.A., Rubins, K.H., Schreriber, R.D., and McDevitt, H.O. (2008). Interferon-alpha initiates type 1 diabetes in nonobese diabetic mice. Proc Natl Acad Sci U S A *105*, 12439-12444.

Li, X.D., Sun, L., Seth, R.B., Pineda, G., and Chen, Z.J. (2005). Hepatitis C virus protease NS3/4A cleaves mitochondrial antiviral signaling protein off the mitochondria to evade innate immunity. Proc Natl Acad Sci U S A *102*, 17717-17722.

Li, X.D., Wu, J., Gao, D., Wang, H., Sun, L., and Chen, Z.J. (2013). Pivotal roles of cGAS-cGAMP signaling in antiviral defense and immune adjuvant effects. Science *341*, 1390-1394.

Li, Y.R., Li, J., Zhao, S.D., Bradfield, J.P., Mentch, F.D., Maggadottir, S.M., Hou, C., Abrams, D.J., Chang, D., Gao, F.*, et al.* (2015). Meta-analysis of shared genetic architecture across ten pediatric autoimmune diseases. Nat Med *21*, 1018-1027.

Lindahl, T., Gally, J.A., and Edelman, G.M. (1969). Properties of deoxyribonuclease 3 from mammalian tissues. J Biol Chem *244*, 5014-5019.

Ling, Z., Hannaert, J.C., and Pipeleers, D. (1994). Effect of nutrients, hormones and serum on survival of rat islet beta cells in culture. Diabetologia *37*, 15-21.

Linterman, M.A., Pierson, W., Lee, S.K., Kallies, A., Kawamoto, S., Rayner, T.F., Srivastava, M., Divekar, D.P., Beaton, L., Hogan, J.J.*, et al.* (2011). Foxp3+ follicular regulatory T cells control the germinal center response. Nat Med *17*, 975-982.

Liu, R., Wu, Q., Su, D., Che, N., Chen, H., Geng, L., Chen, J., Chen, W., Li, X., and Sun, L. (2012). A regulatory effect of IL-21 on T follicular helper-like cell and B cell in rheumatoid arthritis. Arthritis Res Ther *14*, R255.

Liu, S., Chen, J., Cai, X., Wu, J., Chen, X., Wu, Y.T., Sun, L., and Chen, Z.J. (2013). MAVS recruits multiple ubiquitin E3 ligases to activate antiviral signaling cascades. Elife *2*, e00785.

Liu, S., Wang, H., Jin, Y., Podolsky, R., Reddy, M.V., Pedersen, J., Bode, B., Reed, J., Steed, D., Anderson, S.*, et al.* (2009). IFIH1 polymorphisms are significantly associated with type 1 diabetes and IFIH1 gene expression in peripheral blood mononuclear cells. Hum Mol Genet *18*, 358-365.

Liu, W., Xie, Y., Ma, J., Luo, X., Nie, P., Zuo, Z., Lahrmann, U., Zhao, Q., Zheng, Y., Zhao, Y.*, et al.* (2015). IBS: an illustrator for the presentation and visualization of biological sequences. Bioinformatics *31*, 3359-3361.

Liu, X.Y., Wei, B., Shi, H.X., Shan, Y.F., and Wang, C. (2010). Tom70 mediates activation of interferon regulatory factor 3 on mitochondria. Cell Res *20*, 994-1011.

Locci, M., Havenar-Daughton, C., Landais, E., Wu, J., Kroenke, M.A., Arlehamn, C.L., Su, L.F., Cubas, R., Davis, M.M., Sette, A.*, et al.* (2013). Human circulating PD-1+CXCR3-CXCR5+ memory Tfh cells are highly functional and correlate with broadly neutralizing HIV antibody responses. Immunity *39*, 758-769.

Loder, F., Mutschler, B., Ray, R.J., Paige, C.J., Sideras, P., Torres, R., Lamers, M.C., and Carsetti, R. (1999). B cell development in the spleen takes place in discrete steps and is determined by the quality of B cell receptor-derived signals. J Exp Med *190*, 75-89.

Longhi, M.P., Trumpfheller, C., Idoyaga, J., Caskey, M., Matos, I., Kluger, C., Salazar, A.M., Colonna, M., and Steinman, R.M. (2009). Dendritic cells require a systemic type I interferon response to mature and induce CD4(+) Th1 immunity with poly IC as adjuvant. Journal of Experimental Medicine *206*, 1589-1602.

Lonnrot, M., Lynch, K., Larsson, H.E., Lernmark, A., Rewers, M., Hagopian, W., She, J.X., Simell, O., Ziegler, A.G., Akolkar, B.*, et al.* (2015). A method for reporting and classifying acute infectious diseases in a prospective study of young children: TEDDY. BMC Pediatr *15*, 24.

Lowe, C.E., Cooper, J.D., Brusko, T., Walker, N.M., Smyth, D.J., Bailey, R., Bourget, K., Plagnol, V., Field, S., Atkinson, M.*, et al.* (2007). Large-scale genetic fine mapping and genotype-phenotype associations implicate polymorphism in the IL2RA region in type 1 diabetes. Nat Genet *39*, 1074-1082.

Lu, X.Y., Sachs, F., Ramsay, L., Jacques, P.E., Goke, J., Bourque, G., and Ng, H.H. (2014). The retrovirus HERVH is a long noncoding RNA required for human embryonic stem cell identity. Nature Structural & Molecular Biology *21*, 423-U168.

Ludewig, B., Odermatt, B., Landmann, S., Hengartner, H., and Zinkernagel, R.M. (1998). Dendritic cells induce autoimmune diabetes and maintain disease via de novo formation of local lymphoid tissue. J Exp Med *188*, 1493-1501.

Lukowiak, B., Vandewalle, B., Riachy, R., Kerr-Conte, J., Gmyr, V., Belaich, S., Lefebvre, J., and Pattou, F. (2001). Identification and purification of functional human beta-cells by a new specific zinc-fluorescent probe. J Histochem Cytochem *49*, 519-528.

Luthje, K., Kallies, A., Shimohakamada, Y., Belz, G.T., Light, A., Tarlinton, D.M., and Nutt, S.L. (2012). The development and fate of follicular helper T cells defined by an IL-21 reporter mouse. Nat Immunol *13*, 491-498.

Lyons, P.A., Armitage, N., Lord, C.J., Phillips, M.S., Todd, J.A., Peterson, L.B., and Wicker, L.S. (2001). Mapping by genetic interaction: high-resolution congenic mapping of the type 1 diabetes loci Idd10 and Idd18 in the NOD mouse. Diabetes *50*, 2633-2637.

Ma, J., Zhu, C., Ma, B., Tian, J., Baidoo, S.E., Mao, C., Wu, W., Chen, J., Tong, J., Yang, M.*, et al.* (2012). Increased frequency of circulating follicular helper T cells in patients with rheumatoid arthritis. Clin Dev Immunol *2012*, 827480.

MacFarlane, A.J., Burghardt, K.M., Kelly, J., Simell, T., Simell, O., Altosaar, I., and Scott, F.W. (2003). A type 1 diabetes-related protein from wheat (Triticum aestivum). cDNA clone of a wheat storage globulin, Glb1, linked to islet damage. J Biol Chem *278*, 54-63.

Maksakova, I.A., Mager, D.L., and Reiss, D. (2008). Keeping active endogenous retroviral-like elements in check: the epigenetic perspective. Cell Mol Life Sci *65*, 3329-3347.

Manders, E.M.M., Verbeek, F.J., and Aten, J.A. (1993). Measurement of Colocalization of Objects in Dual-Color Confocal Images. J Microsc-Oxford *169*, 375-382.

Mao, A.P., Li, S., Zhong, B., Li, Y., Yan, J., Li, Q., Teng, C., and Shu, H.B. (2010). Virus-triggered ubiquitination of TRAF3/6 by cIAP1/2 is essential for induction of interferon-beta (IFN-beta) and cellular antiviral response. J Biol Chem *285*, 9470-9476.

Marino, E., Walters, S.N., Villanueva, J.E., Richards, J.L., Mackay, C.R., and Grey, S.T. (2014). BAFF regulates activation of self-reactive T cells through B-cell dependent mechanisms and mediates protection in NOD mice. Eur J Immunol *44*, 983-993.

Marroqui, L., Lopes, M., dos Santos, R.S., Grieco, F.A., Roivainen, M., Richardson, S.J., Morgan, N.G., Op de Beeck, A., and Eizirik, D.L. (2015). Differential cell autonomous responses determine the outcome of coxsackievirus infections in murine pancreatic alpha and beta cells. Elife *4*, e06990.

Martin, A.P., Rankin, S., Pitchford, S., Charo, I.F., Furtado, G.C., and Lira, S.A. (2008). Increased expression of CCL2 in insulin-producing cells of transgenic mice promotes mobilization of myeloid cells from the bone marrow, marked insulitis, and diabetes. Diabetes *57*, 3025-3033.

Martin, R.M., Brady, J.L., and Lew, A.M. (1998). The need for IgG2c specific antiserum when isotyping antibodies from C57BL/6 and NOD mice. J Immunol Methods *212*, 187-192.

Martino, T.A., Petric, M., Weingartl, H., Bergelson, J.M., Opavsky, M.A., Richardson, C.D., Modlin, J.F., Finberg, R.W., Kain, K.C., Willis, N.*, et al.* (2000). The coxsackie-adenovirus receptor (CAR) is used by reference strains and clinical isolates representing all six serotypes of coxsackievirus group B and by swine vesicular disease virus. Virology *271*, 99-108.

Mathew, R., Khor, S., Hackett, S.R., Rabinowitz, J.D., Perlman, D.H., and White, E. (2014). Functional role of autophagy-mediated proteome remodeling in cell survival signaling and innate immunity. Mol Cell *55*, 916-930.

Mathias, S.L., Scott, A.F., Kazazian, H.H., Jr., Boeke, J.D., and Gabriel, A. (1991). Reverse transcriptase encoded by a human transposable element. Science *254*, 1808-1810.

Mavragani, C.P., Sagalovskiy, I., Guo, Q., Nezos, A., Kapsogeorgou, E.K., Lu, P., Zhou, J.L., Kirou, K.A., Seshan, S.V., Moutsopoulos, H.M., and Crow, M.K. (2016). Long interspersed nuclear element-1 retroelements are expressed in

patients with systemic autoimmune disease and induce type I interferon. Arthritis Rheumatol.

Maziarz, M., Hagopian, W., Palmer, J.P., Sanjeevi, C.B., Kockum, I., Breslow, N., Lernmark, A., Swedish Childhood Diabetes, R., Diabetes Incidence in Sweden Study, G., and Type 1 Diabetes Genetics, C. (2015). Non-HLA type 1 diabetes genes modulate disease risk together with HLA-DQ and islet autoantibodies. Genes Immun *16*, 541-551.

McCarthy, E.M., and McDonald, J.F. (2004). Long terminal repeat retrotransposons of Mus musculus. Genome Biol *5*, R14.

McClintock, B. (1950). The origin and behavior of mutable loci in maize. Proc Natl Acad Sci U S A *36*, 344-355.

McClintock, B. (1984). The significance of responses of the genome to challenge. Science *226*, 792-801.

Medzhitov, R., Preston-Hurlburt, P., and Janeway, C.A., Jr. (1997). A human homologue of the Drosophila Toll protein signals activation of adaptive immunity. Nature *388*, 394-397.

Mellors, R.C., and Mellors, J.W. (1978). Type C RNA virus-specific antibody in human systemic lupus erythematosus demonstrated by enzymoimmunoassay. Proc Natl Acad Sci U S A *75*, 2463-2467.

Mena, I., Fischer, C., Gebhard, J.R., Perry, C.M., Harkins, S., and Whitton, J.L. (2000). Coxsackievirus infection of the pancreas: evaluation of receptor expression, pathogenesis, and immunopathology. Virology *271*, 276-288.

Meylan, E., Curran, J., Hofmann, K., Moradpour, D., Binder, M., Bartenschlager, R., and Tschopp, J. (2005). Cardif is an adaptor protein in the RIG-I antiviral pathway and is targeted by hepatitis C virus. Nature *437*, 1167-1172.

Mi, S., Lee, X., Li, X., Veldman, G.M., Finnerty, H., Racie, L., LaVallie, E., Tang, X.Y., Edouard, P., Howes, S.*, et al.* (2000). Syncytin is a captive retroviral envelope protein involved in human placental morphogenesis. Nature *403*, 785-789.

Michallet, M.C., Meylan, E., Ermolaeva, M.A., Vazquez, J., Rebsamen, M., Curran, J., Poeck, H., Bscheider, M., Hartmann, G., Koenig, M.*, et al.* (2008). TRADD protein is an essential component of the RIG-like helicase antiviral pathway. Immunity *28*, 651-661.

Mogensen, S.C. (1979). Role of macrophages in natural resistance to virus infections. Microbiol Rev *43*, 1-26.

Moles, J.P., Tesniere, A., and Guilhou, J.J. (2005). A new endogenous retroviral sequence is expressed in skin of patients with psoriasis. Brit J Dermatol *153*, 83-89.

Moltchanova, E.V., Schreier, N., Lammi, N., and Karvonen, M. (2009). Seasonal variation of diagnosis of Type 1 diabetes mellitus in children worldwide. Diabet Med *26*, 673-678.

Mond, J.J., Lees, A., and Snapper, C.M. (1995). T-Cell-Independent Antigens Type-2. Annual Review of Immunology *13*, 655-692.

Morita, M., Stamp, G., Robins, P., Dulic, A., Rosewell, I., Hrivnak, G., Daly, G., Lindahl, T., and Barnes, D.E. (2004). Gene-targeted mice lacking the Trex1 (DNase III) 3'-->5' DNA exonuclease develop inflammatory myocarditis. Mol Cell Biol *24*, 6719-6727.

Morton, R.A., Geras-Raaka, E., Wilson, L.M., Raaka, B.M., and Gershengorn, M.C. (2007). Endocrine precursor cells from mouse islets are not generated by epithelial-to-mesenchymal transition of mature beta cells. Mol Cell Endocrinol *270*, 87-93.

Moses, R.G., Matthews, J.A., and Griffiths, R. (1995). Dramatic increase in incidence of insulin-dependent diabetes mellitus in Western Australia. Med J Aust *162*, 111.

Mosmann, T.R., Cherwinski, H., Bond, M.W., Giedlin, M.A., and Coffman, R.L. (1986). Two types of murine helper T cell clone. I. Definition according to profiles of lymphokine activities and secreted proteins. J Immunol *136*, 2348-2357.

Muir, A., Peck, A., Clare-Salzler, M., Song, Y.H., Cornelius, J., Luchetta, R., Krischer, J., and Maclaren, N. (1995). Insulin immunization of nonobese diabetic mice induces a protective insulitis characterized by diminished intraislet interferon-gamma transcription. J Clin Invest *95*, 628-634.

Mukherjee, A., Morosky, S.A., Delorme-Axford, E., Dybdahl-Sissoko, N., Oberste, M.S., Wang, T., and Coyne, C.B. (2011). The coxsackievirus B 3C protease cleaves MAVS and TRIF to attenuate host type I interferon and apoptotic signaling. PLoS pathogens *7*, e1001311.

Mukhopadhyay, S., and Gordon, S. (2004). The role of scavenger receptors in pathogen recognition and innate immunity. Immunobiology *209*, 39-49.

Muller, U., Steinhoff, U., Reis, L.F., Hemmi, S., Pavlovic, J., Zinkernagel, R.M., and Aguet, M. (1994). Functional role of type I and type II interferons in antiviral defense. Science *264*, 1918-1921.

Nagase, F., Nakashima, I., Nagase, N., and Kato, N. (1982). Alterations in the immunogenic properties of sheep erythrocytes by sonic disruption. Microbiol Immunol *26*, 139-151.

Nagy, G., Ward, J., Mosser, D.D., Koncz, A., Gergely, P., Jr., Stancato, C., Qian, Y., Fernandez, D., Niland, B., Grossman, C.E.*, et al.* (2006). Regulation of CD4 expression via recycling by HRES-1/RAB4 controls susceptibility to HIV infection. J Biol Chem *281*, 34574-34591.

Nakayamada, S., Kanno, Y., Takahashi, H., Jankovic, D., Lu, K.T., Johnson, T.A., Sun, H.W., Vahedi, G., Hakim, O., Handon, R.*, et al.* (2011). Early Th1 cell differentiation is marked by a Tfh cell-like transition. Immunity *35*, 919-931.

Nakayamada, S., Poholek, A.C., Lu, K.T., Takahashi, H., Kato, M., Iwata, S., Hirahara, K., Cannons, J.L., Schwartzberg, P.L., Vahedi, G.*, et al.* (2014). Type I IFN induces binding of STAT1 to Bcl6: divergent roles of STAT family transcription factors in the T follicular helper cell genetic program. J Immunol *192*, 2156-2166.

Namjou, B., Kothari, P.H., Kelly, J.A., Glenn, S.B., Ojwang, J.O., Adler, A., Alarcon-Riquelme, M.E., Gallant, C.J., Boackle, S.A., Criswell, L.A.*, et al.* (2011). Evaluation of the TREX1 gene in a large multi-ancestral lupus cohort. Genes Immun *12*, 270-279.

Nejentsev, S., Walker, N., Riches, D., Egholm, M., and Todd, J.A. (2009). Rare variants of IFIH1, a gene implicated in antiviral responses, protect against type 1 diabetes. Science *324*, 387-389.

Nelms, K.A., and Goodnow, C.C. (2001). Genome-wide ENU mutagenesis to reveal immune regulators. Immunity *15*, 409-418.

Nemazee, D.A., and Burki, K. (1989). Clonal deletion of B lymphocytes in a transgenic mouse bearing anti-MHC class I antibody genes. Nature *337*, 562-566.

Neupert, W., and Herrmann, J.M. (2007a). Translocation of proteins into mitochondria. Annu Rev Biochem *76*, 723-749.

Neupert, W., and Herrmann, J.M. (2007b). Translocation of proteins into mitochondria. Annu Rev Biochem *76*, 723-749.

Neyt, K., Perros, F., GeurtsvanKessel, C.H., Hammad, H., and Lambrecht, B.N. (2012). Tertiary lymphoid organs in infection and autoimmunity. Trends Immunol *33*, 297-305.

Ngo, S.T., Steyn, F.J., and McCombe, P.A. (2014). Gender differences in autoimmune disease. Front Neuroendocrinol *35*, 347-369.

Nica, A.C., Ongen, H., Irminger, J.C., Bosco, D., Berney, T., Antonarakis, S.E., Halban, P.A., and Dermitzakis, E.T. (2013). Cell-type, allelic, and genetic signatures in the human pancreatic beta cell transcriptome. Genome Res *23*, 1554-1562.

Nielsen, J.H., Brunstedt, J., Andersson, A., and Frimodt-Moller, C. (1979). Preservation of beta cell function in adult human pancreatic islets for several months in vitro. Diabetologia *16*, 97-100.

Nishimura, H., Nose, M., Hiai, H., Minato, N., and Honjo, T. (1999). Development of lupus-like autoimmune diseases by disruption of the PD-1 gene encoding an ITIM motif-carrying immunoreceptor. Immunity *11*, 141-151.

Noble, J.A., and Erlich, H.A. (2012). Genetics of type 1 diabetes. Cold Spring Harb Perspect Med *2*, a007732.

Nonoyama, S., Smith, F.O., Bernstein, I.D., and Ochs, H.D. (1993). Strain-dependent leakiness of mice with severe combined immune deficiency. J Immunol *150*, 3817-3824.

O'Brien, C.A., and Harley, J.B. (1990). A subset of hY RNAs is associated with erythrocyte Ro ribonucleoproteins. EMBO J *9*, 3683-3689.

O'Shea, J.J., and Paul, W.E. (2010). Mechanisms underlying lineage commitment and plasticity of helper CD4+ T cells. Science *327*, 1098-1102.

Ochsenbein, A.F., and Zinkernagel, R.M. (2000). Natural antibodies and complement link innate and acquired immunity. Immunol Today *21*, 624-630.

Odendall, C., Dixit, E., Stavru, F., Bierne, H., Franz, K.M., Durbin, A.F., Boulant, S., Gehrke, L., Cossart, P., and Kagan, J.C. (2014). Diverse intracellular pathogens activate type III interferon expression from peroxisomes. Nat Immunol *15*, 717-726.

Oikarinen, M., Tauriainen, S., Oikarinen, S., Honkanen, T., Collin, P., Rantala, I., Maki, M., Kaukinen, K., and Hyoty, H. (2012). Type 1 diabetes is associated with enterovirus infection in gut mucosa. Diabetes *61*, 687-691.

Oikarinen, S., Martiskainen, M., Tauriainen, S., Huhtala, H., Ilonen, J., Veijola, R., Simell, O., Knip, M., and Hyoty, H. (2011). Enterovirus RNA in blood is linked to the development of type 1 diabetes. Diabetes *60*, 276-279.

Okazaki, K., Uchida, K., Ohana, M., Nakase, H., Uose, S., Inai, M., Matsushima, Y., Katamura, K., Ohmori, K., and Chiba, T. (2000). Autoimmune-related pancreatitis is associated with autoantibodies and a Th1/Th2-type cellular immune response. Gastroenterology *118*, 573-581.

Oldenborg, P.A., Zheleznyak, A., Fang, Y.F., Lagenaur, C.F., Gresham, H.D., and Lindberg, F.P. (2000). Role of CD47 as a marker of self on red blood cells. Science *288*, 2051-2054.

Onoguchi, K., Onomoto, K., Takamatsu, S., Jogi, M., Takemura, A., Morimoto, S., Julkunen, I., Namiki, H., Yoneyama, M., and Fujita, T. (2010). Virus-infection or 5'ppp-RNA activates antiviral signal through redistribution of IPS-1 mediated by MFN1. PLoS pathogens *6*, e1001012.

Orban, T., Bundy, B., Becker, D.J., DiMeglio, L.A., Gitelman, S.E., Goland, R., Gottlieb, P.A., Greenbaum, C.J., Marks, J.B., Monzavi, R.*, et al.* (2011). Co-stimulation modulation with abatacept in patients with recent-onset type 1 diabetes: a randomised, double-blind, placebo-controlled trial. Lancet *378*, 412-419.

Orci, L., Thorens, B., Ravazzola, M., and Lodish, H.F. (1989). Localization of the pancreatic beta cell glucose transporter to specific plasma membrane domains. Science *245*, 295-297.

Ortis, F., Naamane, N., Flamez, D., Ladriere, L., Moore, F., Cunha, D.A., Colli, M.L., Thykjaer, T., Thorsen, K., Orntoft, T.F., and Eizirik, D.L. (2010). Cytokines interleukin-1beta and tumor necrosis factor-alpha regulate different transcriptional and alternative splicing networks in primary beta-cells. Diabetes *59*, 358-374.

Orzalli, M.H., and Knipe, D.M. (2014). Cellular sensing of viral DNA and viral evasion mechanisms. Annu Rev Microbiol *68*, 477-492.

Palmer, J.P., Asplin, C.M., Clemons, P., Lyen, K., Tatpati, O., Raghu, P.K., and Paquette, T.L. (1983). Insulin antibodies in insulin-dependent diabetics before insulin treatment. Science *222*, 1337-1339.

Pang, K., Mukonoweshuro, C., and Wong, G.G. (1994). Beta cells arise from glucose transporter type 2 (Glut2)-expressing epithelial cells of the developing rat pancreas. Proc Natl Acad Sci U S A *91*, 9559-9563.

Park, S., Juliana, C., Hong, S., Datta, P., Hwang, I., Fernandes-Alnemri, T., Yu, J.W., and Alnemri, E.S. (2013). The mitochondrial antiviral protein MAVS

associates with NLRP3 and regulates its inflammasome activity. J Immunol *191*, 4358-4366.

Pasare, C., and Medzhitov, R. (2005). Control of B-cell responses by Toll-like receptors. Nature *438*, 364-368.

Patel, R.K., and Jain, M. (2012). NGS QC Toolkit: a toolkit for quality control of next generation sequencing data. PLoS One *7*, e30619.

Patterson, C.C. (2000). Variation and trends in incidence of childhood diabetes in Europe. EURODIAB ACE Study Group. Lancet *355*, 873-876.

Paz, S., Vilasco, M., Werden, S.J., Arguello, M., Joseph-Pillai, D., Zhao, T., Nguyen, T.L., Sun, Q., Meurs, E.F., Lin, R., and Hiscott, J. (2011). A functional C-terminal TRAF3-binding site in MAVS participates in positive and negative regulation of the IFN antiviral response. Cell Res *21*, 895-910.

Pedros, C., Zhang, Y., Hu, J.K., Choi, Y.S., Canonigo-Balancio, A.J., Yates, J.R., 3rd, Altman, A., Crotty, S., and Kong, K.F. (2016). A TRAF-like motif of the inducible costimulator ICOS controls development of germinal center TFH cells via the kinase TBK1. Nat Immunol *17*, 825-833.

Pei, J., Kim, B.H., and Grishin, N.V. (2008). PROMALS3D: a tool for multiple protein sequence and structure alignments. Nucleic Acids Res *36*, 2295-2300.

Petrich de Marquesini, L.G., Fu, J., Connor, K.J., Bishop, A.J., McLintock, N.E., Pope, C., Wong, F.S., and Dayan, C.M. (2010). IFN-gamma and IL-10 islet-antigen-specific T cell responses in autoantibody-negative first-degree relatives of patients with type 1 diabetes. Diabetologia *53*, 1451-1460.

Pichlmair, A., Schulz, O., Tan, C.P., Naslund, T.I., Liljestrom, P., Weber, F., and Reis e Sousa, C. (2006). RIG-I-mediated antiviral responses to single-stranded RNA bearing 5'-phosphates. Science *314*, 997-1001.

Pothlichet, J., Niewold, T.B., Vitour, D., Solhonne, B., Crow, M.K., and Si-Tahar, M. (2011). A loss-of-function variant of the antiviral molecule MAVS is associated with a subset of systemic lupus patients. EMBO Mol Med *3*, 142-152.

Powell, R.D., Holland, P.J., Hollis, T., and Perrino, F.W. (2011). Aicardi-Goutieres syndrome gene and HIV-1 restriction factor SAMHD1 is a dGTP-regulated deoxynucleotide triphosphohydrolase. J Biol Chem *286*, 43596-43600.

Prahalad, S., Hansen, S., Whiting, A., Guthery, S.L., Clifford, B., McNally, B., Zeft, A.S., Bohnsack, J.F., and Jorde, L.B. (2009). Variants in TNFAIP3,

STAT4, and C12orf30 loci associated with multiple autoimmune diseases are also associated with juvenile idiopathic arthritis. Arthritis Rheum *60*, 2124-2130.

Precechtelova, J., Borsanyiova, M., Stipalova, D., Sarmirova, S., Gomolcak, P., Berakova, K., and Bopegamage, S. (2015). Pathophysiology of the pancreas after oral infection of genetically diverse mice with coxsackievirus B4-E2. Arch Virol *160*, 103-115.

Pritchard, C.C., Kroh, E., Wood, B., Arroyo, J.D., Dougherty, K.J., Miyaji, M.M., Tait, J.F., and Tewari, M. (2012). Blood cell origin of circulating microRNAs: a cautionary note for cancer biomarker studies. Cancer Prev Res (Phila) *5*, 492-497.

Prochazka, M., Serreze, D.V., Frankel, W.N., and Leiter, E.H. (1992). NOR/Lt mice: MHC-matched diabetes-resistant control strain for NOD mice. Diabetes *41*, 98-106.

Quandt, K., Frech, K., Karas, H., Wingender, E., and Werner, T. (1995). MatInd and MatInspector: new fast and versatile tools for detection of consensus matches in nucleotide sequence data. Nucleic Acids Res *23*, 4878-4884.

Quintana, F.J., and Cohen, I.R. (2001). Autoantibody patterns in diabetes-prone NOD mice and in standard C57BL/6 mice. Journal of autoimmunity *17*, 191-197.

Rabinovitch, A., Suarez-Pinzon, W.L., Sorensen, O., Bleackley, R.C., and Power, R.F. (1995). IFN-gamma gene expression in pancreatic islet-infiltrating mononuclear cells correlates with autoimmune diabetes in nonobese diabetic mice. J Immunol *154*, 4874-4882.

Radaev, S., and Sun, P. (2002). Recognition of immunoglobulins by Fcgamma receptors. Mol Immunol *38*, 1073-1083.

Radbruch, A., Muehlinghaus, G., Luger, E.O., Inamine, A., Smith, K.G.C., Dorner, T., and Hiepe, F. (2006). Competence and competition: the challenge of becoming a long-lived plasma cell. Nature Reviews Immunology *6*, 741-750.

Ramos, P.S., Criswell, L.A., Moser, K.L., Comeau, M.E., Williams, A.H., Pajewski, N.M., Chung, S.A., Graham, R.R., Zidovetzki, R., Kelly, J.A.*, et al.* (2011). A comprehensive analysis of shared loci between systemic lupus erythematosus (SLE) and sixteen autoimmune diseases reveals limited genetic overlap. PLoS Genet *7*, e1002406.

Ramsingh, A.I., Lee, W.T., Collins, D.N., and Armstrong, L.E. (1999). T cells contribute to disease severity during coxsackievirus B4 infection. J Virol *73*, 3080-3086.

Rasilainen, S., Nieminen, J.M., Levonen, A.L., Otonkoski, T., and Lapatto, R. (2002). Dose-dependent cysteine-mediated protection of insulin-producing cells from damage by hydrogen peroxide. Biochem Pharmacol *63*, 1297-1304.

Rathjen, T., Nicol, C., McConkey, G., and Dalmay, T. (2006). Analysis of short RNAs in the malaria parasite and its red blood cell host. FEBS Lett *580*, 5185-5188.

Raulet, D.H., Garman, R.D., Saito, H., and Tonegawa, S. (1985). Developmental regulation of T-cell receptor gene expression. Nature *314*, 103-107.

Rawlings, D.J., Schwartz, M.A., Jackson, S.W., and Meyer-Bahlburg, A. (2012). Integration of B cell responses through Toll-like receptors and antigen receptors. Nat Rev Immunol *12*, 282-294.

Ray, J.P., Marshall, H.D., Laidlaw, B.J., Staron, M.M., Kaech, S.M., and Craft, J. (2014). Transcription factor STAT3 and type I interferons are corepressive insulators for differentiation of follicular helper and T helper 1 cells. Immunity *40*, 367-377.

Rebollo, R., Romanish, M.T., and Mager, D.L. (2012). Transposable elements: an abundant and natural source of regulatory sequences for host genes. Annu Rev Genet *46*, 21-42.

Redondo, M.J., Fain, P.R., and Eisenbarth, G.S. (2001). Genetics of type 1A diabetes. Recent Prog Horm Res *56*, 69-89.

Redondo, M.J., Jeffrey, J., Fain, P.R., Eisenbarth, G.S., and Orban, T. (2008). Concordance for islet autoimmunity among monozygotic twins. N Engl J Med *359*, 2849-2850.

Reilly, S.M., Chiang, S.H., Decker, S.J., Chang, L., Uhm, M., Larsen, M.J., Rubin, J.R., Mowers, J., White, N.M., Hochberg, I.*, et al.* (2013). An inhibitor of the protein kinases TBK1 and IKK-varepsilon improves obesity-related metabolic dysfunctions in mice. Nat Med *19*, 313-321.

Reinhardt, R.L., Liang, H.E., and Locksley, R.M. (2009). Cytokine-secreting follicular T cells shape the antibody repertoire. Nat Immunol *10*, 385-393.

Reynier, F., Pachot, A., Paye, M., Xu, Q., Turrel-Davin, F., Petit, F., Hot, A., Auffray, C., Bendelac, N., Nicolino, M.*, et al.* (2010). Specific gene expression

signature associated with development of autoimmune type-I diabetes using whole-blood microarray analysis. Genes Immun *11*, 269-278.

Rice, G.I., Bond, J., Asipu, A., Brunette, R.L., Manfield, I.W., Carr, I.M., Fuller, J.C., Jackson, R.M., Lamb, T., Briggs, T.A.*, et al.* (2009). Mutations involved in Aicardi-Goutieres syndrome implicate SAMHD1 as regulator of the innate immune response. Nat Genet *41*, 829-832.

Rice, G.I., del Toro Duany, Y., Jenkinson, E.M., Forte, G.M., Anderson, B.H., Ariaudo, G., Bader-Meunier, B., Baildam, E.M., Battini, R., Beresford, M.W.*, et al.* (2014). Gain-of-function mutations in IFIH1 cause a spectrum of human disease phenotypes associated with upregulated type I interferon signaling. Nat Genet *46*, 503-509.

Rice, G.I., Kasher, P.R., Forte, G.M., Mannion, N.M., Greenwood, S.M., Szynkiewicz, M., Dickerson, J.E., Bhaskar, S.S., Zampini, M., Briggs, T.A.*, et al.* (2012). Mutations in ADAR1 cause Aicardi-Goutieres syndrome associated with a type I interferon signature. Nat Genet *44*, 1243-1248.

Richardson, S.J., Leete, P., Dhayal, S., Russell, M.A., Oikarinen, M., Laiho, J.E., Svedin, E., Lind, K., Rosenling, T., Chapman, N.*, et al.* (2014). Evaluation of the fidelity of immunolabelling obtained with clone 5D8/1, a monoclonal antibody directed against the enteroviral capsid protein, VP1, in human pancreas. Diabetologia *57*, 392-401.

Richardson, S.J., Willcox, A., Bone, A.J., Foulis, A.K., and Morgan, N.G. (2009). The prevalence of enteroviral capsid protein vp1 immunostaining in pancreatic islets in human type 1 diabetes. Diabetologia *52*, 1143-1151.

Ricklin, D., Hajishengallis, G., Yang, K., and Lambris, J.D. (2010). Complement: a key system for immune surveillance and homeostasis. Nature Immunology *11*, 785-797.

Rigby, M.R., Harris, K.M., Pinckney, A., DiMeglio, L.A., Rendell, M.S., Felner, E.I., Dostou, J.M., Gitelman, S.E., Griffin, K.J., Tsalikian, E.*, et al.* (2015). Alefacept provides sustained clinical and immunological effects in new-onset type 1 diabetes patients. J Clin Invest *125*, 3285-3296.

Riva, A. (2012). The MAPPER2 Database: a multi-genome catalog of putative transcription factor binding sites. Nucleic Acids Res *40*, D155-161.

Robinson, T., Kariuki, S.N., Franek, B.S., Kumabe, M., Kumar, A.A., Badaracco, M., Mikolaitis, R.A., Guerrero, G., Utset, T.O., Drevlow, B.E.*, et al.* (2011). Autoimmune disease risk variant of IFIH1 is associated with increased sensitivity to IFN-alpha and serologic autoimmunity in lupus patients. J Immunol *187*, 1298-1303.

Rock, K.L., Reits, E., and Neefjes, J. (2016). Present Yourself! By MHC Class I and MHC Class II Molecules. Trends in Immunology *37*, 724-737.

Rodriguez-Calvo, T., Sabouri, S., Anquetil, F., and von Herrath, M.G. (2016). The viral paradigm in type 1 diabetes: Who are the main suspects? Autoimmun Rev *15*, 964-969.

Roep, B.O., Arden, S.D., de Vries, R.R., and Hutton, J.C. (1990). T-cell clones from a type-1 diabetes patient respond to insulin secretory granule proteins. Nature *345*, 632-634.

Romme Christensen, J., Bornsen, L., Ratzer, R., Piehl, F., Khademi, M., Olsson, T., Sorensen, P.S., and Sellebjerg, F. (2013). Systemic inflammation in progressive multiple sclerosis involves follicular T-helper, Th17- and activated B-cells and correlates with progression. PLoS One *8*, e57820.

Rote, N.S., Chakrabarti, S., and Stetzer, B.P. (2004). The role of human endogenous retroviruses in trophoblast differentiation and placental development. Placenta *25*, 673-683.

Roulois, D., Loo Yau, H., Singhania, R., Wang, Y., Danesh, A., Shen, S.Y., Han, H., Liang, G., Jones, P.A., Pugh, T.J.*, et al.* (2015). DNA-Demethylating Agents Target Colorectal Cancer Cells by Inducing Viral Mimicry by Endogenous Transcripts. Cell *162*, 961-973.

Rowe, H.M., and Trono, D. (2011). Dynamic control of endogenous retroviruses during development. Virology *411*, 273-287.

Russell, D.M., Dembic, Z., Morahan, G., Miller, J.F., Burki, K., and Nemazee, D. (1991). Peripheral deletion of self-reactive B cells. Nature *354*, 308-311.

Sabbah, A., and Bose, S. (2009). Retinoic acid inducible gene I Activates innate antiviral response against human parainfluenza virus type 3. Virol J *6*.

Sage, P.T., Francisco, L.M., Carman, C.V., and Sharpe, A.H. (2013). The receptor PD-1 controls follicular regulatory T cells in the lymph nodes and blood. Nat Immunol *14*, 152-161.

Saito, T., and Gale, M., Jr. (2008). Differential recognition of double-stranded RNA by RIG-I-like receptors in antiviral immunity. J Exp Med *205*, 1523-1527.

Sallusto, F., Geginat, J., and Lanzavecchia, A. (2004). Central memory and effector memory T cell subsets: function, generation, and maintenance. Annu Rev Immunol *22*, 745-763.

Sangokoya, C., LaMonte, G., and Chi, J.T. (2010). Isolation and characterization of microRNAs of human mature erythrocytes. Methods Mol Biol *667*, 193-203.

Sarikonda, G., Pettus, J., Phatak, S., Sachithanantham, S., Miller, J.F., Wesley, J.D., Cadag, E., Chae, J., Ganesan, L., Mallios, R.*, et al.* (2014). CD8 T-cell reactivity to islet antigens is unique to type 1 while CD4 T-cell reactivity exists in both type 1 and type 2 diabetes. Journal of autoimmunity *50*, 77-82.

Scherm, M.G., Ott, V.B., and Daniel, C. (2016). Follicular Helper T Cells in Autoimmunity. Curr Diab Rep *16*, 75.

Schmidt, D., Schwalie, P.C., Wilson, M.D., Ballester, B., Goncalves, A., Kutter, C., Brown, G.D., Marshall, A., Flicek, P., and Odom, D.T. (2012). Waves of retrotransposon expansion remodel genome organization and CTCF binding in multiple mammalian lineages. Cell *148*, 335-348.

Schroder, K., Zhou, R.B., and Tschopp, J. (2010). The NLRP3 Inflammasome: A Sensor for Metabolic Danger? Science *327*, 296-300.

Schulte, B.M., Bakkers, J., Lanke, K.H., Melchers, W.J., Westerlaken, C., Allebes, W., Aanstoot, H.J., Bruining, G.J., Adema, G.J., Van Kuppeveld, F.J., and Galama, J.M. (2010). Detection of enterovirus RNA in peripheral blood mononuclear cells of type 1 diabetic patients beyond the stage of acute infection. Viral Immunol *23*, 99-104.

Schulte, B.M., Kers-Rebel, E.D., Prosser, A.C., Galama, J.M., van Kuppeveld, F.J., and Adema, G.J. (2013). Differential susceptibility and response of primary human myeloid BDCA1(+) dendritic cells to infection with different Enteroviruses. PLoS One *8*, e62502.

Schwartz, R.H. (1989). Acquisition of immunologic self-tolerance. Cell *57*, 1073-1081.

Schwickert, T.A., Lindquist, R.L., Shakhar, G., Livshits, G., Skokos, D., Kosco-Vilbois, M.H., Dustin, M.L., and Nussenzweig, M.C. (2007). In vivo imaging of germinal centres reveals a dynamic open structure. Nature *446*, 83-87.

Sebzda, E., Wallace, V.A., Mayer, J., Yeung, R.S., Mak, T.W., and Ohashi, P.S. (1994). Positive and negative thymocyte selection induced by different concentrations of a single peptide. Science *263*, 1615-1618.

Sechi, L.A., Rosu, V., Pacifico, A., Fadda, G., Ahmed, N., and Zanetti, S. (2008). Humoral immune responses of type 1 diabetes patients to Mycobacterium avium subsp. paratuberculosis lend support to the infectious trigger hypothesis. Clin Vaccine Immunol *15*, 320-326.

See, D.M., and Tilles, J.G. (1995). Pathogenesis of virus-induced diabetes in mice. J Infect Dis *171*, 1131-1138.

Seifarth, W., Frank, O., Zeilfelder, U., Spiess, B., Greenwood, A.D., Hehlmann, R., and Leib-Mosch, C. (2005). Comprehensive analysis of human endogenous retrovirus transcriptional activity in human tissues with a retrovirus-specific microarray. J Virol *79*, 341-352.

Serreze, D.V., Ottendorfer, E.W., Ellis, T.M., Gauntt, C.J., and Atkinson, M.A. (2000). Acceleration of type 1 diabetes by a coxsackievirus infection requires a preexisting critical mass of autoreactive T-cells in pancreatic islets. Diabetes *49*, 708-711.

Serreze, D.V., Wasserfall, C., Ottendorfer, E.W., Stalvey, M., Pierce, M.A., Gauntt, C., O'Donnell, B., Flanagan, J.B., Campbell-Thompson, M., Ellis, T.M., and Atkinson, M.A. (2005). Diabetes acceleration or prevention by a coxsackievirus B4 infection: critical requirements for both interleukin-4 and gamma interferon. J Virol *79*, 1045-1052.

Seth, R.B., Sun, L., Ea, C.K., and Chen, Z.J. (2005). Identification and characterization of MAVS, a mitochondrial antiviral signaling protein that activates NF-kappaB and IRF 3. Cell *122*, 669-682.

Sevilla, N., McGavern, D.B., Teng, C., Kunz, S., and Oldstone, M.B. (2004). Viral targeting of hematopoietic progenitors and inhibition of DC maturation as a dual strategy for immune subversion. J Clin Invest *113*, 737-745.

Sharon, D., Chen, M., Zhang, G., Girgis, S., Sis, B., Graham, D., McDougall, C., Wasilenko, S.T., Montano-Loza, A., and Mason, A.L. (2015). Impact of combination antiretroviral therapy in the NOD.c3c4 mouse model of autoimmune biliary disease. Liver Int *35*, 1442-1450.

Shi, Y., Yuan, B., Qi, N., Zhu, W., Su, J., Li, X., Qi, P., Zhang, D., and Hou, F. (2015). An autoinhibitory mechanism modulates MAVS activity in antiviral innate immune response. Nat Commun *6*, 7811.

Shifrin, N., Raulet, D.H., and Ardolino, M. (2014). NK cell self tolerance, responsiveness and missing self recognition. Semin Immunol *26*, 138-144.

Shimizu, F., Hooks, J.J., Kahn, C.R., and Notkins, A.L. (1980). Virus-induced decrease of insulin receptors in cultured human cells. J Clin Invest *66*, 1144-1151.

Simmons, K.M., Gottlieb, P.A., and Michels, A.W. (2016). Immune Intervention and Preservation of Pancreatic Beta Cell Function in Type 1 Diabetes. Curr Diab Rep *16*, 97.

Simpson, N., Gatenby, P.A., Wilson, A., Malik, S., Fulcher, D.A., Tangye, S.G., Manku, H., Vyse, T.J., Roncador, G., Huttley, G.A.*, et al.* (2010). Expansion of circulating T cells resembling follicular helper T cells is a fixed phenotype that identifies a subset of severe systemic lupus erythematosus. Arthritis Rheum *62*, 234-244.

Smelt, M.J., Faas, M.M., de Haan, B.J., and de Vos, P. (2008). Pancreatic beta-cell purification by altering FAD and NAD(P)H metabolism. Exp Diabetes Res *2008*, 165360.

Smyth, D., Cooper, J.D., Collins, J.E., Heward, J.M., Franklyn, J.A., Howson, J.M., Vella, A., Nutland, S., Rance, H.E., Maier, L.*, et al.* (2004). Replication of an association between the lymphoid tyrosine phosphatase locus (LYP/PTPN22) with type 1 diabetes, and evidence for its role as a general autoimmunity locus. Diabetes *53*, 3020-3023.

Smyth, D.J., Cooper, J.D., Bailey, R., Field, S., Burren, O., Smink, L.J., Guja, C., Ionescu-Tirgoviste, C., Widmer, B., Dunger, D.B.*, et al.* (2006a). A genome-wide association study of nonsynonymous SNPs identifies a type 1 diabetes locus in the interferon-induced helicase (IFIH1) region. Nat Genet *38*, 617-619.

Smyth, D.J., Howson, J.M., Payne, F., Maier, L.M., Bailey, R., Holland, K., Lowe, C.E., Cooper, J.D., Hulme, J.S., Vella, A.*, et al.* (2006b). Analysis of polymorphisms in 16 genes in type 1 diabetes that have been associated with other immune-mediated diseases. BMC Med Genet *7*, 20.

Snarski, E., Milczarczyk, A., Torosian, T., Paluszewska, M., Urbanowska, E., Krol, M., Boguradzki, P., Jedynasty, K., Franek, E., and Wiktor-Jedrzejczak, W. (2011). Independence of exogenous insulin following immunoablation and stem cell reconstitution in newly diagnosed diabetes type I. Bone Marrow Transplant *46*, 562-566.

Stark, G.R., Kerr, I.M., Williams, B.R.G., Silverman, R.H., and Schreiber, R.D. (1998). How cells respond to interferons. Annu Rev Biochem *67*, 227-264.

Stene, L.C., Oikarinen, S., Hyoty, H., Barriga, K.J., Norris, J.M., Klingensmith, G., Hutton, J.C., Erlich, H.A., Eisenbarth, G.S., and Rewers, M. (2010). Enterovirus infection and progression from islet autoimmunity to type 1 diabetes: the Diabetes and Autoimmunity Study in the Young (DAISY). Diabetes *59*, 3174-3180.

Stetson, D.B., Ko, J.S., Heidmann, T., and Medzhitov, R. (2008). Trex1 prevents cell-intrinsic initiation of autoimmunity. Cell *134*, 587-598.

Stetson, D.B., and Medzhitov, R. (2006a). Recognition of cytosolic DNA activates an IRF3-dependent innate immune response. Immunity *24*, 93-103.

Stetson, D.B., and Medzhitov, R. (2006b). Type I interferons in host defense. Immunity *25*, 373-381.

Stewart, T.A., Hultgren, B., Huang, X., Pitts-Meek, S., Hully, J., and MacLachlan, N.J. (1993). Induction of type I diabetes by interferon-alpha in transgenic mice. Science *260*, 1942-1946.

Stoye, J.P. (2012). Studies of endogenous retroviruses reveal a continuing evolutionary saga. Nat Rev Microbiol *10*, 395-406.

Strasser, A., and Pellegrini, M. (2004). T-lymphocyte death during shutdown of an immune response. Trends Immunol *25*, 610-615.

Subramanian, A., Tamayo, P., Mootha, V.K., Mukherjee, S., Ebert, B.L., Gillette, M.A., Paulovich, A., Pomeroy, S.L., Golub, T.R., Lander, E.S., and Mesirov, J.P. (2005). Gene set enrichment analysis: a knowledge-based approach for interpreting genome-wide expression profiles. Proc Natl Acad Sci U S A *102*, 15545-15550.

Subramanian, N., Natarajan, K., Clatworthy, M.R., Wang, Z., and Germain, R.N. (2013). The adaptor MAVS promotes NLRP3 mitochondrial localization and inflammasome activation. Cell *153*, 348-361.

Sundaram, V., Cheng, Y., Ma, Z., Li, D., Xing, X., Edge, P., Snyder, M.P., and Wang, T. (2014). Widespread contribution of transposable elements to the innovation of gene regulatory networks. Genome Res *24*, 1963-1976.

Szabo, K., Papp, G., Barath, S., Gyimesi, E., Szanto, A., and Zeher, M. (2013). Follicular helper T cells may play an important role in the severity of primary Sjogren's syndrome. Clin Immunol *147*, 95-104.

Tak, Y.G., and Farnham, P.J. (2015). Making sense of GWAS: using epigenomics and genome engineering to understand the functional relevance of SNPs in non-coding regions of the human genome. Epigenetics Chromatin *8*, 57.

Takahama, Y. (2006). Journey through the thymus: stromal guides for T-cell development and selection. Nature Reviews Immunology *6*, 127-135.

Takahasi, K., Yoneyama, M., Nishihori, T., Hirai, R., Kumeta, H., Narita, R., Gale, M., Jr., Inagaki, F., and Fujita, T. (2008). Nonself RNA-sensing mechanism of RIG-I helicase and activation of antiviral immune responses. Mol Cell *29*, 428-440.

Takeuchi, O., and Akira, S. (2008). MDA5/RIG-I and virus recognition. Curr Opin Immunol *20*, 17-22.

Takeuchi, O., and Akira, S. (2010). Pattern recognition receptors and inflammation. Cell *140*, 805-820.

Tal, M.C., Sasai, M., Lee, H.K., Yordy, B., Shadel, G.S., and Iwasaki, A. (2009). Absence of autophagy results in reactive oxygen species-dependent amplification of RLR signaling. Proc Natl Acad Sci U S A *106*, 2770-2775.

Tangye, S.G., and Good, K.L. (2007). Human IgM+CD27+ B cells: memory B cells or "memory" B cells? J Immunol *179*, 13-19.

Tarlinton, D.M., and Smith, K.G. (2000). Dissecting affinity maturation: a model explaining selection of antibody-forming cells and memory B cells in the germinal centre. Immunol Today *21*, 436-441.

Temin, H.M. (1985). Reverse transcription in the eukaryotic genome: retroviruses, pararetroviruses, retrotransposons, and retrotranscripts. Mol Biol Evol *2*, 455-468.

Tenenbaum, D. (2016). KEGGREST: Client-side REST access to KEGG.

Terrier, B., Costedoat-Chalumeau, N., Garrido, M., Geri, G., Rosenzwajg, M., Musset, L., Klatzmann, D., Saadoun, D., and Cacoub, P. (2012). Interleukin 21 correlates with T cell and B cell subset alterations in systemic lupus erythematosus. J Rheumatol *39*, 1819-1828.

Thomas, J.W., Kendall, P.L., and Mitchell, H.G. (2002). The natural autoantibody repertoire of nonobese diabetic mice is highly active. J Immunol *169*, 6617-6624.

Tivol, E.A., Borriello, F., Schweitzer, A.N., Lynch, W.P., Bluestone, J.A., and Sharpe, A.H. (1995). Loss of CTLA-4 leads to massive lymphoproliferation and fatal multiorgan tissue destruction, revealing a critical negative regulatory role of CTLA-4. Immunity *3*, 541-547.

Todd, J.A. (2014). Constitutive Antiviral Immunity at the Expense of Autoimmunity. Immunity *40*, 167-169.

Todd, J.A., Walker, N.M., Cooper, J.D., Smyth, D.J., Downes, K., Plagnol, V., Bailey, R., Nejentsev, S., Field, S.F., Payne, F.*, et al.* (2007). Robust associations of four new chromosome regions from genome-wide analyses of type 1 diabetes. Nat Genet *39*, 857-864.

Tracy, S., Drescher, K.M., Chapman, N.M., Kim, K.S., Carson, S.D., Pirruccello, S., Lane, P.H., Romero, J.R., and Leser, J.S. (2002). Toward testing the hypothesis that group B coxsackieviruses (CVB) trigger insulin-

dependent diabetes: inoculating nonobese diabetic mice with CVB markedly lowers diabetes incidence. J Virol *76*, 12097-12111.

Tracy, S., Smithee, S., Alhazmi, A., and Chapman, N. (2015). Coxsackievirus can Persist in Murine Pancreas by Deletion of 5 ' Terminal Genomic Sequences. J Med Virol *87*, 240-247.

Tubo, N.J., Pagan, A.J., Taylor, J.J., Nelson, R.W., Linehan, J.L., Ertelt, J.M., Huseby, E.S., Way, S.S., and Jenkins, M.K. (2013). Single naive CD4+ T cells from a diverse repertoire produce different effector cell types during infection. Cell *153*, 785-796.

Tuomilehto, J., Virtala, E., Karvonen, M., Lounamaa, R., Pitkaniemi, J., Reunanen, A., Tuomilehto-Wolf, E., and Toivanen, L. (1995). Increase in incidence of insulin-dependent diabetes mellitus among children in Finland. Int J Epidemiol *24*, 984-992.

Tuvemo, T., Dahlquist, G., Frisk, G., Blom, L., Friman, G., Landin-Olsson, M., and Diderholm, H. (1989). The Swedish childhood diabetes study III: IgM against coxsackie B viruses in newly diagnosed type 1 (insulin-dependent) diabetic children--no evidence of increased antibody frequency. Diabetologia *32*, 745-747.

Tyznik, A.J., Verma, S., Wang, Q., Kronenberg, M., and Benedict, C.A. (2014). Distinct requirements for activation of NKT and NK cells during viral infection. J Immunol *192*, 3676-3685.

Tzartos, J.S., Craner, M.J., Friese, M.A., Jakobsen, K.B., Newcombe, J., Esiri, M.M., and Fugger, L. (2011). IL-21 and IL-21 receptor expression in lymphocytes and neurons in multiple sclerosis brain. Am J Pathol *178*, 794-802.

Ueda, H., Howson, J.M., Esposito, L., Heward, J., Snook, H., Chamberlain, G., Rainbow, D.B., Hunter, K.M., Smith, A.N., Di Genova, G.*, et al.* (2003). Association of the T-cell regulatory gene CTLA4 with susceptibility to autoimmune disease. Nature *423*, 506-511.

Ueda, T., Shirakawa, H., and Yoshida, M. (2002). Involvement of HMGB1 and HMGB2 proteins in exogenous DNA integration reaction into the genome of HeLa S3 cells. Biochim Biophys Acta *1593*, 77-84.

Ueno, H. (2016). T follicular helper cells in human autoimmunity. Curr Opin Immunol *43*, 24-31.

UniProt, C. (2015). UniProt: a hub for protein information. Nucleic Acids Res *43*, D204-212.

Vahedi, G., Kanno, Y., Furumoto, Y., Jiang, K., Parker, S.C., Erdos, M.R., Davis, S.R., Roychoudhuri, R., Restifo, N.P., Gadina, M.*, et al.* (2015). Super-enhancers delineate disease-associated regulatory nodes in T cells. Nature *520*, 558-562.

van Belle, T.L., Coppieters, K.T., and von Herrath, M.G. (2011). Type 1 diabetes: etiology, immunology, and therapeutic strategies. Physiol Rev *91*, 79-118.

Van de Winkle, M., Maes, E., and Pipeleers, D. (1982). Islet cell analysis and purification by light scatter and autofluorescence. Biochem Biophys Res Commun *107*, 525-532.

van den Broek, M.F., Muller, U., Huang, S., Zinkernagel, R.M., and Aguet, M. (1995). Immune defence in mice lacking type I and/or type II interferon receptors. Immunol Rev *148*, 5-18.

Van Dommelen, S.L., and Degli-Esposti, M.A. (2004). NKT cells and viral immunity. Immunol Cell Biol *82*, 332-341.

Vandewinkel, M., and Pipeleers, D. (1983). Autofluorescence-Activated Cell Sorting of Pancreatic-Islet Cells - Purification of Insulin-Containing B-Cells According to Glucose-Induced Changes in Cellular Redox State. Biochem Bioph Res Co *114*, 835-842.

Varela-Calvino, R., Skowera, A., Arif, S., and Peakman, M. (2004). Identification of a naturally processed cytotoxic CD8 T-cell epitope of coxsackievirus B4, presented by HLA-A2.1 and located in the PEVKEK region of the P2C nonstructural protein. J Virol *78*, 13399-13408.

Vavouri, T., McEwen, G.K., Woolfe, A., Gilks, W.R., and Elgar, G. (2006). Defining a genomic radius for long-range enhancer action: duplicated conserved non-coding elements hold the key. Trends Genet *22*, 5-10.

Venkataraman, T., Valdes, M., Elsby, R., Kakuta, S., Caceres, G., Saijo, S., Iwakura, Y., and Barber, G.N. (2007). Loss of DExD/H box RNA helicase LGP2 manifests disparate antiviral responses. J Immunol *178*, 6444-6455.

Victora, G.D., and Nussenzweig, M.C. (2012). Germinal centers. Annu Rev Immunol *30*, 429-457.

Vinuesa, C.G., Linterman, M.A., Yu, D., and MacLennan, I.C.M. (2016). Follicular Helper T Cells. Annual Review of Immunology, Vol 34 *34*, 335-368.

von Herrath, M.G., Coon, B., Wolfe, T., and Chatenoud, L. (2002). Nonmitogenic CD3 antibody reverses virally induced (rat insulin promoter-

lymphocytic choriomeningitis virus) autoimmune diabetes without impeding viral clearance. J Immunol *168*, 933-941.

Vossenkamper, A., Lutalo, P.M., and Spencer, J. (2012). Translational Mini-Review Series on B cell subsets in disease. Transitional B cells in systemic lupus erythematosus and Sjogren's syndrome: clinical implications and effects of B cell-targeted therapies. Clin Exp Immunol *167*, 7-14.

Wang, B., Xi, X., Lei, X., Zhang, X., Cui, S., Wang, J., Jin, Q., and Zhao, Z. (2013). Enterovirus 71 protease 2Apro targets MAVS to inhibit anti-viral type I interferon responses. PLoS pathogens *9*, e1003231.

Wang, G.J., Gao, C.F., Wei, D., Wang, C., and Ding, S.Q. (2009). Acute pancreatitis: etiology and common pathogenesis. World J Gastroenterol *15*, 1427-1430.

Wang, L., Wang, F.S., and Gershwin, M.E. (2015). Human autoimmune diseases: a comprehensive update. J Intern Med *278*, 369-395.

Weets, I., Kaufman, L., Van der Auwera, B., Crenier, L., Rooman, R.P., De Block, C., Casteels, K., Weber, E., Coeckelberghs, M., Laron, Z.*, et al.* (2004). Seasonality in clinical onset of type 1 diabetes in belgian patients above the age of 10 is restricted to HLA-DQ2/DQ8-negative males, which explains the male to female excess in incidence. Diabetologia *47*, 614-621.

Wei, G., Wei, L., Zhu, J., Zang, C., Hu-Li, J., Yao, Z., Cui, K., Kanno, Y., Roh, T.Y., Watford, W.T.*, et al.* (2009). Global mapping of H3K4me3 and H3K27me3 reveals specificity and plasticity in lineage fate determination of differentiating CD4+ T cells. Immunity *30*, 155-167.

West, A.P., Shadel, G.S., and Ghosh, S. (2011). Mitochondria in innate immune responses. Nat Rev Immunol *11*, 389-402.

White, M.J., McArthur, K., Metcalf, D., Lane, R.M., Cambier, J.C., Herold, M.J., van Delft, M.F., Bedoui, S., Lessene, G., Ritchie, M.E.*, et al.* (2014). Apoptotic caspases suppress mtDNA-induced STING-mediated type I IFN production. Cell *159*, 1549-1562.

Wicker, L.S., Clark, J., Fraser, H.I., Garner, V.E., Gonzalez-Munoz, A., Healy, B., Howlett, S., Hunter, K., Rainbow, D., Rosa, R.L.*, et al.* (2005a). Type 1 diabetes genes and pathways shared by humans and NOD mice. Journal of autoimmunity *25 Suppl*, 29-33.

Wicker, L.S., Moule, C.L., Fraser, H., Penha-Goncalves, C., Rainbow, D., Garner, V.E., Chamberlain, G., Hunter, K., Howlett, S., Clark, J.*, et al.* (2005b). Natural genetic variants influencing type 1 diabetes in humans and in the NOD mouse. Novartis Foundation symposium *267*, 57-65; discussion 65-75.

Wickham, H. (2009). ggplot2: Elegant Graphics for Data Analysis. Use R, 1-212.

Willcox, A., Richardson, S.J., Bone, A.J., Foulis, A.K., and Morgan, N.G. (2009). Analysis of islet inflammation in human type 1 diabetes. Clin Exp Immunol *155*, 173-181.

Wilson, S.B., Kent, S.C., Patton, K.T., Orban, T., Jackson, R.A., Exley, M., Porcelli, S., Schatz, D.A., Atkinson, M.A., Balk, S.P.*, et al.* (1998). Extreme Th1 bias of invariant Valpha24JalphaQ T cells in type 1 diabetes. Nature *391*, 177-181.

Wollenberg, I., Agua-Doce, A., Hernandez, A., Almeida, C., Oliveira, V.G., Faro, J., and Graca, L. (2011). Regulation of the germinal center reaction by Foxp3+ follicular regulatory T cells. J Immunol *187*, 4553-4560.

Wong, P., and Pamer, E.G. (2003). CD8 T cell responses to infectious pathogens. Annu Rev Immunol *21*, 29-70.

Wu, J., and Chen, Z.J. (2014). Innate immune sensing and signaling of cytosolic nucleic acids. Annu Rev Immunol *32*, 461-488.

Xu, H., He, X., Zheng, H., Huang, L.J., Hou, F., Yu, Z., de la Cruz, M.J., Borkowski, B., Zhang, X., Chen, Z.J., and Jiang, Q.X. (2014). Structural basis for the prion-like MAVS filaments in antiviral innate immunity. Elife *3*, e01489.

Xu, L.G., Wang, Y.Y., Han, K.J., Li, L.Y., Zhai, Z., and Shu, H.B. (2005). VISA is an adapter protein required for virus-triggered IFN-beta signaling. Mol Cell *19*, 727-740.

Xu, X., Shi, Y., Cai, Y., Zhang, Q., Yang, F., Chen, H., Gu, Y., Zhang, M., Yu, L., and Yang, T. (2013). Inhibition of increased circulating Tfh cell by anti-CD20 monoclonal antibody in patients with type 1 diabetes. PLoS One *8*, e79858.

Yang, B.T., Dayeh, T.A., Kirkpatrick, C.L., Taneera, J., Kumar, R., Groop, L., Wollheim, C.B., Nitert, M.D., and Ling, C. (2011). Insulin promoter DNA methylation correlates negatively with insulin gene expression and positively with HbA(1c) levels in human pancreatic islets. Diabetologia *54*, 360-367.

Yang, Y., Ertl, H.C., and Wilson, J.M. (1994). MHC class I-restricted cytotoxic T lymphocytes to viral antigens destroy hepatocytes in mice infected with E1-deleted recombinant adenoviruses. Immunity *1*, 433-442.

Yang, Y.G., Lindahl, T., and Barnes, D.E. (2007). Trex1 exonuclease degrades ssDNA to prevent chronic checkpoint activation and autoimmune disease. Cell *131*, 873-886.

Yap, I.S., Giddings, G., Pocock, E., and Chantler, J.K. (2003). Lack of islet neogenesis plays a key role in beta-cell depletion in mice infected with a diabetogenic variant of coxsackievirus B4. J Gen Virol *84*, 3051-3068.

Yap, M.W., Nisole, S., Lynch, C., and Stoye, J.P. (2004). Trim5alpha protein restricts both HIV-1 and murine leukemia virus. Proc Natl Acad Sci U S A *101*, 10786-10791.

Yasukawa, K., Oshiumi, H., Takeda, M., Ishihara, N., Yanagi, Y., Seya, T., Kawabata, S., and Koshiba, T. (2009). Mitofusin 2 inhibits mitochondrial antiviral signaling. Sci Signal *2*, ra47.

Yi, T., Li, J., Chen, H., Wu, J., An, J., Xu, Y., Hu, Y., Lowell, C.A., and Cyster, J.G. (2015). Splenic Dendritic Cells Survey Red Blood Cells for Missing Self-CD47 to Trigger Adaptive Immune Responses. Immunity *43*, 764-775.

Yin, H., Berg, A.K., Tuvemo, T., and Frisk, G. (2002). Enterovirus RNA is found in peripheral blood mononuclear cells in a majority of type 1 diabetic children at onset. Diabetes *51*, 1964-1971.

Yoneyama, M., Kikuchi, M., Matsumoto, K., Imaizumi, T., Miyagishi, M., Taira, K., Foy, E., Loo, Y.M., Gale, M., Jr., Akira, S.*, et al.* (2005). Shared and unique functions of the DExD/H-box helicases RIG-I, MDA5, and LGP2 in antiviral innate immunity. J Immunol *175*, 2851-2858.

Yoneyama, M., Onomoto, K., Jogi, M., Akaboshi, T., and Fujita, T. (2015). Viral RNA detection by RIG-I-like receptors. Curr Opin Immunol *32*, 48-53.

Yoon, J.W., Austin, M., Onodera, T., and Notkins, A.L. (1979). Isolation of a virus from the pancreas of a child with diabetic ketoacidosis. N Engl J Med *300*, 1173-1179.

Yoon, J.W., McClintock, P.R., Bachurski, C.J., Longstreth, J.D., and Notkins, A.L. (1985). Virus-induced diabetes mellitus. No evidence for immune mechanisms in the destruction of beta-cells by the D-variant of encephalomyocarditis virus. Diabetes *34*, 922-925.

Yoon, J.W., Onodera, T., and Notkins, A.L. (1978). Virus-induced diabetes mellitus. XV. Beta cell damage and insulin-dependent hyperglycemia in mice infected with coxsackie virus B4. J Exp Med *148*, 1068-1080.

Young, G.R., Mavrommatis, B., and Kassiotis, G. (2014). Microarray analysis reveals global modulation of endogenous retroelement transcription by microbes. Retrovirology *11*, 59.

Young, J.C., Hoogenraad, N.J., and Hartl, F.U. (2003). Molecular chaperones Hsp90 and Hsp70 deliver preproteins to the mitochondrial import receptor Tom70. Cell *112*, 41-50.

Yu, D., dos Santos, C.O., Zhao, G., Jiang, J., Amigo, J.D., Khandros, E., Dore, L.C., Yao, Y., D'Souza, J., Zhang, Z.*, et al.* (2010). miR-451 protects against erythroid oxidant stress by repressing 14-3-3zeta. Genes Dev *24*, 1620-1633.

Yu, P. (2016). The potential role of retroviruses in autoimmunity. Immunol Rev *269*, 85-99.

Yui, M.A., Muralidharan, K., Moreno-Altamirano, B., Perrin, G., Chestnut, K., and Wakeland, E.K. (1996). Production of congenic mouse strains carrying NOD-derived diabetogenic genetic intervals: an approach for the genetic dissection of complex traits. Mamm Genome *7*, 331-334.

Zeng, M., Hu, Z., Shi, X., Li, X., Zhan, X., Li, X.D., Wang, J., Choi, J.H., Wang, K.W., Purrington, T.*, et al.* (2014). MAVS, cGAS, and endogenous retroviruses in T-independent B cell responses. Science *346*, 1486-1492.

Zerbino, D.R., Johnson, N., Juetteman, T., Sheppard, D., Wilder, S.P., Lavidas, I., Nuhn, M., Perry, E., Raffaillac-Desfosses, Q., Sobral, D.*, et al.* (2016). Ensembl regulation resources. Database (Oxford) *2016*.

Zhang, H., Wada, J., Hida, K., Tsuchiyama, Y., Hiragushi, K., Shikata, K., Wang, H.Y., Lin, S., Kanwar, Y.S., and Makino, H. (2001). Collectrin, a collecting duct-specific transmembrane glycoprotein, is a novel homolog of ACE2 and is developmentally regulated in embryonic kidneys. Journal of Biological Chemistry *276*, 17132-17139.

Zhao, Y., Sun, X., Nie, X., Sun, L., Tang, T.S., Chen, D., and Sun, Q. (2012). COX5B regulates MAVS-mediated antiviral signaling through interaction with ATG5 and repressing ROS production. PLoS pathogens *8*, e1003086.

Zust, R., Cervantes-Barragan, L., Habjan, M., Maier, R., Neuman, B.W., Ziebuhr, J., Szretter, K.J., Baker, S.C., Barchet, W., Diamond, M.S.*, et al.* (2011). Ribose 2'-O-methylation provides a molecular signature for the distinction of self and non-self mRNA dependent on the RNA sensor Mda5. Nat Immunol *12*, 137-143.